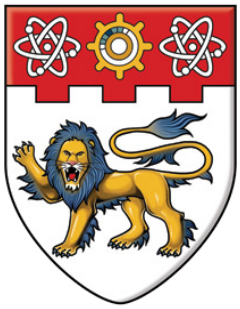

NANYANG TECHNOLOGICAL UNIVERSITY

A MICROFLUIDIC PLATFORM TO STUDY PATHOGEN-HOST INTERACTIONS AT SINGLE CELL LEVEL

ZHANG RUI

SCHOOL OF MECHANICAL AND AEROSPACE ENGINEERING

Nanyang Technological University

2012

A MICROFLUIDIC PLATFORM TO STUDY PATHOGEN-HOST INTERACTIONS AT SINGLE CELL LEVEL

ZHANG RUI

School of Mechanical and Aerospace Engineering

A thesis submitted to the Nanyang Technological University

in partial fulfillment of the requirement for the degree of

Doctor of Philosophy

2012

Thesis Advisors

Main supervisor: Prof. Thomas Hai-Qing GONG, BioMEMS lab, School of Mechanical and Aerospace Engineering, Nanyang Technological University, Singapore.

Co-supervisor: Prof. Sze Chun Chau, Division of Molecular Genetics and Cell Biology, School of Biological Sciences, Nanyang Technological University, Singapore.

ACKNOWLEDGEMENTS

I would like to convey my appreciation to all those who helped me with this thesis. I want to thank the School of Mechanical and Aerospace engineering for giving me the opportunity to commence my PhD study program in the first place and to do innovative research work. I also want to thank the School of Biological Sciences, Mr. Charles Tan and Ms. Chew Lay Byan who confirmed the permission for me to utilize the laboratory facility.

I am deeply indebted to my supervisor Prof. Gong Hai Qing and Prof. Sze Chun Chau whose guidance, inspiring advice and warm encouragement help me in all the time of my PhD research and thesis writing.

I am obligaed to staff in Star Array Pte Ltd in Singapore for their contributions and discussions in conceptualization, designing, fabricating and testing of the liquid phase nucleic acid extraction chip shown in Figure 4.2, 4.3 and 4.4, and the PCR array chip shown in Figure 3.2 and 3.4 of this thesis.

I am obliged to my colleagues who support me in my research work. I want to thank them for all their kind help and valuable technical suggestions. Especially, want to say thank you to Mr. Lou Chao Ping, Dr. Liu Hao Bing. Mr. Dai Chang Chun, Mr. Wu Bo, Ms. Wang Hui, in the area of chip fabrication, testing and instrumentation, and Dr. Miao Huang, Ms. Ng Chow Goon and Ms. Shalini Ratnasingam in the area of biological knowledge. Your friendship is a valuable and wonderful gift for me during my 4-year PhD study. I also want to thank Ms. Chan Sock Hoai who offered her help on instrument operation and data analysis to me in her spare time.

I would like to give my special thanks to my husband Shang Yang. Thank you for your unconditional trust and support. Thank you for the countless night spent with me in the lab. Your love and patient enabled me to complete this work.

Abstract

In this study, a high throughput poly(dimethylsiloxane) (PDMS) array chip consisting of multiple micro-wells and microfluidic channels was developed to analyze two biological perspectives of pathogen-host interactions – adherence and gene transcription – at single cell level, that current techniques are unable to cater to. The association of a common human pathogen, *Pseudomonas aeruginosa*, in either single or mixed (with *Staphylococcus aureus*) infection context, to the host human lung epithelial A549 cells was selected as the in vitro model to evaluate the performance of the chip. Single A549 cells were isolated into the individual micro-wells by one-step vacuum driven microfluidics when cell density was pre-adjusted to less than 0.3 cell/well. On-chip quantitative PCR was carried out with species-specific primer and probe sets to quantify the adhered bacteria. Single bacterium detection with the success rates of 90% for *P. aeruginosa* and 94% for *S. aureus* can be achieved with good reproducibility using the optimized DNA isolation protocol. Association profiling of *P. aeruginosa* and *S. aureus* in single infection context to A549 cells at three time points revealed different adherence patterns of these two pathogens. The attachment profiling of *P. aeruginosa* and *S. aureus* in mixed infection context was also obtained by on-chip multiplex q-PCR assay, from which *P. aeruginosa* association to the host A549 cells was identified to be significantly inhibited in the presence of *S. aureus* at 4 hours and 6 hours of infection.

This chip was further developed for gene transcriptional regulation analysis by incorporation of a novel microfluidic phase partitioning technology for bacterial nucleic acid purification. DNA or RNA from *P. aeruginosa* and *S. aureus* in the range of 5000 down to a single cell in the sample volume of 1 μl or 125 nl, can be selectively recovered and directly put through on-chip quantitative PCR assay. The aqueous phase bacterial lysate was isolated in an array of micro-wells, after which an immiscible organic (phenol-chloroform) phase was introduced in a headspace channel connecting the micro-well array. Continuous flow of the organic phase increases the interfacial contact with the aqueous phase to achieve purification of target nucleic acid through phase partitioning. Significantly enhanced nucleic acid recovery yield, up to 10 fold higher, was achieved

using the chip based liquid phase nucleic acid purification technique compared to that obtained by the conventional column based solid phase nucleic acid extraction method. One step vacuum-driven microfluidics allowed an on-chip quantitative PCR assay to be carried out in the same micro-wells within which bacterial nucleic acids were isolated, avoiding sample loss during liquid transfer. Using this nucleic acid purification device set in a two-dimensional (2D) array format of 900 micro-wells, it was demonstrated for the first time that high-throughput extraction of RNA coupled with direct on-chip PCR analysis from single bacterial cells could be achieved. The mRNA transcripts of *rmd* gene (an important gene involved in O antigen synthesis) of *P. aeruginosa* attached to single A549 cells were quantified using the 2D nucleic acid purification chip. The up-regulation of this gene in positive correlation with the number of *P. aeruginosa* adhered was reported.

In summary, the proposed microfluidic platform that integrated liquid phase nucleic acid purification and on-chip quantitative PCR presents a simple and effective "all-in-one" solution for high throughput bacterial nucleic acid analysis down to single cell sensitivity and can be applied for both automated bacteria quantification and transcriptional profiling.

List of Publications

[1] **Rui Zhang**, Hai-Qing Gong, XuDong Zeng, ChaoPing Lou and Chun Chau Sze; A microfluidic liquid phase nucleic acid purification chip to selectively isolate DNA or RNA from low copy/single bacterial cells in minute sample volume followed by direct on-chip quantitative PCR assay. ***Analytical Chemistry*** 2013 *85* (3), 1484-1491.

[2] **Rui Zhang**, Hai-Qing Gong Xu Dong Zeng and Chun Chau Sze; A high throughput microfluidic PDMS array chip to quantify bacteria adhesion to single host cells by real time PCR assay. ***Analytical and Bioanalytical Chemistry*** 02/2013 (published on line first).

[3] **Rui Zhang**, Hai-Qing Gong Bo Wu and Chun Chau Sze; Interaction of *P. aeruginosa* and *S. aurues* in mixed infection context to human lung epithelial A549 cells. To be submitted to ***Cellular Microbiology.***

[4] Majid Ebrahimi Warkiani, Longqing Chen, Chao-Ping Lou, Hao-Bing Liu, **Rui Zhang**, and Hai-Qing Gong; Capturing and recovering of Cryptosporidium parvum oocysts with polymeric micro-fabricated filter. ***Journal of Membrane Science***. Volume 369, Issues 1–2, 1 March 2011 Pages 560-568.

[5] Naveen Ramalingam, **Rui Zhang**, Hao-Bing Liu, Chang-Chun Dai, Rajni Kaushik, Bandi Ratnaharika and Hai-Qing Gong; Real-time PCR-based microfluidic array chip for simultaneous detection of multiple waterborne pathogens. ***Sensors and Actuators B: Chemical*** Volume 145, Issue 1, 4 March 2010, Pages 543-552.

Contents

List of Figures

List of Tables

Chapter 1 Introduction

1.1 Introduction

Single cells represent the basic unit of all living organisms. However, the majority of the knowledge in life sciences is based on the investigations on cell populations but not on individual cells. Only until recently, it has been well recognized that some key fundamentals in both systematic and developmental biology, including those related to cell differentiation, heterogeneity in gene expression, and the origins of some diseases can only be solved at the single-cell level. The success in single-cell biology is inseparable from the development of novel engineering techniques that can accurately quantify chemical components of single cells in extremely small quantities. Flow cytometry and fluorescence microscopy are two commonly employed bench top platforms to analyze single cell behavior. However, their usage is only limited to a small number of species that can be either genetically modified to express fluorescent proteins or probed with target-specific fluorophores.

Microfluidics is an emerging discipline that refers to analyze the liquid behavior in small volumes from picoliters to nanoliters and to control it within micro-structured devices. These micro-fabricated devices enable the integration of multi-step procedures of cell isolation, lysis, and analysis of cell components of various types and have become a promising tool for single-cell study in fully automated fashion with minimum human interference. Therefore, microfluidic single cell analytical devices are of great interest and have a broad range of applications in both clinical and research laboratories. One critical application of microfluidic platform in single cell analysis is to quantify gene

transcriptional kinetics, which is an important perspective in biological researches to unambiguously identify co-regulated genes, especially in minority disease-relevant cell populations. Current technologies for transcripts quantification include quantitative reverse transcription polymerase chain reaction (q-RT-PCR) [1], mRNA sequencing [2], and hybridization based single molecule counting [3]. Of all these methods, q-RT-PCR outperforms in both sensitivity and specificity, and therefore serves as the first choice in microfluidic platforms for single cell study. A successful microfluidic q-RT-PCR platform must incorporate the following basic functionalities of cell manipulation and isolation, RNA purification, cDNA synthesis and q-PCR amplification assay. Although each step is challenged with certain technical limitations, the major obstacle remains in the nucleic acid sample preparation at microscales. Current microfluidic nucleic acid extraction techniques mainly focus on the miniaturization of the solid phase nucleic acid purification method based on the fact that nucleic acids can be selectively absorbed onto specific solid phase medium in high ionic strength buffer and can later be eluted in low ionic strength buffer after unwanted impurities are washed away. However, solid phase extraction technology is not well suited for single cell assay due to the unsatisfactory nucleic acid recovery. Additionally, the elution volume of the purified nucleic acids is usually more than ten microliter, which is not compatible with downstream microfluidic q-RT-PCR assay. Moreover, this method is low throughput in nature so that only limited number of cells can be analyzed per each run. In order to circumvent this situation, existing high throughput microfliudic platforms for single cell mRNA transcription assay are developed in a way to avert the necessities for RNA purification by designing primers to anneal to sequences in exons on both sides of an intron [4]. However, this method cannot be applied

to single bacterium assay as extron is not present in bacterial mRNA transcripts. Until now, microfluidic platforms for single bacterium nucleic acid assay have not been developed.

1.2 Objective and methods

A breakthrough microfluidic device for PCR based bacterial nucleic acid analysis down to single bacterium sensitivity was developed in this study. The proposed device integrated all necessary procedures for single bacterium assay including single bacterium separation, cell lysis, and nucleic acid purification. This microfluidic device is of simple structure with 900 micro-wells holding the liquid of around 125 nl/well, a headspace channel, a sample inlet channel and a sample outlet channel. Sample and reagent were distributed into the micro-wells by single step vacuum driven microfluidics. Single bacterium was isolated in the individual wells probabilistically by pre-adjusting the cell densities to less than 0.3 cell/well. Bacteria were then lysed by on-chip thermal lysis in an optimized buffer with minimum nucleic acid loss. Nucleic acids were purified in the micro-wells by novel phase partitioning technology developed in this study. PCR reagent was then distributed into the micro-wells for on-chip amplification assay so that sample loss caused by liquid transfer can be avoided. Enhanced nucleic acid recovery was validated as compared with solid phased based nucleic acid purification method. Successful high throughput purification of RNA from single bacterium with compatible on-chip q-RT-PCR assay was reported for the first time.

This chip was applied to investigate two biological perspectives of pathogen-host interactions, including both bacterial association and gene transcriptional regulation of

Pseudomonas aeruginosa with human lung epithelial A549 cells in either single or mixed infection context with *Staphylococcus aureus* at single host cell level. *P. aeruginosa* is an important opportunistic human pathogen widespread throughout the environment, which can cause life-threatening respiratory tract infection, especially in patients with cystic fibrosis (CF). *P. aeruginosa* associated lung damage is initiated by the bacterium's successful colonization to the human lung epithelium. The highly infectious nature of *P. aeruginosa* is contributed by the large number of virulence and pathogenicity associated genes it is equipped with. Therefore, understanding how *P. aeruginosa* regulates the adhesion and transcription of virulence and pathogenesis associated genes to single host cells provides better insights to the disease development. In recent years, mixed infections induced by *P. aeruginosa* and *S. aureus* are reported with increased frequency, especially in lower airway of CF patient [5]. A variety of complicated interactions are likely to occur between the bacteria involved, which may lead to intensified pathogenesis with increased severity of infection. However, despite this recognized possibility, the interaction of *P. aeruginosa* with other bacteria during lung infection is poorly understood.

In this study, single A549 cells at the endpoint of bacterial infection were isolated into the individual wells of the chip by one step vacuum driven microfluidics. The number of adhered bacteria was quantified by optimized on-chip q-PCR assay without the necessities for DNA extraction. *P. aeruginosa* RNA was further isolated by novel high throughput liquid phase nucleic acid purification technique to analyze transcriptional regulation of the selected gene by on-chip q-RT-PCR assay. Biological knowledge is incorporated to the chip design to reduce engineering complexity, which in return simplifies the chip based assay in life sciences researches, showing the potential value of

this interdisciplinary study. The proposed microfluidic platform is easy to fabricate, cost effective, and presents a promising tool for biologist to study pathogen-host interaction at single cell level. The flow chart of methods adopted in this thesis is shown in Fig. 1-1.

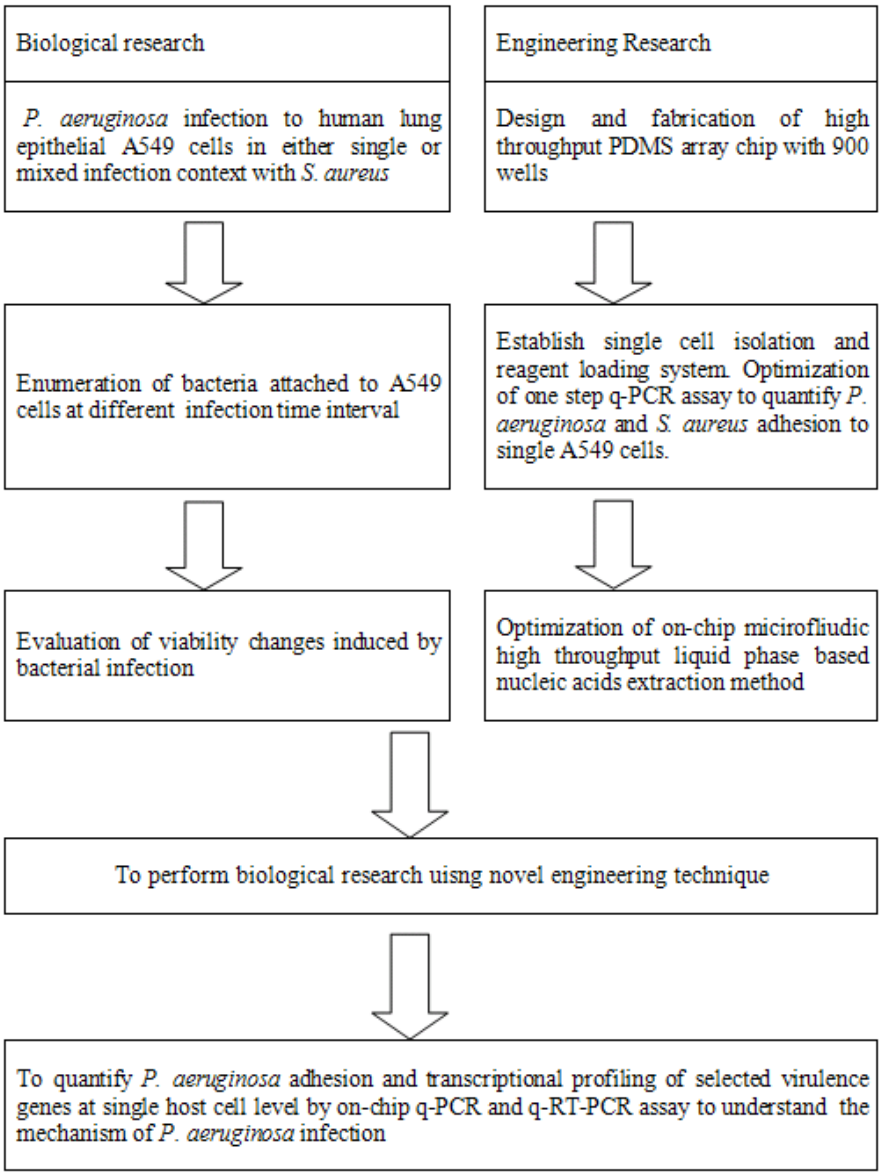

Fig. 1-1 Flow chart of methods adopted in this thesis.

1.3 Thesis organization

Chapter 2: Literature review

This chapter reviewed the current state of art microfluidic technologies in single cell isolation, nucleic acid extraction, and high throughput PCR assay. *P. aeruginosa* and *S.aureus* associated respiratory infections were also reviewed in this chapter.

Chapter 3: High throughput microfluidic PDMS array chip to quantify bacteria adhesion to single host cells

This chapter discussed the design and fabrication of a simple and cost effective high throughput microfluidic platform to analyze bacteria-host interaction at single cell level based on q-PCR assay. The proposed chip consisted of a two-dimensional array of 900 micro-wells, one inlet and one outlet micro-channel. The association of a common human pathogen, *Pseudomonas aeruginosa*, in both single infection and mixed infection contexts with *S. aureus* to the host human lung epithelial A549 cells was selected as the in vitro model to evaluate the performance of the chip.

Chapter 4: High throughput microfluidic liquid phase nucleic acid purification chip to quantify transcriptional gene regulation of bacteria attached to single host cells

This chapter discussed the design and fabrication of a novel microfluidic liquid phase nucleic acid purification chip to isolate nucleic acids from small numbers of bacterial cells followed by on-chip quantitative polymerase chain reaction (q-PCR) or quantitative reverse transcription polymerase chain reaction (q-RT-PCR) analysis based on novel phase partitioning techniques. Enhanced nucleic acids recovery was observed

using the chip based liquid phase nucleic acid purification technique as compared with traditional column based solid phase nucleic acid extraction methods. The liquid phase nucleic acid purification device was further modified into a two dimensional format of 900 micro-wells to study the transcriptional regulations of the selected gene of *P. aeruginosa* attached to single A549 cells at different infection time intervals.

Chapter 6: Conclusion and future work.

Results and conclusions of this research were summarized in this chapter. Future study was proposed.

Chapter 2 Literature Review

2.1 Overview of single cell analysis

The existence of independence in individual cell behavior within a cell population has been recognized for a long time. However, only until recently has this phenomenon, named cellular heterogeneity been appreciated and considered important in understanding key fundamentals in both systematic and developmental biology [6, 7]. Conventional technologies of fluorescence microscopy and flow cytometry are two commonly employed bench top platforms to observe and analyze single cell behavior with the advantages of high information content acquisition and high throughput sample screening respectively [8]. However, their usage for single cell analysis is restricted to species that can be either genetically modified to express fluorescent proteins or probed with target-specific fluorophores.

The rapid development of microfluidic technologies has led to the invention of many miniaturized chips with the ability to integrate multiple procedures of cell separation, lysis, and genetic analysis in the liquid volume of nanoliter to microliter scale. With these unique features, microfluidic platform has become a promising tool for automated single cell analysis with minimum risk of errors from human operations. Besides, the cost in sample and reagent can be significantly reduced in miniaturized micro-devices.

2.2 Isolation of single cell in microfluidic platforms

Isolation of single cells is the first step for heterogeneous behaviour analysis. Normally, a single mammalian cell weighs a few nanogram, with the volume around 1 picoliter and the diameter around 10 micrometer. Bacterial cells are even smaller with the size around 0.2-2 micrometer. With the capability to handle extremely small volume of liquid, single cell can be separated in microfludic chips of trap, pattern, droplet, or well based structure [9].

2.2.1 Micro-well based microfluidic platform for single cell isolation

A commonly adopted way to isolate single cell is to mechanically confine each individual cell into one micro-well with physical boundaries from other cells. With miniaturized sizes and volumes of the micro-wells, the target molecules of interest can be effectively concentrated for downstream testing with improved sensitivity and accuracy as compared with conventional plastic multiwell plates. Additionally, the sample processing time is significantly shortened because of the decreased liquid distribution distance. With the advanced micro-fabrication techniques, micro-wells of different shapes and sizes can be patterned in different materials, depending on the proposed applications. Micro-channels and micro-valves are often integrated to control and direct the flow of the cells and reagent.

The early design of single cell analytical chip consists of a cell-sized micro-well array for high throughput single cell isolation and imaging [10]. The two dimensional high density poly(dimethylsiloxane) (PDMS) well matrix is placed in petri dish, after

which cells in cultured medium are dispensed directly onto the micro-wells. Single cells are settled and isolated in the individual wells of the array chip by gravity. To avoid air bubble being trapped in the hydrophobic PDMS wells, cell feeding is carried out in a special custom-made CO_2 chamber as CO_2 molecules can be easily dissolved into the fluid. With optimized well diameter of 20 μm and depth of 27 μm, single cells can be isolated with more than 80% occupancy of the micro-well array. This PDMS chip is simply structured and easy to fabricate. However, downstream assays that require multiple steps of reagent loading such as fluorescence in situ hybridization (FISH), nucleic acid extraction, and polymerase chain reaction (PCR) assay cannot integrated. Besides, meticulous operations have to be implemented to avoid cells being dislodged from the chip.

In order to incorporate on-chip multi-step single cell assay, micro-valves and micro-pumps of various types have been designed and integrated into microfluidic analytical chips to control the sequential flow of different reagent. The elastomeric PDMS micro-valves and micro-pumps fabricated by the multilayer soft lithography technique provide a straightforward method to confine single cells and direct the inflow and outflow of various reagent for complicated single cell analysis [11-13]. Fig. 2-1 illustrates the structure and operation of a typical PDMS micro-valve. The key components of the device consist of a top channel layer, a bottom valve layer and a middle thin elastomeric membrane. To separate different reagents, the microfluidic channel is patterned in a double-T format. The opening and closing of the channel layer is controlled by the external pressure applied on the valve layer to deform the membrane layer in between. Single cells can be isolated in tens of picoliter volume, chemically lysed and derivatized

for further analysis [13]. Other types of micro-valves including magnetic micro-valves [14], thermopneumatic micro-valves [15, 16], electrostatic micro-valves [17, 18] have also been developed by different research groups. Compared with these micro-valves, PDMS micro-valves outperform in easy fabrication process and relatively small retaining volumes because of the thermal polymerization and highly hydrophobic property of this material respectively.

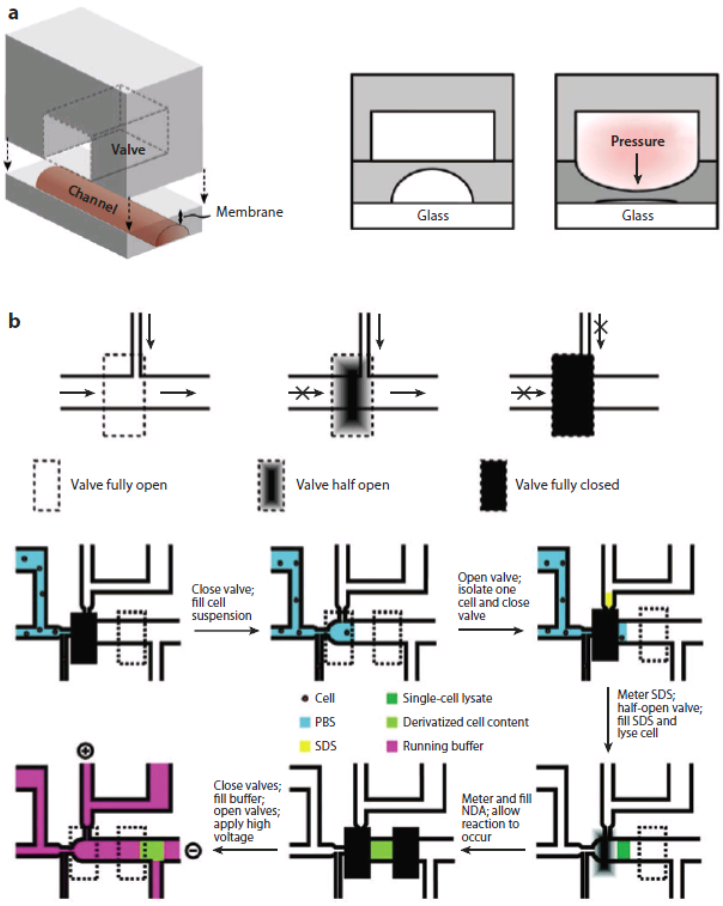

Fig. 2-1 Overview of the structure and operation of a typical single cell analytical chip.(a) Three-dimensional diagram of the channel, membrane, and valve layer and pneumatic actuation of a PDMS micro-valve. (b) Schematic illustration of a three-state valve and its application for single-cell isolation, lysis and derivatization. Abbreviations: NDA, naphthalene-2,3-dicarboxaldehyde; PBS, phosphate-buffered saline; SDS, sodium dodecyl sulfate. Picture was adapted from [8].

Although integration of micro-valves in single cell analytical chip opens the possibility of complex single cell assay, efficient reagent mixing in micro-channels is still problematic because of the property of laminar flow at low-Reynolds-number. To solve this problem, micro-pumps in connection with micro-valves are introduced in the design of microfluidic single cell analytical devices. The concept of rotary micro-pump for reagent mixing is first described by Chou et al. [19] in the year of 2001. This device is formatted in two layers, a top layer of pneumatic actuation channels and a bottom layer of finger shaped fluidic channels and an additional central circulation loop. Fluid in the circulation loop can be pumped in selected direction with a serial of on and off actuation sequences. Enhanced mixing is evidenced by rapid diffusion of fluorescent microbeads from one flow stream to the other. Tseng et al. present another innovative microfluidic rotary device with four micro-pumps combined with two micro-valves to transport and mix two different kinds of reagents at micro-liter scales [20]. The micro-pump is designed in annular layout with four compatible sized membranes. Maximum mixing index of 96.3% can be achieved after three cycles of mixing under the external air pressure over 10 psi.

Integration of microfluidic components including micro-wells, micro-channels, micro-valves and micro-pumps leads to the development of numerous micro-devices to perform single cell analysis [13, 21-23]. However, these analytic chips are typically of complicated structure with an array of micro-valves and micro-pumps to control the flow of different reagents into and out of each micro-well containing isolated single cell [21, 22, 24]. Cells may also be individually isolated with minimum number of micro-valves and lysed one by one within the same micro-channel, but are at high risks of sample cross contamination between each assay [13, 25]. Therefore, innovative microfluidic platforms

of simple structure and standard operation process are still needed for single cell study in biological laboratories.

2.2.2 Patterning and trapping based microfluidic platform for single cell isolation

Patterning and tapping based single cell isolation microfluidic platforms are usually used for long term single cell culturing and analysis. Patterning refers to the chemical modification of the surface of a substrate to create cytophilic (cell friendly) and cytophobic (cell repelling) regions so that single cells can be positioned for growth and analysis [26, 27]. Similarly, single cells can also be separated in micro-traps of various shapes in microfluidic chips. Single cell trapping is usually considered as a low throughput technique with some exceptions as shown by Carlo et al. [28]. As illustrated in Fig. 2-2, the proposed microfluidic device is designed with high density arrays of "U" shaped mechanical traps with specific geometry to isolate single cells. After constant perfusion of culture media for 24 hours, more than 85% of cells are maintained in the original trapping locations while around 95% cells remain viable. Further development of the "U" shaped trappings with a larger front-side and a smaller back-side capture cups leads to high throughput pairing of two cells [29]. Single cells are first isolated in the smaller back-side cup until the array is saturated and then transferred into the opposing larger front-side cup. Following this, the second cell population is loaded to pair with the previously trapped cells. Although patterning and trapping based microfluidic platforms enable fast and effective single cell isolation, analysis of the intra-cellular components using these devices is rather difficult as cell lysate cannot be confined.

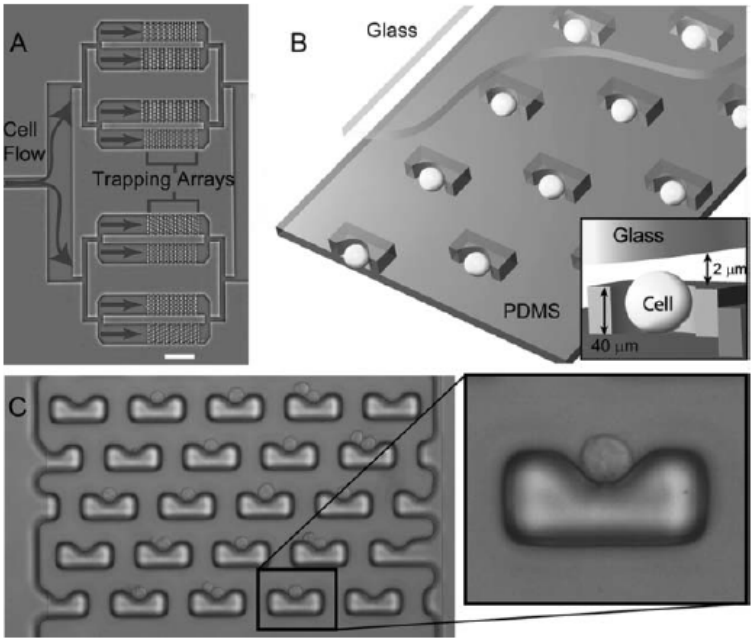

Fig. 2-2 Microfluidic single cell trapping device. (A) Structure of the cell trapping device. (B) Diagram of the device and working mechanism for single cell trapping. (C) Observation of trapped single cells under microscope. Picture adapted from [28].

2.2.3 Droplet based microfluidic platforms for single cell isolation

In addition of confining individual cells in isolated compartment, single cells can also be encapsulated in separated droplets of low volumes with minimized risk of cross contamination. Droplet based single cell analysis can be adapted to a wide range of applications based on fluorescence detection. Generally, droplets of water are formed in carrier oil by high frequency droplet generator in microfluidic devices with the possibilities to be merged, spitted, or sorted for complex single cell analysis [30-32]. However, the variation in the number of encapsulated cells per drop is problematic in single cell analysis due to stochastic cell loading. This limitation can be overcome by evenly spacing cells within a microchannel as proposed by Edd et al. [33]. Concentrated

cells are emulsified and arranged into an array in alternating pattern from one side of the micro-channel to the other by flow focusing geometry with nearly 100% single cell isolation (Fig. 2-3).

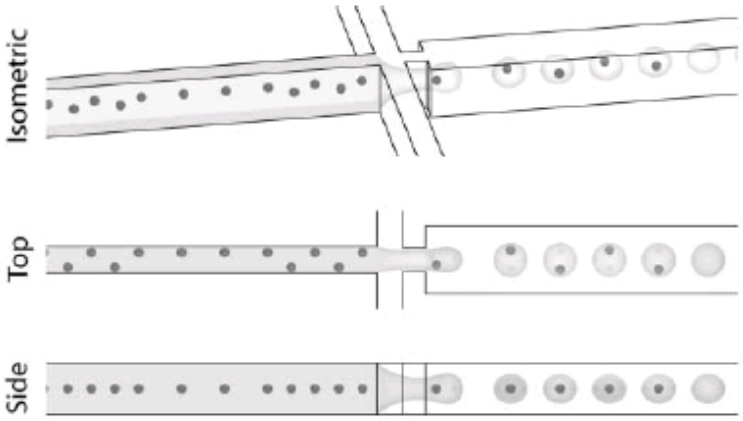

Fig. 2-3 Cell arrangement along one direction or into alternating pattern in micro-channel by flow focusing geometry. Picture adapted from [33].

One promising application of droplet-based microfluidic devices is for high throughput screening of bio-markers of single cells at low concentrations, as exampled by enzyme activity monitoring with laser induced cells lysis [34]. However, potential risks of nutrient reduction and the toxic metabolite accumulation still need to be taken into consideration before applying droplet based analytical devices for long term single cell assays.

2.3 Microfludic platforms for single cell nucleic acid analysis

2.3.1 Analysis of nucleic acids by quantitative PCR (q-PCR) technology

Identification and quantification of nucleic acids in single cells are important in many fields such as species recognition, disease diagnostics, pathogen detection, and

transcriptional regulation profiling. Of all the current nucleic acid analytical technologies, q-PCR outperforms in both detection sensitivity (less than 5 copies) and precision (less than 2% standard deviation) [35].

PCR is an enzyme catalyzed reaction, which amplifies a specific region of single or double strand DNA through temperature cycling. Assuming the PCR reaction is 100% efficient, the PCR product will increase with exponential order after each cycle. The PCR kinetics can be monitored by specifically labeling the PCR product with fluorescent dye, which is termed as quantitative PCR (q-PCR). q-PCR amplification curve is represented by the fluorescence intensity versus reaction cycle. Quantification of the initial DNA template can be achieved by comparing the number of PCR reaction cycles required to reach a certain threshold (Ct) fluorescence signal level. q-PCR standard curve is constructed by plotting the Ct values against known DNA copy number, which allows absolute quantification unknown DNA sample. In order to enumerate messenger RNA (mRNA) transcripts by q-PCR assay, mRNA need to be first converted to single strand cDNA, the process of which is referred to as reverse transcription. Reverse transcription can be performed using either gene specific primers or random primers of short oligoes. Random primers are advantageous in reverse transcription reaction as the whole transcriptome can be copied into cDNA for downstream analysis. This technique is entitled as quantitative reverse transcription PCR (q-RT-PCR). To compare gene transcription under different conditions by q-RT-PCR assay, normalization is required to compensate the difference in the amount of starting biological materials. The most commonly adopted standards for mRNA transcripts normalization include total RNA,

ribosomal RNA (rRNA), externally added RNA standard, and internal reference genes. The q-PCR amplification curve is illustrated in Fig. 2-4.

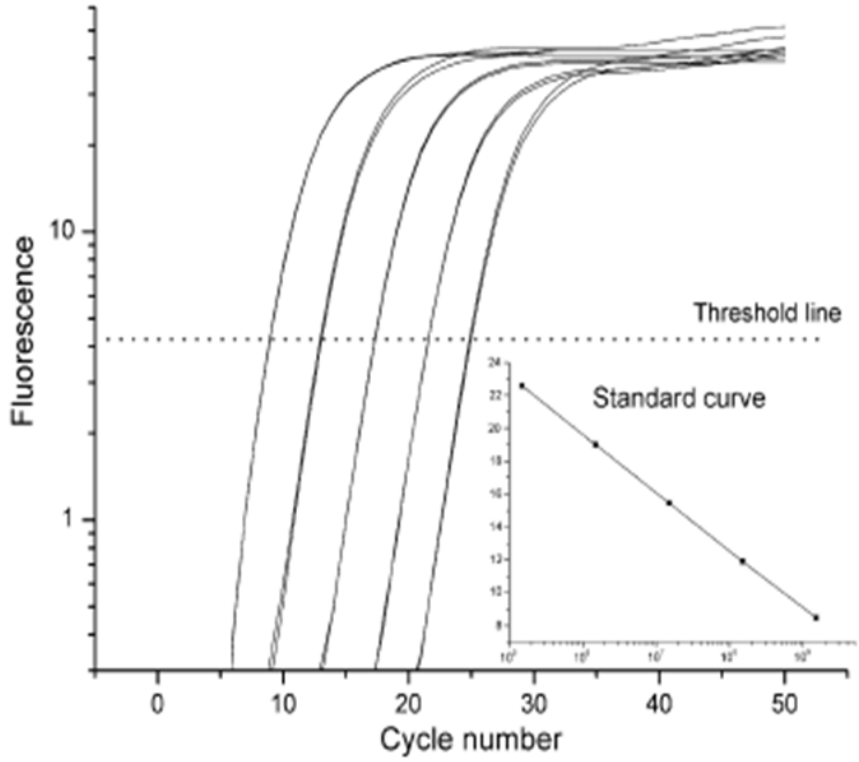

Fig. 2-4 q-PCR amplification curve crossed by threshold line of five standard samples are shown in logarithmic scale. The standard curve is constructed by plotting Ct values against DNA copy number. Picture adapted from [36].

Two most popular fluorescent dyes in q-PCR assay are Syber Green DNA intercalator and TaqMan probe. Sybr Green can non-specifically bind to the newly synthesized double-stranded DNA and emits fluorescence so that the PCR amplification can be monitored in real time fashion. One major problem associated with Sybr Green q-PCR technique is the PCR by-product primer dimer formation. Primer dimer is generated by attachment of one primer to each other in the presence of complementary bases. Primer dimer can be amplified by DNA polymerase and labeled by Syber Green as a false

positive signal in q-PCR reaction. Consequently, PCR product needs to be confirmed by either DNA gel electrophoresis or melting curve analysis. Taqman probe is a short single strand DNA oligo with a reporter fluorescent dye attached to the 5' end and a quencher dye attached to the 3'end. Taqman probe can be hydrolyzed by DNA polymerase due to the 5' to 3' exonuclease activity of this enzyme so that the reporter fluorophore is released from the proximate quencher. Hence, the fluorescence signal detected is directly proportional to the amount of target DNA template in the PCR reaction mixture (Fig. 2-5). One major advantage to use Taqman probed based q-PCR assay is that primer dimmer formation will not be reflected in the amplification curve. TaqMan and Sybr Green based q-PCR methods are usually considered as equally sensitive and accurate, but the latter is more cost effective [37].

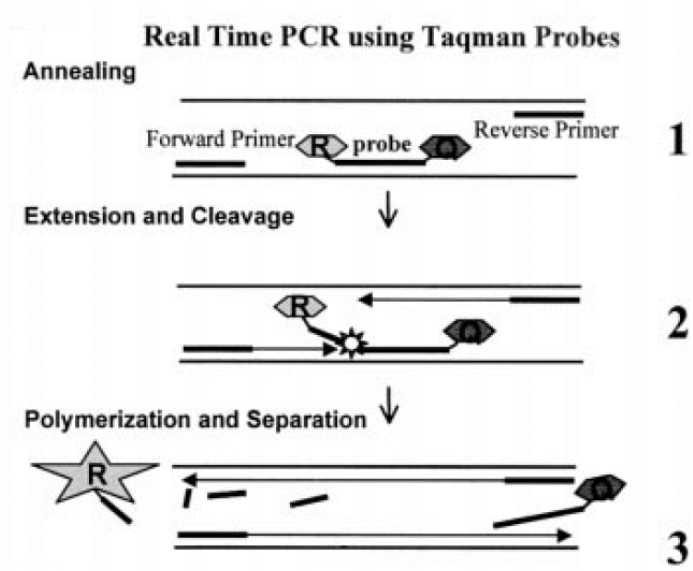

Fig. 2-5 Taqman probes based q-PCR assay (1) Probes and primers hybridize to target sequence. Taqman probes are attached with a fluorescence reporter (R) and a quencher (Q). (2) During each extension cycle, the exonuclease activity of Taq DNA polymerase degrade the reporter dye from the probe. (3) The reporter dye emits the fluorescence signial once separated from the quencher, which is detected in every cycle of PCR reaction. Picture adapted from [38].

2.3.2 High throughput microfluidic platform for q-PCR analysis

q-PCR technology has traditionally been considered as a low throughput technology until the recent development of large scale microfluidic PCR platform. The early PCR chip design mainly focuses on the PCR reactor miniaturization and sample volume reduction [39]. Although cost effective assay with accelerated thermal cycling can be achieved using these systems, they are not suitable for high throughput PCR analysis.

In order to address this problem, multi-reactor microfluidic device are developed by different research groups [40, 41]. Although parallel q-PCR assay can be achieved in these platforms, either tedious manual loading or expensive dispensing instrument is required to transfer samples and reagent into the reactors.

A breakthrough of high throughput PCR array chip is accomplished by Nagai et al., who successfully fabricate an integrated picoliter chamber PCR array chip with silicon substrate. q-PCR is performed in micro-chambers ranging from 1.3 pl to 32 μl. [42]. Although promising high throughput application is achieved, manual reagent loading is still required, leaving the problem of tedious sample delivery unaddressed.

Liu et al. demonstrate a microfluidic polydimethylsiloxane (PDMS) PCR matrix with the capability to automatically distribute 2 μL PCR mixture into 400 isolated wells using 2860 integrated valves (Fig.2-6) [43]. PDMS is a polymer substrate with increasing popularity in PCR chip fabrication due to its excellent thermal stability and bio-compatibility [44, 45]. PDMS presents in viscous liquid form at room temperature and can be irreversibly solidified when mixed with curing agent at higher temperature. Therefore,

chip fabrication using PDMS is much simpler as no micromachining or photolithography processing is required. Nonetheless, this PCR array chip is still costly due to its complicated structure.

2.3.3 Microfluidic platforms for nucleic acid purification

2.3.3.1 Nucleic acid purification overview

In most cases, nucleic acids need to be released out of the cells or to be separated from other cell components for q-PCR analysis. Typically, cell membranes are first disrupted by chemical combined with enzymatic lysis [46], thermal lysis [47],or mechanical lysis [48], the lysate of which are passed through selected solid phase medium [49, 50] or partitioned with organic phase [51, 52] for nucleic acid recovery.

Solid phase nucleic acid purification technique is developed based on the fact that nucleic acids can be selectively absorbed onto specific solid phase medium in high ionic strength buffer solutions and later be eluted out in low ionic strength buffer after washing away the unwanted impurities. Many nucleic acid purification kits are now commercially available (e.g. Qiagen, Biorad, Epicentre). The most commonly used solid phase mediums include silica gel, membranes, or glass matrix. Although DNA and RNA can be successfully isolated using the solid phase based purification methods from a variety of sources, however, compromised nucleic acid recovery is reported due to insufficient binding of nucleic acids to silica gel, loss during washing, or failure to be eluted because of irreversible bonds [53].

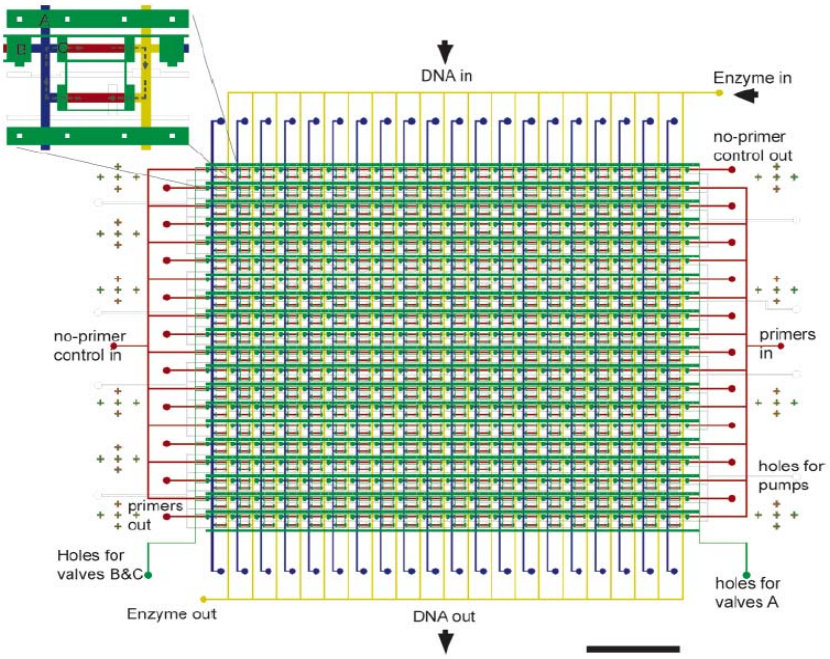

Fig.2-6 PDMS based high throughput PCR matrix. Schematic diagram of the N 20 matrix chip layout, showing the various input, output, and control ports. Inset: a single reactor color coded to indicate control lines (green), template sample (blue), DNA polymerase (yellow), primers (red), and rotary pump (white). Picture adapted from [43].

Liquid phase extraction offers a simpler and more effective way to separate nucleic acids from other cellular impurities. Conventionally, cell lysate in the aqueous phase is vigorously mixed with equal volume of an immiscible phenol:chloroform:isoamyl alcohol (PCI) mixture which is referred to as the organic phase. To reduce interaction surface energy, denatured proteins and other membrane components are spontaneously transferred from the aqueous phase to the organic phase, while charged nucleic acids are retained in the aqueous phase. This process is given the termed “phase partitioning”. DNA and RNA can also be separated in a pH dependent manner. Although still controversial, it is reported that liquid phase nucleic acid

purification technique outperforms in both efficiency [54, 55] and purity [56] as compared with solid phase nucleic acid extraction methods.

2.3.3.2 Solid phase microfluidic platforms for nucleic acid isolation

Microfluidic platforms enable rapid and automated nucleic acid isolation from sample in minute liquid volumes, which is extremely important in single cell nucleic acid analysis. Micro-systems with integrated functions including cell lysis, nucleic acid purification and q-PCR have been developed by many research groups. Until now, researches in microfluidic nucleic acid purification platforms have mainly focused on miniaturizing solid phase extraction rather than liquid phase extraction method.

One well documented solid phase medium in chip based nucleic acid isolation module involves micro-pillars or micro-columns coated with silica gel [57]. Cady et al. design an array of square pillars covered with a silicon dioxide layer in a microfluidic channel for nucleic acid purification (Fig. 2-7). Maximum 6-fold increase in the surface area with the etch depth of 50 μm could be achieved compared with the micro-channel alone. However, only 10% of the absorbed DNA could be recovered in the first 50 μl of elution buffer so that the possibility of integration with downstream microfluidic q-PCR platforms is limited. Insufficient DNA recovery of less than 20% using the solid phase medium of pillar like structure is also reported by Hindson et al. [58].

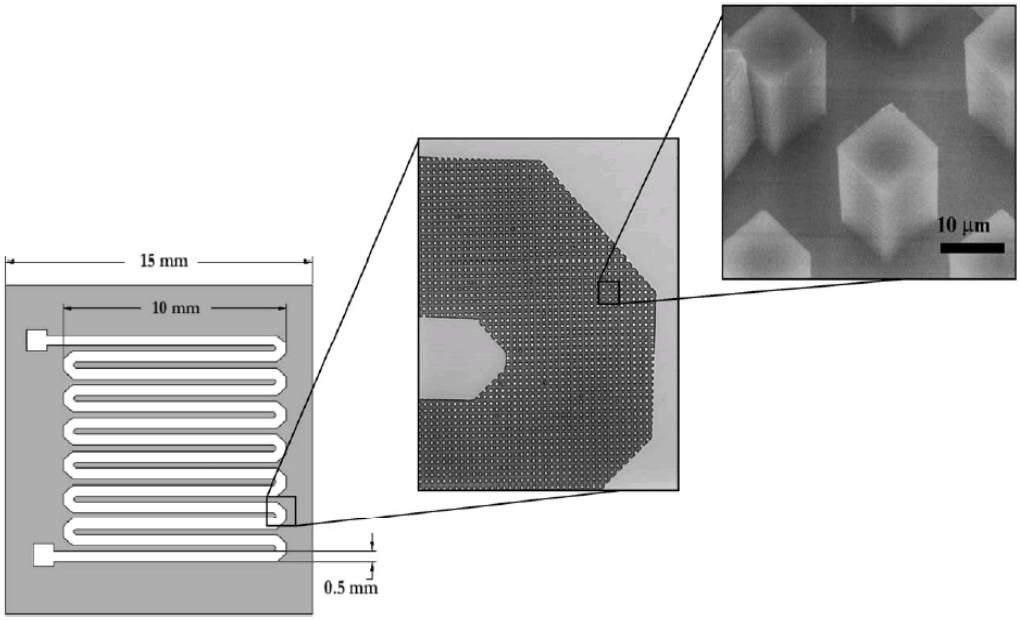

Fig. 2-7 Schematic view of micro-channels containing micro-fabricated pillars coated with silica gel. Scanning Electron Microscopy (SEM) imaging of micro-fabricated silica pillars is shown. The spacing between micro-pillars is kept at 10 μm. The etch depth of the channels is adjustable between 20 and 50 μm. Picture adapted from [57].

Another popular solid phase medium for nucleic acid purification in microfluidic devices is silica beads immobilized in sol-gel packed in micro-channels [59, 60]. Sol-gel helps to trap the silica beads in the channel, to prevent liquid obstruction as well as to increase absorption area (Fig. 2-8). Around 50% of human genomic DNA and 70% λ DNA can be recovered in 10 μl elution buffer at the optimal pH and flow rate. DNA from highly concentrated bacterial samples can also be isolated with successful off chip PCR amplification but the extraction efficiency is not reported. Besides, manual loading of the sample, washing buffer, and elution buffer is required for the proposed microfluidic DNA isolation device.

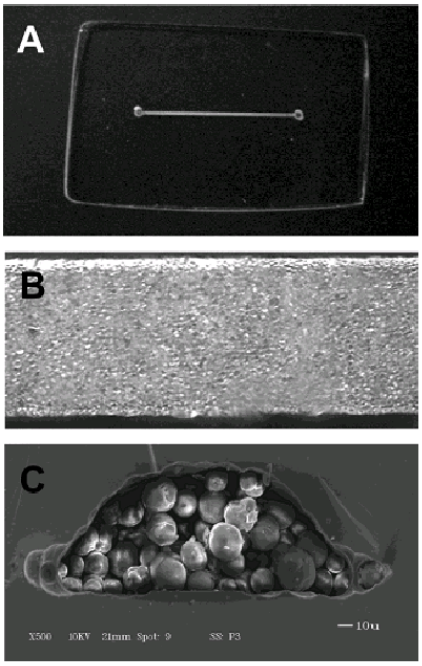

Fig. 2-8 Micro-channel packed with silica particles immobilized in sol-gel. (A) Image of micro-channel under 1× magnification (B) Image of micro-channel under10 × magnification; (C) SEM image of packed channel (cross session) under 500× magnification. Picture adapted from [60].

Although micro-devices with packed sol-gel matrix exhibit effectiveness in nucleic acid isolation, poor nucleic acid purity is reported due to the decreased surface area as a result of the bonding and shrinkage between the micro-channel wall and the matrix. To solve this problem, a glass microchip packed with tetramethyl orthosilicate-based sol-gel matrix for DNA extraction is developed by Wu et al [61]. Pores at micrometer-scale are formed by adding poly-ethylene glycol (PEG) to the precursor mixture to increase the total DNA binding surface area with reduced flow-induced back pressure (Fig. 2-9). Enhanced DNA extraction efficiencies of 70% for human genomic DNA and 85% for λ DNA from human blood are demonstrated. However, unsatisfactory

bacterial DNA recovery of less than 30% is reported due to the insufficient conditioning of the solid phase matrix.

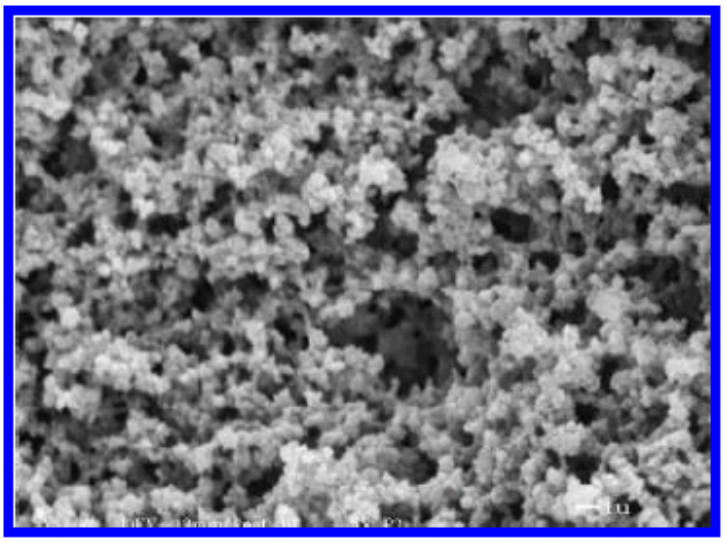

Fig. 2-9 SEM picture of tetramethyl orthosilicate-based sol-gel matrix as the solid phase for DNA extraction. Picture adapted from [61].

Photopolymerized silica-based monolithic column as the solid phase for DNA extraction is proposed by Wen et al. [62]. Micro-column is fabricated with the sol-gel solution of trimethoxysilylpropyl methacrylate (TMSPM) monomer and photo-initiator. This monomer can form a polyacrylate matrix around the silica backbone up on UV induced photopolymerization. The monolith surface of the micro-column is derivatized by tetramethyl orthosilicate (TMOS) at the optimal concentration of 85% v/v to increase the DNA binding capacity. The maximum DNA extraction efficiency is about 85.6% when using purified human genomic DNA, but decreases to 59.9% when mixing the DNA sample with human blood due to insufficient protein removal. Purified DNA can be recovered in 1 μl elution buffer, which is preferable for downstream PCR assay in

microfluidic platforms. In order to improve the protein removal efficiency, a two-stage microfluidic device is designed by integrating the TMSPM/TMOS DNA extraction column with a C18 reversed-phase micro-column with high affinity for hydrophobic proteins (Fig. 2-10) [63]. 70% protein is retained in the first stage C18 column with 99% DNA passing through in a 10 μL load of whole blood, resulting in an overall of 69% DNA recovery from the second stage TMSPM/TMOS column in 20 μl elution buffer. However, the elution volume is still too large to be coupled with microfludic PCR analytical chips. Besides, incorporation of C18 column significantly increases the cost of this DNA extraction device.

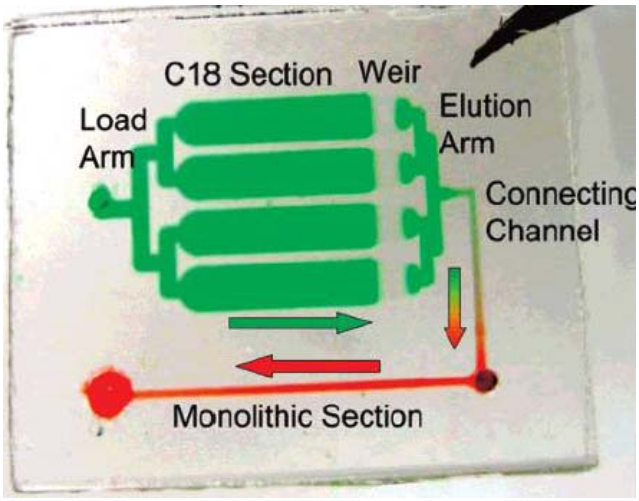

Fig. 2-10 Two-stage microfluidic DNA extraction device. The channels are filled with dyes to visualize the protein and nucleic acid capture phase regions. Arrow indicated flow direction from stage 1 to stage 2. Picture adapted from [63].

Although silica gel packed in micro-channels provides suitable solid phase medium for nucleic acid extraction, samples and reagents need to be either loaded by manual pipetting or by applied external air pressure at high risks of air bubbles being trapped, both of which may lead to reduced nucleic acid extraction efficiency. The

situation is circumvented by introduction of functionalized magnetic beads coated with silica gel or short oligo probes that can specifically bind to the target nucleic acids [64-67]. One major advantage to use functionalized magnetic beads as the solid phase medium for nucleic acid extraction is that they can be freely suspended in solution and then collected in specific location. The movement of the magnetic beads is controlled by magnetic field so that air bubbles trapped can be easily removed from the solid phase medium. Jong et al. [66] propose a complicatedly structured chip processor with 54 integrated micro-mechanical valves to allow sequential flow of lysis buffer, wash buffer and elution buffer into and out of reaction chambers for nucleic acid purification. Micro-mechanical valves are controlled by external pneumatic activation. The parallel architecture of this microfluidic device enables eight samples to be processed at the same time (Fig. 2-11). Cells and lysis buffer are introduced first into the device and mixed through a rotary micro-pump. The mixture is then flushed in to the resuspend the magnetic beads that are preloaded in the device. Washing buffer is subsequently pumped in to remove the impurities. Finally, nucleic acids are eluted out for off-chip PCR assay. This microfluidic nucleic acid purification chip is designed in fully automatic fashion. mRNA from as little as a single mammalian cell and DNA from 28 bacterial cells can be isolated with successful PCR amplification. Nonetheless, important issues such as initial sample volume, reproducibility, nucleic acid extraction efficiency and sample carryover are not reported in this article.

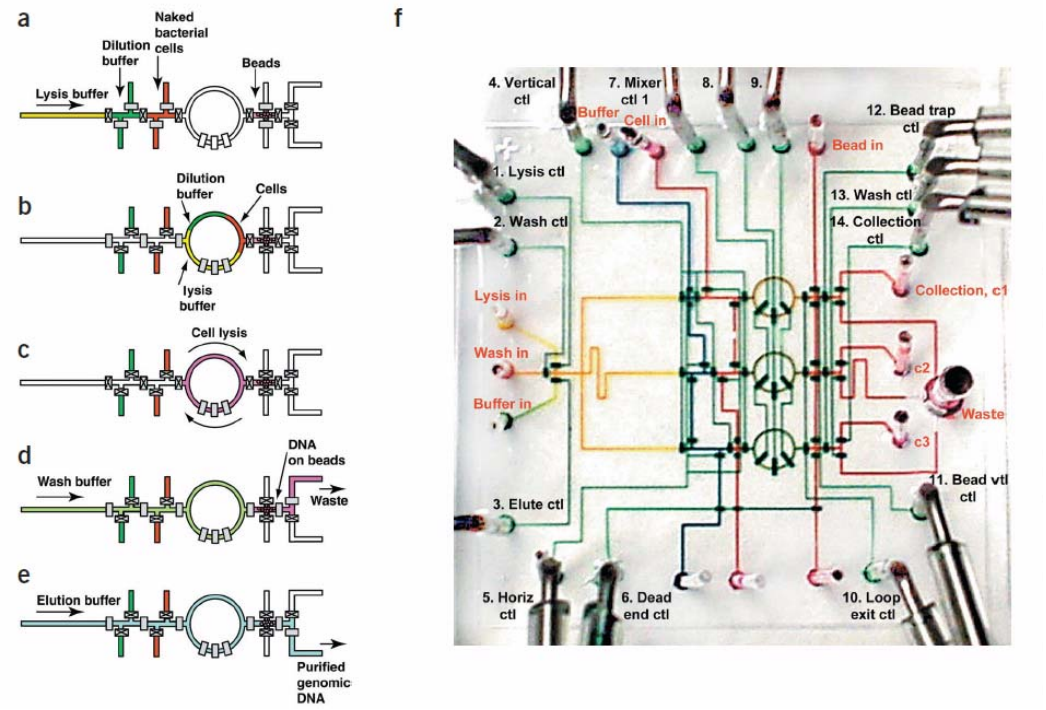

Fig. 2-11 Schematic illustration of the DNA purification process (a-e) and image of the microfluidic DNA extraction chip with parallel architecture (f). Picture adapted from [66].

In summary, the development of solid phase microfluidic nucleic acid extraction platforms realizes nucleic acid sample processing at microliter scales. However, the extraction efficiency is still unsatisfactory for single cell analysis. Furthermore, as micro-valve controlled microfluidics of all steps including cell loading, washing, and nucleic acids elution is required, high throughput nucleic acid extraction from different samples cannot be easily achieved in these micro-systems.

2.3.3.3 Liquid phase based microfluidic platforms for nucleic acid isolation

Nucleic acid purification by phase partitioning techniques have been long established and widely used [51]. But liquid phase microfluidic nucleic acid purification platforms have only been proposed recently as chaotic mixing and separation of two

immiscible phases in microfludic devices cannot be easily achieved. The first step towards a miniaturized chip for liquid phase nucleic acid extraction is taken by Reddy et al. [68] through analysis of the two phase fluidic behavior and interface stabilization in micro-channels. Stable stratified micro-flows can be created by adding surfactant to the aqueous phase with reduce interfacial tension (Fig. 2-12). In addition, experimental and computational examination of DNA and protein partitioning between the organic and aqueous phase through droplet formation is presented by Mao et al. [69].

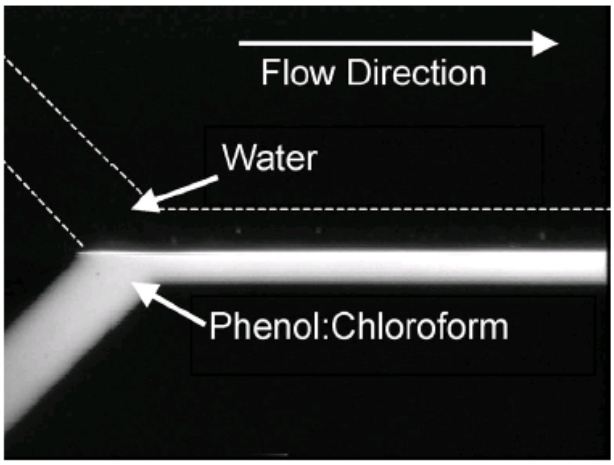

Fig. 2-12 Stable stratified flow of water (aqueous phase) and phenol:chloroform (organic phase). The organic phase was fluorescent labeled and visualized under epifluorescent microscopy. Picture adapted from [68].

Morales et al. design two microfluidic platforms including both stratified and droplet-based flow conditions to achieve high throughput DNA purification using liquid phase extraction techniques (Fig. 2-13) [70]. Enhanced mass transfer is observed through convective recirculation flow within discrete droplets in a glass micro-channel. As high as 92% plasmid DNA from bacterial lysate can be recovered using the droplet-based

microfluidic platform. However, the organic phase that is incompatible with downstream PCR assay cannot be removed from the aqueous phase.

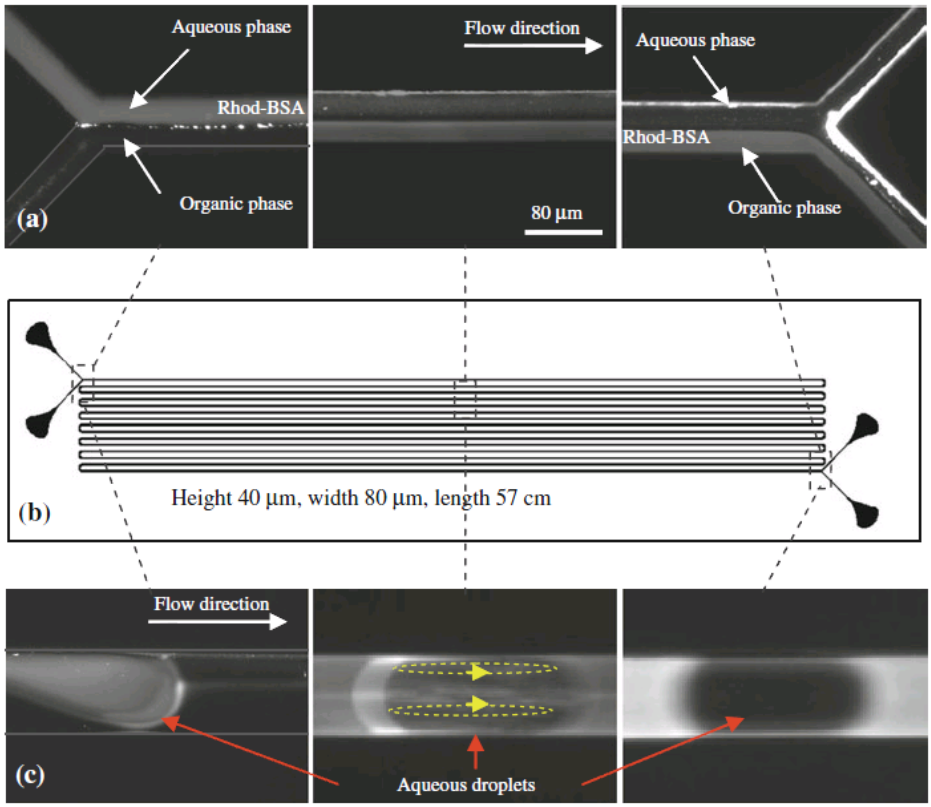

Fig. 2-13 Images of (a) stratified flow, (b) the device structure design, and (c) droplet based flow. Fluorescence labeled bovine serum albumin (BSA) was partitioned from the aqueous phase at the device inlet into the organic phase at the outlet. Picture adapted from [70].

Besides passive diffusion in stratified flow and internal recirculation in droplet based flow, mixing of two immiscible phases can also be accomplished by introducing electrohydrodynamic (EHD) instability at the interface (Fig. 2-14) [71]. The initial EHD instability is modeled for interfacial stresses from both fluid and electrical stress tensors. At the electric field of $8.0 \cdot 10^5$ V/m, phase instability is experimentally proved by

labeling the organic phase with a fluorescent dye to visualize interfacial turbulence under microscope. The level of chaotic mixing increases with the escalating electric field.

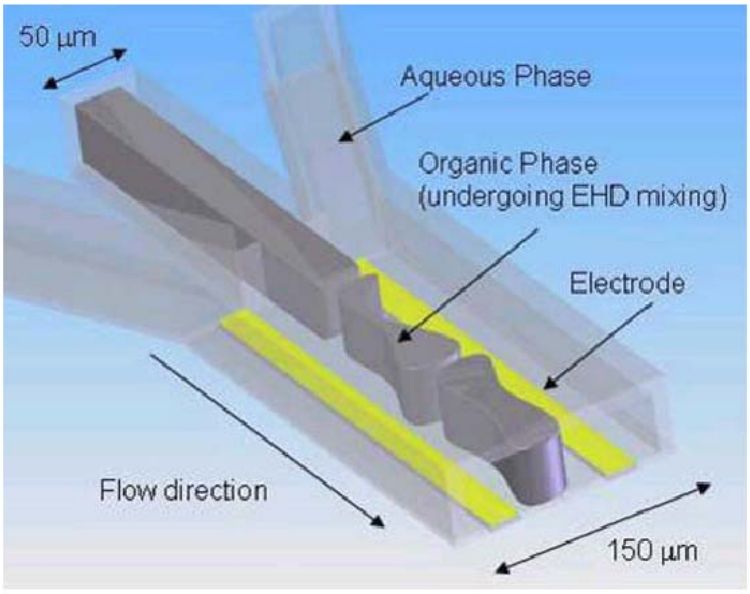

Fig. 2-14 Schematic of the three inlet micro-device with electrodes for instability phase mixing. Picture adapted from [71].

2.3.4 Microfluidic PCR platforms for single cell DNA analysis

2.3.4.1 Microfluidic PCR platforms for single mammalian cell DNA analysis

Analyzing single cell genomic DNA is not considered necessary in isogenic pure culture. However, in cases where genetic mutation within a cell population is expeted to occur, genome characterization for single cells is essential. For example, detection of DNA mutation in single cancer cells may help researchers to understand stochastic molecular mechanisms of the disease development. Kumaresan et al. present a high-throughput droplet based microfluidic platform to rapidly isolate single DNA molecule or cell [32]. Micro-pump is integrated in the device to generate droplet with uniform size,

and controllabe frequency. Microbeads attached with specific primers is incorporated into the droplets together with the PCR reagent mixture to amplifiy the target gene in single copy genome. The droplets are then lysed to recover the beads associated with fluorescence labeled amplicons for flow cytometry analysis (Fig. 2-15). The generated droplets are of excellent thermal emulsion stability without DNA exchange during thermal cycling. The false positive results generated from unspecific binding of fluorescence labeled probes are reported to be less than 3%. However, only 40% PCR efficiency is attained for beads based droplet PCR. Moreover, random trapping of two or more cells in one droplet is observed which may result in compromised accuracy for single cell DNA profiling. False negative results may also originate from unsuccessful incorporation of microbeads into droplets with single cell encapsulated.

To overcome these technical limitations, a novel microfluidic device with improved performance in single cell capture and PCR efficiency is proposed by Fan et al. to study the combination of alleles on each of the homologous copies of the chromosomes from a single human metaphase cell [72]. Single cell is identified microscopically and isolated in a micro-cell sorter with 100% separation efficiency. Chromosomes of single cells are then released by protease digestion in a separated micro-chamber, partitioned into 48 long micro-channels and amplified by PCR. Microfluidics in the device is controlled by a serial of membrane valves actuated by air pressure. Around 99.8% detection accuracy for up to 96% of all single nucleotide polymorphism assays is accomplished. Nonetheless, sample carryover is unavoidable as lysis and PCR amplification of all cells are performed in the same channel. Besides, this platform is only suitable for low throughput analysis.

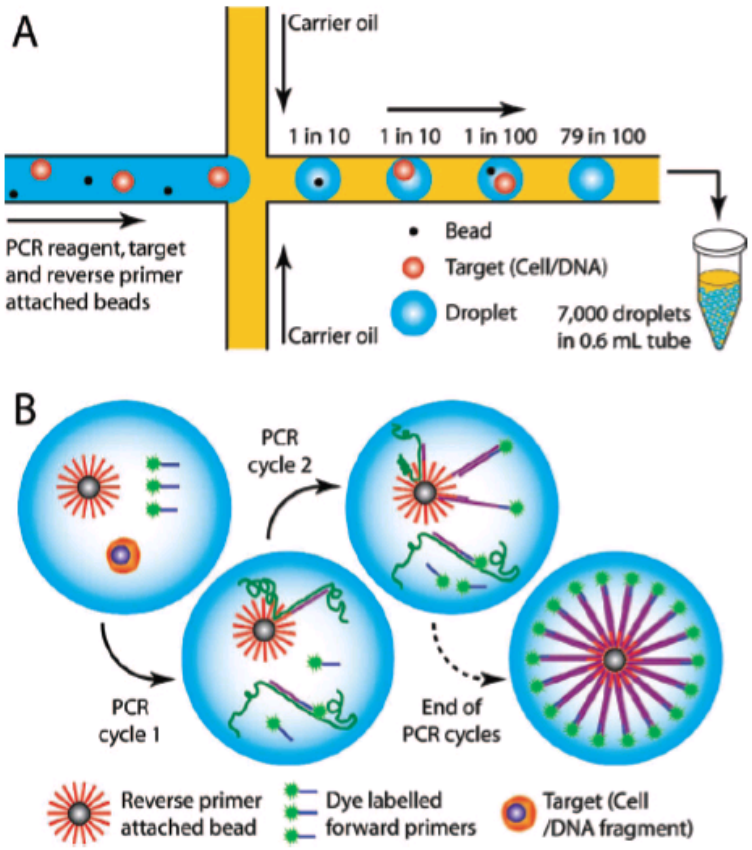

Fig. 2-15 Schematic of single cell isolation and microbeads incorporation into micro-droplet (A) and beads based PCR amplification of target gene (B). Picture adapted from [32].

2.3.4.2 Microfluidic PCR platforms for single bacterium DNA analysis

Another representative example in single cell DNA analysis is in the study of microbial communities. As only 1% of bacterial species existing in nature are culturable, identification of unculturable bacterial populations in majority mainly depends on DNA based sequencing analysis. Microfluidic PCR platforms facilitate researches in this area to unravel information encoded in genomic DNA by amplification of specific genes in individual bacterial cells. For this purpose, Ottesen et al. design a high throughput micro-chip that can amplify two different target genes within individual bacterial cells by

multiplex PCR (Fig. 2-16) [73]. Single bacterial cell is isolated probabilistically by adjusting cell density to less than 33% of the total 1176 reaction wells of a sample panel. This platform enables single bacterium identification by on-chip PCR amplification of the formyltetrahydrofolate synthetase (FTHFS) gene and the phylogeneticmarker 16S rRNA gene, but only applicable to the bacterial cells that can be thermally lysed. Otherwise, DNA purification chip should be integrated for single bacterium PCR amplification. In another single bacterium genotyping application, one pathogenic *E. coli* can be detected out of 10^5 of non-pathogenic bacteria in a droplet based microfluidic system for digital PCR assay [74].

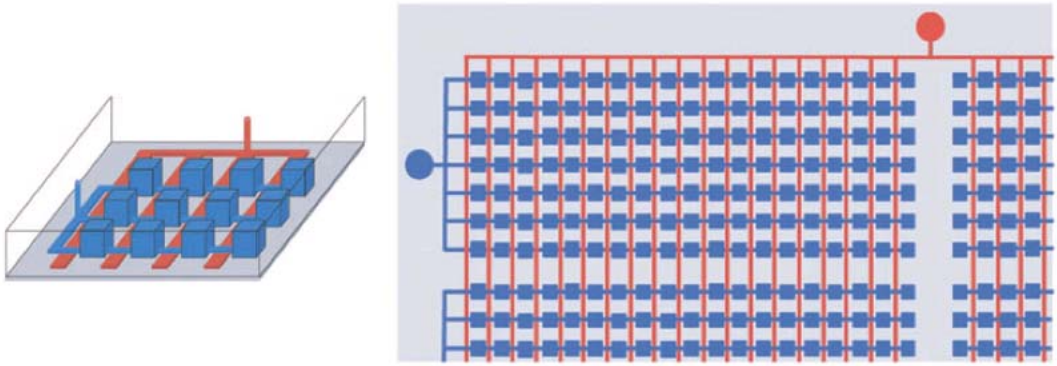

Fig. 2-16 Schematic diagram of a microfluidic chip for single bacterium identification by multiplex PCR. Picture adapted from [73].

Microfluidic PCR platforms also enable whole genome sequencing by multiple-displacement amplification (MDA) as presented by Marcy et al. [75]. Eight fluorescence labelled single bacteria can be separated into 3 nl chambers in parallel. Microscopic images are taken to ensure that single bacterium is captured. The MDA amplification chip consists of four micro-chambers, including a template chamber, a cell lysis chamber, a neutralization chamber and a PCR reaction chamber, each of which is designed for a

single step of MDA protocol. The flow of different reagents into and out of micro-chambers is directed by 24 control lines with 225 integrated micro-valves. Amplification bias is reported to be significantly reduced in nanoliter volumes. But the application of this microfluidic chip is only limited to bacterial strains that can be genetic modified to express fluorescent proteins.

2.3.5 Microfluidic PCR platforms for single cell RNA analysis

2.3.5.1 Microfluidic PCR platforms for single mammalian cell RNA analysis

Quantitative reverse transcription PCR (q-RT-PCR) now serves as the golden standard to measure RNA transcripts with excellent specificity and sensitivity, and is the first choice for gene transcription profiling in single cell studies [76]. Quantification of single cell RNA transcripts in microfluidic platforms is usually achieved by miniaturizing the standard q-RT-PCR protocol. RNA transcripts are first reverse transcribed into complementary DNA (cDNA), the products of which are then analyzed by q-PCR amplification. Minute RNA targets from single cells can be effectively concentrated in micro PCR reaction chambers of picoliters to nanoliters in volume with enhanced q-RT-PCR detection sensitivity [77]. Nevertheless, application of the microfluidic platforms for single cell RNA analysis is challenged by both throughput and cost. A commercial microfluidic PCR system, Dynamic Array^{TM} (Fluidigm), is now available to provide sensitive q-RT-PCR detection at low-volume and high throughput. Studies of differentiated gene transcription and micro-RNA regulation of single cancer cells using this microfluidic platform have lead to a number of significant scientific discoveries in related disease development [78-80]. However, manual single cell isolation, RNA

extraction and reverse transcription are required so that only a limited number of single cells can be analyzed in each run. In order to address this problem, Zhang et al. present a microfluidic device to perform high throughput single cell RT-PCR using agarose droplet [81]. Uniform picoliter agarose emulsion droplets are produced from a two-aqueous-inlet droplet generator. Diluted target cells are introduced into the device through one inlet portal and mixed with PCR and cell lysis reagent injected from the other inlet portal within one droplet. Droplets are then collected in PCR tube for thermal cycling. Following this, agarose droplets are solidified, stained with Sybr Green, and analyzed by flow cytometry (Fig. 2-17). Millions of agarose droplets can be produced within less than one hour so that single cell RNA assay at large scales can be achieved. However, endpoint PCR method is adopted using this microfluidic platform with compromised accuracy for RNA transcript quantification. Besides, this chip must be coupled with flow cytometry instrument for detection. Other microfluidic single cell RNA analytical platforms with basic functions including single cell capturing [29], RNA purification and cDNA synthesis [82, 83] are also demonstrated but these chips are only applicable to off-chip PCR analysis.

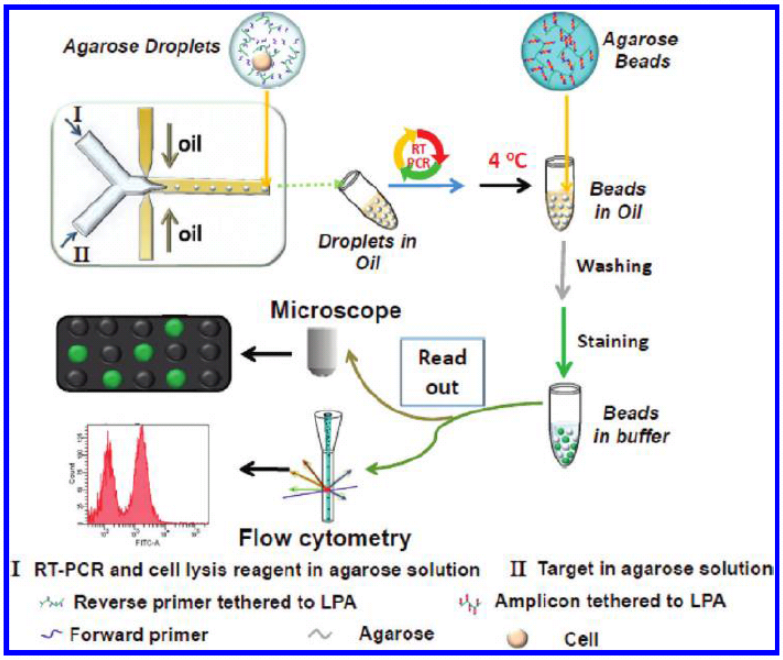

Fig. 2-17 Schematic overview of the working principle of a droplet based high throughput microfluidic chip for single cell RNA analysis. Single cells are isolated and mixed with PCR reagent in one droplet. Droplets are then collected in PCR tube for thermal cycling. Following this, agarose droplets are solidified, stained with SYBR Green, and analyzed by flow cytometry assay. Picture adapted from [81].

Although the above mentioned microfluidic systems facilitate mRNA profiling in single cells, human interference in either sample preparation or off-chip PCR processing is required. Consequently, automated single cell RNA analytical micro-platforms are still necessary to minimize sample loss during liquid transference. Towards this end, Toriello et al. develop an integrated micro-device equipped with all steps of single cell isolation, lysis, cDNA synthesis, and q-PCR analysis [84]. This single cell mRNA analytical micro-device consists of 4 independently controllable micro-systems, each of which contained 4 regions for sample transportation, single cell processing, PCR amplicons purification, and the size-based separation and quantification of PCR product (Fig. 2-18). Cells are first labeled with a 20-base oligonucleotide on the surface and then captured on a gold pad

immobilized with oligonucleotide of complimentary sequence based on DNA hybridization. mRNA was released by repeated free-thaw cycling. Silencing of GAPDH gene in individual Jurkat cell is measured using this micro-device, revealing the presence of cell populations of moderate or complete silencing. Although single cell can be analyzed in fully automated fashion, pre-labeling of target cell with potential risks of altered gene transcription profile is compulsory for this approach. Bontoux et al. describe a microfluidic platform in the same year to accomplish single cell RNA assay in label-free manner [25]. Cell capture, lysis and reverse transcription were integrated in a 10 nl PDMS rotary mixer followed by on-chip PCR amplification. Sample and reagents transportation is controlled by 11 micro-valves. However, only one gene of one single cell can be analyzed at each run, limiting the application of this device for single cell RNA assay at large scales.

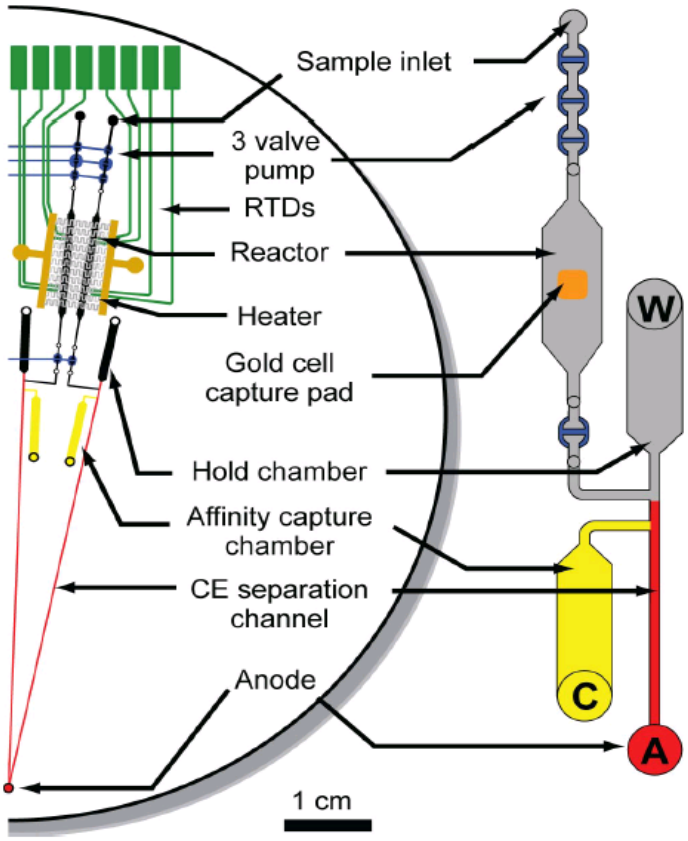

Fig. 2-18 Schematic overview showing overlay of half of the device. The micro-device contain 4 regions. The first region is a 3-valve pump for sample transportation. The reactor region consists of gold pad for single cell isolation in the center, a 200-nl PCR reaction chamber with resistance temperature detection (RTD) and a heater for thermal cycling. The amplicon purification region comprises a gold chamber and an affinity capture chamber (yellow). Finally, the PCR products were analyzed on the CE separation channel (red). Picture adapted from [84].

The first fully integrated microfluidic q-RT-PCR platform providing "front to end" solution for high throughput single cell RNA assay is only described in the year of 2011 by White et al. [4]. The prototype device comprises six independently controllable sample loading lanes, each with 50 cell processing unit so that 300 single cell can be analyzed per each run. Single cells are isolated by cell traps of cup structure. Upstream deflectors are incorporated to push cells into the central streamlines for effective capturing. At optimal

flow rate, high single-cell occupancy of 89.3% in the cell traps can be achieved. Captured single cells are then washed to remove extra-cellular impurities and thermally lysed to release RNA in the same micro-chamber. RT-PCR reagents are infused into the corresponding reaction chambers for downstream analysis (Fig. 2-19). The combined reactor is designed to hold a total liquid volume of 60.6 nl, which consists of a 0.6 nl cell isolation chamber, a 10 nl RT reaction chamber, and a 50 nl q-PCR reaction chamber to minimize the reaction inhibition by sufficient dilution between each step. Advantages of this microfluidic platform include reduced detection noise, enhanced sensitivity and single nucleotide specificity. However, the cell capture efficiency is only 5%, which means that majority of sample injected will be lost before testing. Moreover, the microfluidic platform is still of complicated structure with relative high cost for general biological laboratory usage.

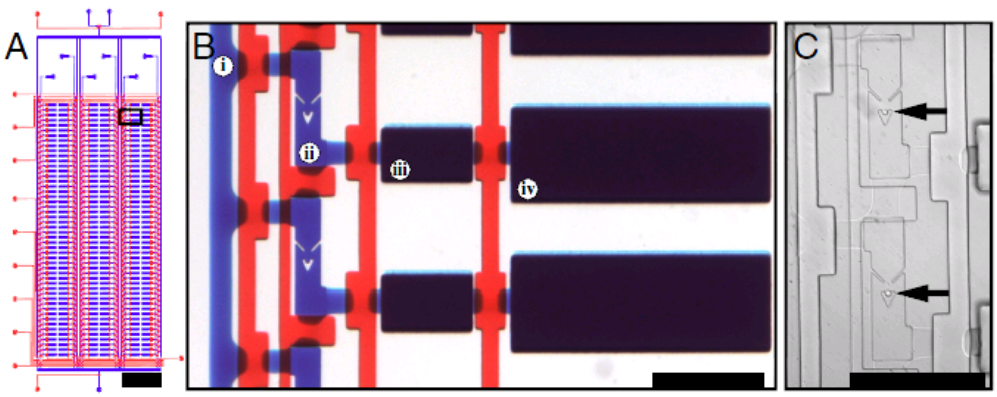

Fig. 2-19 Design of the microfluidic platform for single cell RNA analysis. (A) Schematic of microfluidic device with 6 sample input channels, each containing 50 reaction chambers. (B) Optical micrograph of array unit. Each unit comprises a reagent injection line (i), a cell capture chamber with cell traps (ii), a reverse transcription reaction chamber (iii), and a PCR reaction chamber. (C) Optical micrograph of two trapped single cells cell in capture chambers indicated by black arrows. Picture adapted from [4].

2.3.5.2 Microfluidic PCR platforms for bacterial cell RNA analysis

The importance of variations in gene expression of single bacterium within a microbial population has only been recognized until recently, as exampled by antibiotic resistant persister *Escherichia coli* cells and competence development in *Bacillus subtilis* [85]. Flow cytometry and fluorescence microscopy are two most commonly used methods in single bacterium gene expression studies. Generally, bacterial cells are either genetically modified to tag the target gene product with fluorescent proteins [86] or transformed with plasmids that carry the promoter sequence fused with fluorescent proteins [87, 88]. Cells are then visualized under fluorescence microscope or analyzed by flow cytometry. These methods require specialized and labor intensive molecular biological techniques for sample processing and are at high risk of misinterpretation because of the unknown consequences of exogenous DNA introduction. Alternatively, bacteria can also be labeled with fluorescent probes that specifically bind to target RNA of interest [89]. This method is less labor intensive but is easily subjected to information loss and misleading conclusion due to nonspecific bindings of the probes with other RNA targets during sample preparations.

The feasibility of applying q-RT-PCR as a label-free technique to quantify gene transcripts from single bacterium is demonstrated by Gao et al. [90]. In their study, single bacterium is picked up by a vision based cell manipulation system which can aspirate a single bacterial cell under light microscopy. RNA from single bacterium is then purified and concentrated by commercial RNA extraction kit followed by tube based q-RT-PCR assay. However, this method is low throughput in nature so that only a small number of bacteria can be studied each time with undetermined RNA loss during sample processing.

High throughput microfluidic PCR platforms for single bacterium RNA analysis have not been developed mainly because of two technical obstacles. First, bacterial cells are usually tens to hundreds fold smaller than mammalian cells so that microscopic dependent methods for single bacterium isolation are desirable. Second, RNA purification is essential to remove the background signals generated from DNA amplification in q-RT-PCR assay. This may not be a serious problem in mammalian cell q-RT-PCR amplification as the false positive signals from DNA can be eliminated by designing primers to anneal to sequences in exons on both sides of an intron which is absent in bacterial cells. Unfortunately, current microfluidic bacterial RNA purification technologies are low throughput with unsatisfactory extraction efficiencies. As a result, breakthrough in microfluidic devices for single bacterium RNA analysis is needed to facilitate researches in the area of both bacterial detection and infectious disease development.

2.4 Overview of *Pseudomonas aeruginosa* pathogenesis in respiratory infections

P. aeruginosa is an opportunistic human pathogen that is responsible for both acute and chronic respiratory tract infections, especially for immune-compromised patients, sick children and the elderly. Of infants born with low birth weight, the mortality rate associated with *P. aeruginosa* lung infections can reach as high as 50%-87% (Fig. 2-20) [91]. In cystic fibrosis (CF) patients, chronic lung infections associated with *P. aeruginosa* is the major cause of morbidity and mortality in spite of the aggressive antibiotic therapy the patients are put through [92]. CF is a congenital disorder with the disease incidence of 1 in 2,000 newborns in Caucasian populations. In Europe, around 35,000 children and young adults suffer from CF [93]. Chronic *P. aeruginosa* infections

induce intensive lung epithelial surface damages and airway obstruction in CF patients which are associated with pulmonary function decline. Intense inflammations provoked by frequent activation of immune cells and various oxidants released by neutrophil also contribute to exaggerated lung injury and increased mortality. The prevalence of *P. aeruginosa* lung infections in end stage CF patients is up to 80 to 90% [94]. The previously reported remaining life time in 50% of CF patients is less than 5 years after the commencement of chronic *P. aeruginosa* infections. Studies have shown that *P. aeruginosa* bacteria have developed a variety of strategies to be adapted in lung tissues with dramatic diversification in morphology. *P. aeruginosa* strains isolated from the same patient may differ significantly in morphotypes and antibiotic resistant patterns [95] (Fig. 2-21). *P. aeruginosa* also contributes to high mortality rate in ventilator-associated pneumonia.

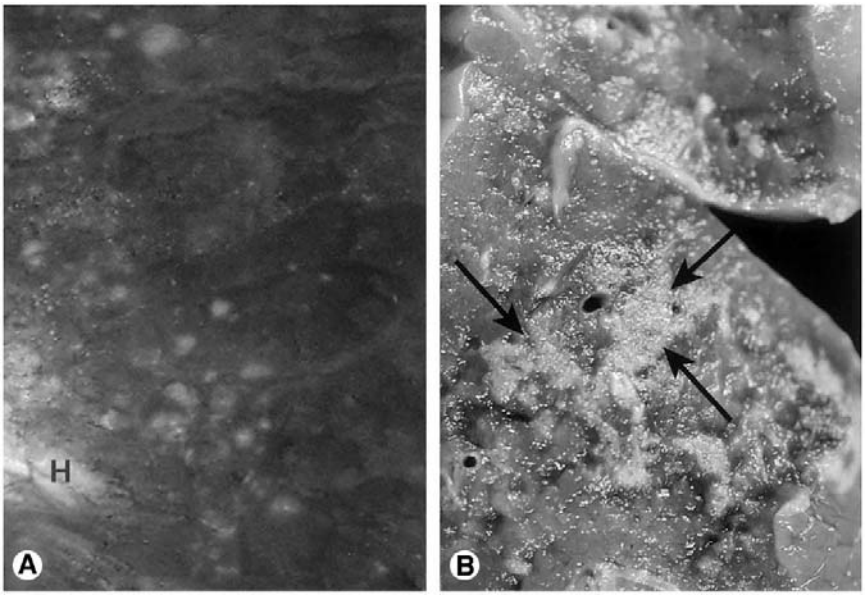

Fig. 2-20 Lung infections due to *P. aeruginosa* infection in newborn infants . (A) The pleural surface with intensive necrosis. H repersented hilar bronchus in this image. (B) The cut surface of the lung tissue. Lesions in lung tissue were arrowed. Picture adapted from [91].

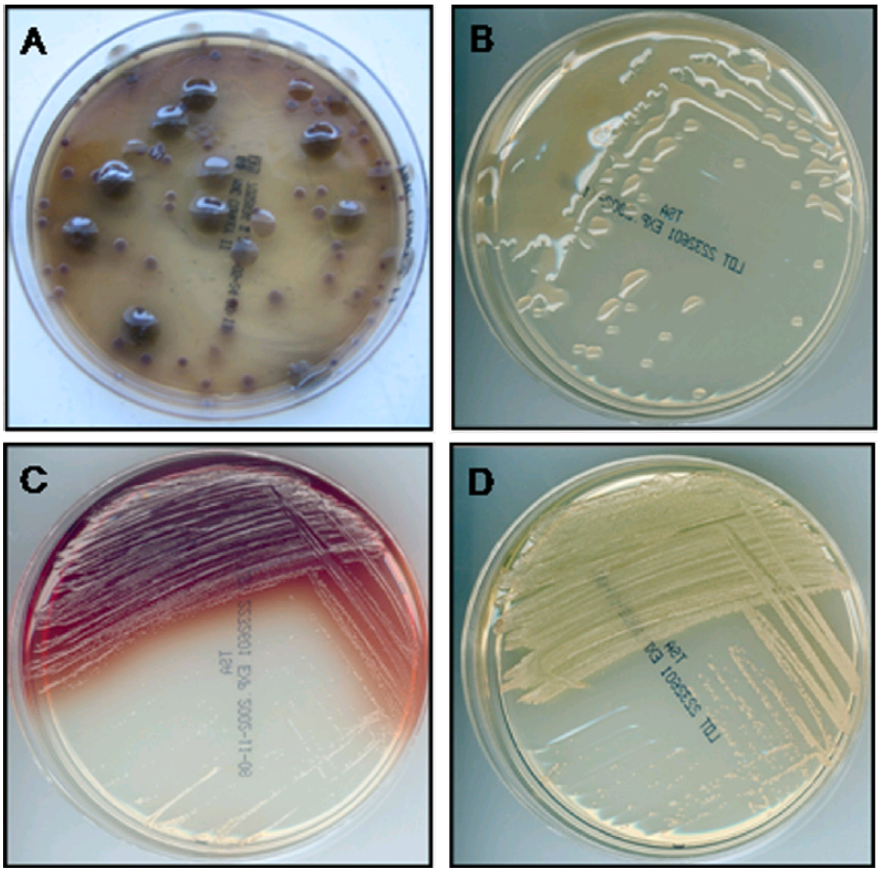

Fig. 2-21 Morphological diversity of *P. aeruginosa* isolates from the same CF patient. (A) *P. aeruginosa* recovered from one sputum sample, (B) mucoid variants, (C) non mucoid pyomelanin producing variants, and (D) non-pigmented LPS-rough variants. Picture adapted from [95].

2.5 Current methods in quantification of bacterial adhesion to the host cells

P. aeruginosa-associated lung infection is initiated by bacterial contact and colonization to human respiratory epithelium, which is mediated through surface appendages, such as flagella and pili, of the bacteria [96]. Lipopolysaccharide (LPS) functions similarly as an adhesin to bind to the epithelial surface glycolipid asialo-GM1 [96]. Understanding the detail adhesion dynamics between *P. aeruginosa* and the host cells is important to comprehend the mechanism of pathogenesis. However, in spite of this,

only limited number of techniques is now available to quantify bacterial adhesion to the host cells. Traditional methods applied to enumerate bacterial adhesion include the counting of plated colony forming units (CFU) or microscopic counting [97, 98]. CFU counting is the most commonly adopted method to quantify the total amount of bacteria attached to the whole population of infected host cells. Briefly, at the endpoint of infection, unattached bacteria are removed by extensive washing after which the bound bacteria are released from the host cells by treatment with mild detergent such as Triton X100 [97]. The bacterial suspension is then serial diluted and plated on appropriate agar. The colonies that appear on the agar plate after incubation in optimal temperature for more than 24 hours are counted. Each colony forming unit is considered to be derived from a single bacterium so that the original number of bacterial cells can be calculated based on the dilution factors. This method is labor intensive, time consuming and furthermore, applicable only to the culturable subpopulation of the bacteria. Besides, the detailed profiling of bacterial attachment to individual host cells, which provides deeper level of biological information related to pathogenesis, cannot be obtained [99].

Microscopic visualization of infected host cells is performed by pre-labeling of bacteria with fluorochromes [100-102] prior to the commencement of the infection (Fig. 2-22), or post-labeling of adhered bacteria with fluorochrome-tagged antibodies after the completion of the infection. Although this method is no less labor intensive than CFU counting, analysis of bacterial attachment to single infected host cells is possible under high resolution fluorescence microscope. However, the bacterial association kinetic cannot be profiled. This is because the attachment of the bacteria proliferated during the infection cannot be pre-labeled with fluorochromes and visualized under microscope.

Besides, the surface characteristics might be changed in fluorochromes labeled bacteria, so that the true adhesion properties may not be reflected [103]. This problem can be overcome by labeling bacteria with species specific-antibodies conjugated with fluorochromes only at the end of infection [104]. Although the natural structure of both mammalian cells and attached bacteria can be well preserved, the application of this method is still limited because of the lack of availability of antibodies to most bacteria of interest, as well as the antibody cross reaction between related species. Moreover, only a very small number of infected mammalian cells can be investigated in one experiment, which may result in misleading interpretations.

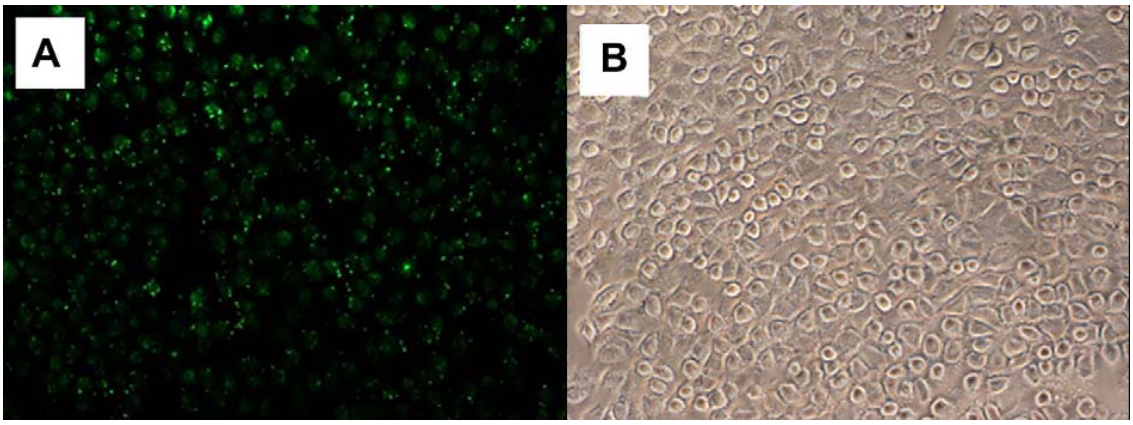

Fig. 2-22 Epifluorescence image of the attachment of *P. aeruginosa* pre-labeled with fluorescence dye to A549 cells (A) and control A549 cells under bright field. Picture adapted from [102] with a few modifications.

Flow cytometry (FCM) is a high throughput platform to study bacteria-host interactions [105, 106]. However, the bacteria still need to be either genetically modified to express fluorescent proteins or labeled with fluorochromes prior to flow cytometry experiment. Quantification of bacteria adhered to single host cells is possible as the fluorescence signal of adhered bacteria can be collected when infected host cells pass

through the laser detection system in cell-by cell fashion but with compromised accuracy due to the lack of standardized interpretation of FCM [107, 108].

Quantitative PCR (q-PCR) is a sensitive and reliable method to quantify bacterial adhesion to the host cells but is traditionally used to enumerate the total amount of bacteria attached to the whole population of infected cells [109, 110]. The rapid development of microfluidic technologies has led to the invention of many miniaturized chips for q-PCR based single cell analysis. Some micro-devices have been successfully demonstrated to quantify bacterial DNA at single copy level [73, 111], which showed promising potentials to precisely quantify the number of bacteria associated to single host cells. However, these analytic chips are relatively costly or need to be coupled with flow cytometry instrument to carry out q-PCR investigations [112, 113] as discussed in section 2.3.4.

2.6 Profiling of *P. aeruginosa* gene regulation during lung infection

Upon successful attachment, Type III secretion system of *P. aeruginosa* is activated to allow four effector proteins, ExoS, ExoT, ExoU and ExoY, to be introduced directly into the cytoplasm of the human lung epithelium cells, resulting in disruption of host cell functions [114]. Other virulence factors secreted into the outer space, such as exotoxin A, elastase, alkaline phosphatase, and phospholipase C disrupt the tight junction of lung epithelium to facilitate further invasion [115]. *P. aeruginsoa* regulates reversible gene expression in response to external environmental stimuli to adapt and survive in the host tissues. However, during chronic infection in CF patients, sometimes, reversible gene regulation in *P. aeruginosa* is lost, leading to the emergence of mutants strains that

differ in morphology from the original infecting strains as described above. This long term adaptation of *P. aeruginosa* is referred to as microevolution and understood as an in vivo selection process [116]. Recent reports have shown that the mutant *P. aeruginosa* strains in CF patient is transmissible, more virulent and antibiotic resistant, associated with increased morbidity in both infected patients and laboratory animal models [117]. Therefore, understanding the gene regulation during *P. aeruginosa* microevolution in chronic lung infections, especially at single host cell level, is important to gain detailed mechanisms related to disease development and may provide better insights to the progression of infection, thus contributing to new therapeutic drug development. Current technologies for bacterial gene transcripts quantification include quantitative reverse transcription polymerase chain reaction (q-RT-PCR) [1], mRNA sequencing [2], and hybridization based single molecule counting [3]. Of all these methods, q-RT-PCR outperforms in both sensitivity and specificity. However, high throughput q-RT-PCR platforms to study transcriptional gene regulations of bacterial cells have not been developed yet due to the lack of innovative technologies to isolate nucleic acids from small amount bacteria at large scales as discussed in section 2.3.5.

2.7 Lung infections induced by mixed infection of *P. aeruginosa* and *S. aureus*

S. aureus is another infectious human pathogen that is frequently found to co-infect with *P. aeruginosa*, especially in respiratory tract of CF patients [118]. It is reported that additive effect is observed in the level of expression of the lower airway inflammatory marker when *P. aeruginosa* and *S. aureus* co-infected, which highlights the significance of polymicrobial infection in lung disease [119]. However, beyond this observation, little is known about the influence of *P. aeruginosa* and *S. aureus* on each

other during mixed lung infection, such as changes in gene expression and altered progress of pathogenesis.

In this study, a novel microfluidic platform was designed and fabricated to study the interaction of *P. aeruginosa* with human lung epithelial A549 cells in either single or mixed infection context with *S. aureus* at single cell level. Single A549 cell at the endpoint of infection was isolated by one step vacuum driven microfluidics controlled by one external mechanical valve. The number of adhered bacteria was quantified by optimized on-chip q-PCR assay. *P. aeruginosa* RNA was isolated by novel chip based liquid phase nucleic acids purification technique down to single bacterium sensitivity reported for the first time. Transcriptional profiling of the selected virulence associated gene of *P. aeruginosa* was analyzed by on-chip q-RT-PCR assay. This platform offered a convenient and effective solution to study pathogen-host interactions at single cell level and can also be applied to other PCR based single cell investigations.

Chapter 3 High throughput microfluidic PDMS array chip to quantify bacterial adhesion to single host cells

3.1 Overview

To simplify the analysis of bacteria-host cells interactions for general biological laboratories, a PDMS array chip with 900 micro-wells, one sample inlet channel and one sample outlet channel was designed to achieve high throughput and label-free quantification of bacterial adhesion to single host cells by on-chip q-PCR assay. Interactions of *P. aeruginosa* and *S. aureus* with the host human lung epithelial A549 cell line in both single and mixed infection contexts were selected as the in vitro model [97] to demonstrate the performance of this chip. Single A549 cells at the endpoint of infection were isolated probabilistically into the individual micro-wells of the array chip by single step vacuum driven microfluidics controlled by one external mechanical valve followed by on-chip q-PCR quantification of the adhered bacteria. Single bacterium detection with the success rates of 90% for *P. aeruginosa* and 94% for *S. aureus* can be achieved with good reproducibility using the optimized DNA isolation protocol. Association profiling of *P. aeruginosa* and *S. aureus* in single infection context to A549 cells at three time points revealed different adherence patterns by these two pathogens. The attachment profiling of *P. aeruginosa* and *S. aureus* in mixed infections was also obtained by on-chip multiplex q-PCR assay, from which *P. aeruginosa* association with host A549 cells was identified to be significantly inhibited in the presence of *S. aureus* at 4 hours and 6 hours. The proposed microfluidic platform is easy to fabricate, cost effective, and presentes a

promising tool for biologists to study pathogen-host interaction at single cell level. The flow chart of methods adopted in this thesis is shown in Fig. 3-1.

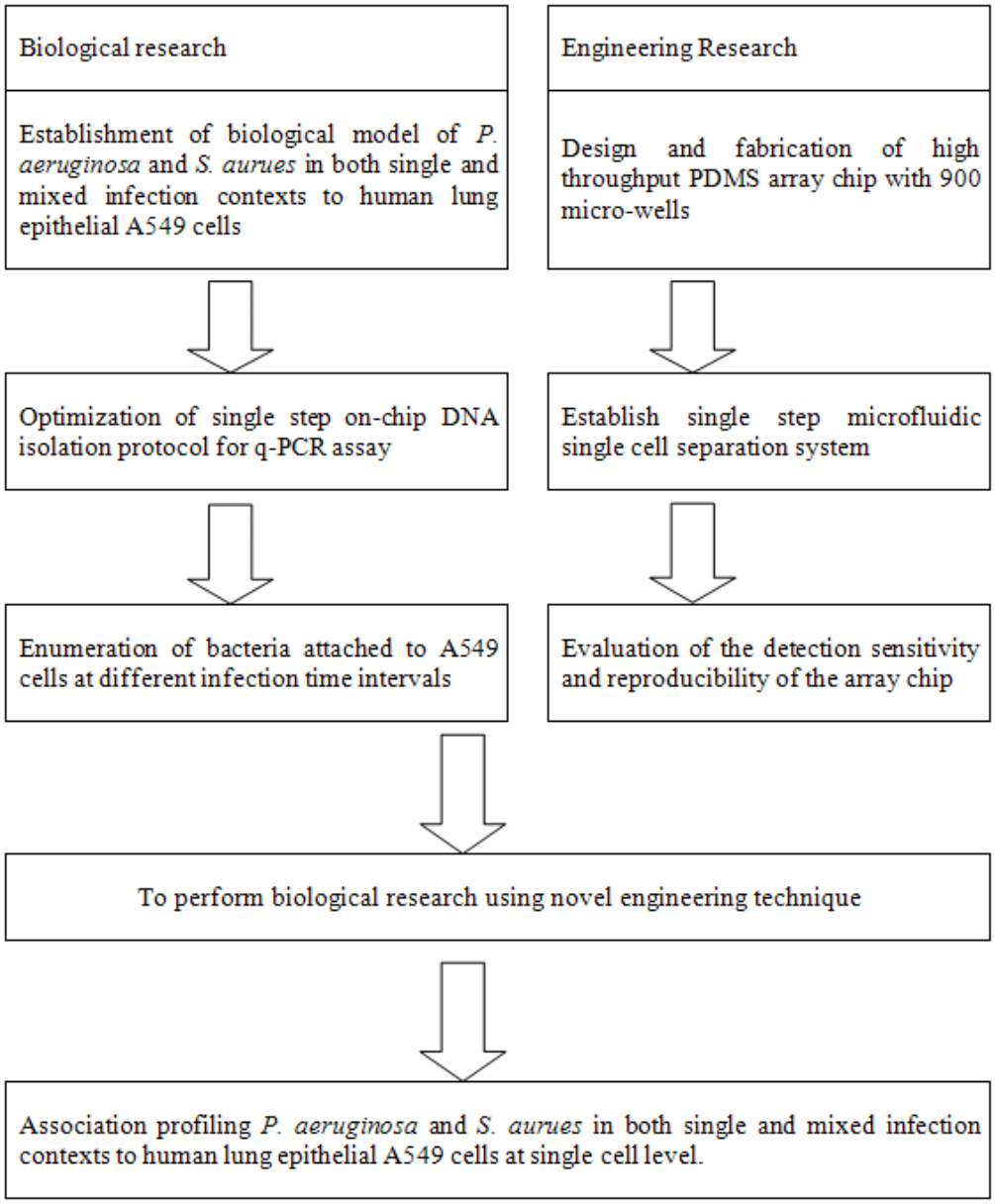

Fig. 3-1 Flow chart of methods adopted in this chapter.

3.2 Materials and Methods

3.2.1 Chip design and fabrication

The prototype microfluidic PDMS array chip with 900 micro-wells was modified from the PCR array matrix previously developed by Liu et al. [45]. Each well had a dimension of 0.5 mm×0.5mm×0.5mm to hold the sample liquid of around 125 nl. The chip also contained one inlet capillary channel, one outlet capillary channel and one headspace channel connecting the micro-wells for sample loading (Fig. 3-2). The chip had a total dimension of 40 mm× 40 mm. The PDMS micro-well layer was replicated from a stainless steel mold, which was fabricated by electrical discharge machining (EDM) process. To replicate the PDMS well layer, 4 ml of curing mixture containing 3.6 ml of PDMS Sylgard Silicone Elastomer 184 and 0.4 ml Sylgard Curing Agent 184 (Dow Corning Corporation Midland, MI, USA) was poured onto the surface of the metal mold and subjected to vacuum for 20 minutes to remove air bubbles. Following this, another metal block with smooth surface was placed on top of the PDMS polymer and the entire assembly was placed at 80 ˚C for 2 h for curing. The solid PDMS layer was then peeled off, cut to the desired size and attached to 1 mm thick acid-washed borosilicate glass substrate (Herenz Medizinalbedarf, Hamburg, Germany). Finally, a 1 mm acrylic head spacer was glued for sample loading. The chip cover was a piece of acrylic plate with two glass capillaries of 1 cm immobilized at diagonal positions. The chip and the cover was bond together using vacuum grease (Dow Corning, Singapore). The two capillaries were connected with silicon tubing as the sample inlet and outlet channels (Fig. 3-2). The image of micro-wells of the PDMS array chip visualized under bright filed microscope using 4 times magnification was shown in Fig. 3-3.

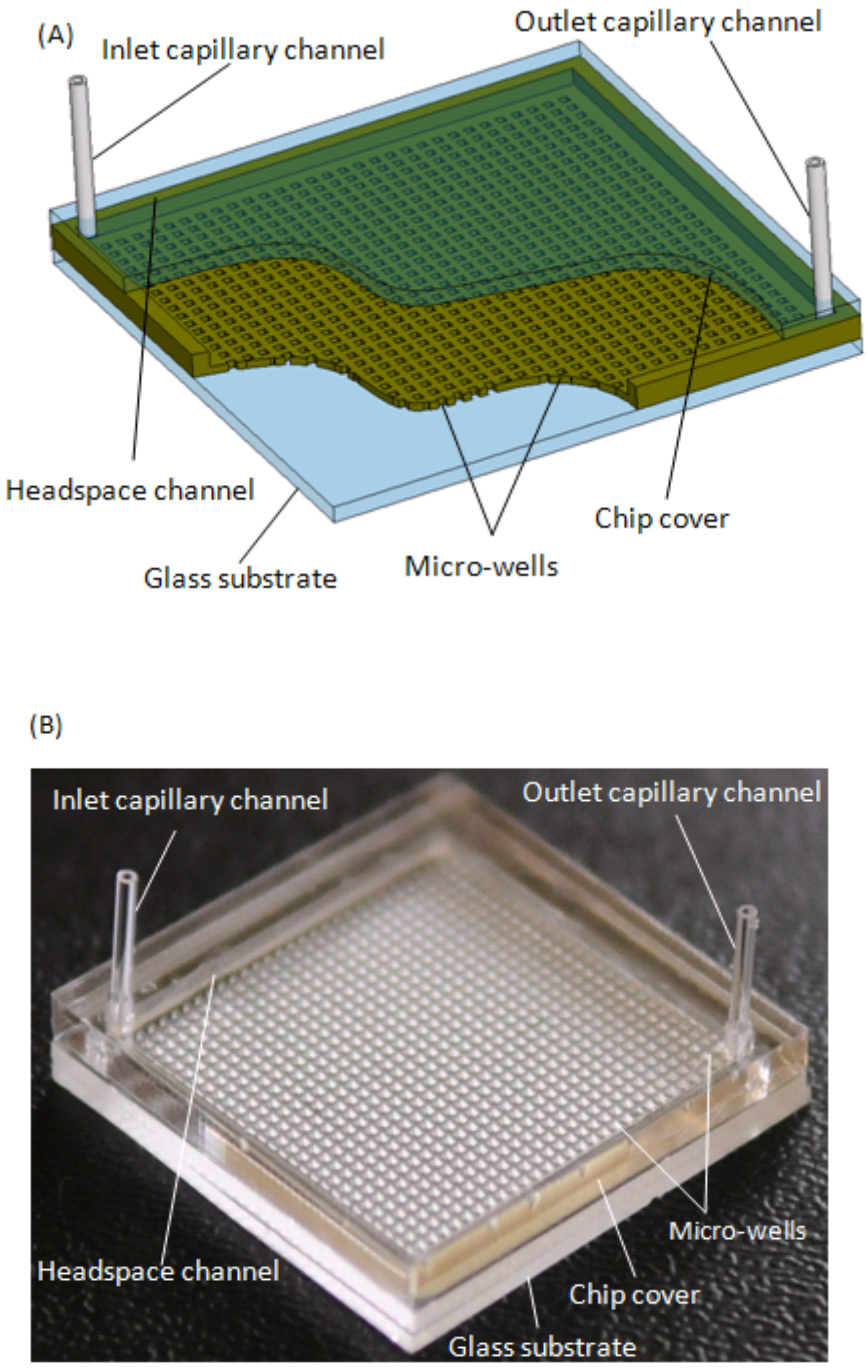

Fig. 3-2 Schematic (A) and photo (B) of the PDMS array chip. This PDMS array chip consisted of 900 micro-wells. Each well has a dimension of 0.5 mm×0.5 mm×0.5 mm that can hold the sample liquid around 125 nl.

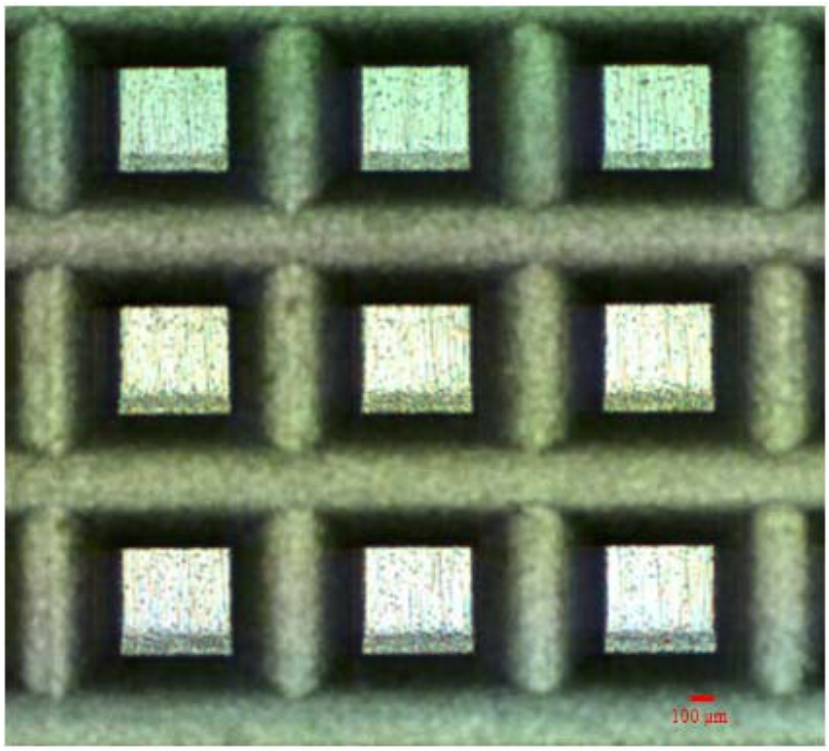

Fig. 3-3 Micro-wells of the PDMS array chip visulized under bright field microscope using 4 times megnificaiton.

3.2.2 Microfluidic operation of the PDMS array chip

q-PCR reagent containing the sample of interest was loaded into the PDMS array chip by one step vacuum driven microfluidics as previously described [45] with a few modifications. As illustrated in Fig. 3-4, the sample inlet channel of the PDMS array chip was connected to the reservoir tip to hold the PCR reagent mixture, the flow of which was controlled by an external mechanical pinch valve. The sample outlet channel was connected to an air buffering chamber to prevent accidental liquid leakage to the vacuum pump. To load PCR reaction mixture into the micro-wells of the PDMS array chip, vacuum pump was powered on with the pinch valve closed until the system's internal pressure was below 2 Torr. Afterwards, the mechanical valve was released so that the

PCR reagent mixture in the reservoir tip can be driven into the micro-wells. The microfluidic operation of the PDMS array chip was illustrated in (Fig. 3-5).

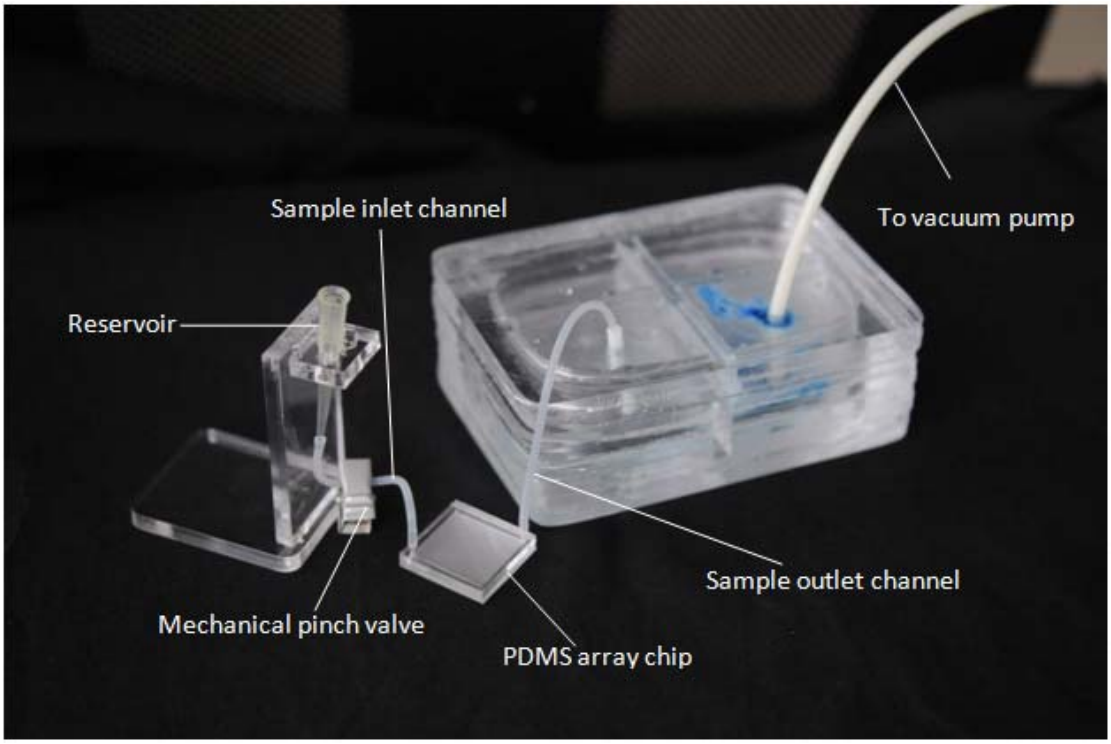

Fig. 3-4: Vacuum system setup for sample loading into the micro-wells of the PDMS array chip. PCR reagent was transferred into the micro-wells by vacuum driven fluidics controlled by an external mechanical pinch valve.

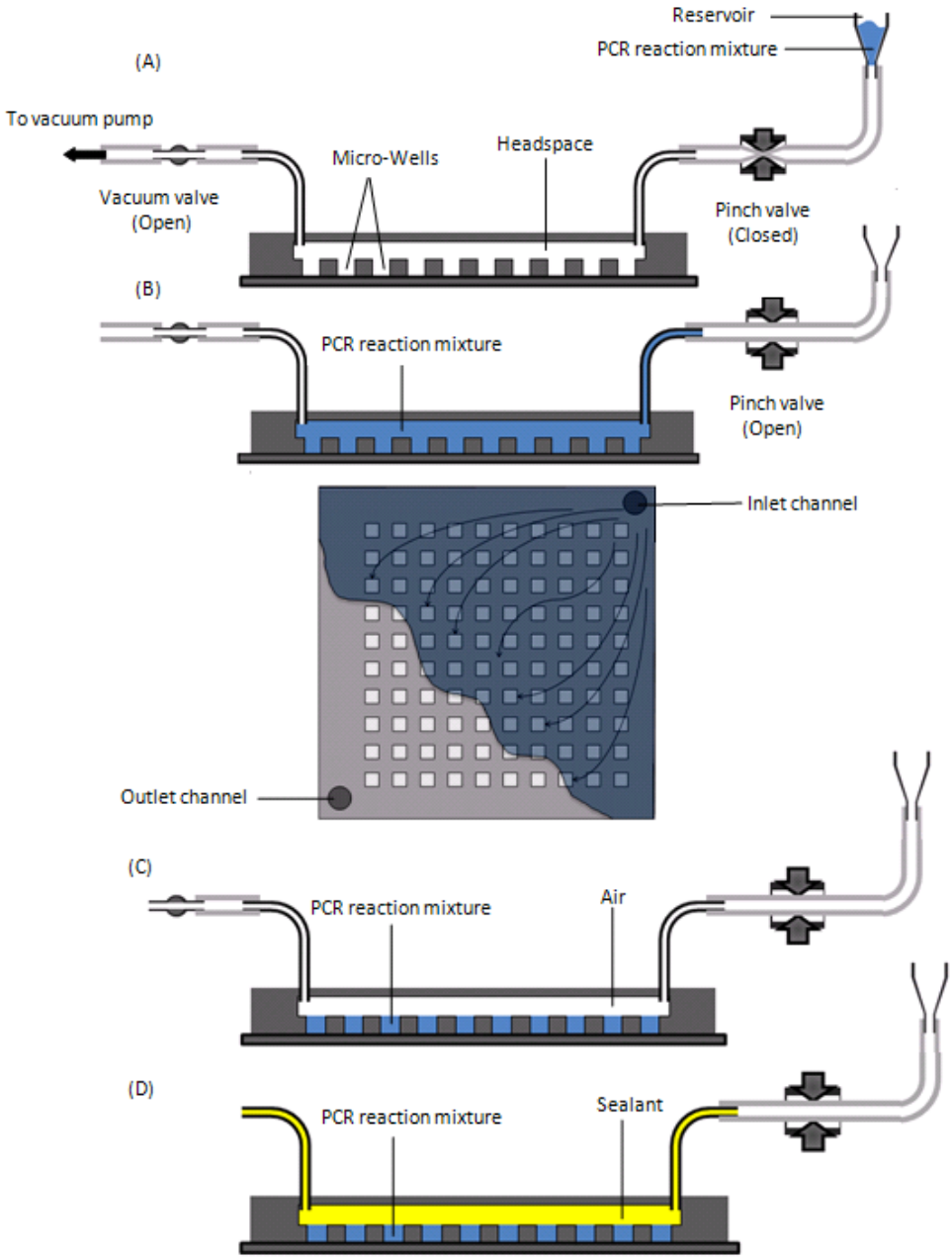

Fig. 3-5 Microfluidic operations of the PDMS array chip modifed from the previous method developed by Liu et al [45]. (A) Vacuum was established and monitored. PCR reaction mixture was loaded into the reservoir tip. (B) Pinch valve was opened to allow the PCR reaction mixture flow into the micro-wells. (C) Vacuum was still on to remove the excess liquid in the headspace and to isolate the micro-wells. (D) Vacuum closed and sealant was injected into the headspace for on-chip PCR assay.

3.2.3 Isolation of single A549 cells by vacuum driven microfluidics

Human lung epithelial A549 cell line (ATCC CCL 165) was kindly provided by Prof. Hui Kam Mun, National Cancer Center, Singapore. The cells were maintained in 10% fetal calf serum in F-12K Medium (Kaighn's Modification of Ham's F-12 Medium, ATCC, USA). Cultured A549 cells were first trypsinized, washed once with phosphate buffered saline (PBS) solution and then resuspended in q-PCR reaction mixture of dissolved Ready-To-Go PCR Beads (GE healthcare, USA) supplemented with 3mM $MgCl_2$ according to the manufacturer's protocol. The cell density of A549 was pre-adjusted to less than 2400 cell/ml (equivalent to 0.3 cell/well) and then loaded into the array chip by vacuum driven microfluidics as described in Fig. 3-5 to ensure that single cells can be isolated into the individual micro-well by probability (Fig. 3-6) [120]. To confirm the presence of the isolated single cells, A549 cells were stained with 4',6'-diamidino-2-phenylindole (DAPI) of 1 μg/ml for 10 minutes in dark to prior to cell loading. DAPI is a fluorescence dye that can penetrate into both viable and non-viable cells with enhanced fluorescence emission upon binding to DNA. A549 cells isolated in the micro-wells of the PDMS array chip was visualized under the microscope (Nikon, Japan) using 10 times magnification of both bright field and fluorescence field with the excitation and emission wavelengths of 350 nm and 450 nm respectively.

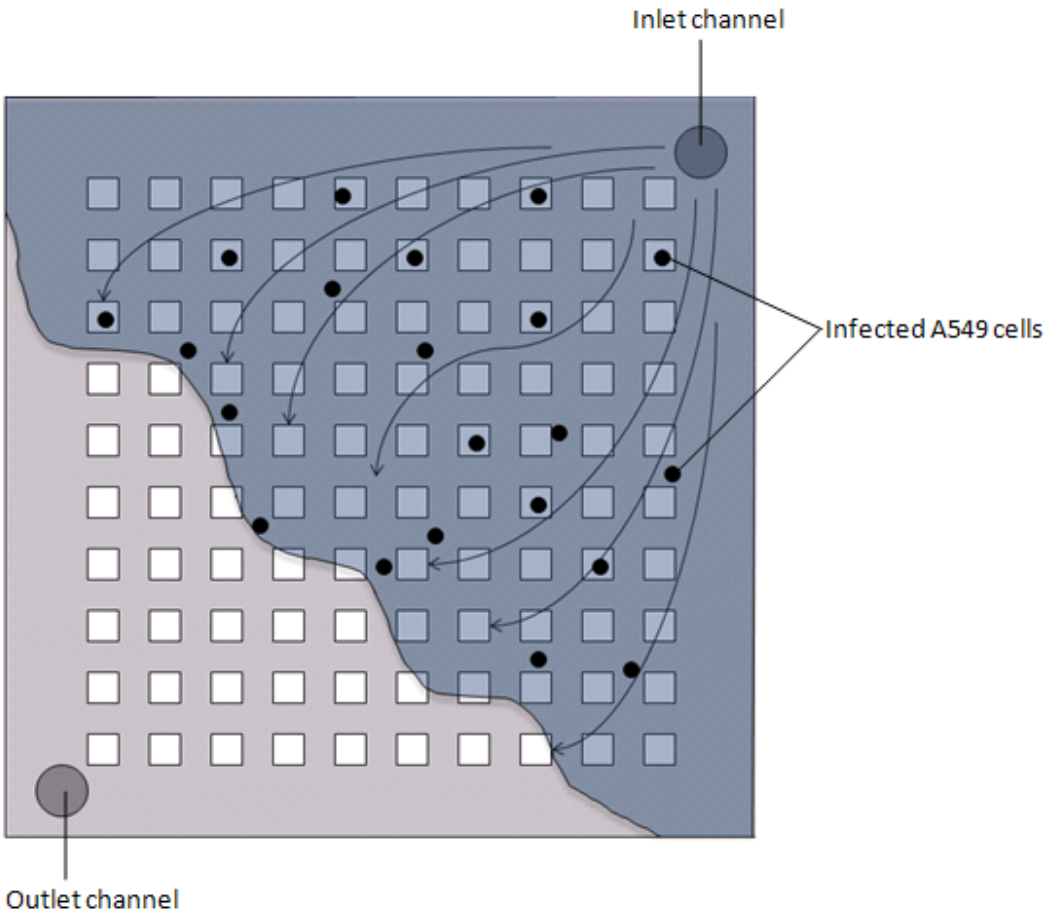

Fig. 3-6 Single cell isolation into the individual micro-wells of the PDMS chip by probability based on vacuum driven microfluidics.

3.2.4 Optimization of single step q-PCR protocol for *P. aeruginosa* and *S. aureus* quantification

To achieve single step q-PCR quantification of *P. aeruginosa* and *S. aureus*, without the need for a separate DNA purification procedure, bacterial DNA extraction by thermal lysis was incorporated with the initial DNA denaturation cycle of q-PCR at 95 ˚C for 5 minutes. The thermal lysis rate of *P. aeruginosa* and *S. aureus* in this condition was verified by staining the unlysed bacteria with 1:1,000 (vol/vol) Sybr Green I (Invitrogen,

USA) in dark for 10 minutes after the lysed bacteria were removed by centrifugation at 12000 rpm. The number of unlysed bacteria was counted under the fluorescence microscope using 40 times magnification with the excitation and emission wavelength of 490 and 520 respectively. *P. aeruginosa* and *S. aurous* at the same cell densities but was not subjected to thermal lysis were also stained with SYBR Green. Bacterial thermal lysis efficiency was estimated by the percentage of unlysed cells within five fields of view counted under the microscope. As it turned out that *S. aureus* was resistant to thermal lysis, lysostaphin of 200 µg/ml and two-fold serial dilutions to 12.5 µg/ml was added in the PCR reaction mixtures. *S. aureus* was incubated with the PCR reaction mixture supplemented with lysostaphin at various concentrations at 37 ˚C for 5 minutes prior to thermal lysis at 95 ˚C to find the optimal enzyme concentration to facilitate DNA release. The potential PCR inhibition effect of this enzyme was also tested by adding lysostaphin of various concentrations to q-PCR reaction mixture and amplified with *S. aureus* genomic DNA purified by Qiagen DNeasy® Blood & Tissue kit according to the manufacturer's protocol. q-PCR analysis was carried out using Ready-To-Go PCR Beads (GE healthcare, USA) supplemented with 3mM $MgCl_2$ and the corresponding primers and probes at initial denaturation temperature of 95 ˚C for 5 minutes followed by 40 cycles of denaturation at 95 ˚C for 30 s, annealing at 60 ˚C for 30 s and extension at 72 ◦C for 30 s using Rotor-Gene 3000 real time thermal cycler (Qiagen, Germany). DNA extraction efficiency of bacterial cells at various densities using optimized thermal lysis method was evaluated by comparison of the Ct values with appropriate dilutions from purified *P. aeruginosa* and *S. aureus* genomic DNA, extracted using Qiagen DNeasy Blood & Tissue kit, as reference control for 100% efficiency. PCR products was validated by capillary

electrophoresis chip (DNA Labchip 1000) using Agilent 2100 bioanalyzer (Agilent Technologies, USA) according to the manufacturer's protocol. Primers and probes used in this experiment have been selected based on the previously published paper [121] and were summarized in Table 3-1.

Table 3-1 Primer and probes for q-PCR assay

Species	Gene names	Product size (bp)	Forward primer	Taqman probe	Reverse primer
P. aeruginosa	PA 0708	211	CCGACTGACGC CAACGA	FAM-5'-CCACTGCACAGACCAGAGAA- 3' -TAMRA	CGACCCTACCTCC CACGAAT
S. aureus	ViK	319	AAACAACTACA ATCCCTTCA	CYS- 5'-ACGAAAAGGGCTCCGTAAAT-3'-IBRQ	TACGGTTAGACT GCTTCG

3.2.5 Construction of q-PCR standard curve

To realize absolute quantification of bacterial attachment to single A549 cell, q-PCR standard curve was constructed by loading the q-PCR reaction mixtures with *P. aeruginosa* and *S. aureus* at the cell densities from 3×10^6 cell/ml to 3×10^3 cell/ml, which is equivalent to a range of 300 cell/well to 0.3 cell/well into the proposed microfluidic PDMS array chip. q-PCR analysis was carried out using the optimized DNA extraction protocol with Ready-To-Go PCR Beads supplemented with 3mM $MgCl_2$ at an initial denaturation temperature at 95 °C for 5 minutes followed by 40 cycles of denaturation at 95 °C for 30 s, annealing at 60 °C for 30 s and extension at 72 °C for 30 s using an in-

house real-time PCR cycler with multiple integrated functions including thermo-cycling control, real time fluorescence imaging, on line image processing and data analysis as described previously [45] (Fig. 3-7). *P. aeruginosa* and *S. aureus* cell densities were estimated by measuring the optical density at 660 nm (OD_{660}) and confirmed by CFU counting on plates. q-PCR standard curve was constructed by plotting threshold Ct values obtained against logarithm of bacterial concentrations. The success rate for single bacterium detection was estimated by the number of total positive amplifications with bacterial concentration of 0.3 cell/well divided by the theoretical positive amplifications calculated according to Poisson statistics [120].

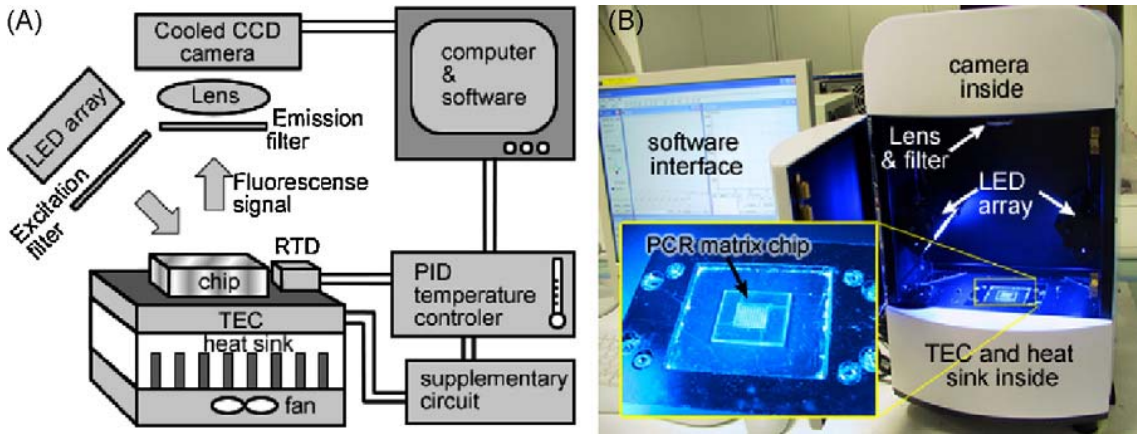

Fig. 3-7: Schematic structure (A) and photo (B) of the prototype real time PCR instrument. The temperature of the array chip was controlled by thermoelectric cooler (TEC). Fluorophore was excited using an array of blue light-emitting diode (LED) with appropriate filter. Fluorescence image was captured by cooled coupled device (CCD) camera. The design and fabrication of this instrument was not included in this thesis Picture adapted from [45].

3.2.6 Quantification of *P. aeruginosa* and *S. aureus* adherence to A549 cells in both single and mixed infection contexts by CFU counting assay

P. aeruginosa PAO1 and *S. aureus* (ATCC 25923) were purchased from American Type Culture Collection (ATCC) and were maintained in Luria broth (1% tryptone, 0.5% yeast extract, 0.5% sodium chloride). Bacteria taken from overnight culture in LB agar was resuspended in PBS (Phosphate buffered saline) solution. Prior to adhesion assays, the bacteria were harvested by centrifugation at 8,000 *g* for 10 min and washed once with PBS. Bacterial concentration was determined by measuring the optical density at 660 nm (OD_{660}) and confirmed by CFU counting. The human lung epithelial A549 cell line (ATCC CCL 165) was kindly provided by Prof. Hui Kam Mun, National Cancer Center, Singapore. The cells were maintained in 10% fetal calf serum supplemented F-12K Medium (Kaighn's Modification of Ham's F-12 Medium, ATCC) and incubated at 37°C in 5% CO_2. A549 cells were seeded at 5×10^5 cells/well in a 24-well plate one day before the adhesion assay. To quantify the binding kinetics of *P. aeruginosa* and *S. aureus* adhesion in a single infection condition, 1ml bacterial suspension was added to give a final multiplicity of infection (MOI) of 400 bacteria per cell and incubated for the time intervals of 2h, 4h, and 6h. For mixed infection assay, mixtures containing both *P. aeruginosa* and *S. aureus* at the MOI of 400 each were added to A549 cells. Unbound bacteria were excluded by intensive washing of A549 cells with PBS for four times. A549 cells were then trypsinized at the end of the infection and collected by centrifugation at 800 *g*. Bound *P. aeruginosa* and *S. aureus* were released by lysis of the A549 cells in 1% triton-X100 and enumerated by CFU counting on MacConkey agar and Mannitol Salt

Phenol Red agar (Sigma, Singapore) respectively. Viability of infected A549 cells was analyzed by trypan blue exclusion assay as described previously [122].

3.2.7 Quantification of bacterial adhesion to single A549 cells using the microfludic PDMS array chip

At the endpoint of bacterial infections, A549 cells were trypsinized, pelleted by centrifugation at 800 *g*, and washed once with PBS. Infected A549 cells were then directly resuspened in the q-PCR reaction mixture of dissolved Ready-To-Go PCR Beads (GE healthcare, USA) supplemented with 3mM $MgCl_2$ and the corresponding primers and probes. The density of infected A549 cells were adjusted to less than 2400 cell/ml (equivalent to 0.3 cell/well) and were loaded into the PDMS array chip by vacuum driven microfluidics to isolate single cells in the individual micro-wells. For *S. aureus* related infection assays, lysostaphin at the concentration of 50 μg/ml was pre-loaded and dried in the micro-wells. The micro-wells were then sealed with PCR grade mineral oil (Sigma, USA) followed by q-PCR assay as described in section 3.2.5. The number of adhered *P. aeruginosa* and *S. aureus* was calculated according to the q-PCR standard curve and the sample Ct values as described previously [36, 110, 123].

3.3 Results and discussions

3.3.1 Single A549 cell isolation

Isolation of single cells is a key step for heterogeneous behaviour analysis. Microfluidic devices provide excellent platforms for single cell separation because of their capabilities to control and manipulate small quantities of fluids using an array of

delicately designed microvalves and microchannels [22]. However, the complicated manufacturing process and the lack of standard operation in current microfluidic platforms remain a barrier for their routine usage in biological laboratory. Presented here is simple and easy to fabricate PDMS array chip of 900 micro-wells, one sample inlet channel and one sample outlet channel. A549 cell suspension can be loaded into the array chip by one step vacuum driven microfluidics, the flow of which is easily controlled by only one external mechanical valve. As shown in Fig. 3-8 (left), single A549 cell can be effectively separated into the individual micro-wells of the PDMS array chip probabilistically, the presence of which is confirmed by DAPI staining Fig. 5 (right), given that the cell density was pre-adjusted to less than 0.3 cell/well. According to Poisson statistics, the vast majority of the micro-wells contain no more than a single cell in this condition [120]. 97.8% of A549 cells maintained their viability after loading as assessed by trypan blue staining. Since the ultimate interest in this study is to quantify the number of bacteria attached to A549 cells during the infection process, immersing A549 cells in the PCR reaction mixtures should not result in the dissociation of the bacterial cells from A549 cells. To test this, infected A549 cells were incubated in the PCR reaction mixture buffer for 10 minutes, and centrifuged at 800 g for 5 minutes. The supernatant was then plated on LB agar. No positive bacteria growth was observed, indicating that bacteria remained attached to the host cells in PCR reaction mixture.

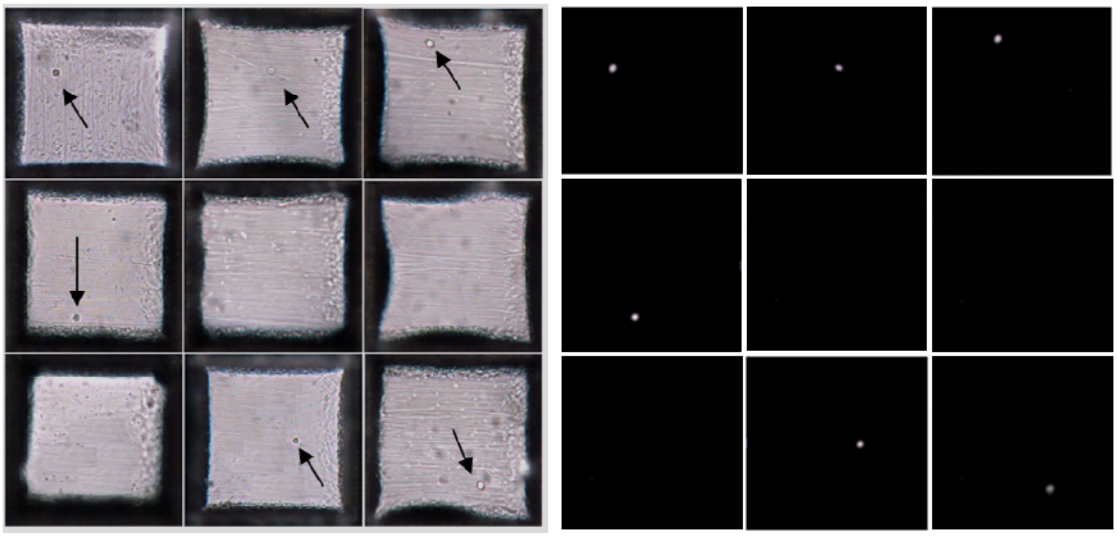

Fig. 3-8 Observation of single A549 cell isolated in the individual micro-wells of the PDMS array chip. Cells were stained with DAPI before loading into the chip. 3×3 wells were imaged under 10 times bright field microscopy (left) and fluorescence microscopy (right). Cells were isolated in one/zero per well patten by probability. Single cells isolated in micro-wells were arrowed.

3.3.2 Optimization of bacterial lysis protocol

In most cases DNA has to be released out of the cells for q-PCR analysis to be performed. In order to minimize device complexity and avert the need for DNA purification, an on-chip bacterial DNA extraction protocol that is compatible with the commercial q-PCR kit was optimized. Bacterial thermal lysis was first attempted to be incorporated with the first cycle of q-PCR amplification at 95 ˚C for 5 minutes. To verify thermal lysis efficiency in this condition, *P. aeruginosa* and *S. aureus* were suspended in 100 μl PCR reaction mixture at the concentration of around 10^8 CFU/ml followed by heat treatment at 95˚C for 5 minutes. Cells were then centrifuged at 12000 rpm for 10 minutes and the supernatant containing the lysed bacteria were removed. The pellets of the unlysed bacteria were resuspended in 100 μl PBS buffer and stained with 1:1000 (vol/vol) SYBR Green I (Invitrogen, USA) in the dark for 10 minutes [124]. SYBR Green I is a

fluorescence dye that can penetrate into both viable and nonviable bacteria and bind to DNA to form DNA-dye-complex, emitting green fluorescence. As a control, *P. aeruginosa* and *S. aureus* of the same cell densities but without heat treatment were also stained with SYBR Green I. Cells were then enumerated under fluorescence microscope using 40 times magnification. Bacterial thermal lysis efficiency was estimated by the percentage of unlysed bacteria counted within five fields of views under microscope. As shown in Fig. 3-9, *P. aeruginosa* was susceptible to thermal lysis in PCR reaction buffer (Fig. 3-9 A and B) while *S. aureus* was heat resistant in the same circumstance (Fig. 3-9 C and D) probably because of the complex outer cell wall structure of *S. aureus*. [125]. 93.9% *P. aeruginosa* can be effectively lysed compared with only 4.5% for *S. aureus* (Fig. 3-10).

To further improve thermal lysis efficiency, *S. aureus* was pre-treated with lysostaphin, an enzyme that can selectively digest the outer membrane of *S. aureus* [126], at the concentrations of 200 μg/ml, 100 μg/ml, 50 μg/ml, 25 μg/ml and 12.5 μg/ml in PCR reaction mixture at 37 ˚C for 5 minutes, and then subjected to thermal lysis at 95 ˚C for 5 minutes. Following this, *S. aureus* were stained with SYBER Green I as described above. As illustrated in Fig. 3-11 and Fig. 3-12, pre-treatment with lysostaphin significantly enhanced the thermal lysis efficiency of *S. aureus* at the enzyme concentrations ≥ 50 μg/ml.

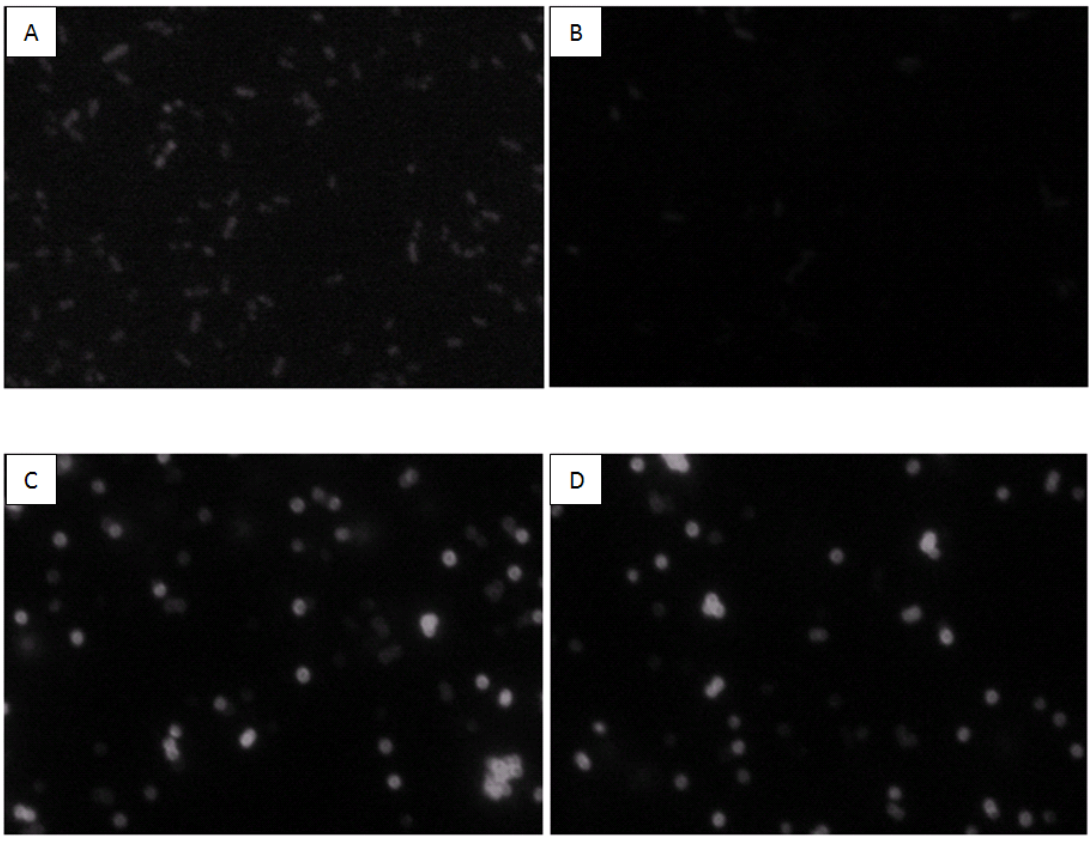

Fig. 3-9 Microscopic images of *P. aeruginosa* and *S. aureus* cells subjected to thermal lysis in the PCR reaction buffer. *P. aeruginosa* and *S. aureus* without heat treament were shown in image A and C respectively. Unlysed *P. aeruginosa* and *S. aureus* in the PCR reaction buffer at 95 ˚C for 5 minutes were shown in image B and D respectively. Cells were stained with Sybrgreen I and visualized under 40 times fluorescence microscopy.

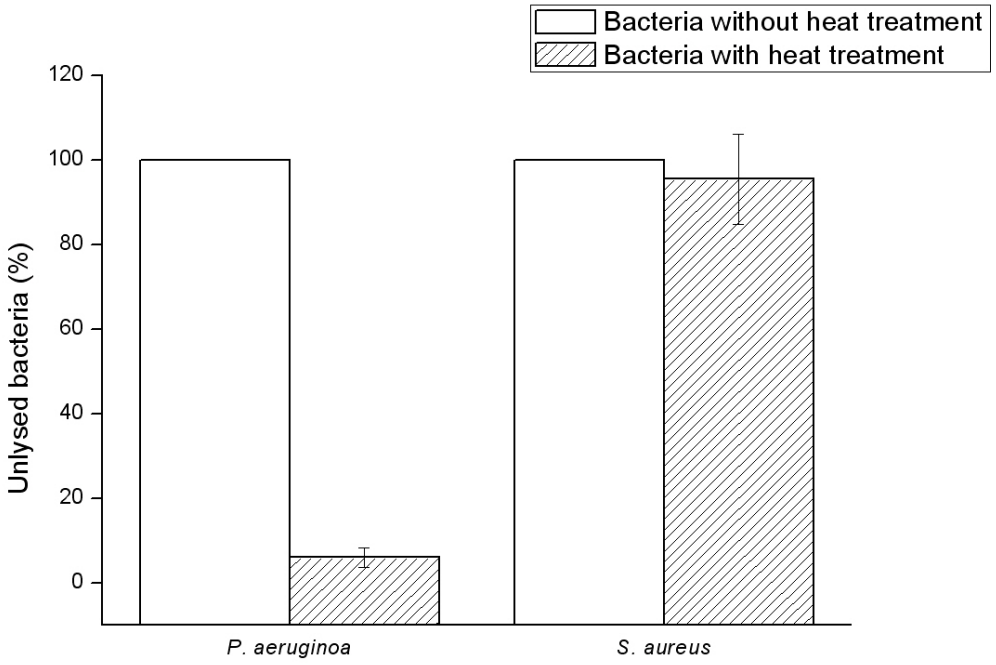

Fig. 3-10 Bacterial thermal lysis efficiency in the PCR reaction buffer at 95 ˚C for 5 minutes, estimated by the number of unlysed bacteria divided by the number of untreated bacteria counted under the microscope of five fields of views. Each point represents the mean ± standard error of three replicated experiments.

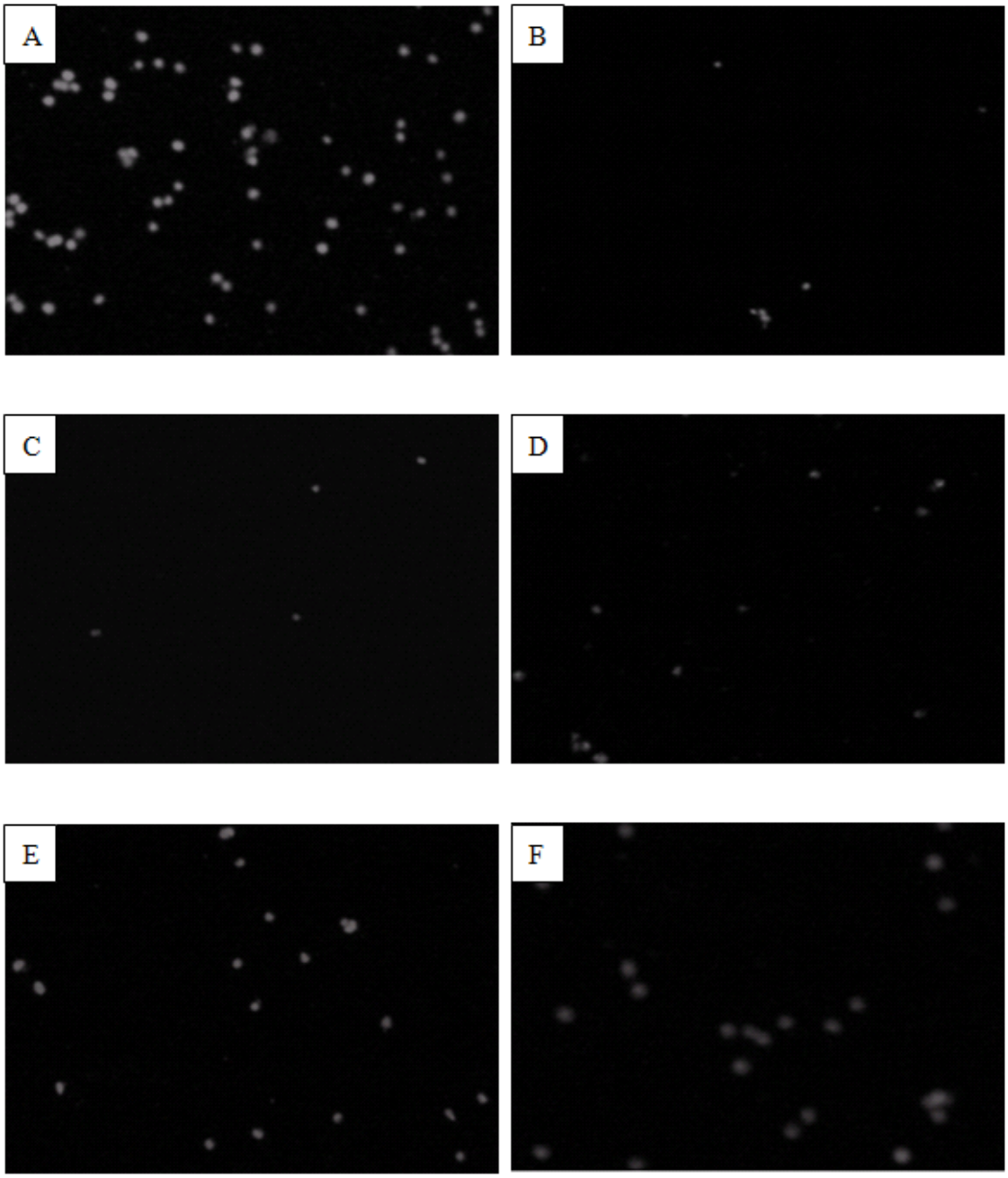

Fig. 3-11 Microscopic images of unlysed *S. aureus* subjected to thermal lysis in PCR reaction mixture with lysostaphin pre-treatment at concentrations of 200 µg/ml (B), 100 µg/ml (C), 50 µg/ml (D), 25 µg/ml (E) and 12.5 µg/ml (F) and *S. aureus* with no thermal and enzymetic treatment (A). Cells were stained with Sybrgreen I and visualized under 40 times fluorescence microscopy

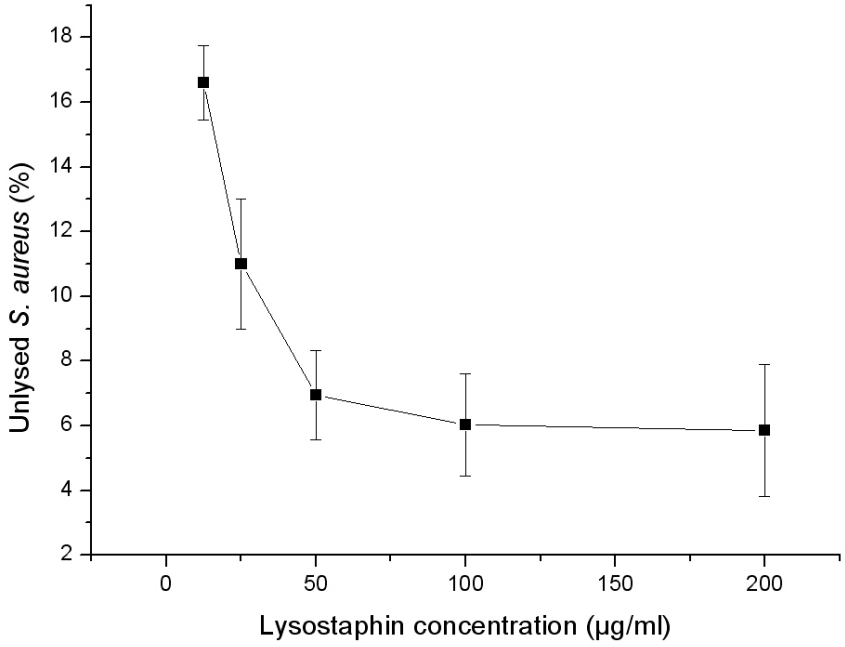

Fig. 3-12 Thermal lysis efficiency of *S. aureus* in PCR reaction mixture at 95 ˚C for 5 minutes with lysostaphin pre-treatment at 37 ˚C for 5 minutes estimated by the average number of unlysed bacteria divided by the number of untreated bacteria counted under the microscope of five different views. Each point represents the mean ± standard error of three replicated experiments.

To verify if lysostaphin acts as a potential PCR inhibitor, lysostaphin was added to the PCR reaction mixture at the final concentrations of 200 µg/ml, 100 µg/ml, 50 µg/ml, 25 µg/ml and 12.5 µg/ml. Purified *S. aureus* DNA was then added to the PCR reaction mixtures containing lysostaphin at various concentrations and analyzed by PCR as described in section 3.2.4. As shown in Fig. 3-13, inhibition of PCR was observed with lysostaphin at concentrations ≥100 µg/ml, but this inhibitory effect was not present in diluted concentrations ≤ 50 µg/ml. Consequently, lysostaphin of 50 µg/ml was chosen for future experiments.

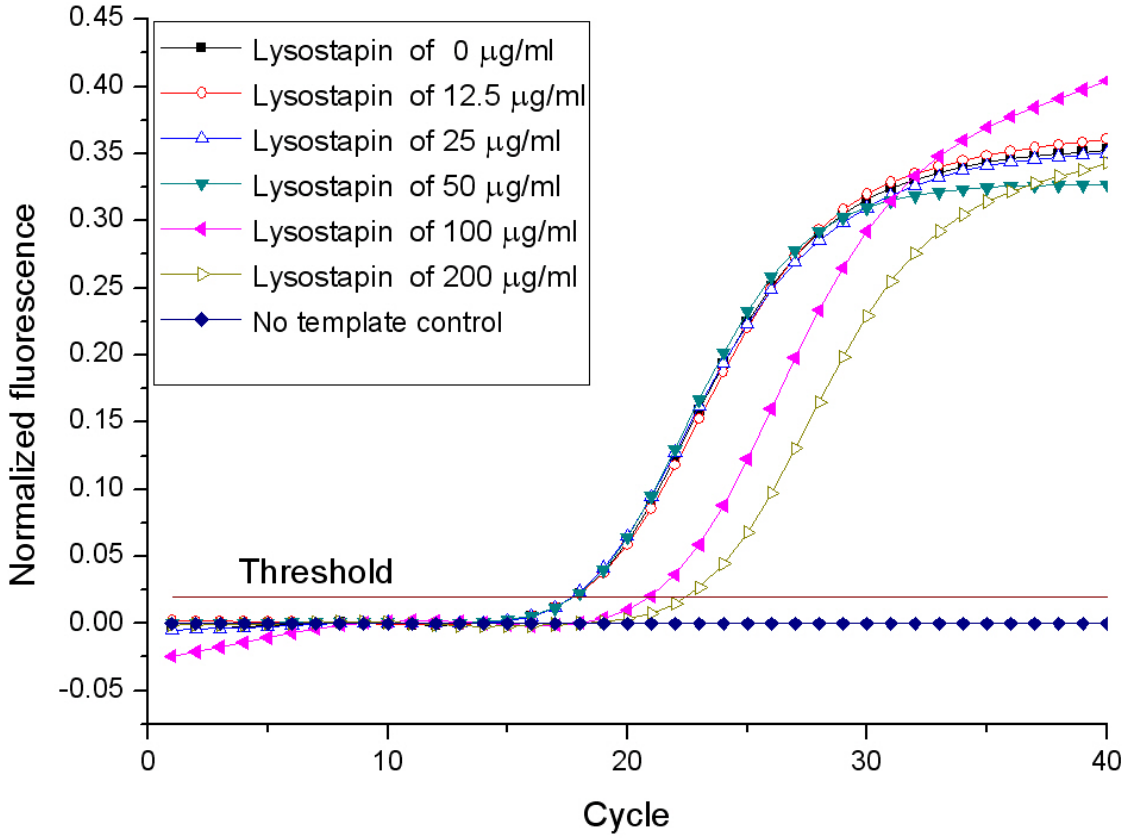

Fig. 3-13 q-PCR amplifications of *S. aureus* genomic DNA with lysostapin at the concentrations of 200 μg/ml, 100 μg/ml, 50 μg/ml, 25 μg/ml,12.5 μg/ml and 0 μg/ml.

Although pre-incubation of *S. aureus* with lysostaphin at 50 μg/ml significantly enhanced the bacterial thermal lysis efficiency without notable inhibitory effect on q-PCR assay, *S. aureus* infected A549 cells cannot be mixed directly with lysostaphin to avoid bacterial dissociation prior to single cell isolation in the PDMS array chip. One simple solution to circumvent this problem is to pre-load and dry lysostaphin into the micro-wells of the array chip. However, enzyme activity loss during sample loading and rehydration process is the key issue that needs to be taken into consideration. To validate the enzyme stability during dehydration and rehydration processing, lysostaphin was loaded and dried into the micro-wells of the array chip as described in Fig. 3-5. Distilled water was then

loaded into the chip to rehydrate the enzyme, the suspension of which was rinsed out by pipetting. No apparent enzyme activity loss was observed as assessed by *S. aureus* thermal lysis efficiency assay as described in section 3.2.4 (Fig. 3-14). This finding is consistent with the previously reported activity restoration of lysozme (another enzyme with similar bacterial lysis functionality as lysostaphin) after rehydration [127]. The possibility of enzyme loss during sample loading may also arise from the momentary connection of all wells with the headspace above. It is previously demonstrated that pre-dried DNA oligoes remained in the micro-wells during the sample loading as the incubation time of fluidically connected wells is much shorter than the DNA resuspension time [45]. To verify if the same scenario also applies to lysostaphin, the enzyme was first tagged with fluorescein isothiocyanate (FITC) fluorophore using FluoroTag™ FITC Conjugation Kit (Sigma, USA) according to the manufacture's protocol. FITC conjugated lysostaphin was loaded and vacuum dried into the micro-wells of the array chip, and then resuspended by a second round of loading of the distilled water into the micro-wells. Fluorescence images of FITC conjugated lysostaphin in the micro-wells at different time points were shown Fig. 3-15. It took around 1 minute for the lysostaphin to be fully resuspended in water without significant loss in quantity. In summary, pre-dried lysostaphin retained its activity and quantity in the micro-wells during the sample loading, which means that this method is suitable to be incorporated for on-chip quantification of *S. aureus* adhered to single A549 cells by q-PCR assay.

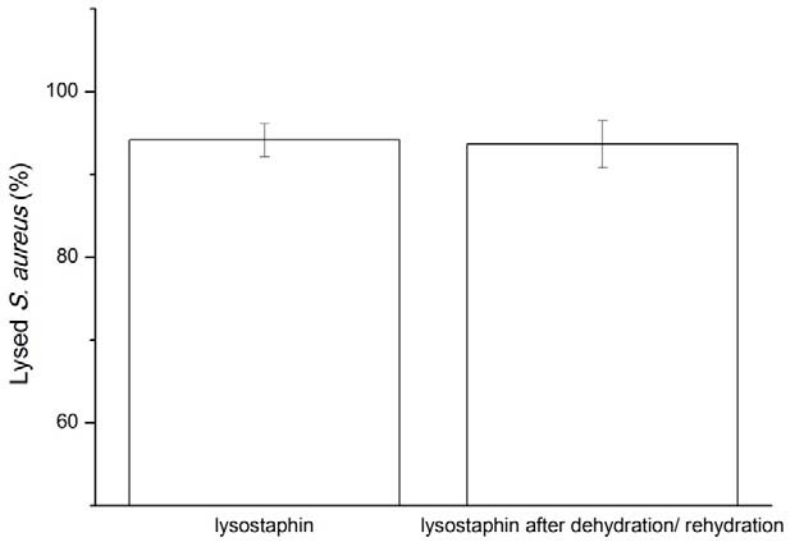

Fig. 3-14 Thermal lysis efficiency of *S. aureus* pre-treated with lysostaphin in its natural state and lysostaphin with one round dehydration and rehydration process as estimated by the percentage of lysed bacteria counted under the microscope of five different views. Each point represents the mean ± standard error of three replicated experiments.

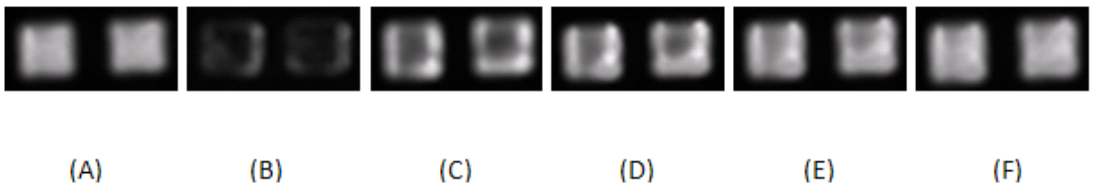

Fig. 3-15 Visualization of the resuspension process of pre-dried lysostaphin after sample loading. (A) Fluorophore tagged lysostaphin before dehyration. (B) Lysostaphin dried in micro wells. (C-F) Fluorescence images shot after 5 seconds, 10 seconds, 30 seconds, and 1 minute after a second round loading of distill water.

As genomic DNA purification was not integrated in the proposed PDMS array chip, another potential PCR inhibition source may come from the crude thermal lysate of *P. aeruginosa*, *S. aureus* and A549 cells. Consequently, q-PCR inhibition caused by

sample overloading should be investigated. *S. aureus* DNA template was therefore put through q-PCR assay in the presence and absence of the thermal lysates of *P. aeruginosa* and A549 cells at various cell densities. Similarly, q-PCR with *P. aeruginosa* DNA template in the presence and absence of *S. aureus* and A549 thermal lysates at different cell densities was also performed. ΔCt was derived from the Ct value obtained from q-PCR with cell lysate subtracted from the Ct value from identical control samples without foreign cell lysate. PCR inhibition was indicated by ΔCt values above zero. As illustrated in Fig. 3-16, significant PCR inhibition was observed with cell lysates at cell densities above10^7 CFU/μl for *P. aeruginosa*, 10^6 CFU/μl for *S. aureus*, and 10^4 cell/μl for A549 cells. Considering that the total volume of the micro-wells in the PDMS array chip is only around 100 nl, up to 10^6 *P. aeruginosa* and 10^5 *S. aureus* adhered to single A549 cells can be detected without compromised accuracy. As A549 cell is around 400 times larger than *P. aeruginosa* and *S. aureus* in surface area, the saturated number of bacteria attached is estimated to be less than 400 per cell with no bacterial association more than this ratio reported to date. In this study, the maximum number of bacteria adhered to single A549 cell was later found to be around 40 for *P. aeruginosa* and 90 for *S. aureus* when verified by CFU counting method (Fig. 3-28), which is within the loading limit indicated above.

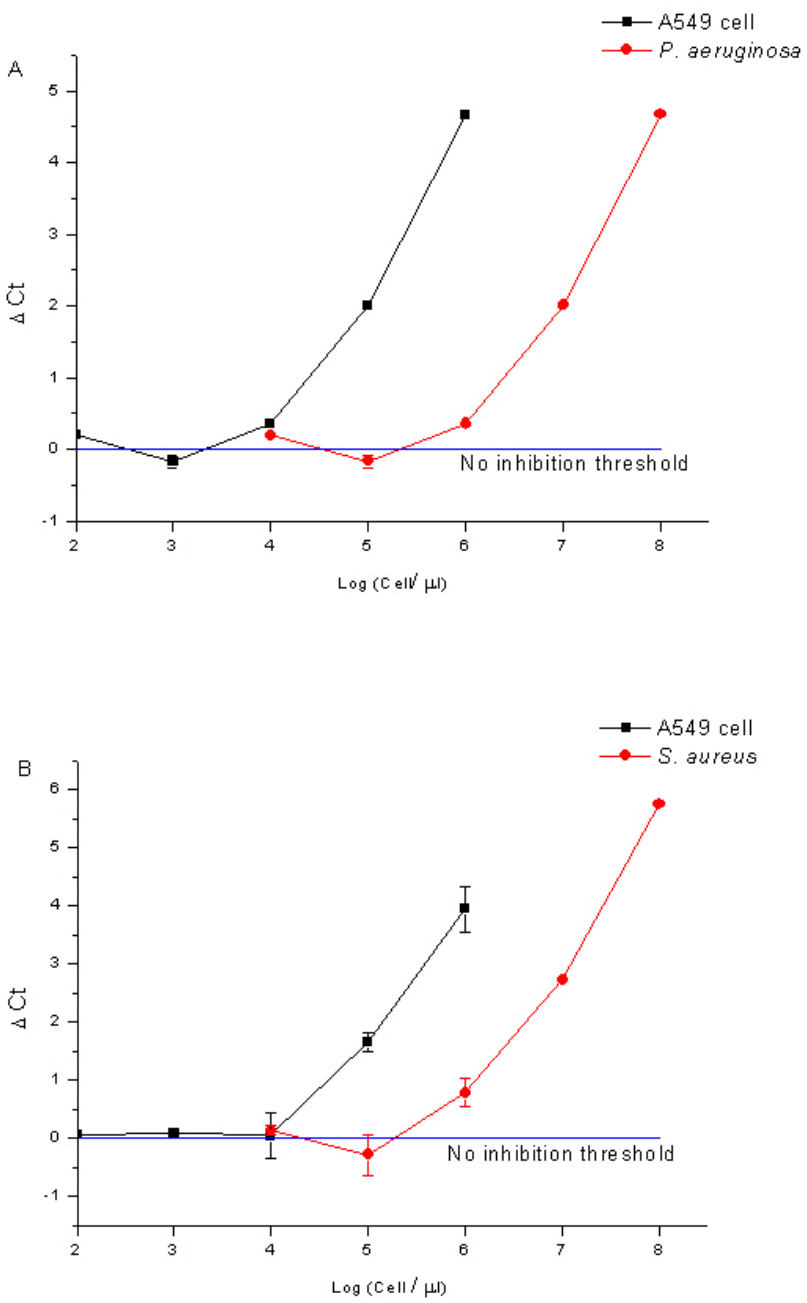

Fig. 3-16 PCR inhibition induced by the thermal lysate of A549 cells and *P. aeruginosa* using *S. aureus* genomic DNA as template (A) and PCR inhibition induced by thermal lysate of A549 cells and *S. aureus* targeting *P. aeruginosa* genomic DNA (B). ΔCt corresponded to the Ct value derived from q-PCR amplifications with cell lysate subtracted from the Ct value from identical samples without foreign cell lysate.

3.3.3 Primer specificity and q-PCR efficiency evaluation

Primer design is a crucial factor for successful q-PCR assay [128]. As the aim of this experiment is to identify one type of bacteria in a mixture of three different species from different genera, one important criterion for the primer design is to ensure that primers are at least genus specific. Therefore, the primer specificity was first evaluated by sequence alignment using NCBI online nucleotide blast tools (http://blast.ncbi.nlm.nih.gov/) and was then tested by q-PCR assay in the presence of genomic DNA of the other two species respectively in order to eliminate the possibilities of non-specific cross reactions. As demonstrated in Fig. 3-17, the designed primers exhibited excellent specificity without any undesired amplifications.

Another important factor to consider in primer design is the amplification efficiency. In this study, four orders of magnitude of *P. aeruginosa* and *S. aureus* genomic DNA copy number were tested. Aliquots with 10000, 1000, 100 and 10 copies of genomic DNA template per PCR reaction were prepared by appropriate dilutions from purified DNA extracted from of 5×10^8 CFU/ml of the respective bacterial cultures, using Qiagen DNeasy® Blood & Tissue kit. This set of DNA was used as the positive control representing 100% DNA recovery according to the kit specifications provided by the manufacture. Ct values obtained from q-PCR using DNA prepared by thermal lysis, whereby viable *P. aeruginosa* and *S. aureus* were directly added to the PCR reaction mixture at the final cell densities of 10000, 1000, 100 and 10 CFU per tube were compared against the genomic DNA copy range described above which was referenced as 100% DNA recovery to evaluate the DNA extraction efficiency by thermal lysis method. In the case of *S. aureus* related experiment, lysostaphin was added to the PCR reaction

mixture at a final concentration of 50 μg/ml and incubated with *S. aureus* cells at 37˚C for 5 minutes prior to q-PCR assay. As described in Fig. 3-18, the Ct values obtained by q-PCR analysis using diluted bacterial DNA extracted by Qiagen kit as the template as opposed to direct thermal lysis of bacterial cells without DNA purification procedure were comparable. The differences in the average Ct value between each dilution were 3.47, 3.39 and 3.27 for *P. aeruginosa*, 3.60, 3.29 and 3.97 for *S. aureus* respectively. Since the ideal Ct value difference between each 10 fold serial dilution is around 3.324 cycles, the amplification efficiency for *P. aeruginosa* and *S. aureus* primers were 95% and 90% respectively according to the equation $E=10^{(-1/\lambda)}-1$, where E is the PCR amplification efficiency and λ represents the slope of the q-PCR standard curve [36]. The physical presence of PCR products were confirmed by capillary electrophoresis chip (DNA Labchip 1000) using Agilent 2100 bioanalyzer (Agilent Technologies, USA) according to the manufacturer's protocol (Fig. 3-19), indicating that the fluorescence signals which allowed the Ct values to be derived were indeed due to productive PCR amplifications.

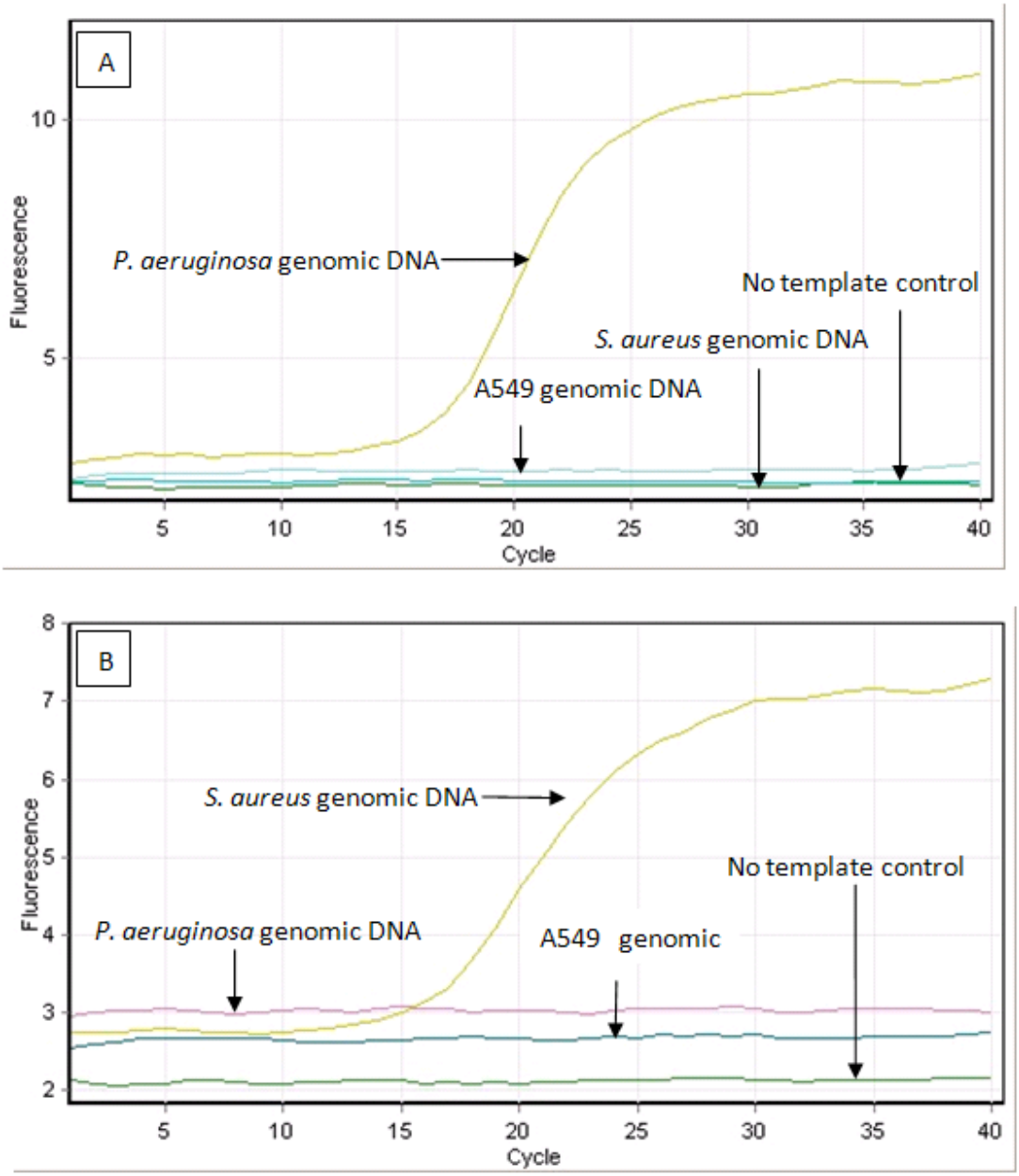

Fig. 3-17 Primer specificity validation. Primers desinged for *P. aeruginosa* were tested with genomic DNA from *S. aureus* and A549 cells (A). Similarly, primers designed for *S. aureus* were tested with genomic DNA from *P. aeruginosa* and A549 cells (B). No non-specific amplifications were observed.

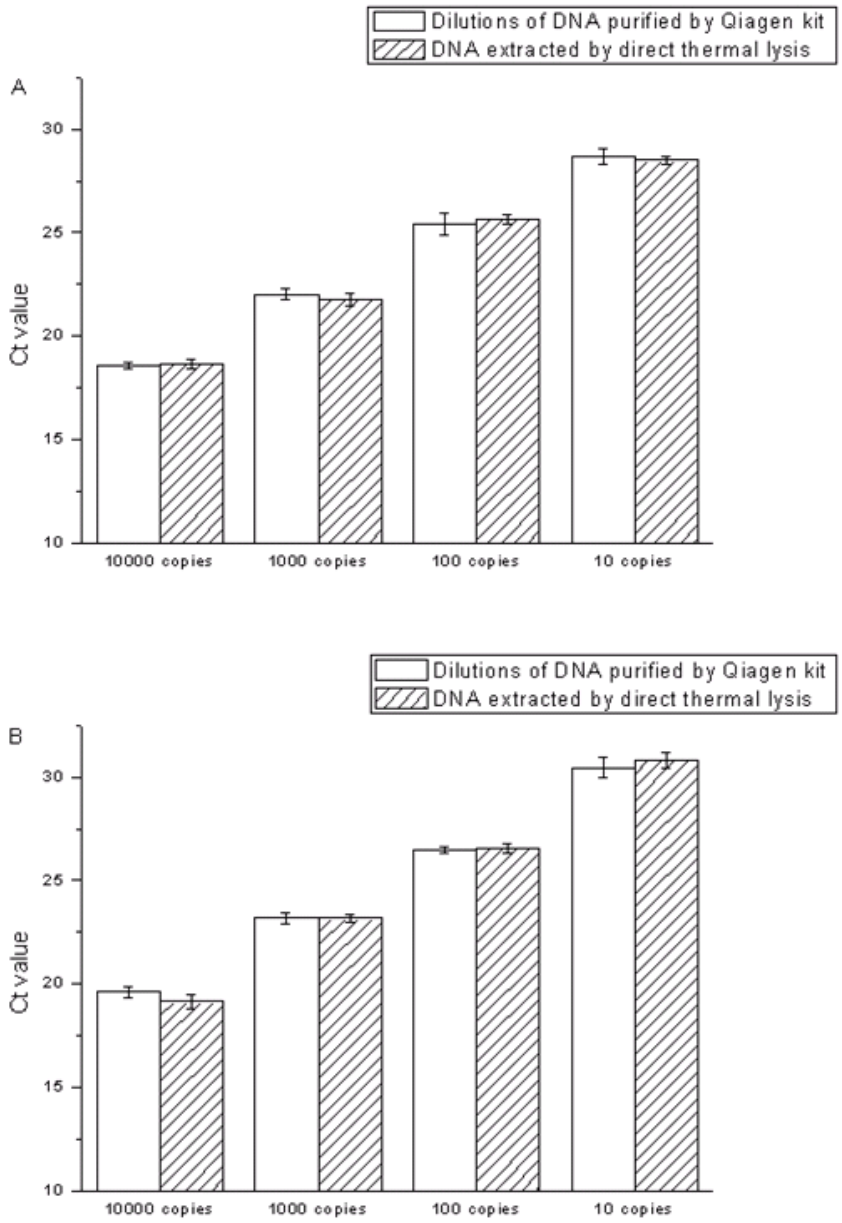

Fig. 3-18 Comparision of Ct values obtained by q-PCR assay using DNA prepared by Qiagen kit and optimal thermal lysis method from *P. aeruginosa* (A) and *S.aureus* (B) of different concentrations.

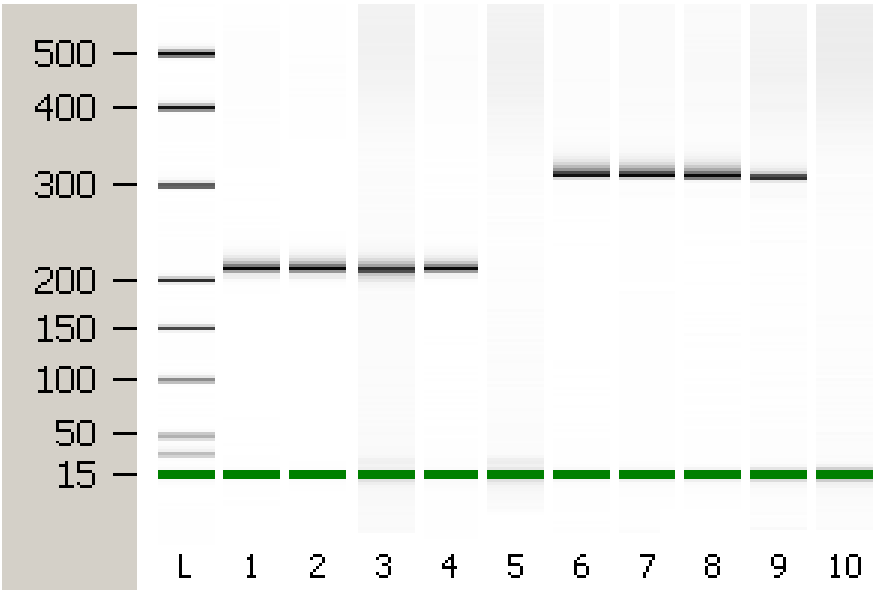

Fig. 3-19 Gel-like image of PCR products by capillary electrophoresis on a DNA Labchip 1000 using Agilent 2100 bioanalyzer. Lane L is the ladder. Lanes 1-4, PCR products with the *P. aeruginosa* DNA ranging from 10000 to 10 copy per reaction. Lane 6-9, PCR products with the *S. aureus* DNA ranging from 10000 to 10 copy per reaction. Lane 5 and Lane 10 are no template control reaction of *P.aeruginosa* and *S. aureus* genomic DNA respectively.

3.3.4 Attachment of *P. aeruginosa* and *S. aureus* in single infection context to A549 cells by CFU counting assay

The aim of this study is to develop a microfluidic system to profile the bacterial association to single host cells. To provide a biological basis to test such an application the adherence of *P. aeruginosa* and *S. aureus* to A549 cells in the single infection context was first quantified, using the CFU counting assay. As discussed in section 3.1, the method allows the bulk population of adhered bacteria to be counted and the average number per host A549 cell to be derived, but not the adherence heterogeneity between individual host cells. Monolayer of A549 cells were incubated with suspension of bacteria for 2 to 6 h at a ratio of 400 bacteria per A549 cell. Following the removal of non-

adherent bacteria by extensive washing, *P. aeruginosa* and *S. aureus* attached to A549 cells were enumerated by CFU counting using MacConkey agar to selectively recover *P. aeruginosa* and Mannitol Salt Phenol Red agar to selectively recover *S. aureus*. 62% of *P. aeruginosa* were recovered on MacConkey agar and 89% of *S. aureus* were recovered on Mannitol Salt Phenol Red agar as referenced with bacterial recovery in LB agar (data not shown). As shown in Fig. 3-20, time dependent increase of the adherence of both *P. aeruginosa* and *S. aureus* to A549 cells was observed. However, the *P. aeruginosa* association rate to A549 cells was significantly slower compared with *S. aureus*. Linear increase of bound *P. aeruginosa* with the input ratio of 400 bacteria/cell, was observed, which did not exceed 2-fold increase after six hours of infection. However, at the same MOI of 400, from a small fraction of *S. aureus* that were associated with A549 cell after two hours of infection, a more rapid increase to approximately 4-fold at four hours of infection could be observed, which then slowed down in the last two hours of infection. As a result, it can be postulated that the initial adhesion of *S. aureus* may change the cellular state of the host to attract more bacteria to migrate and bind to A549 cells.

The data showed that the average number of adherent *P. aeruginosa* and *S. aureus* per A549 cells is less than 40 and 90 respectively. Based on the optimization work described in section 3.2.2, the overloading threshold that could lead to inhibition of PCR was 10^6 and 10^5 cells per well for *P. aeruginosa* and *S. aureus* respectively. It was highly likely that the microfluidic PDMS array chip could be used to quantify the number of adherent *P. aeruginosa* or *S. aureus* to a single A549 cell without compromised detection sensitivity. Hence the single infection context was analyzed using the on-chip system as discussed in the following section.

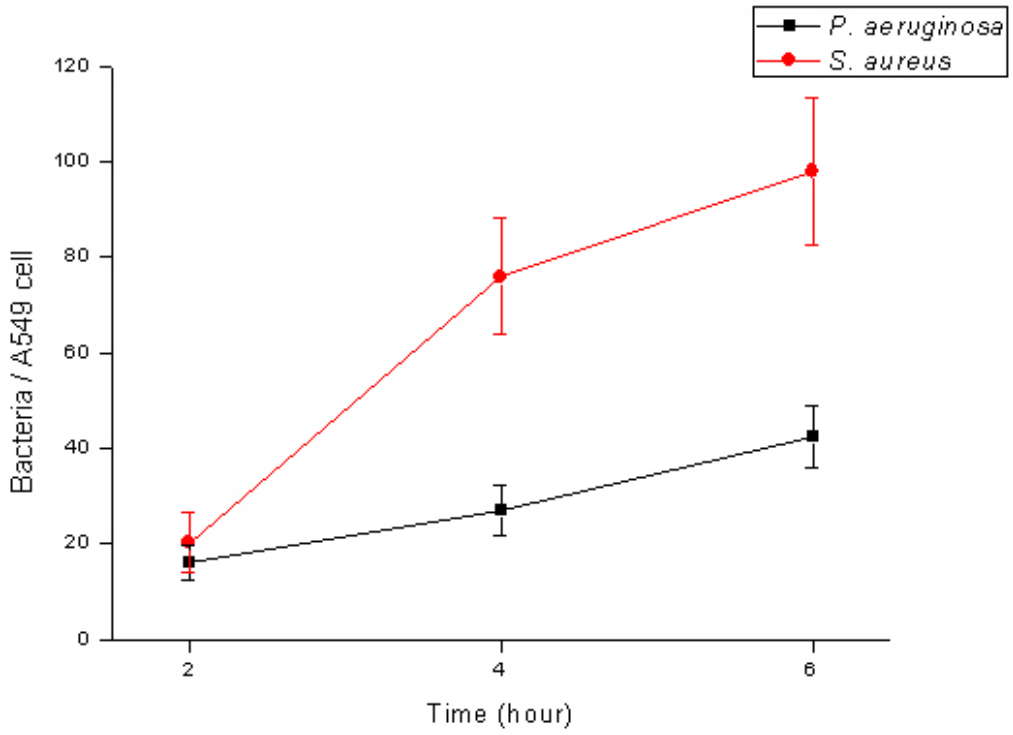

Fig. 3-20 Binding kinetics of *P. aeruginosa* and *S. aureus* to A549 cells. The association of *P. aeruginosa* and *S. aureus* with A549 cells was estimated at bacteria-to-cell ratios of 400:1. The binding data are expressed as the mean± standard error of the mean of three experiments.

3.3.5 On-chip q-PCR assay for quantification of adhered *P. aeruginosa* and *S. aureus* to single A549 cell

3.3.5.1 Thermal stability of the PDMS array chip

PCR is temperature cycling dependent reaction to amplify a specific region of DNA template. Normal PCR cycle requires denaturing the double stranded DNA at 95 ˚C to allow primer binding. As a result, thermo stable array chip with minimal liquid evaporation is important to achieve successful PCR amplification. Fig. 3-21 showed the image of the PDMS array chip loaded with FITC fluorescence dye after the first and last

thermo cycle. Fluorescence intensity of five randomly chosen wells over 40 PCR cycles were also recorded (Fig. 3-22). No significant fluorescence intensity shift was observed, indicating good thermo-stability of the PDMS array chip. PCR temperature profiling was shown in Fig. 3-23.

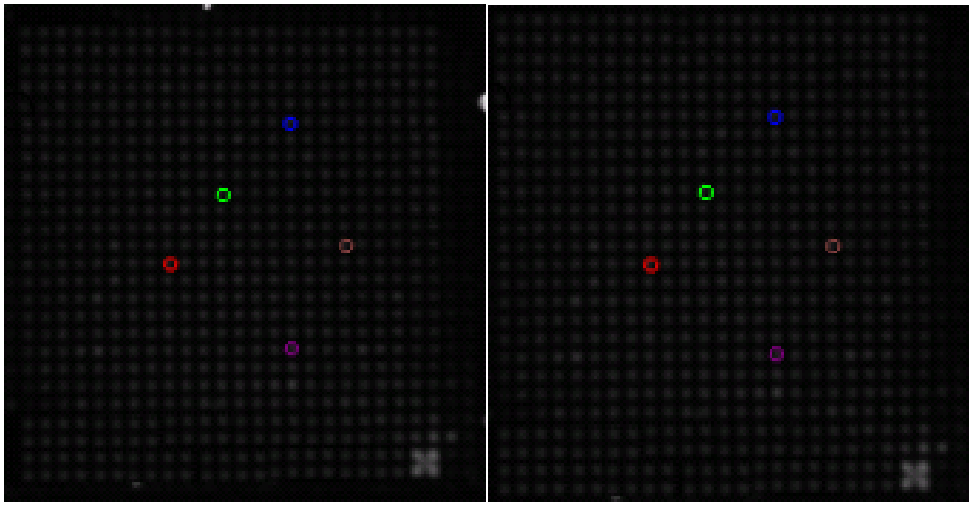

Fig. 3-21 Images of the chip loaded with fluorescence dye after the first (left) and fortieth cycle of PCR reaction.

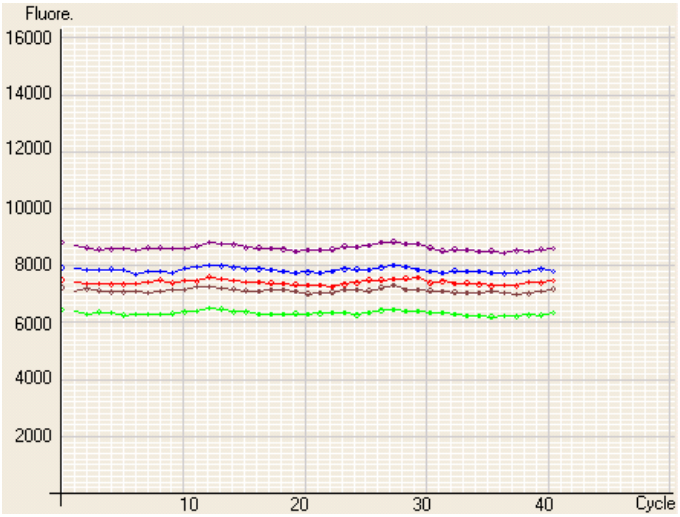

Fig. 3-22 The fluorescence intensity curve versus 40 PCR reaction cycles of five randomly chosen wells (circled).

Fig. 3-23. Temperature profiling of PCR reaction. The PCR reaction was carried out at an initial temperature at 95˚C for 5 min followed by 40 cycles of 95˚C for 30 s, 60˚C for 30 s and 72˚C for 30 s.

3.3.5.2 Construction of q-PCR standard curve

To evaluate the reproducibility and detection sensitivity of the proposed on-chip q-PCR assay, standard q-PCR amplification curves were constructed (Fig. 3-24) with four orders of magnitude of *P. aeruginosa* and *S. aureus* at 300, 30, 3, 0.3 cells per well (equivalent to 2400, 240, 24 and 2.4 cells/μl). Bacterial cells at various concentrations were loaded into the PDMS array chip as described in Fig. 3-5. The wells were then sealed with PCR grade mineral oil followed by on-chip q-PCR assay. For *S. aureus* related assays, lysostaphin of 50 μg/ml was first loaded and dried into the micro-wells of the array chip. The pre-dried lysostaphin was resuspended when *S. aureus* cell suspensions were loaded into the array chip. An additional incubation at 37˚C for 5 minutes was carried out prior to q-PCR assay. Amplification curves of single *P. aeruginosa* and *S. aureus* were acquired from wells exhibiting positive PCR amplifications with *P. aeruginosa* and *S. aureus* loaded at the cell densities of 0.3 cells per well. A total of 213 out of 900 wells showed positive amplifications at the cell density of 0.3 cells per well for *P. aeruginosa* and 205 out of 900 wells showed positive amplifications for *S. aureus* at the same cell density (Fig. 3-25). Since the theoretical detection frequency is 233 according to Poisson statistics [120], the data indicate that the

overall successful rate for single *P. aeruginosa* and *S. aureus* cell detection was 90% and 94% respectively. No amplifications were observed in the negative control (for Fig. 3-25) without *P. aeruginosa* or *S. aureus* added to the PCR reaction mixture. Ct values obtained in the different wells showing positive PCR amplifications were well clustered for each cell density level with the standard deviations of less than 0.35. Primer dimer formation was not observed in this experiment. The standard curves were therefore considered adequate to be used as the reference to quantify *P. aeruginosa* and *S. aureus* adherence to single A549 cells.

3.3.5.3 *P. aeruginosa* and *S. aureus* association kinetics to single A549 cell

Bacterial pathogens do not infect the host tissue in a cell-by-cell fashion. However, as the infection progresses, the number of adhered bacteria does differ within the host cell population [129, 130]. The proposed microfluidic PDMS array chip provided a convenient tool to study the consequences of this heterogeneity in bacterial adherence profile without the necessities to label the bacteria with fluorescence probes. Attachment of *P. aeruginosa* and *S. aureus* to single A549 cells, infected to the endpoints of 2h, 4h, and 6h were quantified by on-chip q-PCR assay. As shown in Fig. 3-26, the number of *P. aeruginosa* attached to single A549 cells was clustered within 14-20 at the endpoint of 2h infection. However, when A549 cells were exposed to *P. aeruginosa* for 4 hours of infection, a minority group of around 20% of the A549 cells was associated with more *P. aeruginosa* cells in the range of 32-41 as compared with 80% of the A549 cells with 21-31 *P. aeruginosa* attached. This deviation was further enlarged to 30% of the A549 cell population with 46-59 *P. aeruginosa* cells attached, compared with 70% with only 35-45 bacteria adhered at the endpoint of 6 hours of infection. Assuming that the binding of the

bacteria to the host cell is irreversible, it can be postulated that an increasing proportion of the A549 cells had become more prone to bacterial association when the host cells were challenged with infection for prolonged period of time. Considering that *P. aeruginosa* is an opportunistic human pathogen, it is possible that host cells which have differentiated as a consequence of bacterial adherence in the earlier stage have become more susceptible to further bacterial adherence and hence disease development.

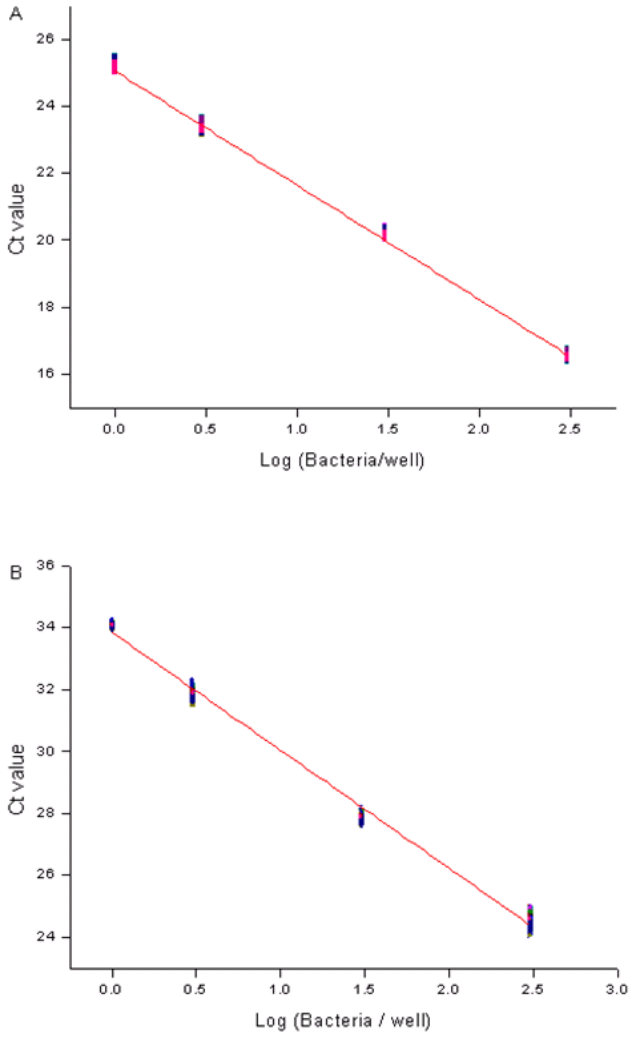

Fig. 3-24 q-PCR standard curve of *P. aeruginosa* (A) and *S. aureus* (B) at 300, 30, 3, and single cell levels.

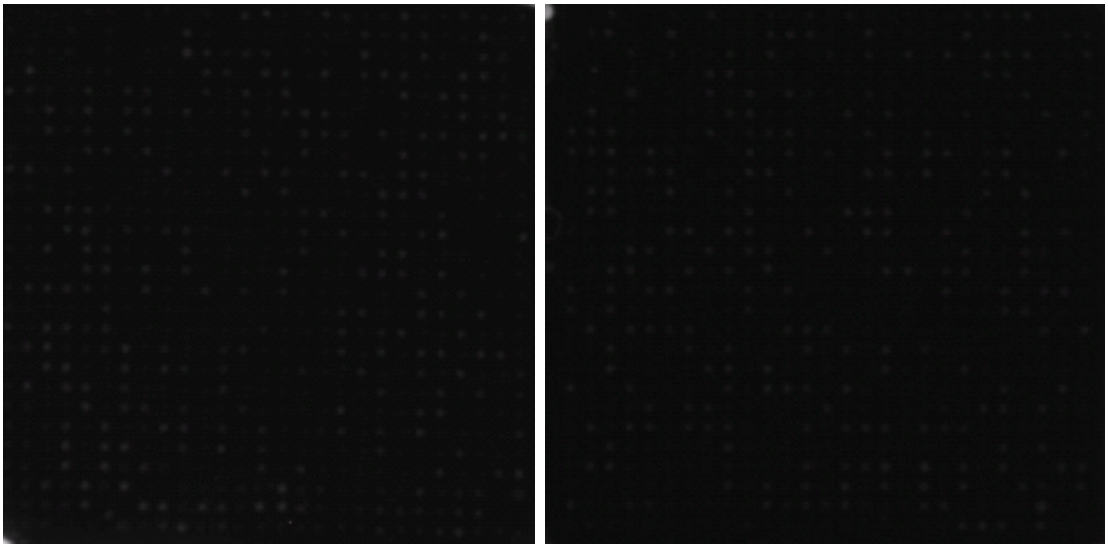

Fig. 3-25 q-PCR amplification of *P. aeruginosa* (left) and *S. aureus* (right) at single cell level. Image of the microfluidic PDMS array chip was taken after the completion of PCR cycling.

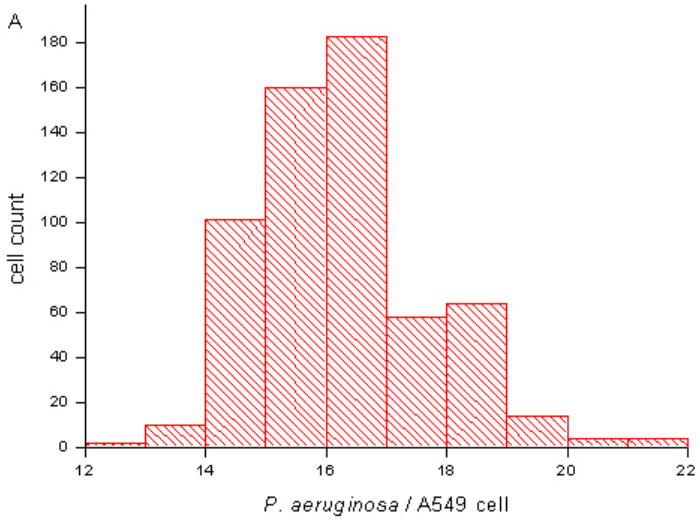

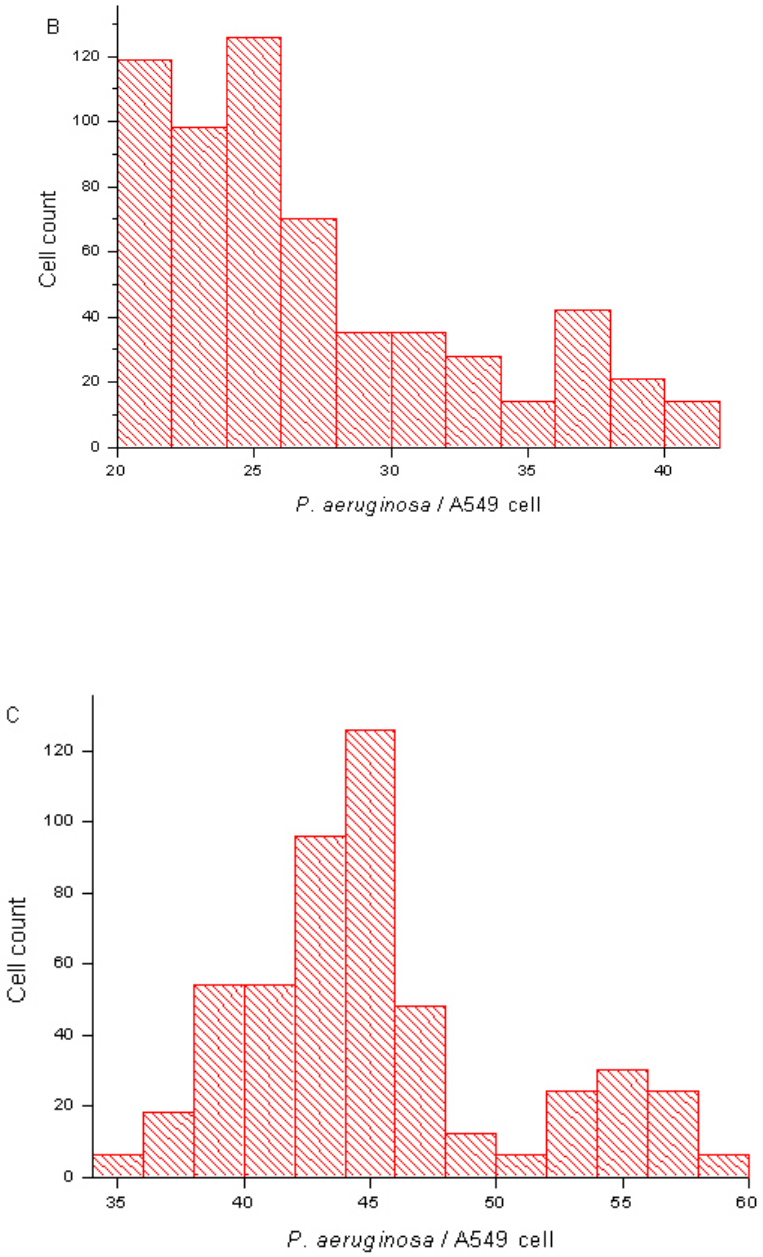

Fig. 3-26 *P. aeruginosa* association profiling to single A549 cells at the end of 2h (A), 4h (B) and 6h (C) infection. Data were representative of results collected from three independent experiments.

On the other hand, this bimodal distribution in the number of *S. aureus* associated to single A549 cells was observed as early as 2h of infection, with around 54% of A549

cells associated with 16-20 cells of *S. aureus* compared to 46% of A549 cells associated with 21-24 cells of *S. aureus* (Fig. 3-27 A). At the endpoint of 4h infection, the association profile of *S. aureus* to single A549 cells resembled a trimodal distribution with 11% of A549 cells attached with 51-57 of *S. aureus*, 74% of A549 cells with 58-70 of *S. aureus*, 15% of A549 cells with 71-77 of *S. aureus* (Fig. 3-27 B.). When A549 cells were challenged to bacterial infection for 6h, the majority of A549 cells (nearly 90%) were associated with *S. aureus* cells in the numerical range of 85-100 (Fig. 3-27 C).This phenomenon revealed a different infection pattern of *S. aureus* as compared with *P. aeruginosa*. When A549 cells were infected with *S. aureus* for a short period of 2 hours, the host population could be differentiated into two groups in near half and half ratio with one group appearing more capable to attract more bacteria than the other group. However, this differentiation of host cells in bacterial attachment was reduced as infection progress to 6 hours with the rapid overall increase in bacterial association of up to 4 folds.

The data in this experiment demonstrated that by analyzing the bacterial adherence to single host cells using the microfluidic platform, biological information at a deeper level can be derived than by conventional analysis of adhered bacterial population averaged to per host cell (Fig. 3-20). Such information can pave the way towards clearer elucidation of the mechanism of bacterial pathogenesis.

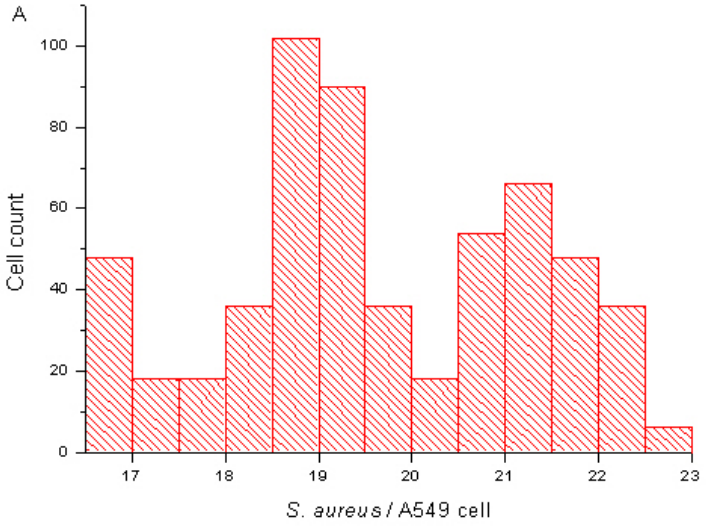
A
Cell count
0
20
40
60
80
100
17
18
19
20
21
22
23
S. aureus / A549 cell

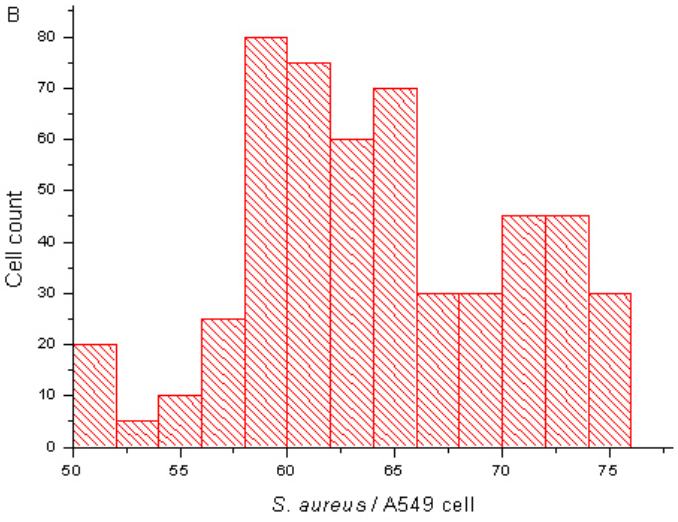
B
Cell count
0
10
20
30
40
50
60
70
80
50
55
60
65
70
75
S. aureus / A549 cell

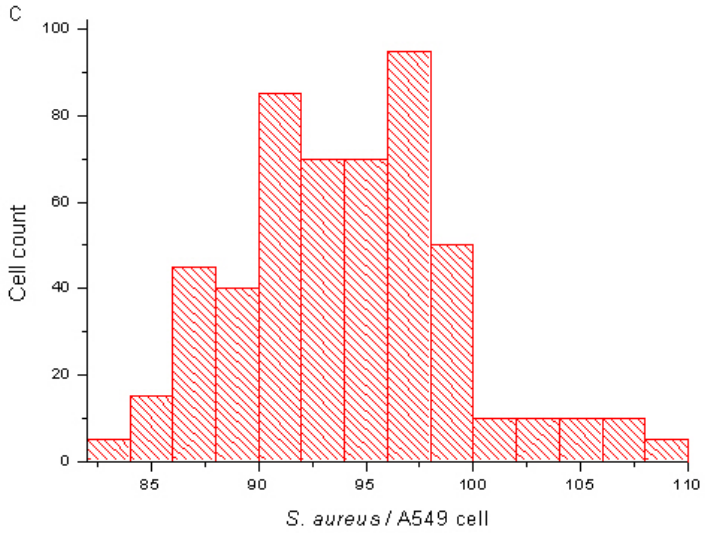

Fig. 3-27 *S. aureus* association profiling to single A549 cells at the end of 2h (A), 4h (B) and 6h (C) infection. Data were representative of results collected from three independent experiments.

3.3.6 Quantification of *P. aeruginosa* and *S. aureus* in mixed infection context

Co-existence *of P. aeruginosa* and *S. aureus* during cystic fibrosis lung infections has been demonstrated by various techniques [129, 130]. However, beyond that, not much more is known about the lung infections caused by mixed *P. aeruginosa* and *S. aureus* communities currently. The proposed microfluidic q-PCR system could also contribute to this area of study in bacterial attachment profiling of adhered *P. aeruginosa* and *S. aureus* to single A549 cells by incorporating on-chip multiplex q-PCR assay. The primer specificity for multiplex q-PCR assay was validated in section 3.3.3. Similar to bacterial infection analysis in single infection context, the associated bacteria was first enumerated by CFU counting assay. As shown in Fig. 3-28, at the endpoint of 2 hour infection, the bound *S. aureus* and *P. aeruginosa* in mixed infection was comparable to the number of attached bacteria in single infection context. However, the number of adhered *P.*

aeruginosa decreased by approximately 40% when mixed infected with *S. aureus* after 4 hours and 6 hours of infection. Slight inhibition of *S. aureus* attachment around 8% was also observed in co-infection with *P. aeruginosa* at the same time point. Therefore, it can be speculated that the *S. aureus* and *P. aeruginosa* compete for the binding sites to the host cells during mixed infection. For instance, the rapid association *S. aureus* may have covered some binding sites of A549 for *P. aeruginosa*.

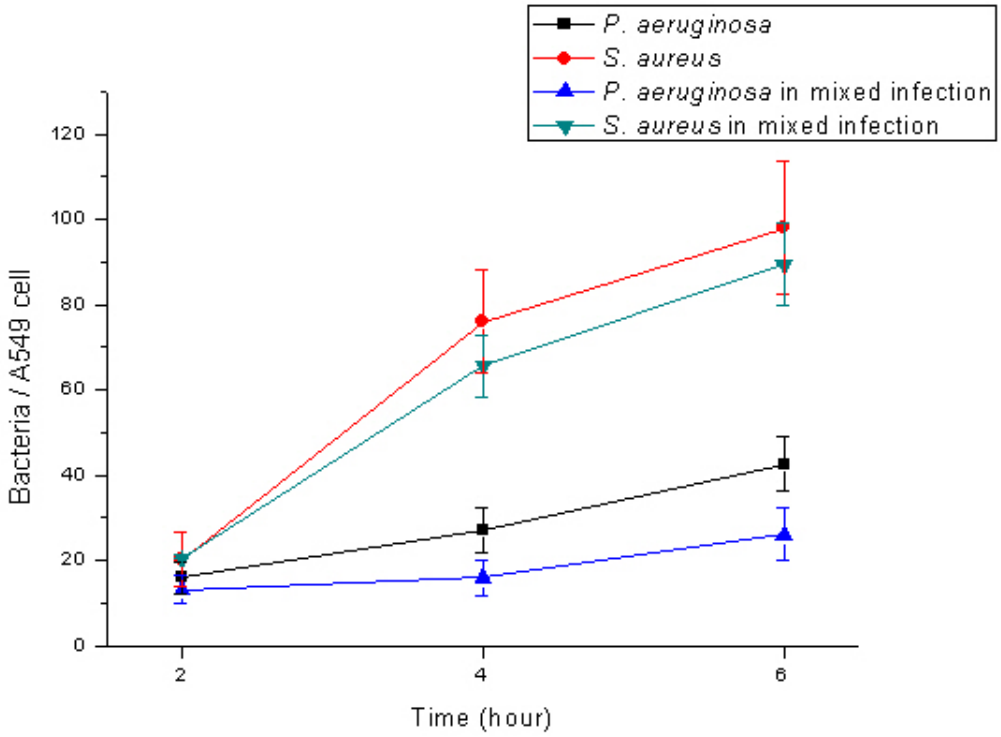

Fig. 3-28 The association of *P. aeruginosa* and *S. aureus* with A549 cells during mixed infection. Cultured A549 cells were incubated with bacterial mixtures containing *S. aureus* and *P. aeruginosa* with the MOI of 400. The binding data are expressed as the mean± standard error of the mean of three experiments.

Mutiplex q-PCR is a technique to simultaneously quantify more than one DNA target in one reaction by TaqMan® probe–based assays [35]. In multiplex q-PCR analysis,

the PCR products of different DNA targets are monitored by TaqMan® probes labelled with specific fluorescent dye, resulting in different emission colours for each amplification assay. This method was incorporated in the microfluidic PDMS array chip to quantify the adhesion of *P. aeruginosa* and *S. aureus* to single A549 cells during mixed infection. At the endpoint of mixed infections at different time intervals, single A549 cells were isolated into the individual micro-wells together with primers and probes for both bacteria. Amplification curves of *P. aeruginosa* and *S. aureus* were obtained by multiplex q-PCR with FAM and Cys-5 labelled TaqMan® probe respectively as summarized in Table 3-1. The number of *P. aeruginosa* and *S. aureus* to the same A549 cell was estimated according to Ct values attained and the corresponding standard curves. The attachment profile of *P. aeruginosa* and *S. aureus* in mixed infection was shown in Fig. 3-29 with each dot representing a single A549 cell with the number of *P. aeruginosa* and *S. aureus* matched in the horizontal axis and the vertical axis respectively. When A549 cells were exposed to mixed infection after 2 hours, the attachment of *P. aeruginosa* and *S. aureus* showed no apparent correlation (Fig. 3-29A scatter plot), being independent from each other and comparable to the number of attached bacteria in single infection context. The association profiles of both bacteria (Fig. 3-29A histogram) were similar when compared to their single infection context (Fig. 3-26/Fig. 3-27, A). However, when A549 cells were infected for prolonged periods of 4 hours and 6 hours, *P. aeruginosa* adhesion is significantly inhibited in the presence of *S. aureus* as evidenced by the negatively correlation between the number of *P. aeruginosa* and *S. aureus* association to single A549 cells (Fig. 3-29 B and C scatter plots). This finding was consistent with the previous postulation that *S. aureus* and *P. aeruginosa* compete for binding sites to the host cells

during mixed infection and that the rapid association of *S. aureus* may have covered some binding sites of A549 cells for *P. aeruginosa* as shown by CFU counting assay (Fig. 3-28). The association profiles of both bacteria during mixed infection at 4 hours and 6 hours (Fig. 3-29 B and C, histograms) were different when compared to their single infections at the corresponding time points (Fig. 3-26/Fig. 3-27, B and C). The mixed infection setting showed (i) lower number of bacterial cells attached to individual host cell and (ii) enlarged variations of the number of bacteria attached, as a result of the interference by the other bacteria.

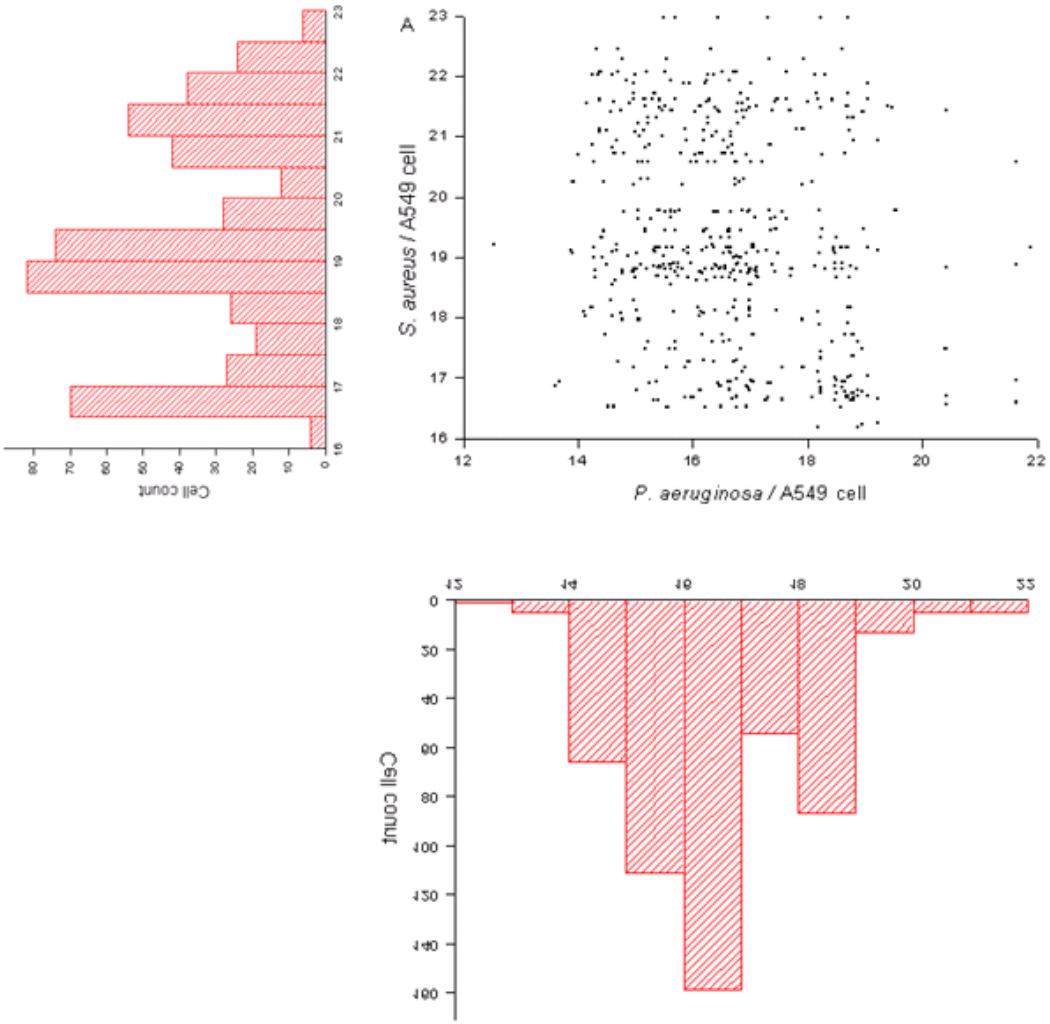

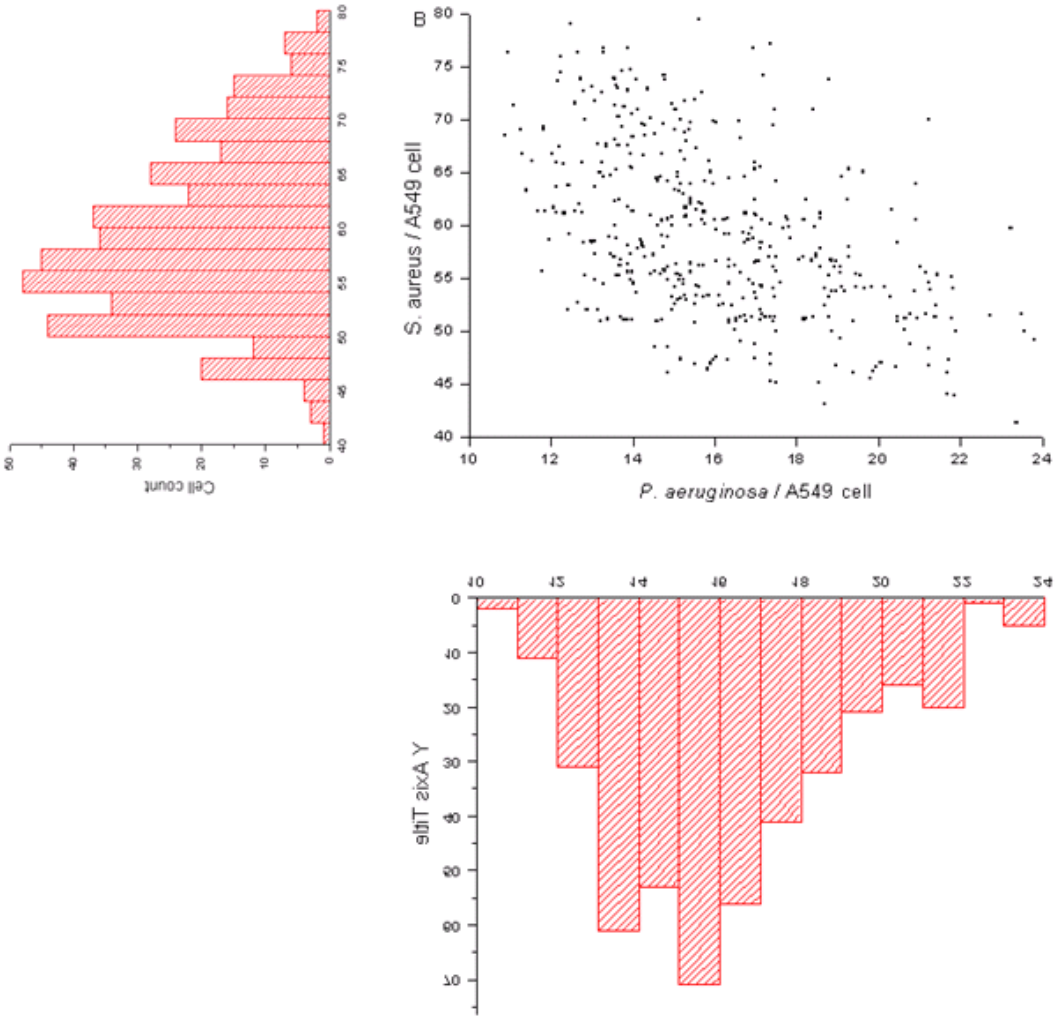
B
S. aureus / A549 cell
P. aeruginosa / A549 cell
Cell count
Y Axis Title

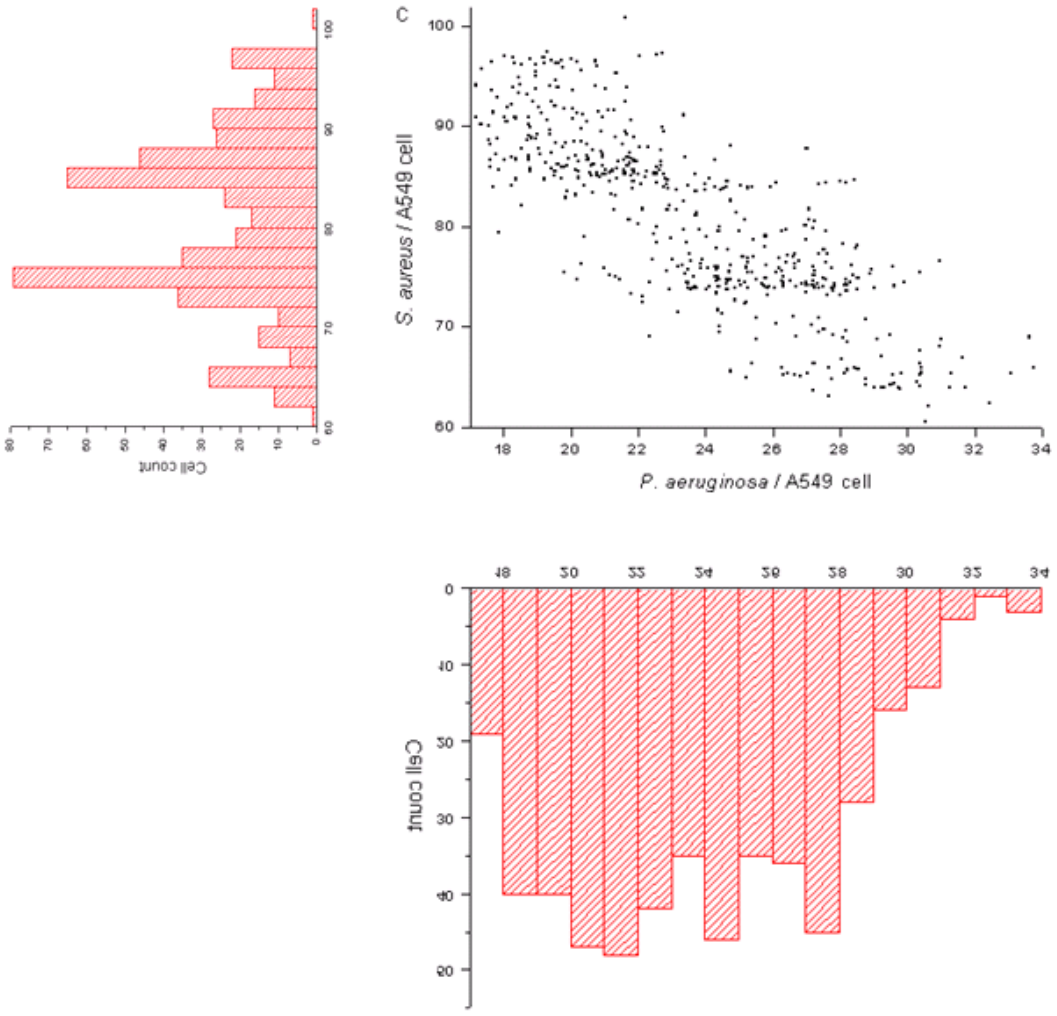

Fig. 3-29 *P. aeruginosa* and *S. aureus* association profiling in mixed infection context to single A549 cells at the end of 2h (A), 4h (B) and 6h (C). The histograms of *P. aeruginsoa* and *S. aureus* adherance profile to single A549 cell in mixed infections were shown next to the corresponding axes for ease of comparison with the histograms obtained during single infections (Fig 3-25 and 3-26). Data were representative of results collected in three independent experiments.

3.3.7 Cytotoxicity of *P. aeruginosa* and *S. aureus* to A549 cells

Bacteria can manipulate the host cell death via necrosis or apoptosis, leading to what is observed as "cytotoxicity". In this experiment, trypan blue exclusion assay was used to determine the cytotoxic effect of *P. aeruginosa* and *S. aureus* to A549 cells.

Trypan blue is a pigment dye that can selectively penetrate into the dead cells with blue stain while live cells with intact membrane will not be colored [131]. A549 cells without bacteria inoculation served as a control. The viability of bacteria infected A549 cells were accessed by cell counting under the microscope. As shown in Fig. 3-30, *P. aeruginosa* PAO1 was not cytotoxic to the host A549 cells while *S. aureus* was slightly cytotoxic only after 6 hours of infection. This cytotoxic effect was inhibited in mixed infection with *P. aeruginosa* (Fig. 3-31), possibly due to the reduced attachment of *S. aureus* to the host cells (Fig. 3-28). A549 cells were treated with 1% paraformaldehyde to serve as the positive control for trypan blue exclusion assay. This is because such treatment would render the cells nonviable, and therefore, would be colored by trypan blue dye. Typan blue stains more than 99.99% of paraformaldehyde treated A549 cells but non-treated cells were not colored, indicating that the true cytotoxic effect of *P. aeruginosa* and *S. aureus* to A549 cells can be reflected by Fig. 3-30 and Fig. 3-31.Since there appears to be a correlation between the cytotoxic effect of *S. aureus* and its cumulative association with the host A549 cell, the microfluidic PDMS array chip developed in this study may be utilized in combination with related experiments to provide greater insight to this process of disease development.

3.4 Conclusion

In this study, a high throughput microfluidic PDMS array chip for quantification of bacterial adherence to single host cells by q-PCR assay was demonstrated. The chip was robust, cost-efficient, easy to fabricate, and allows label-free quantification of adhered bacteria with one-step microfluidic operation. The platform is able to detect down to single *P. aeruginosa* and *S. aureus* with good reproducibility. Using this new device,

the association profiling of *P. aeruginosa* and *S. aureus* to single human lung epithelial A549 cells at different time point of infection in both single and mixed infection contexts was successfully obtained, the information of which provide a deeper level elucidation of the mechanism of bacterial pathogenesis. The introduction of this microfluidic PDMS array chip to biological laboratories will provide a convenient tool to investigate pathogen-host interactions, as well as other genetic analysis for single mammalian cells.

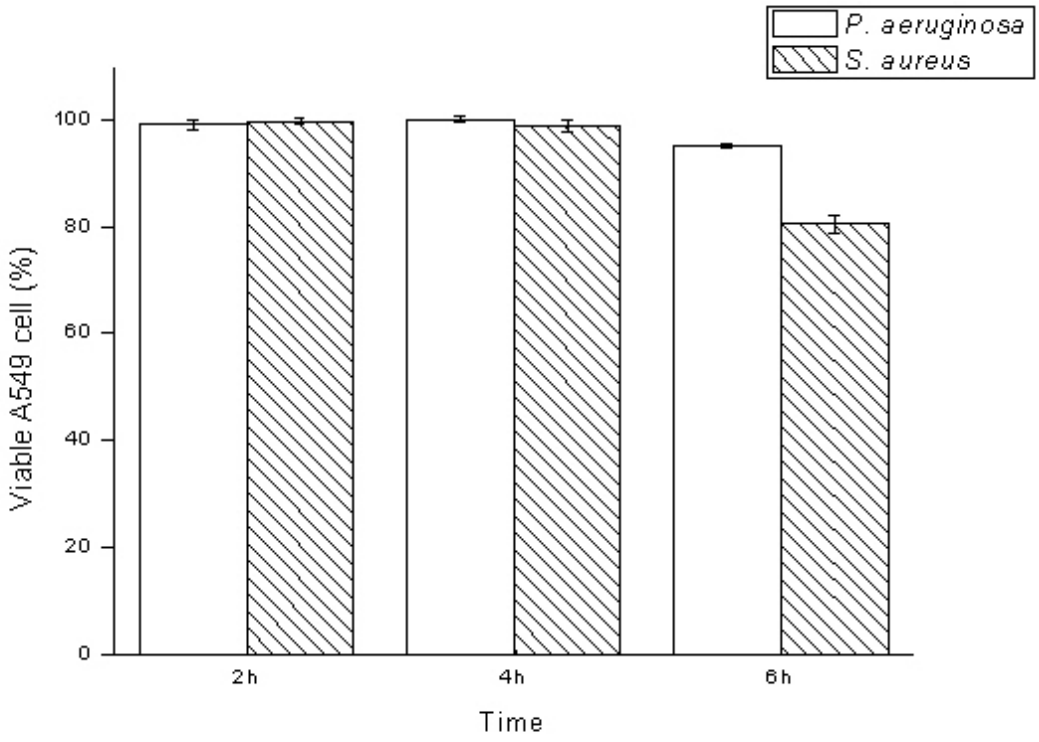

Fig. 3-30 Cytotoxicity of *P. aeruginosa* and *S. aureus* A549 cells evaluated by trypan blue exclusion assays. A549 cells (5×10^5) were co-cultured with each strain at a multiplicity of infection of 400. Cell viability was accessed by observation under microscope. Each point represents the mean ± standard error of the mean of three replicated experiments.

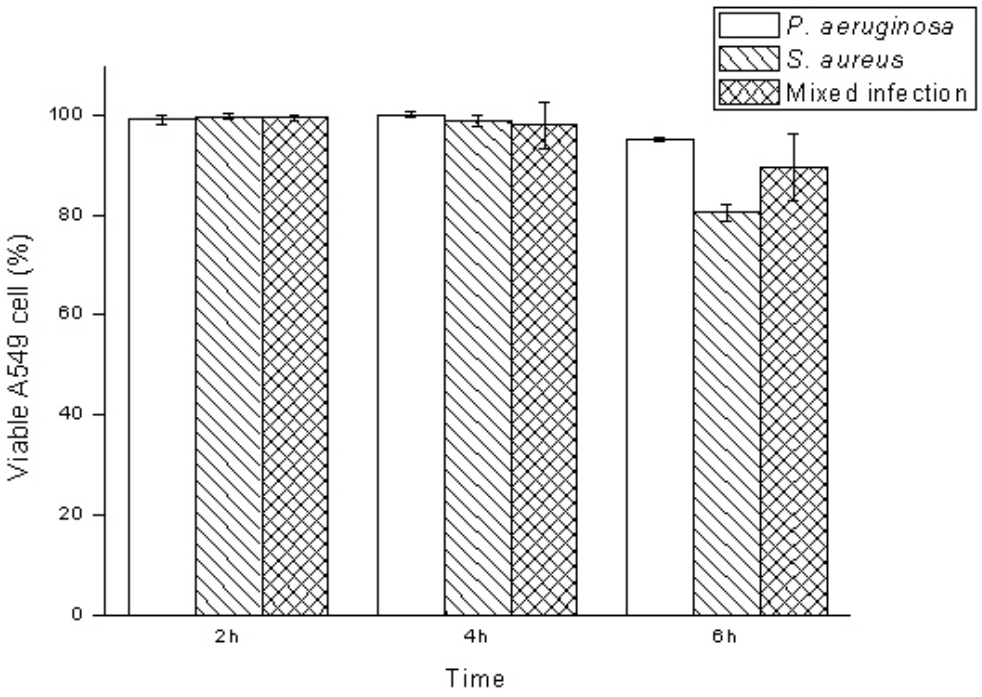

Fig. 3-31. Cytotoxicity of A549 cells mixed infected with *P. aeruginosa* and *S. aureus* evaluated by trypan blue exclusion assay. Cultured A549 cells were incubated with bacterial mixtures containing *S. aureus* and *P. aeruginosa* with the MOI of 400. Each point represents the mean ± standard error of the mean of three replicated experiments.

Chapter 4 High throughput microfluidic liquid phase nucleic acid purification chip to quantify transcriptional gene regulation of bacteria attached to single host cells

4.1 Overview

Purification of nucleic acids from small amount of bacteria in minute volume is important in many clinical and biological applications. A novel microfluidic liquid phase nucleic acid purification chip was developed in this study to selectively isolate DNA or RNA from a small number of bacterial cells in the range of 5000 down to single bacterium in 1 μl or 125 nl sample volume and directly detectable by on-chip quantitative PCR in the same micro-wells. The aqueous phase bacterial lysate was isolated in an array of micro-wells, after which an immiscible organic (phenol-chloroform) phase was introduced in a polydimethylsiloxane (PDMS) headspace channel connecting the micro-well array. Continuous flow of the organic phase increases the interfacial contact with the aqueous phase for sufficient partitioning of the undesirable bio-molecules from the aqueous phase into the organic phase to achieve purification of target nucleic acid in the micro-wells. Residual organic phase was removed by repeated washing and vacuum evaporating with 70% ethanol. PCR reaction mixture was then distributed into the micro-wells array by vacuum facilitated microfluidics for on-chip amplification to avoid loss of nucleic acids caused by liquid transfer. DNA or RNA from 5000 to 5 bacteria, including both gram-positive (*S. aureus*) and gram-negative (*P. aeruginosa*) bacteria in 1μl sample volume, can be selectively isolated depending on the pH of the organic phase and amplified by both off-chip and on-chip quantitative PCR. The nucleic acid recovery yield

was up to 10 folds higher compared with the conventional column based nucleic acid extraction method. To accomplish high throughput nucleic acid analysis from single bacterium, the nucleic acid purification device was further modified into a two dimensional format with 900 micro-wells to hold the liquid of around 125 nl. Single bacterium was trapped in the individual wells by loading diluted cell suspensions of less than 0.3 CFU/well. High throughput RNA extraction from single bacterium compatible with on-chip PCR analysis was achieved for the first time. This liquid phase nucleic acid purification device presents a simple and effective solution for nucleic acid preparation and analysis and can be integrated for automated bacterial pathogen detection and high throughput transcriptional profiling assays. This chip was further applied to investigate the transcriptional gene regulation of *P. aeruginosa* to single human lung epithelial A549 cells and reported the up regulation of a gene involved in *P. aeruginosa* outer membrane antigen synthesis, named as *rmd* gene, in response to greater adherence of *P. aeruginosa* population. The flow chart of methods adopted in this chapter is outlined in Fig. 4-1.

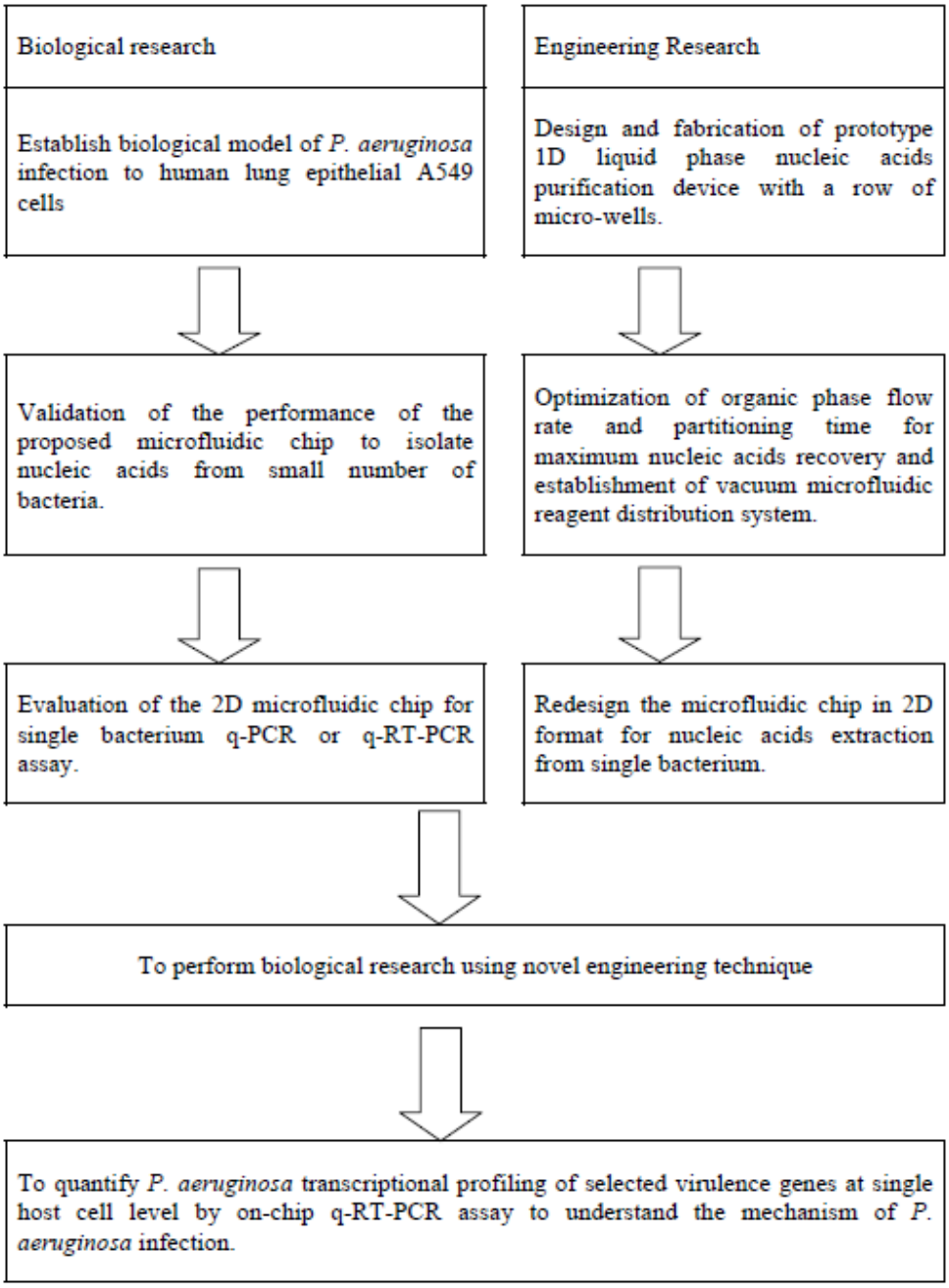

Fig. 4-1 Flow chart of methods adopted in this chapter.

4.2 Materials and Methods

4.2.1 Chip design and fabrication

As shown in Fig. 4-2, the core structure of the liquid phase nucleic acid purification chip consisted of a one dimensional array of PDMS micro-wells of 1mm×1mm×1mm that can the hold sample liquid of approximate 1 μl, a PDMS headspace channel of 20 mm (length) × 3 mm (width) × 1 mm (height) connecting the well array for phase partitioning, and a PDMS protector layer with two round fluidic openings of 3.18 mm in diameter at both ends of the headspace channel. The PDMS structure were patterned using a pulsed CO_2 laser cutting instrument as previously described [132]. Briefly, Dow Corning Sylgard 184 PDMS polymer (10:1 parts A and B) were homogenously mixed and then subjected to vacuum for 30 min to remove the air bubbles. Desired thickness of the PDMS layers was achieved by volume controlled casting of PDMS mixture on an elevated surface in an oven at 80 ˚C for 3 hours. The PDMS layer was then patterned using a commercial CO_2 laser cutting instrument (VersaLaser VLS 2.30 from Universal Laser System Inc). The PDMS core structure was sandwiched by a piece of glass slide to form the bottom of the micro-wells and an acrylic embracer placed on top of the protector layer to form the headspace channel. The inflow and outflow of the organic phase were directed by an inlet and an outlet Teflon tubing with the inner diameter of 1.32 mm and outer diameter of 1.93 mm. Both inlet and outlet Teflon tubings were connected to the headspace channel by insertion into silicon tubing with an inner diameter of 1.60 mm and an outer diameter of 3.18 mm to prevent liquid leakage. The inlet Teflon tubing was connected to a polypropylene syringe. Flow rate of the organic phase was controlled by a programmable syringe pump.

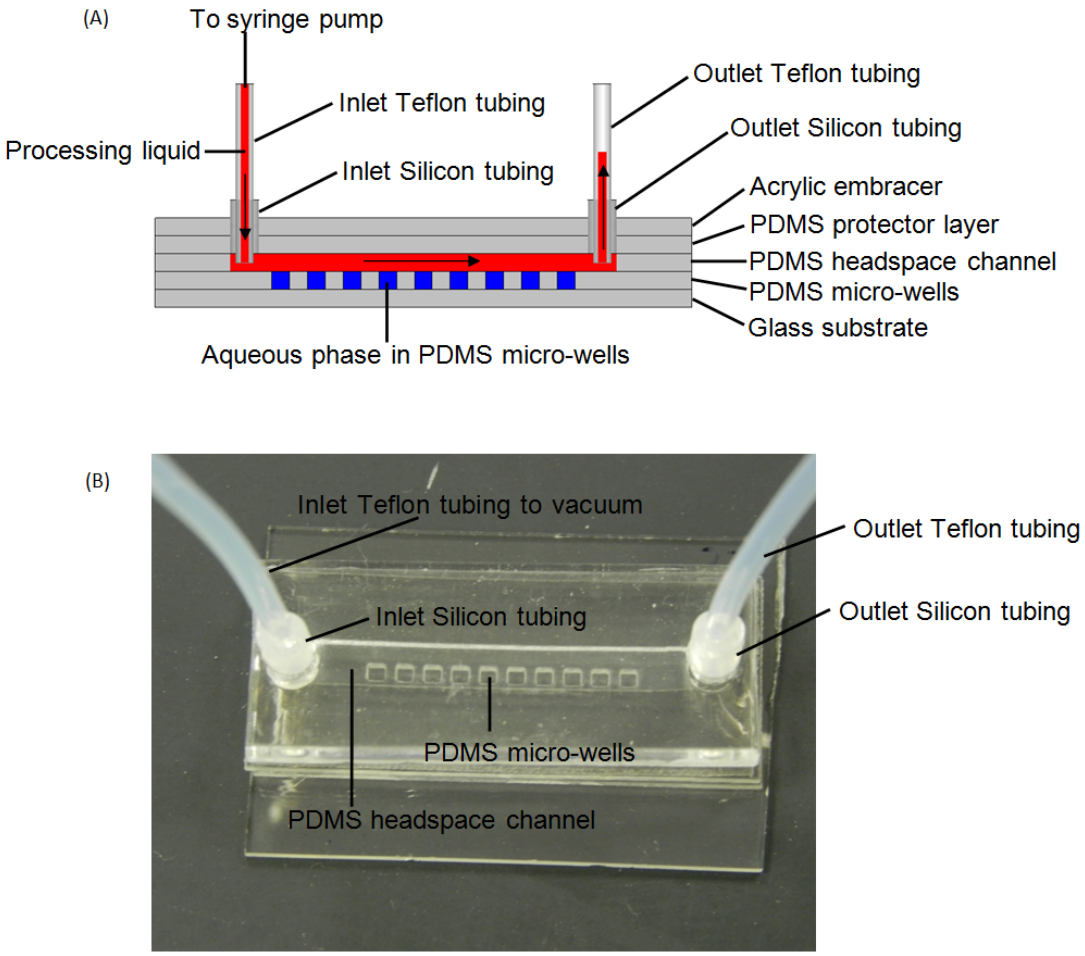

Fig. 4-2 Schematic (A) and photo (B) of the liquid phase nucleic acid purification chip. The processing liquid includes PCI organic phase, 70% ethanol and PCR reaction mixture depending on different steps of nucleic acid extraction and on-chip PCR analysis.

4.2.2 pH dependent phase partitioning of protein, DNA and RNA in the nucleic acid purification chip

Fig. 4-3 shows the working principle of the proposed liquid phase nucleic acid purification chip. Aqueous phase containing DNA, RNA and protein as the model macro-biomolecule analytes were isolated in the array of micro-wells after which the immiscible organic phase was introduced into the headspace channel at different flow rates to

evaluate the on-chip phase partitioning efficiency. Bovine serum albumin (BSA) protein conjugated with fluorescein isothiocyanate (FITC) fluorescence dye (Sigma, Singapore), genomic DNA or total RNA purified from *P. aeruginosa* PAO1 cells (ATCC, USA) were dissolved in either Tris-EDTA (TE) buffer (10 mM Tris base, 1mM EDTA, 0.1% Triton X-100, pH 8) or Sodium acetate-Acetic acid- EDTA (SAE) buffer (5 mM Sodium acetate, 5 mM Acetic acid, 1mM EDTA, 0.1% TritonX-100, pH 4.6) as the aqueous phase. The organic phase was a mixture of phenol, chloroform, and isoamyl alcohol (Ambion, USA) at the volume ratio of 25: 24:1 (pH 8) for DNA extraction and 125:24:1 (pH 4.6) for RNA extraction (Ambion, USA) respectively. The organic phase was equilibrated with either TE buffer to SAE buffer prior to usage. The analytes at the concentration of 0.1 μg/μl were pipetted into the micro-wells of the nucleic acid purification chip. The organic phase at either pH 8.0 or pH 4.6 was then introduced into the headspace channel at the flow rates of 0.25 ml/min, 0.45 ml/min, and 0.65 ml/min in 5 s cycles of continuous forward and backward flow over a duration of 15 min to facilitate phase partitioning of the analytes in the micro-wells (Fig. 4-3 A-C). Fluorescence labeled BSA retained in the aqueous phase after phase partitioning was quantified using a fluorescence imager (StarCycler, Star Array Pte Ltd, Singapore) [45], while DNA and RNA were rinsed out of the micro-wells and quantified by Picogreen DNA quantization kit and Ribogreen RNA quantification kit respectively (Invitrogen, USA) following the manufacturer's protocol.

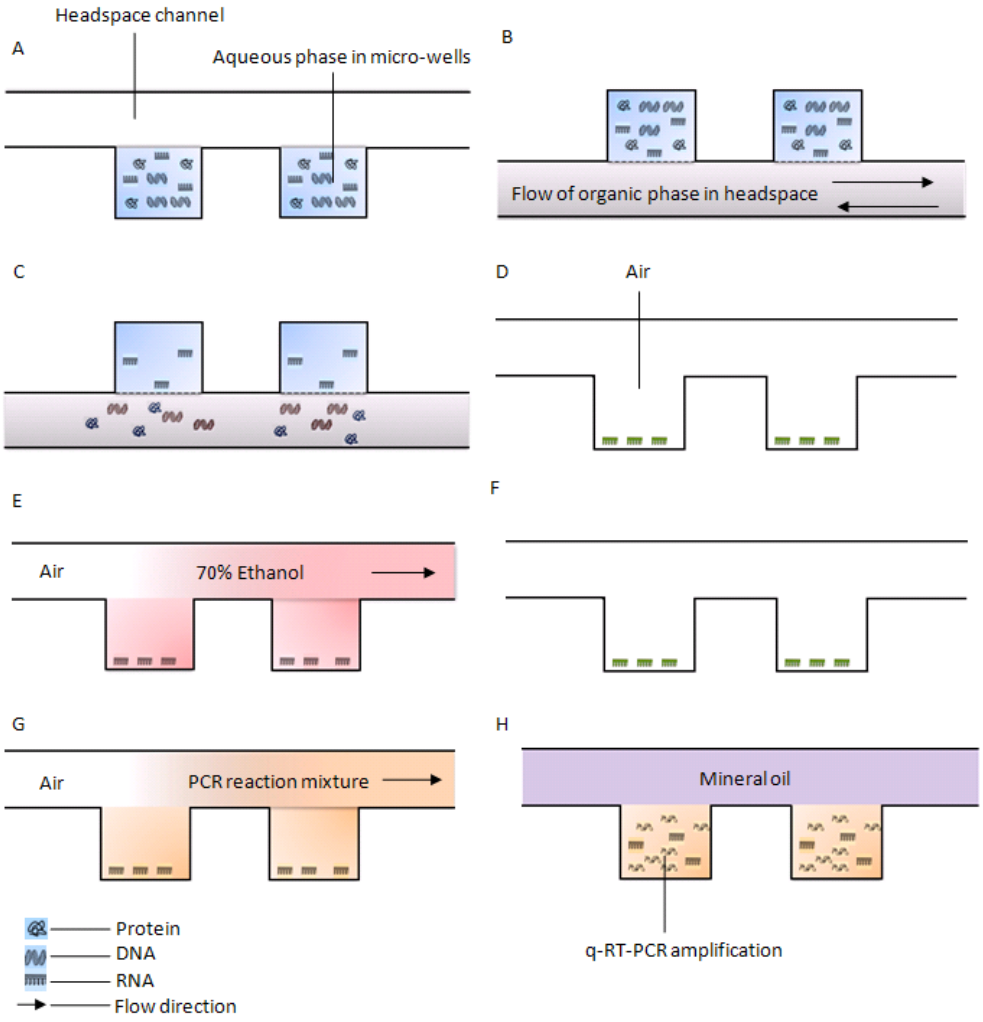

Fig. 4-3 Schematic of the RNA purification process using the liquidphase nucleic acid purification chip. (A) An aqueous phase containing DNA, RNA, and protein as the model macrobiomolecules of bacterial lysate was isolated in the micro-wells. (B) Organic phase of PCI equilibrated at pH 4.6 was introduced into the headspace channel with continuous forward and reverse flow. In the case of on-chip DNA extraction, an organic phase with a pH of 8.0 was introduced into the headspace channel instead. The nucleic acid purification chip was inverted in this step as the organic phase has greater density than the aqueous phase. (C) Protein and DNA were transferred from the aqueous phase into the organic phase, while RNA was retained in the aqueous phase. (D) The organic phase was expelled from the headspace channel and evaporated under vacuum while purified RNA in the micro-well was concurrently dried (E, F). Residual organic phase was further decontaminated by repetitive washing and vacuum evaporating with 70% ethanol. (G) q-RT-PCR reaction mixture was loaded into the micro-wells. (H) Microwells were covered with mineral oil followed by on-chip q-RT-PCR amplification.

4.2.3 Comparison nucleic acid recovery yield of chip based liquid phase and column based solid phase extraction methods

4.2.3.1 Preparation of bacterial nucleic acids by chip based liquid phase and column based solid phase extraction method

DNA or RNA from bacterial lysate was prepared by chip based liquid phase and column based solid phase purification technology. Bacterial nucleic acids were released by enzymatic treatment followed by thermal lysis. Gram-negative bacteria *P. aeruginosa* PAO1 (ATCC, USA) and Gram-positive bacteria *S. aureus* (ATCC 25923, ATCC, USA) were maintained in Luria broth. Suspensions of *P. aeruginosa* or *S. aureus* cells were serially diluted by 10-fold and treated with an enzyme mixture containing 1 unit/ µl Ready-Lyse Lysozyme (Epicenter Biotechnologies)-50 µg/mL proteinase K (Qiagen) or 50 µg/mL lysostaphin (Sigma)-50 µg/mL proteinase K, respectively. For DNA extraction, an enzymatic reaction was carried out in TE buffer (pH 8) at 37 °C for 5 min, followed by thermal lysis at 85 °C for 5 min. For RNA extraction, an enzymatic reaction was carried out in 1 mM EDTA buffer (pH 7.0) with subsequent thermal lysis in SAE buffer at 85 °C for 5 min. Bacterial concentration was determined by measuring the optical density at 660 nm (OD660) and confirmed by CFU counting. 1 µl *P. aeruginosa* or *S. aureus* bacterial cell lysate from the serial 10-fold dilutions containing from 5000 CFU to 5 CFU of bacteria was pipetted into the micro-wells of the liquid phase nucleic acid purification chip. The corresponding organic phase was introduced at the flow rate of 0.65 ml/min in 5 s cycles of continuous forward and backward flow over a duration of 15 min (Fig. 4-3, panels A−C) to achieve phase partitioning for isolation of the target nucleic acid in the micro-wells. The organic phase was subsequently pumped out of the headspace channel

and further removed by vacuum evaporation for 5 min (Fig. 4-3 D). 70% ethanol was then infused in and pumped out of the chip to wash away the residual organic phase. The remaining 70% ethanol was air dried and decontaminated under vacuum for 5 min (Fig. 4-3, panels E-F). Purified DNA or RNA in the micro-wells was rinsed out by repeated pipitting and quantified by off chip q-PCR or q-RT-PCR analysis. Correspondingly, DNA and RNA from the same series of 1 μl bacterial lysate were purified by Qiagen DNeasy Blood and Tissue Kit and RNeasy Mini Kit (Qiagen), respectively, following the manufacturer's protocol. DNA eluted in TE buffer was first dialyzed against water using Slide-A-Lyzer Dialysis Cassettes, 10K MWCO (Fisher Scientific, USA) to remove the TE interference for off-chip q-PCR assay and then vacuum dried in PCR tube. RNA recovered in distilled water was vacuum dried in PCR tube directly. DNA or RNA of *P. aeruginosa* and *S. aureus* at 5×10^8 CFU/ml was also prepared using Qiagen DNeasy Blood & Tissue Kit and RNeasy Mini Kit respectively. The purified DNA and RNA were diluted in distilled sterile water to give theoretically equivalent quantities of nucleic acids for each bacterial dilution as reference control for 100% recovery.

4.2.3.2 Off chip quantitative PCR analysis to compare nucleic acid recovery yield of chip based liquid phase and column based solid phase extraction method

DNA and RNA purified by both chip based liquid phase and column based solid phase purification technology were quantified by off-chip q-PCR and q-RT-PCR assay respectively to compare the nucleic acid recovery yield using RotorGene 3000 thermal cycler (Qiagen, Germany). One q-PCR reaction mixture consisted of 10 μl of 10 mM Tris–HCl (pH equal to 9.0), 50 mM KCl, 0.1% Triton X-100, 0.2 mM each of dATP, dCTP, dTTP and dGTP, 3 mM $MgCl_2$, 0.2 μM each of forward and reverse primer, 0.2

U/μl of Platinum Taq DNA polymerase (Invitrogen, USA), 1 μg/μl of BSA, and 1× Syber green (Invitrogen, USA). q-PCR was performed at an initial denaturation at 95 ˚C for 5 minutes followed by 40 cycles of denaturation at 95 ˚C for 30 s, annealing at 60 ˚C for 30 s and extension at 72 ˚C for 30 s. q-RT-PCR assay was carried out in a volume of 10 μl with 3 mM $MgSO_4$ using SuperScript III Platinum One-Step Quantitative RT-PCR Kit (Invitrogen, USA) following the manufacturer's protocol at an initial 50˚C for 20 minutes, then a denaturation temperature at 95°C for 2 minutes followed by 40 cycles of denaturation at 95°C for 15 s, annealing and extension at 60°C for 30 s. Contamination of genomic DNA in the purified RNA was examined by replacing SuperScript III RT/Platinum® *Taq* Mix with 2 units of Platinum® *Taq* DNA polymerase according to the manufacture's protocol. Primers for two target genes of *P. aeruginosa* (16S rRNA, gene PA 0708) and two target genes of *S. aureus* (16S rRNA and ViK) were shown in Table 4-1.

Table 4-1 Primer pairs for q-PCR and q-RT-PCR assay

Species	Gene names	Assay type	Product size (bp)	Forward primer	Reverse primer
P. aeruginosa	PA 0708	q-PCR	211	CCGACTGACGCCAACGA	CGACCCTACCTCCCACGAAT
	16S rRNA	q-RT-PCR	196	GCTCGTGTCGTGAGATGTT	GTTTCGCTGCCCTTTGTATTGT
S. aureus	ViK	q-PCR	319	AAACAACTACAATCCCTTCA	TACGGTTAGACTGCTTCG
	16S rRNA	q-RT-PCR	215	CAAAACTACTGAGCTAGAGTACG	AAGATCTCAAGGATCCCAACGGCT

4.2.4 On-chip quantitative PCR analysis

Vacuum facilitated reagent loading was performed as previously described with a few modifications [45] for on-chip PCR assay in the same micro-wells in which nucleic acids were isolated to avoid sample loss caused by liquid transfer as well as to demonstrate the feasibility of the nucleic acid purification chip in providing "all in one" solution for bacterial nucleic acid analysis. As pictured in Fig.4-4, the inlet Teflon tubing of the liquid phase nucleic acid purification device was connected to a pipette tip as the reservoir for PCR reagent mixture, the flow of which was controlled by an external mechanical pinch valve. 1 mM $CaCl_2$ was supplemented in the PCR reaction mixture to remove the PCR inhibition induced by EDTA retained in the aqueous phase after phase partitioning. The outlet Teflon tubing was connected to an air buffering chamber to prevent accidental liquid leakage to the vacuum pump. To load PCR reaction mixture into the micro-wells of the nucleic acid purification device, the vacuum pump was powered on with the pinch valve closed until the system's internal pressure was below 2 Torr. Afterwards, the pinch valve was released to load PCR reagent mixture held in the pipette tip into the micro-wells by vacuum driven microfluidics. The well array was then overlaid by mineral oil followed by q-PCR or q-RT-PCR assay using StarCycler quantitative PCR machine (Star Array Pte Ltd, Singapore) with multiple integrated functions, including thermo-cycling control, real time fluorescence imaging, on line image processing and data analysis as described previously [45] (Fig. 4-3 G-H). The microfluidic operation of for PCR reaction mixture loading was illustrated in Fig. 4-5.

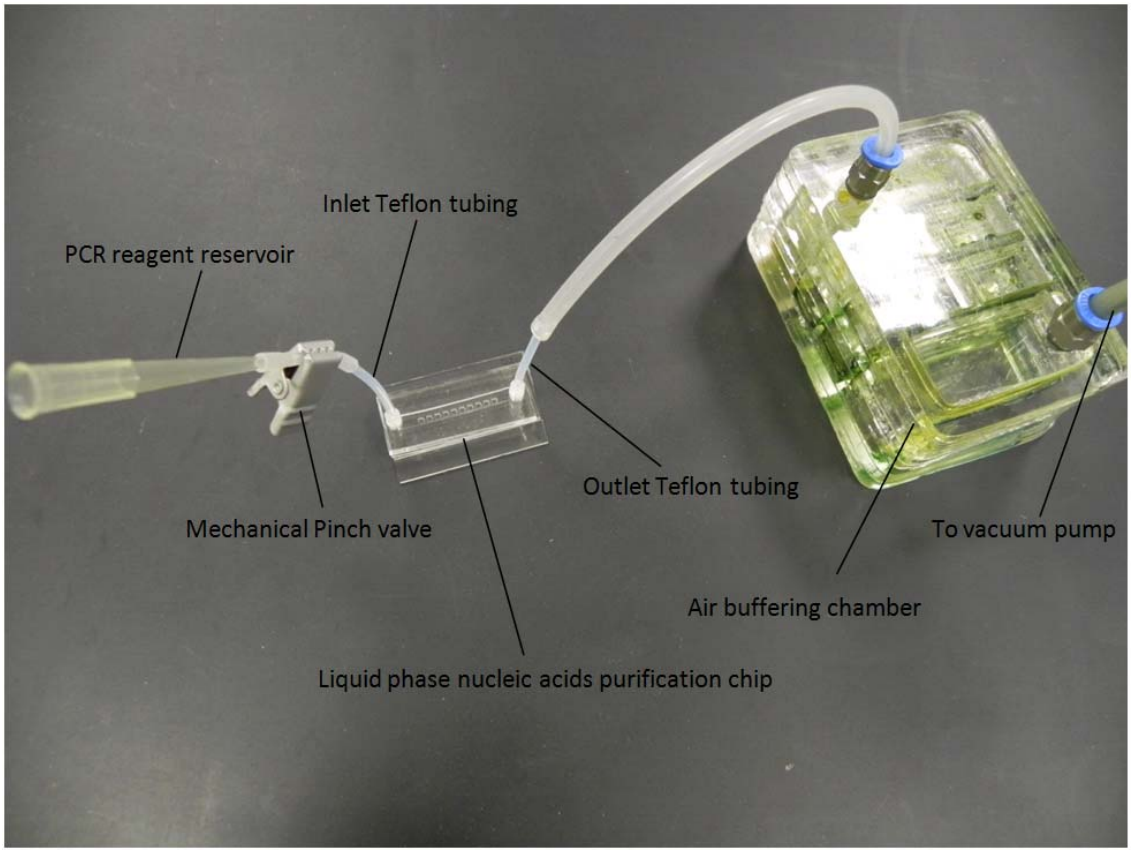

Fig.4-4 The vacuum system setup for PCR reaction mixture loading into the micro-wells of the liquid phase nucleic acid purification device.

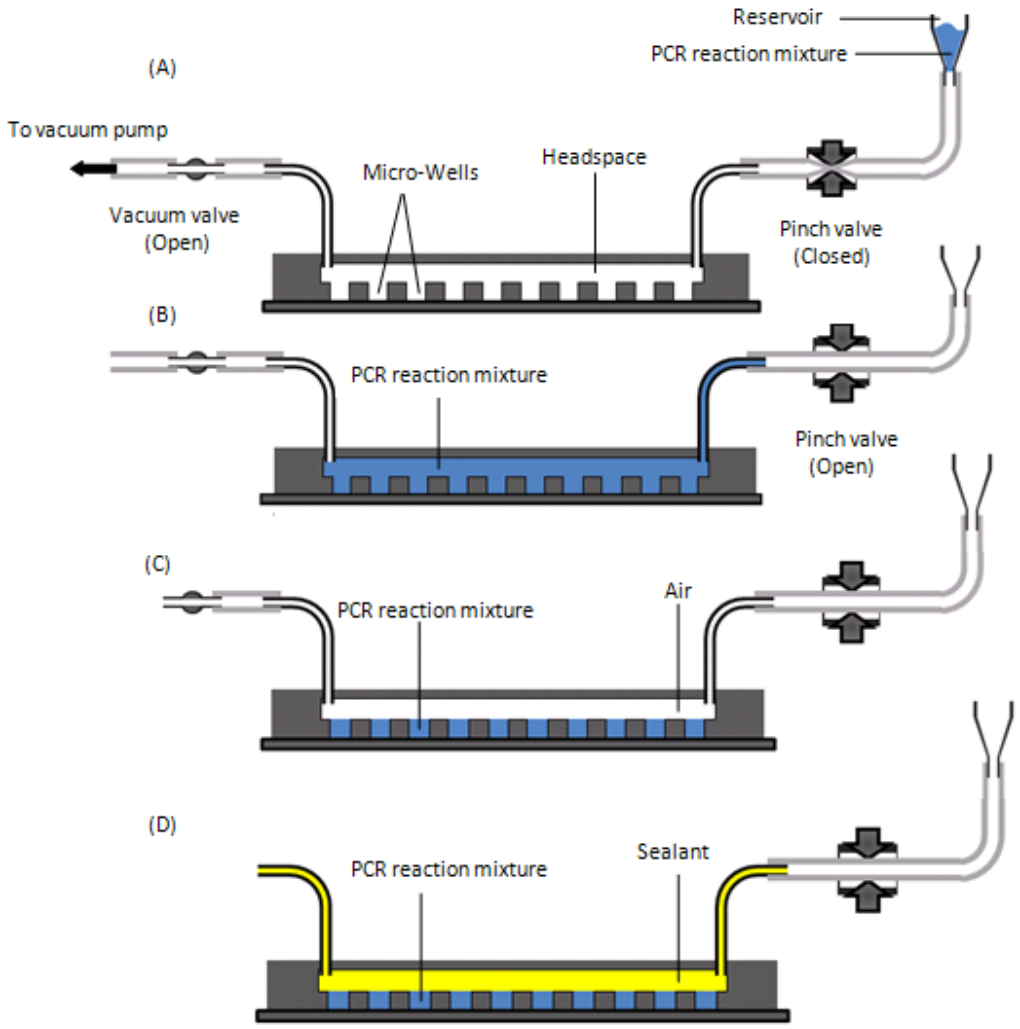

Fig. 4-5 Microfluidic operations to load PCR reaction mixture into the micro-wells of the nucleic acid purification chip modified from the previous method developed by Liu et al [45]. (A) Vacuum was established and monitored. PCR reaction mixture was loaded into the reservoir. (B) The pinch valve was opened to allow the PCR reaction mixture flow into the well array. (C) Vacuum was still on to remove the excess liquid in the headspace and to isolate the micro-wells. (D) Sealant was injected into the headspace for PCR assay.

4.2.5 High throughput nucleic acid extraction from single bacterium

To achieve high throughput analysis DNA or RNA from single bacterial cells, the nucleic acid purification chip was redesigned into a 2-dimension (2D) format containing

900 micro-wells with a glass headspace channel as shown in Fig. 4-6. An additional 0.5 mm PDMS protector layer was placed on top of the headspace channel to shield the acrylic chip cover from chloroform corrosion. Two capillaries were immobilized at the diagonal positions of the chip cover as the inlet and outlet channel. Each well has a dimension of 0.5 mm×0.5 mm×0.5 mm to hold liquid of approximate 125 nl. Sample and reagent were loaded into the micro-wells of the 2D nucleic acid purification chip by one step vacuum driven microfluidics as described in Fig. 3-5. Enzyme mixture of 1 U/μl Ready-Lyse™ Lysozyme - 50 μg/ml Proteinase K or 50 μg/ml Lysostaphin - 50 μg/ml Proteinase K was pre-dried in micro-wells to facilitate lysis of *P. aeruginosa* and *S. aureus* respectively. Single bacterium was isolated into the individual micro-wells by loading *P. aeruginosa* or *S. aureus* cell suspensions of less than 0.3 CFU/well. According to Poisson statistics, majority of the micro-wells contain no more than a single bacterium in this condition [120] (Fig. 4-7). For single bacterial DNA extraction, *P. aeruginosa* and *S. aureus* were diluted in TE buffer and loaded into the 2D chip after which a low-viscosity PCR encapsulation reagent (Vapor-Lock, Qiagen, Germany) was infused into the headspace channel. The chip was subjected to heat treatment at 37˚C for 5 minutes and then at 85˚C for 5 minutes to lyse the captured bacteria. Following this, Vapor-Lock reagent was withdrawn from the channel. To isolate RNA from single bacterium, *P. aeruginosa* and *S. aureus* culture were first stabilized by adding 1/5 volume of ice cold phenol: ethanol (5:95) [133] to minimize RNA degradation, and adjusted to the desired cell densities in 1mM EDTA buffer (pH 7.0). Bacterial cells were then loaded into the 2D chip with the appropriate enzyme mixture pre-dried in the micro-wells. The 2D chip was incubated at room temperature for 5 minutes and then heated at 37 ºC until the liquid in

the micro-wells was fully evaporated to avoid repeated usage of PCR encapsulation reagent. Buffer mixture of 5 mM sodium acetate and 5 mM acetic acid was then loaded into the 2D chip to adjust the pH to 4.6 for RNA recovery. The on-chip single bacterium isolation and lysis for RNA extraction was illustrated in Fig. 4-8. The micro-wells were overlaid with Vapor-Lock reagent and heated at 85 ºC for 5 minutes to lyse the captured bacteria. DNA and RNA from single bacterium were prepared by chip based liquid phase extraction using PCI with the pH of 8 and 4.6 respectively at the flow rate of 0.65 ml/min as described in Fig. 4-3. Residue organic phase in the micro-wells was decontaminated by repeated washing with 70% ethanol. PCR reaction mixture with corresponding primers was loaded into the chip followed by q-PCR or q-RT-PCR analysis.

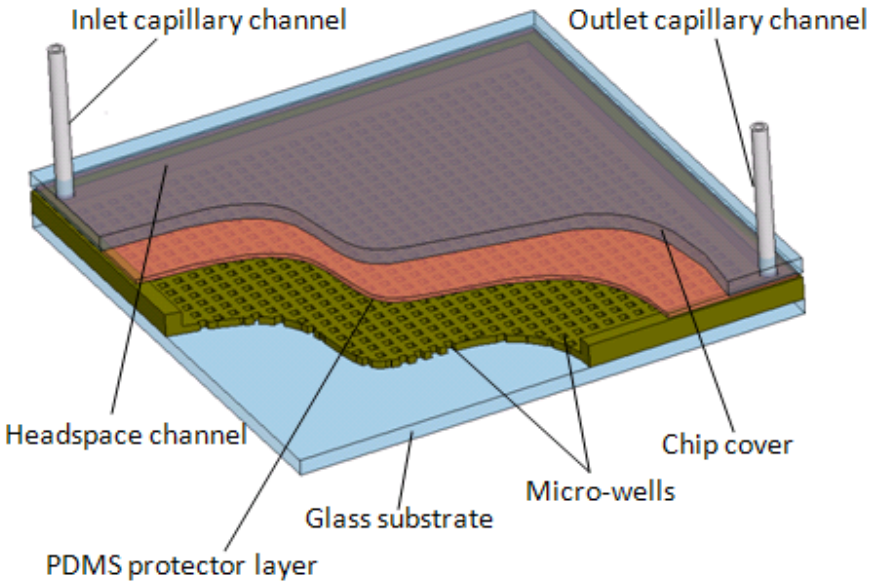

Fig. 4-6 Schematic of the 2D liquid phase nucleic acid purification chip

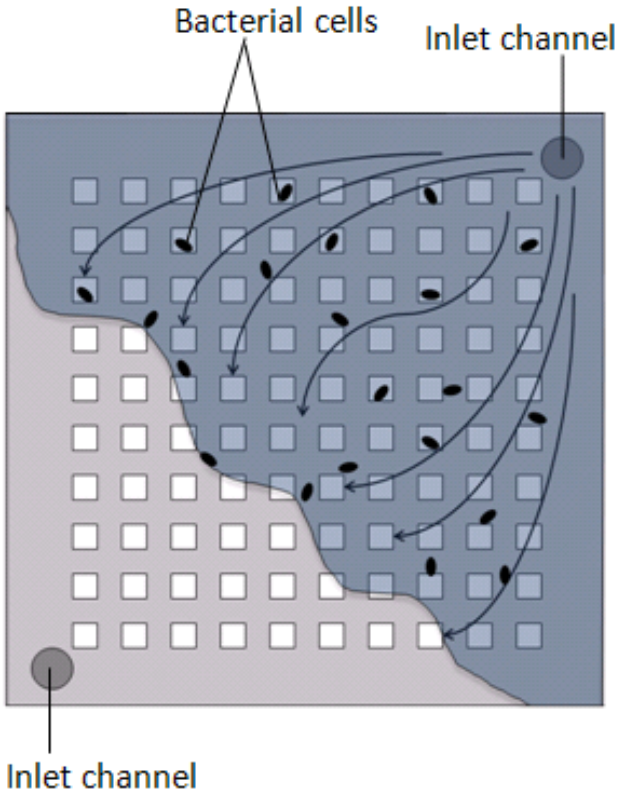

Fig. 4-7 Single bacterium isolation in the individual micro-wells of the 2D nucleic acid purification chip by probability based on vacuum driven microfluidics.

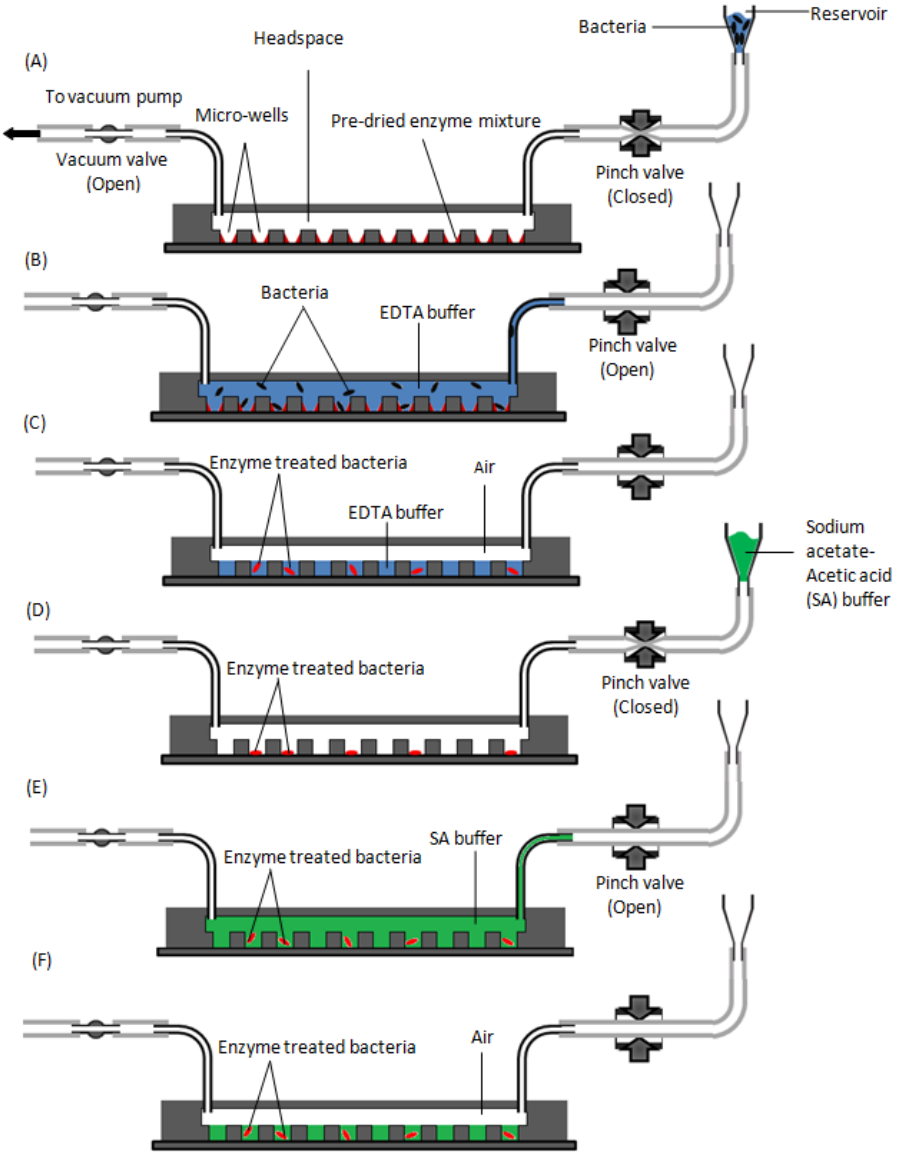

Fig. 4-8 On-chip single bacterium isoaltion and lysis for RNA extraction. (A) Vacuum was established and monitored. Bacteria in EDTA buffer were loaded into the reservoir. Micro-wells were pre-dried with appropriate enzyme mixture. (B) Pinch valve was opened to allow the liquid in the reservoir flow into the well array. Single bacterium was isolated into the individual micro-wells by probability (C) Vacuum was still on to remove the excess liquid in the headspace and to isolate the micro-wells. Bacteria were lysed by enzymatic treatment. (D) Liquid in micro-wells was evaporated under vacuum. Pinch valve was closed. SA buffer was loaded into the reservoir. (E) Pinch valve was opened to allow the SA buffer in the reservoir flow into the well array. (F) Vacuum was still on to remove the excess liquid in the headspace and to isolate the wells. Sealant was then infused in the headspace followed by thermal lysis at 85 ˚C (Image not shown).

4.2.6 Quantification of *rmd* gene transcripts of *P. aeruginosa* adhered A549 cells

To quantify the average gene transcript level of *P. aeruginosa* adhered to the whole population of A549 cells, *P. aeruginosa* infection to A549 cells were performed as described in section 3.2.6. At the endpoint of 2h, 4h, and 6h of infection, A549 cells were washed with PBS three times to remove the unbound bacteria, trypsinized and then centrifuged at 800 *g* to collect the infected cells. Total RNA was isolated by Qiagen RNeasy Mini Kit following the manufacturer's protocol. The relative *rmd* gene transcription ratio was determined according to the Ct values of *rmd* gene as referenced to the Ct values of 16S rRNA gene transcripts, obtained by multiplex q-RT-PCR assay [36] using SuperScript III Platinum One-Step Quantitative-RT-PCR Kit (Invitrogen, USA) in a volume of 10 µl supplemented with 3 mM $MgSO_4$ following the manufacturer's protocol. q-RT-PCR was carried out at an initial step at 50˚C for 20 minutes, then denaturation at 95°C for 2 minutes followed by 40 cycles of denaturation at 95°C for 30 s, annealing and extension at 60°C for 30 s. Relative gene transcription ratio was calculated according to the following equation: normalized gene transcription ratio=$2^{-\Delta\Delta Ct}$, where ΔΔCt=ΔCt (test)-ΔCt(calculator) and ΔCt= Ct (*rmd*)-Ct(16S rRNA) [36]. The *rmd* gene transcription level of *P. aeruginosa* adhered to A549 cells after 2 hours of infection was used as the calculator with the relative gene transcription level defined as 1. Primers and probes for *rmd* gene and the reference 16S rRNA gene used are summarized in Table 4-2. The number of adhered *P. aeruginosa* to A549 cells was determined by CFU counting assay as described in section 3.2.6. Primers and probes were designed using Beacon Designer 8 software. Primer specificity was first evaluated using online sequence alignment blast tools (http://blast.ncbi.nlm.nih.gov/) and confirmed by q-RT-PCR assay to ensure that the

designed primers and probes for *P. aeruginosa rmd* and 16S rRNA analysis do not cross react with total RNA from A549 cells.

Table 4-2 Primer pairs for multiplex q-RT-PCR assay

Gene names	Product size (bp)	Forward primer	Taqman probe	Reverse primer
Rmd	208	GCGCCGTCTATAACGTCTGT	FAM-5'-AGAAGATTCGCGAGCTGATC-3'-TAMRA	CGCAGGGACTGTTTTATGGT
16S rRNA	203	AAGCAACGCGAAGAACCTTA	CYS- 5'-CAGCTCGTGTCGTGAGATGT -3'-IBRQ	CACCGGCAGTCTCCTTAGAG

To quantify the *rmd* gene transcript level of *P. aeruginosa* attached to single A549 cells, infected host cells were loaded into the 2D liquid phase nucleic acid purification chip with the cell density pre-adjusted to less than 0.3 cell/well. RNA was isolated as described in section 4.2.5 followed by on-chip multiplex q-RT-PCR assay using primers and probes for both *rmd* and 16S rRNA genes. q-RT-PCR standard curve of 16S rRNA was constructed by loading the reaction mixture containing total RNA isolated from bacteria spanning four orders of magnitude at 3000, 300, 30, and 3 cells per well (equivalent to 24000, 2400, 240, 24 and cells /μl) into the chip, followed by on-chip q-RT-PCR analysis as described above. The number of *P. aeruginosa* associated with single A549 cells was estimated by the Ct value of 16S rRNA from wells with positive amplifications and the standard curve accordingly. The relative *rmd* gene transcript ratio

was calculated according to the Ct values of *rmd* gene and that of the reference 16S rRNA gene as described above [36].

4.3 Results and discussion

4.3.1 DNA and RNA isolation from *P. aeruginosa* and *S. aureus* bacterial cells

4.3.1.1 Optimization of bacterial thermal lysis protocol for nucleic acid isolation

In most cases, nucleic acids need to be released out of the bacterial cells before moving on to the next purification step. Thermal lysis offered a simple and effective way to disrupt bacterial cell wall for downstream nucleic acid purification [134-136]. One major advantage to incorporate thermal lysis technique into microfluidic nucleic acid extraction devices is that the engineering complexity of the chip design can be significantly reduced, provided that bacterial cells can be effectively lysed with minimal nucleic acid sample loss. A bacterial thermal lysis protocol (section 3.2.2) was previously optimized for DNA extraction from *P. aeruginosa* and *S. aureus*. When pre-treated with enzyme mixture of lysozyme-proteinase K (for *P. aeruginosa* lysis) or lysostahpin-proteinase K (for *S. aureus* lysis) in TE buffer, 94.5% *P. aeruginosa* and 93.7% *S. aureus* can thermally lysed at 85 ˚C for 5 minutes without significant DNA degradation. However, RNA was validated to be unstable at high temperature in alkaline TE buffer as assessed by q-RT-PCR assay targeting 16S rRNA transcripts as described in section 4.2.3.2 (Fig. 4-9). This is because alkali will react with the exposed OH group present in the second carbon of nucleotide of single stranded RNA [137]. On the contrary, RNA is reported to be more stable in acidic buffer [138]. Nonetheless, whether the RNA molecules can withstand high temperature in acidic conditions has not been documented yet. In this study, an acidic

thermal lysis buffer system containing 5 mM sodium acetate, 5 mM acetic acid and 1 mM EDTA (SAE) with the pH of 4.6 was optimized for bacterial RNA extraction. The purpose of EDTA supplement is to inhibit bacterial endogenous RNase activity [139]. RNA stability in SAE buffer at elevated temperatures of 65˚C, 75˚C, 85˚C and 95˚C for 5 minutes was evaluated by q-RT-PCR assay. ΔCt was derived from the Ct value obtained from q-RT-PCR assay using RNA template with heat treatment subtracted from the Ct values of identical non-heated RNA control. RNA degradation was indicated by ΔCt values above zero. As illustrated in Fig. 4-10, significant RNA degradation in SAE buffer was only observed at 95˚C as evidenced by the delayed Ct value, which opened the possibility to thermally lyse bacteria for RNA extraction with minimal sample loss.

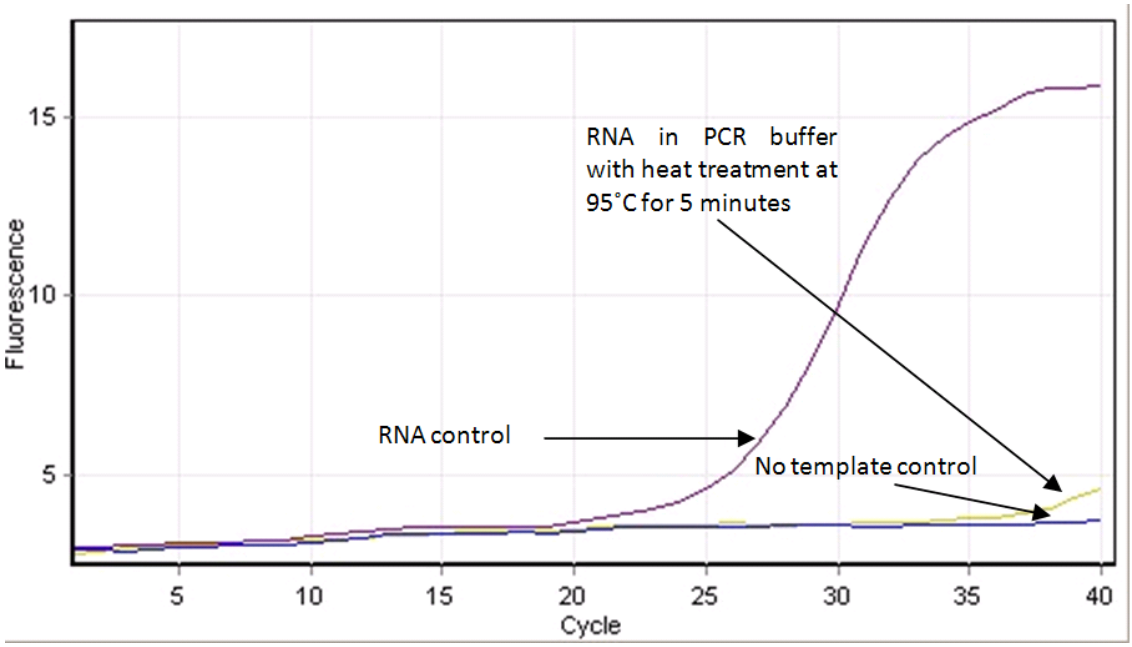

Fig. 4-9 RNA detradation in alkaline TE buffer. RNA purified from *P. aeruginosa* was incubated in alkaline TE buffer at 85 ˚C for 5 minutes followed by q-RT-PCR assay targeting 16S rRNA. RNA witout thermal treatment served as control.

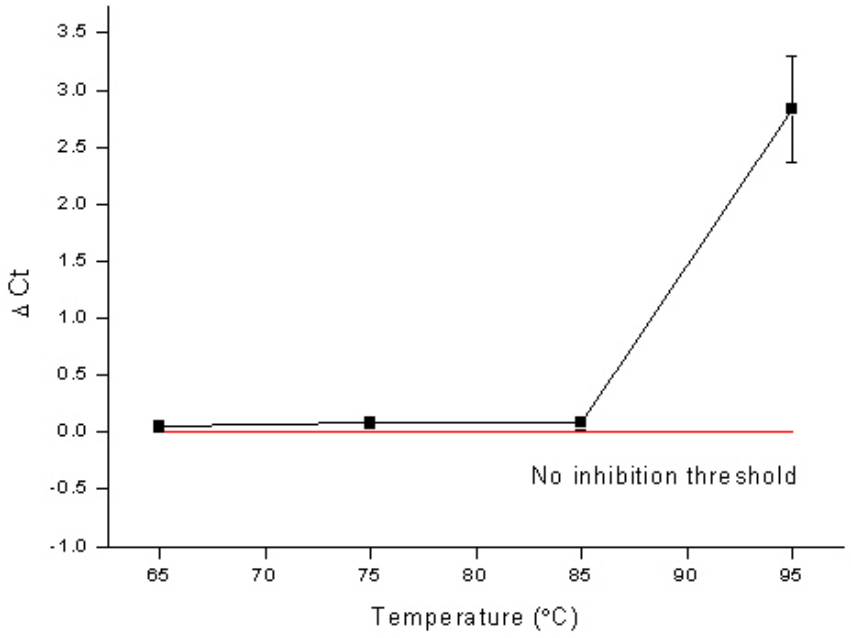

Fig. 4-10 RNA detradation in acidic SAE buffer. RNA purified from *P. aeruginosa* was incubated in SAE buffer at 65˚C, 75˚C, 85˚C and 95˚C for 5 minutes followed by q-RT-PCR assay tageting 16S rRNA. ΔCt represented the Ct value derived from q-RT-PCR using RNA template with heat treatment subtracted from the Ct values of non-heated RNA control.

The next attempt was to validate whether bacteria can be thermally lysed effectively by incubation of *P. aeruginosa* and *S. aureus* cells in SAE buffer at 85˚C for 5 minutes. Unlysed bacteria were stained with SyberGreen I and counted under the fluorescence microscope after lysed bacteria were removed by centrifugation as previously described in section 3.2.4. As shown in Fig. 4-11, both *P. aeruginosa* and *S. aureus* were resistant to thermal lysis in SAE buffer at 85˚C. To enhance bacterial thermal lysis efficiency, *P. aeruginosa* and *S. aureus* cells were pre-treated with enzyme mixture of 1 U/µl Ready-Lyse™ Lysozyme-50 µg/ml Proteinase K and 50 µg/ml lysostaphin-50 µg/ml Proteinase K respectively. As the activity of lysozyme and lysostaphin was

significantly weakened in acidic buffer [140], enzymatic reaction was carried out in 1 mM EDTA (pH 7.0) at 37˚C for 5 minutes with subsequent thermal lysis in SAE buffer at 65ºC, 75, ºC and 85ºC for 5 minutes. As described in Fig. 4-12, the thermal lysis efficiency of both bacteria increased with temperature, with the most satisfactory lysis rate of 94.1% for *P. aeruginosa* and 90.7% for *S. aureus* respectively at 85˚C.

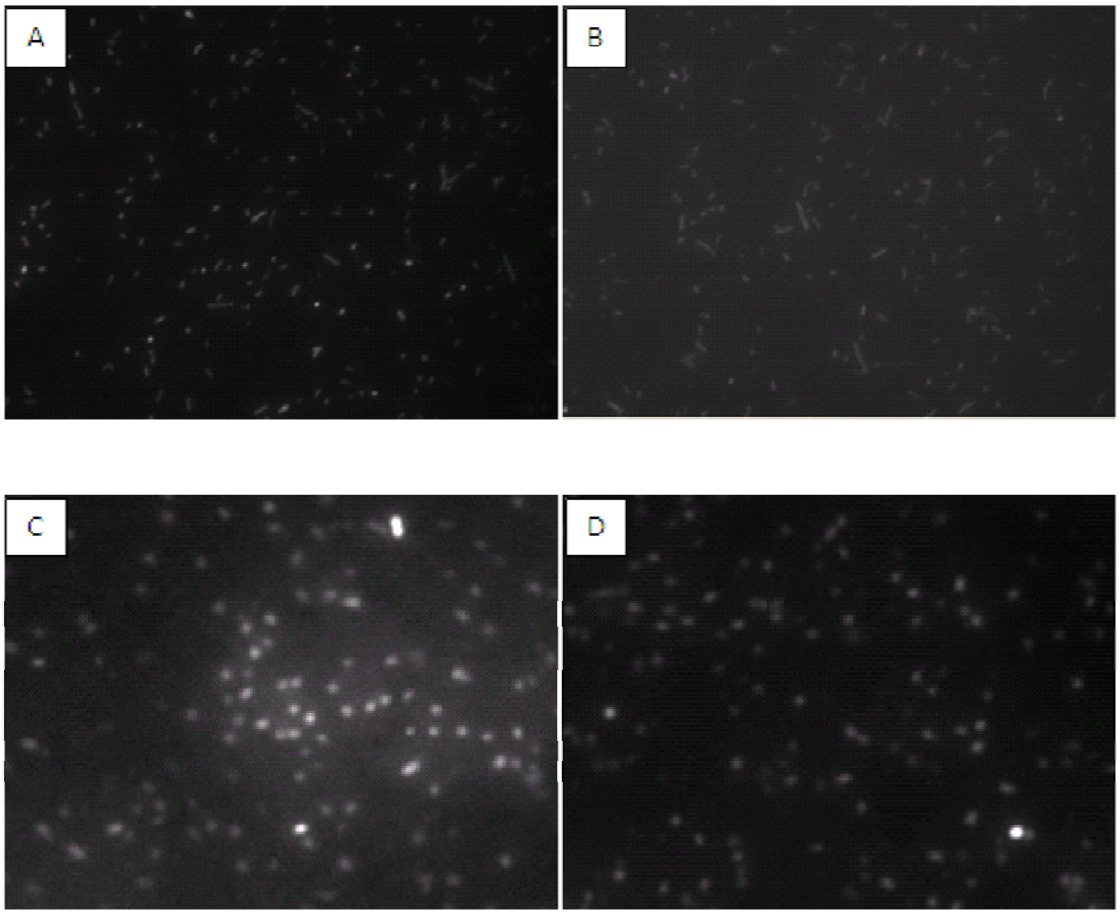

Fig. 4-11 *P. aeruginosa* and *S. aureus* without heat treatment were shown in image A and C respectively. Unlysed *P. aeruginosa* and *S. aureus* in SAE buffer at 85 ˚C for 5 minutes were shown image B and D respctivly. Cells were stained with Sybrgreen I and observed under 40 × fluorescence microscopy.

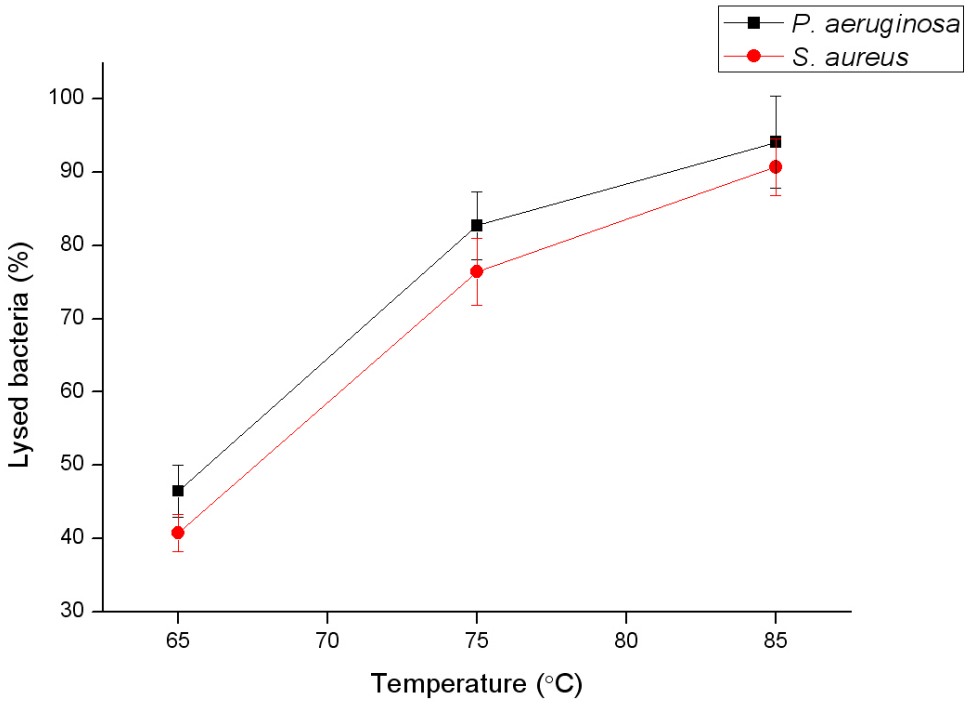

Fig. 4-12 Thermal lysis efficiency of *P. aeruginosa* and *S. aureus* in SAE buffer at different temperature with enzyme pre-treatment at 37 ˚C for 5 minutes. Lysis efficiency was estimated by the percentage of lysed bacteria. Each point represents the mean ± standard error of the mean of three replicated experiments.

In the proposed liquid phase nucleic acid purification chip, removal of chemicals that interfere with the following on-chip q-RT-PCR assay performed in the same micro-wells in which nucleic acids are isolated (discussed later in section 4.3.2) mainly depends on evaporation technique only. As a result, another important criterion in choosing bacterial thermal lysis buffer is that the chemical component retained in the micro-wells after vacuum evaporation must be compatible with the downstream on-chip q-RT-PCR assay. Of all the three chemicals compounds in SAE buffer, acetic acid can be effectively vaporized under vacuum and sodium acetate of 5 mM is not a q-RT-PCR inhibitor (data not shown). Therefore, it can be predicted that the potential q-RT-PCR inhibition may

come from the EDTA salt, which was later validated by off-chip tube based q-RT-PCR assay. To mimic the scenario for on-chip nucleic acid analysis (Fig. 4-3, G-H), purified *P. aeruginosa* RNA was aliquoted in SAE buffer and dried in PCR tube by vacuum evaporation to first deplete acetic acid from the mixture. q-RT-PCR reagent was added followed by amplification assay using Rotogen real time thermal cycler. It was demonstrated that the q-RT-PCR amplification was inhibited but can be effectively reversed by addition of 1 mM $CaCl_2$ in the q-RT-PCR reaction mixture to neutralize the EDTA chelating reagent (Fig. 4-13).

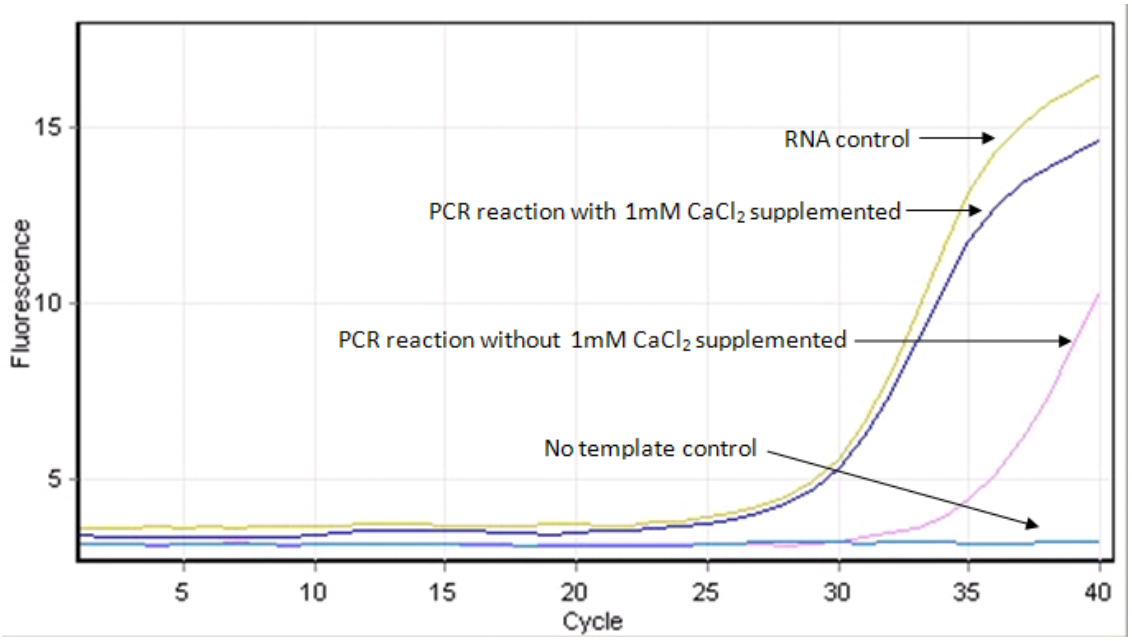

Fig. 4-13 Removal of q-RT-PCR inhibition by 1mM $CaCl_2$. Purified *P. aeruginsoa* RNA was aliquoted in SAE buffer and dried in PCR tube under vacuum evaporation. q-RT-PCR reagent was added in followed by amplification assay with or without $CaCl_2$ supplement.

Based on the above-mentioned analysis, TE and SAE were used as the thermal lysis buffer for bacterial DNA and RNA extraction respectively because of the following reasons. First, when pre-treated with appropriate enzymes, bacterial cells can be

effectively lysed at optimal temperature with minimal nucleic acid degradation. Second, the non-volatile compounds that retained in the thermal lysis buffer after vacuum evaporation is compatible with the downstream on-chip PCR assay provided that 1mM $CaCl_2$ is supplemented in the PCR reaction mixture.

4.3.1.2 Optimization of microfludic phase partitioning protocol for bacterial nucleic acid purification

After bacterial thermal lysis protocol was finalized, the chip based liquid phase purification method was optimized to achieve maximum nucleic acid recovery from small amount of bacterial cells in minute sample volume. During liquid phase extraction, components of bacterial cell lysate are selectively distributed into the organic phase or retained in the aqueous phase with mass transport occurring at the organic–aqueous interface. Hence maximizing the contact area of the two immiscible phases is important for effective separation of nucleic acids from other cell components. This can be conveniently achieved by using a vortex mixer to generate chaotic flow fields of the two phases in macrofluidic systems. However, in microfluidic modules, extensive mixing of two immiscible liquid phases cannot be easily accomplished, so that phase partitioning mainly depends on passive diffusion in stratified or droplet based flow of the two phases, as proposed by Morales et al [70]. Nonetheless, in these scenarios, the residual organic phase that remains with the aqueous phase will interfere with downstream nucleic acid assays. Present here is a novel microfluidic liquid phase nucleic acid purification chip in which the aqueous phase cell lysate was isolated in an array of micro-wells while the organic phase can then be introduced into the headspace channel connecting the micro-well array with repeated forward and reverse flow, achieving intensive mixing of the two

phases. The organic phase were then pumped out of the headspace channel and further decontaminated by repeated washing and evaporating with 70% ethanol, leaving the target nucleic acid of interest dried in the micro-wells for subsequent q-PCR or q-RT-PCR analysis. The partitioning efficiency of three major types of analytes – DNA, RNA and protein – as the model macro-biomolecules present in bacterial lysate with the organic phase at the different flow rates of 0 ml/min, 0.25 ml/min 0.45 ml/min, and 0.65 ml/min were examined. Fluorophore-conjugated BSA was selected to study the protein phase partitioning as previously proposed [70]. Unmodified DNA and RNA purified from *P. aeruginosa* cells were chosen as the nucleic acid analytes to eliminate potential bias that might be introduced when using short synthetic DNA or RNA labeled with fluorescence dye because of their significant variations in molecular weights and structures as compared with natural nucleic acids. These analytes were dissolved in bacterial thermal lysis buffer of either TE or SAE to serve as the aqueous phase to determine the optimal flow rate of the organic phase for maximum recovery of DNA or RNA. As illustrated in Fig. 4-14, 92.9% protein and 93.2% RNA can be partitioned from the aqueous phase into the organic phase (pH 8) at the flow rate of 0.45 ml/min, with further enhancement at 0.65 ml/min. However, when the organic phase was at pH 4.6, it was observed that only at the flow rate of 0.65 ml/min, did sufficient DNA partitioning (more than 99.9% removal from the aqueous phase) occur. DNA and RNA at 93.3% and 94.2%, respectively, were recovered in the aqueous phase when partitioned with the organic phase at pH 8 and 4.6, respectively, at this flow rate.

The effect of partitioning time on the phase partitioning efficiency of DNA, RNA, and protein was also evaluated at the optimal organic phase flow rate of 0.65 ml/min. As

demonstrated in Fig.4-15, recovery of nucleic acids in the aqueous phase decreases with prolonged partitioning by approximately 10% every 10 minutes, probably because of the exacerbated interface instability and the oxidization of the nucleic acids molecules [141]. However, as incomplete removal of both BSA and unwanted nucleic acids were observed at the endpoint of 5 minute partitioning, the phase partitioning protocol for nucleic acid extraction was finalized at 0.65 ml/min for 15 minutes in future experiments.

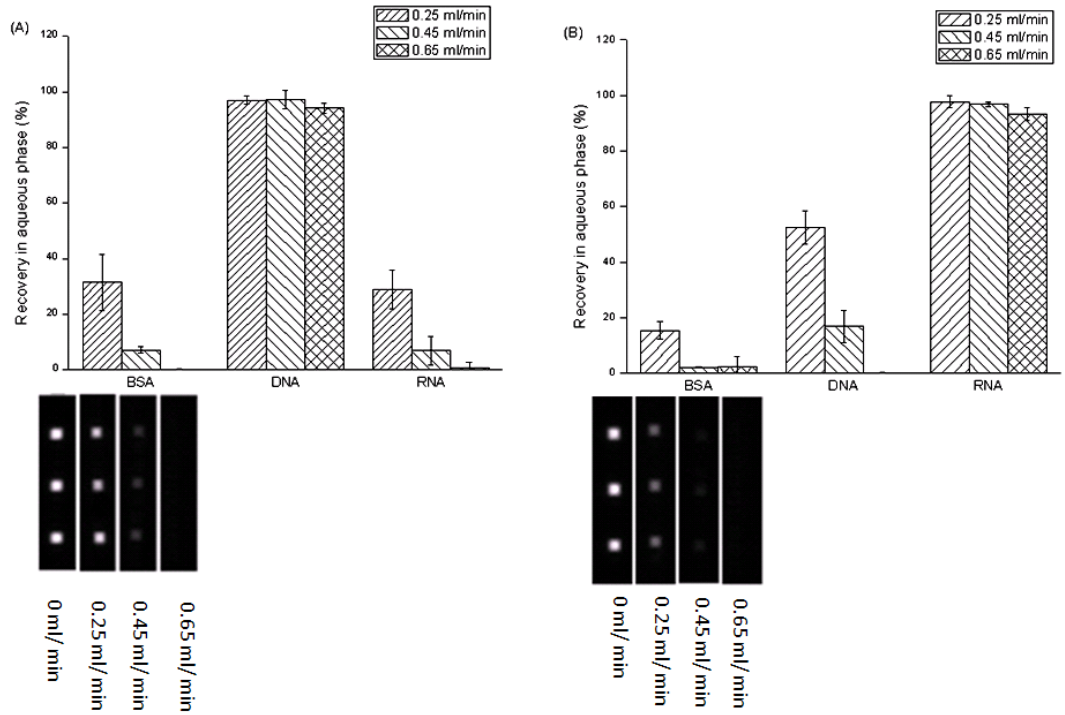

Fig. 4-14 Recovery of fluorescence labeled BSA, DNA and RNA in aqueous phase. Aqueous phase containing fluorescence labeled BSA, purified *P. aeruginosa* DNA or RNA was isolated in the micro-wells of the nulceic acids purification chip and partitioned with PCI at the pH of 8 (A) and 4.6 (B) at the flow rate of 0.25 ml/min, 0.45 ml/min and 0.65 ml/min. Recovery of BSA, DNA and RNA in the aqueous phase were evaluated by fluorescence imaging, Picogreen and Ribogreen quantification assay respectively. Images of fluorescence labeled BSA retained in the aqueous phase were shown beneath the corresponding BSA recovery bars with non-partitioned BSA in the far left image. Each point represents the mean ± standard error of three replicated experiments.

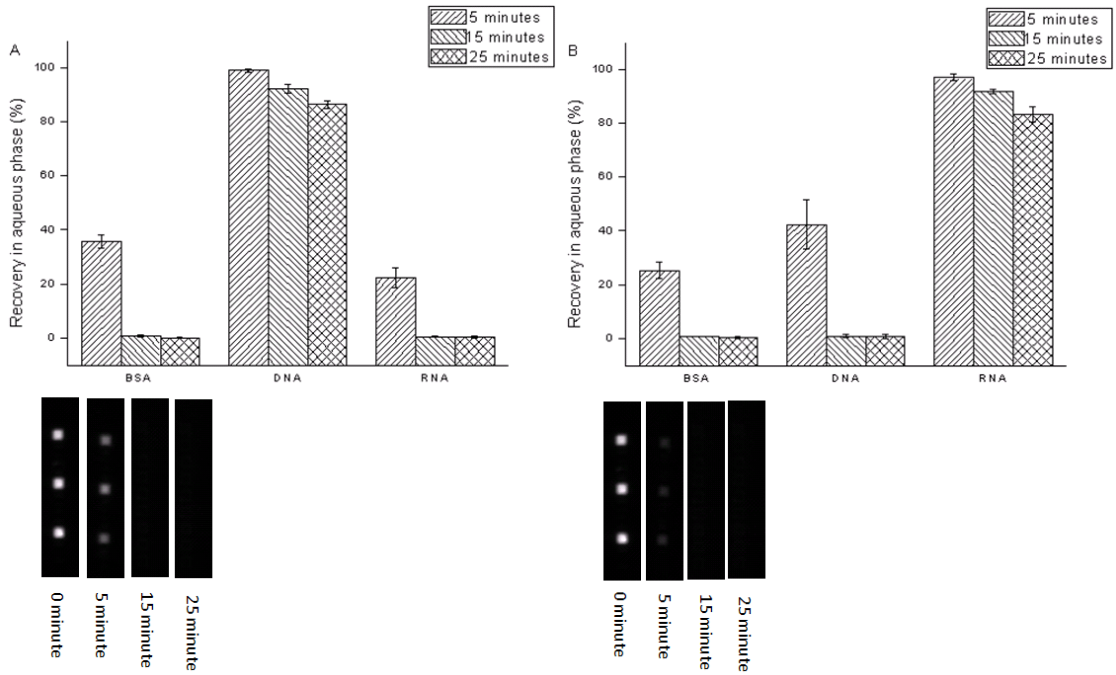

Fig.4-15 Recovery of fluorescence labeled BSA, DNA and RNA in aqueous phase. Aqueous phase containing fluorescence labeled BSA, purified *P. aeruginosa* DNA or RNA was isolated in the micro-wells of the nucleic acid purification chip and partitioned with PCI with the pH of 8 (A) and 4.6 (B) for 5 minutes, 15 minutes, and 25 minutes respectively at the flow rate of 0.65 ml/min. Recovery of BSA, purified DNA and RNA were evaluated by fluorescence imaging, Picogreen and Ribogreen quantification assay respectively. Images of fluorescence labeled BSA partitioned with PCI organic phase at different time were shown beneath the corresponding BSA recovery bars with non-partitioned BSA in the far left image. Each point represents the mean ± standard error of three replicated experiments.

In the proposed chip based liquid phase nucleic acid purification method, 70% ethanol was utilized to wash away the residue organic phase after phase partitioning. To examine if this washing step would lead to nucleic acid loss, 1 μl purified *P. aeruginosa* DNA or RNA were aliquoted and vacuum dried in the micro-wells. 70% ethanol was then infused in, air dried, and further decontaminated by vacuum evaporation. After this, DNA and RNA were rinsed out followed by Picogeen and Rigoreen quantification assay according to the manufacturer's protocol. Nucleic acid of the same concentration served

as the non-ethanol-washed control. As illustrated in Fig. 4-16, no apparent nucleic acid loss was found in the 70% ethanol washing step. This is in consistency with the previously published report that nucleic acids can non-specifically bind to glass substrate without the interference of ethanol washing [142].

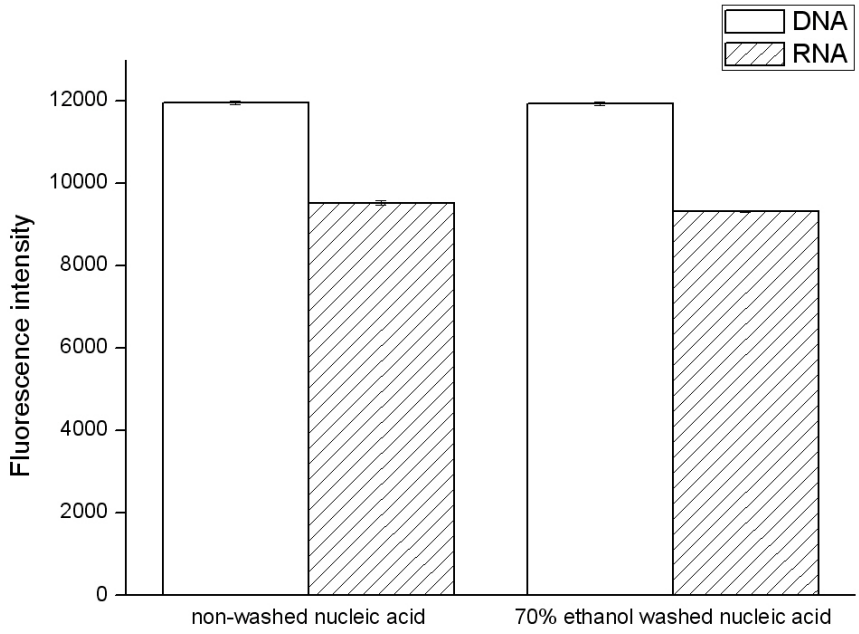

Fig. 4-16 Quantification of nucleic acids with or without 70% ethanol washing by Picogeen and Ribogreen quantification assay respectively.

4.3.1.3 Comparison of solid phase and liquid phase nucleic acid extraction efficiency by off-chip PCR assay

Nucleic acids were isolated from *P. aeruginosa* or *S. aureus* cell suspensions ranging from 5000 CFU to 5 CFU in 1 μl sample volume using both chip based liquid phase and Qiagen column based solid phase nucleic acid purification methods, and

analyzed by q-PCR or q-RT-PCR assay. Threshold Ct values of nucleic acids isolated by both methods were compared with those obtained from purified nucleic acids extracted from the respective bacterial suspensions at high cell density (5×10^8 CFU/mL) using Qiagen DNeasy/RNeasy DNA/RNA purification kit with dilutions corresponding to the 5000 to 5 CFU/μl series referenced as 100% nucleic acid recovery (Fig. 4-17). 16S rRNA was selected as the RNA target for q-RT-PCR because of their rich abundance in bacteria, so as to eliminate the factor of sensitivity limit of q-RT-PCR technology itself. The quantity of nucleic acid recovered was determined as described previously [36] based on the standard curve constructed using the Ct values of reference nucleic acid against each bacterial dilution and Ct values obtained with nucleic acids purified by chip based liquid phase or column based solid phase extraction method. As shown in Fig. 4-18, recovery of nucleic acids prepared by Qiagen solid phase technology was significantly reduced when the input bacterial cell density decreased, with the lowest limit of 50 CFU for DNA recovery, 5 CFU for RNA recovery, and in both cases achieving only 15−20% recovery. In contrast, using the chip-based nucleic acid purification method, 85%−120% of nucleic acids could be recovered from the entire range of bacterial cell densities tested, with an exception of RNA extraction from *S. aureus* which exhibited only a 70%−80% recovery, possibly due to insufficient removal of endogenous RNase during phase partitioning.

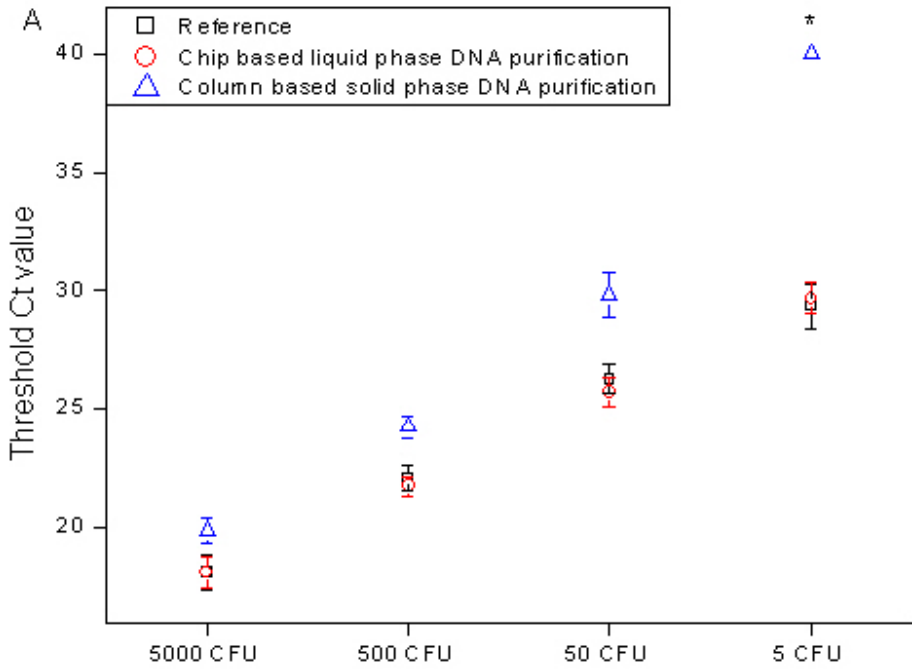
A
Reference
Chip based liquid phase DNA purification
Column based solid phase DNA purification
*
Threshold Ct value
40
35
30
25
20
5000 CFU
500 CFU
50 CFU
5 CFU

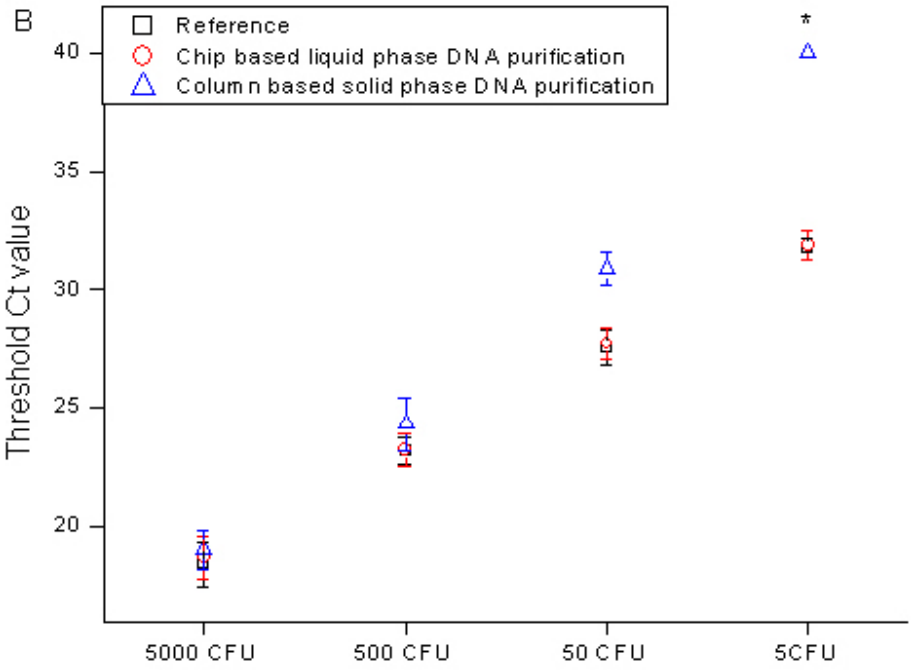
B
Reference
Chip based liquid phase DNA purification
Column based solid phase DNA purification
*
Threshold Ct value
40
35
30
25
20
5000 CFU
500 CFU
50 CFU
5CFU

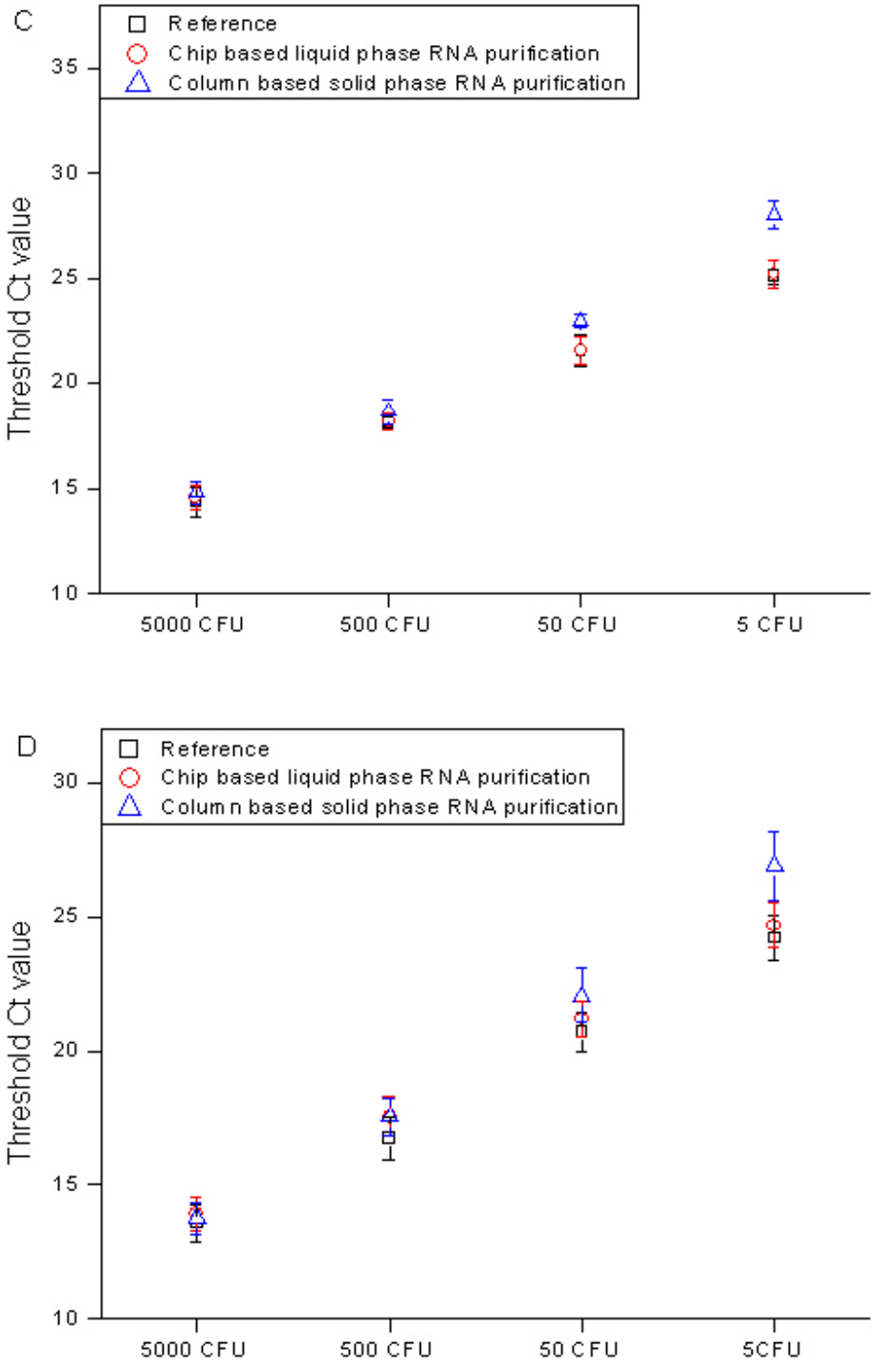

Fig. 4-17 Ct values obtaiend by off-chip q-PCR and q-RT-PCR analysis of DNA (A and B) and RNA (C and D) isolated by chip based liquid phase and column based solid phasse nucleic acid purification methods from *P. aeruginosa* (A and C) and *S. aureus* (B and D) ranging from 5000 CFU to 5 CFU. * No amplification.

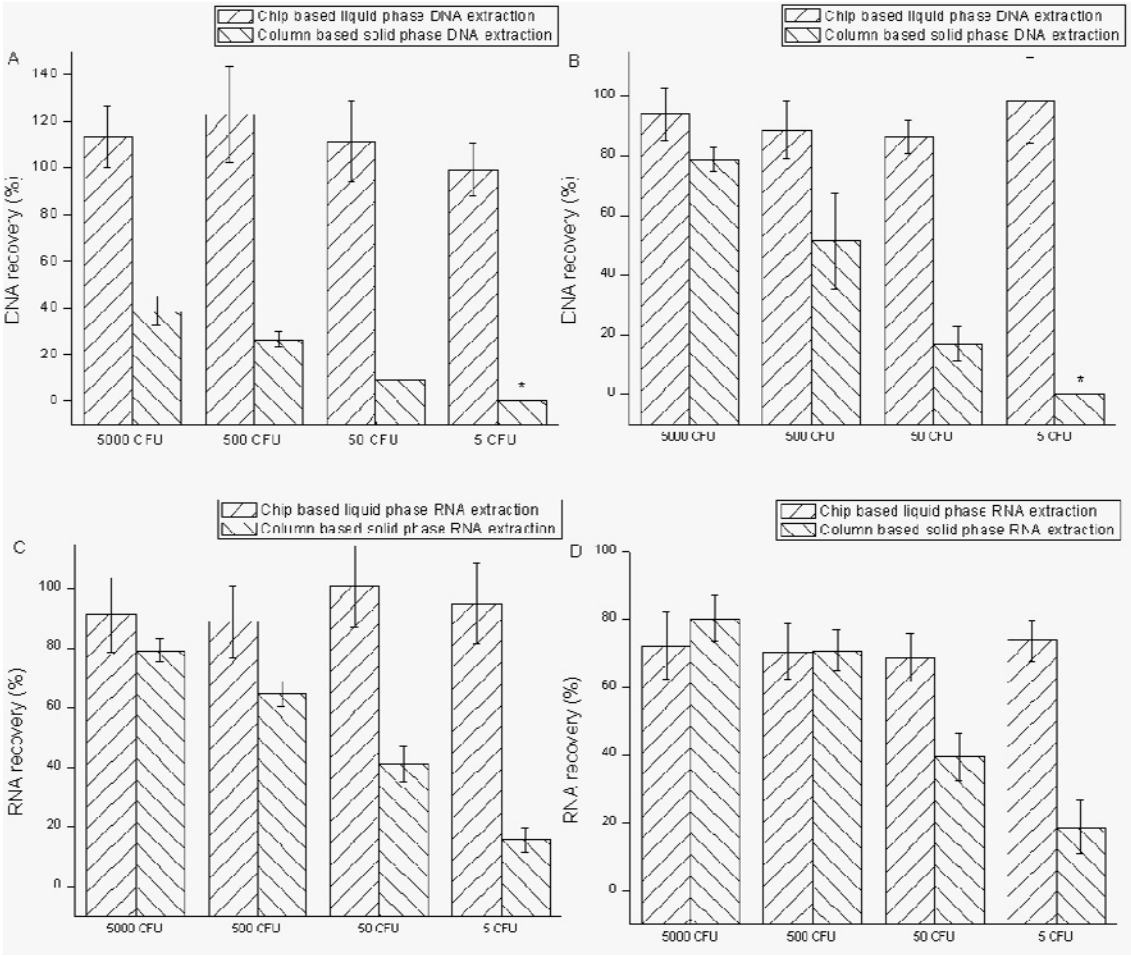

Fig. 4-18 Recovery of DNA (A and B) and RNA (C and D) isolated by chip based liquid phase and column based solid phasse nucleic acid purification methods from *P. aeruginosa* (A and C) and *S. aureus* (B and D) ranging from 5000 CFU to 5 CFU. * No recovery.

Elimination of DNA contamination in RNA sample preparation is important for q-RT-PCR assay as false positive amplification signals generated from DNA may lead to misleading results for RNA quantification. In this experiment, contamination of genomic DNA in RNA extracted using the chip based nucleic acid purification method was validated by replacing SuperScript III RT/Platinum® *Taq* Mix with 2 units of Platinum® *Taq* DNA polymerase in the PCR reaction mixture according to the manufacturer's protocol. As demonstrated in Fig. 4-19, minute DNA contamination was found in RNA

extracted from *P. aeruginosa* of 5000 CFU and 500 CFU. However, the difference in Ct values was more than 10 cycles as compared with those obtained with RNA template purified from bacterial cells at the same density. In this case, the DNA interference in result interpretation can be neglected. No DNA contamination was found in RNA isolated from *P. aeruginosa* of 50 CFU and 5 CFU. Similar results were gained from RNA isolated from *S. aureus* (data not shown).

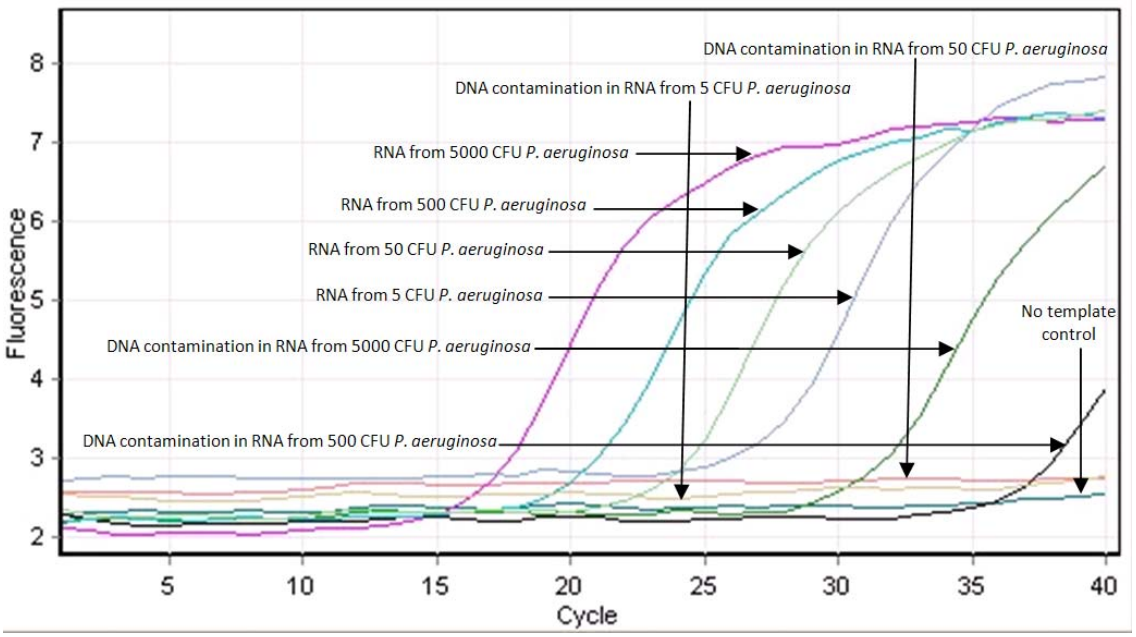

Fig. 4-19 DNA contamination in RNA isolated from *P. aeruginosa* of 5000 to 5 CFU using liquid phase nucleic acid purification chip.

In this study, a novel chip based nucleic acid purification method was developed with optimized protocol for bacterial thermal lysis, phase partitioning, and ethanol washing to ensure the maximum nucleic acid recovery. Compared with conventional column based solid phase nucleic acid extraction technique, the chip based liquid phase nucleic acid purification method outperformed in nucleic acid recovery yield up to 10

folds higher. This finding is in accordance with the previously published results that the nucleic acid recovery yield was higher with the liquid phase phenol-chloroform extraction compared with the column based purification method [143-145]. Besides, the success in nucleic acid extraction from bacterial cells in small and minute sample volume using the liquid phase nucleic acid purification chip paves the way to many critical applications, such as high throughput single bacterium transcriptional regulation assay, that current solid phase based microfluidic nucleic acid extraction platforms are unable to cater to.

4.3.2 On-chip q-PCR and q-RT-PCR assay

Currently, the nucleic acid purification and on-chip PCR assay in most microfluidic platforms [4, 84] are carried out in different reaction chambers with potential risks of sample loss during liquid transfer. This is especially problematic in nucleic acid analysis of bacteria in small amount and minute sample volume. Liu et al. previously developed an PDMS array matrix using vacuum facilitated single step sample loading method for on-chip PCR analysis with primers pre-dried in micro-wells [45]. In this study, we utilized this scenario for on-chip q-PCR or q-RT-PCR assay in the same micro-wells in which bacterial nucleic acids were isolated without the necessity to use a separate PCR reaction chamber to avoid nucleic acid sample loss during transference. Whether the purified nucleic acids in the micro-wells would be lost in the following reagent loading step was first validated by off-chip quantitative PCR assay. *P. aeruginosa* genomic DNA or total RNA were aliquoted and dried in the micro-wells of alternative position of well 1, well 3, and well 5, leaving well 2, well 4, and well 6 empty (Fig. 4-20). Following this, the PCR reaction mixture was loaded into the wells as described in Fig. 4-5. The liquid suspensions in all wells were rinse out and quantified by q-PCR or q-RT-PCR assay using

RotorGene 3000 thermal cycler. In consistency with the previous results [45], although micro-wells of the nucleic acid purification chip were momentarily connected by the PCR reagent, pre-dried nucleic acids were retained without considerable loss in quantity as evidenced by comparable Ct values obtained with the positive control nucleic acids of identical concentration (Fig. 4-21). Besides, q-PCR amplification was not observed with liquid suspension in wells without pre-dried DNA template. The late q-RT-PCR amplification from wells with no pre-aliquoted RNA was due the primer dimer formation as confirmed by analyzing the PCR product using Agilent DNA 1000 kit (Agilent Technologies, USA) according to the manufacture's protocol (Fig. 4-22). Based on the above-mentioned analysis, it can be concluded that the temporary fluidic connection of the micro-wells by during sample loading did not result in nucleic acid loss nor cross contamination, the mechanism of which is illustrated in the paper previously published by Liu et al. [45]. In summary, the proposed on-chip PCR assay has two major advantages. First, on-chip PCR reaction is carried out in the same micro-wells in which the nucleic acids are isolated so that the sample loss during liquid transfer can be avoided to ensure maximum detection sensitivity. Second, as micro-pumps and micro-valves to control the liquid flow from each nucleic acid purification chamber to the PCR reaction chamber, the strategy of which is adopted by most microfluidic nucleic acid analytical platform currently, are not required, the engineering complexity in the chip design can be reduced. This opens the possibility to accomplish high throughput nucleic acid analysis in a cost effective way.

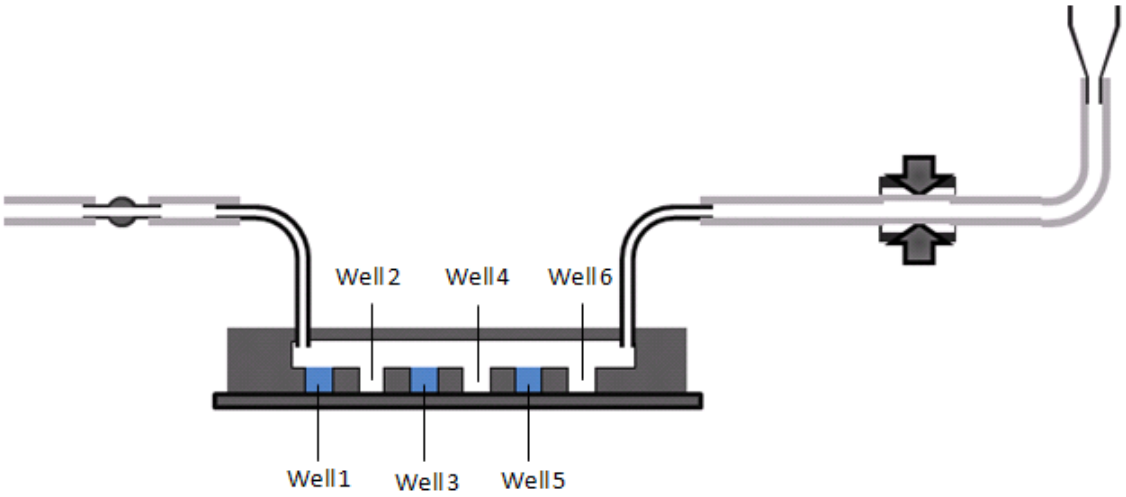

Fig. 4-20 *P. aeruginosa* genomic DNA or total RNA aliquoted in the micro-wells (blue colored) of alternative position of well 1, well 3, and well 5, leaving well 2, well 4, and well 6 empty.

On-chip q-PCR and q-RT-PCR amplifications with nucleic acids isolated from 5000 to 5 *P. aeruginosa* and *S. aureus* bacterial cells using chip based nucleic acid purification method were shown in Fig. 4-23. 1mM $CaCl_2$ was supplemented in the PCR reaction mixture to neutralize the amplification inhibition induced by EDTA retained in the micro-wells after vacuum evaporation as described in section 4.3.1.1. The controls carrying no template were occasionally amplified in the RNA based q-RT-PCR assay due to primer dimer formation. However, these products emerged significantly later than the amplification with RNA isolated from bacteria of 5 CFU and can therefore be differentiated. In addition, the Tm values of these controls were different from those of the samples with templates, hence positive PCR reaction with RNA extracted from bacterial samples can specifically be recognized (Fig. 4-24).

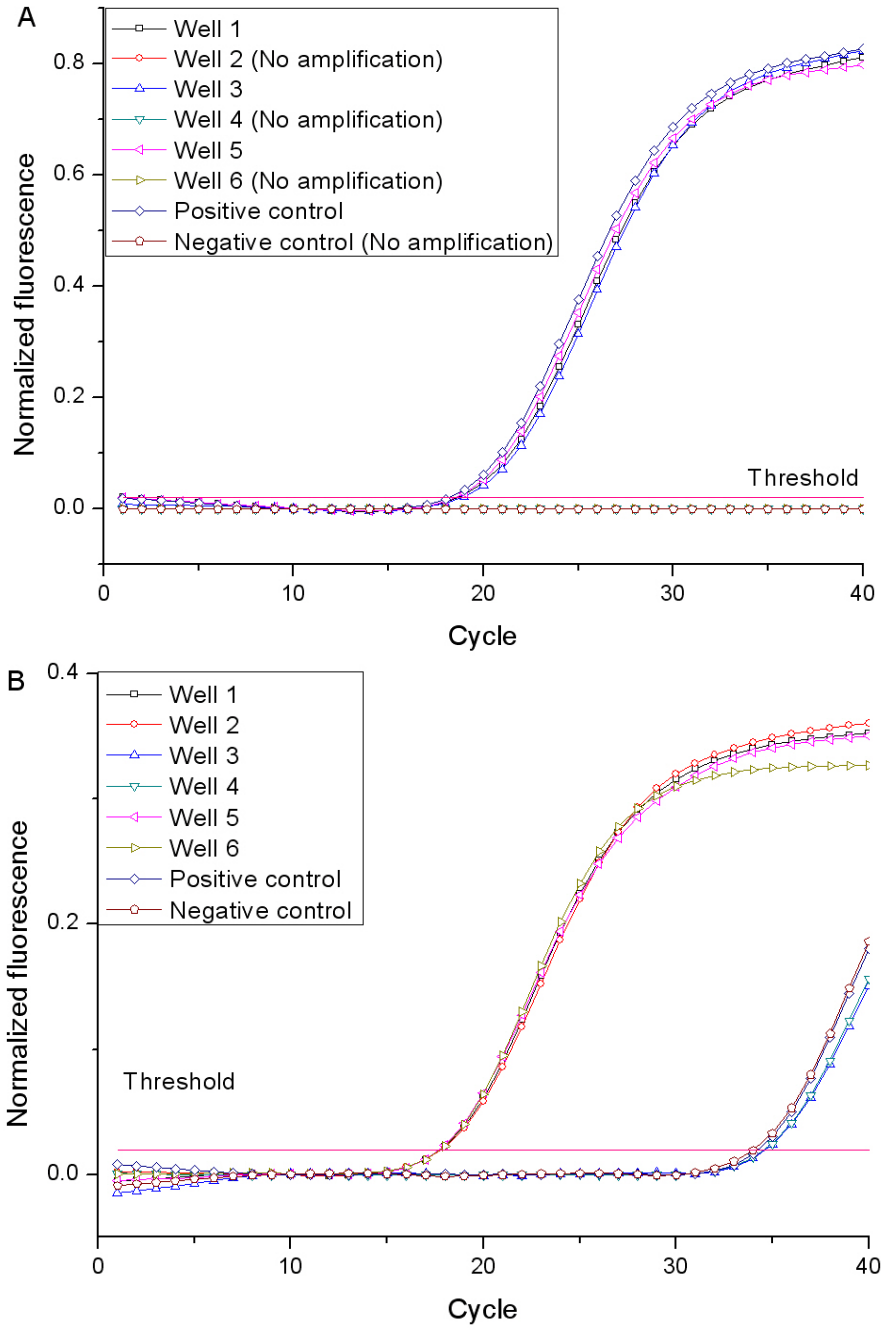

Fig. 4-21 DNA based q-PCR (A) and RNA based q-RT-PCR (B) amplification of nucleic acids in liquid suspension in all wells after sample loading. Negative control represted the no template control in PCR reaction.

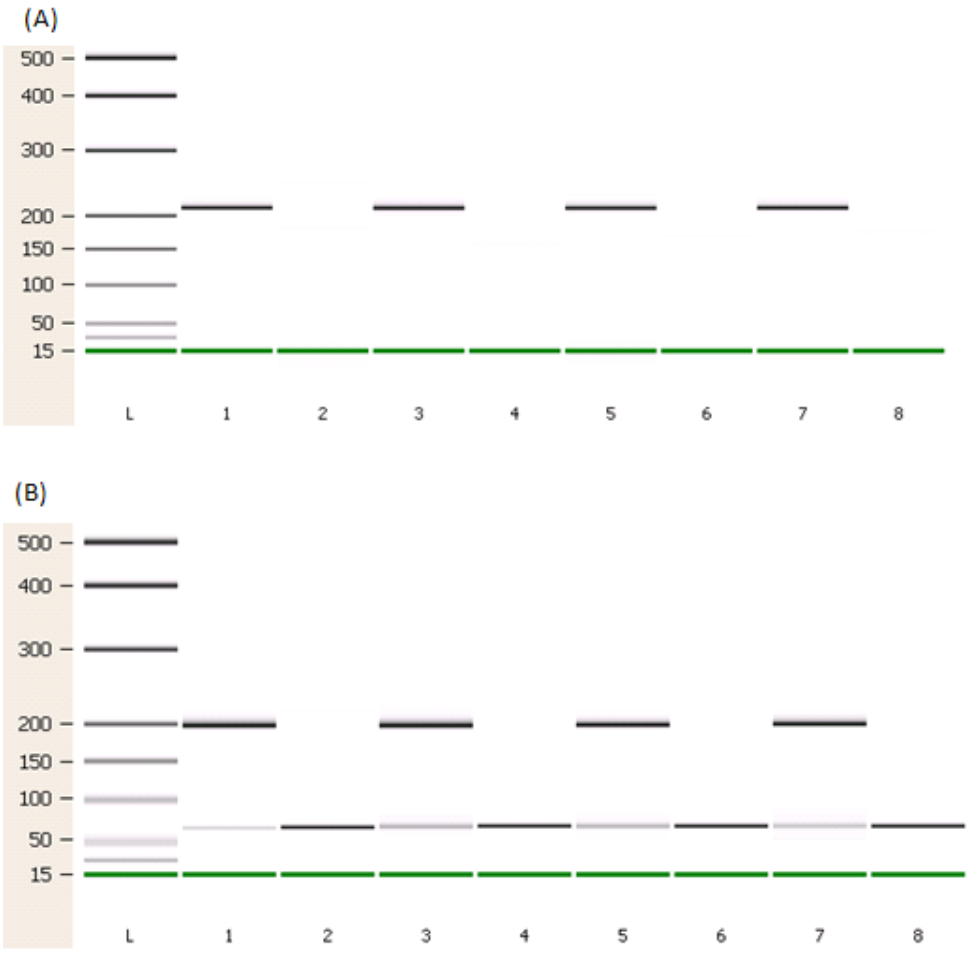

Fig. 4-22 Gel-like image of PCR products by capillary electrophoresis on DNA Labchip 1000 using Agilent 2100 bioanalyzer. Lane L is the ladder. Lanes 1-6, PCR products with *P. aeruginosa* DNA (A) or RNA (B) from well 1 to well 6. Lane 7 and Lane 8 are positive and no template control of q-PCR product targeting *P.aeruginosa* DNA(A) and q-RT-PCR product targeting *P.aeruginosa* RNA (B) respectively.

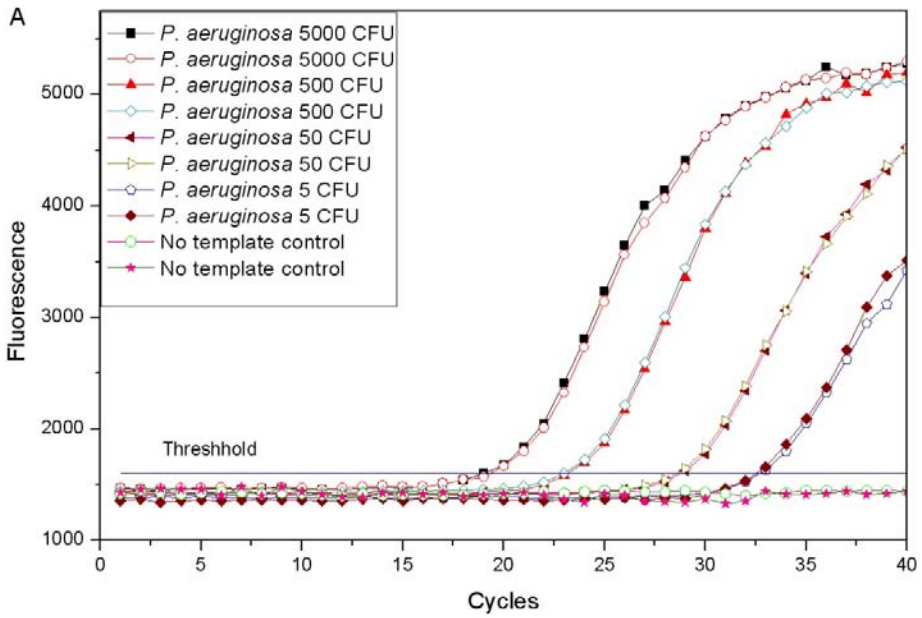
A
P. aeruginosa 5000 CFU
P. aeruginosa 5000 CFU
P. aeruginosa 500 CFU
P. aeruginosa 500 CFU
P. aeruginosa 50 CFU
P. aeruginosa 50 CFU
P. aeruginosa 5 CFU
P. aeruginosa 5 CFU
No template control
No template control
Threshhold
Fluorescence
Cycles

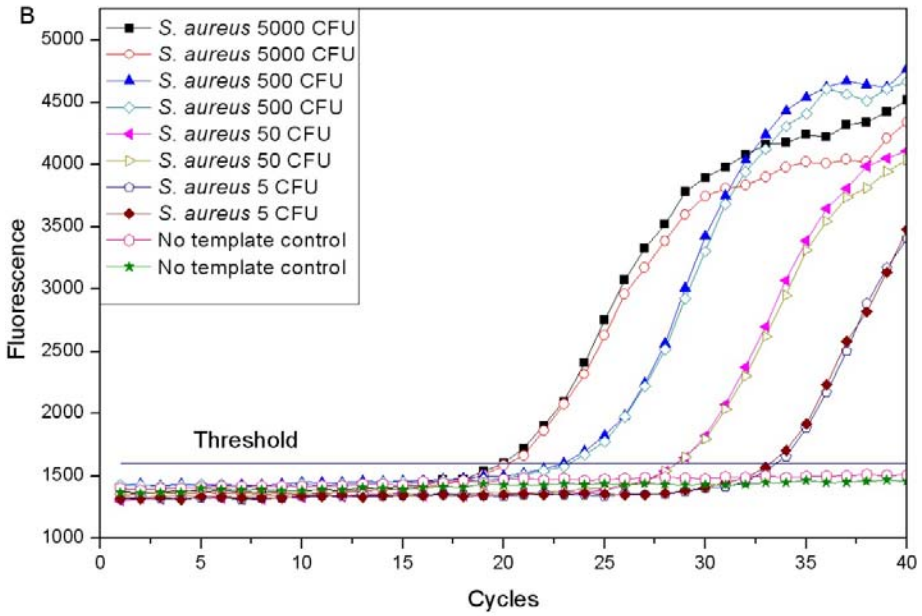
B
S. aureus 5000 CFU
S. aureus 5000 CFU
S. aureus 500 CFU
S. aureus 500 CFU
S. aureus 50 CFU
S. aureus 50 CFU
S. aureus 5 CFU
S. aureus 5 CFU
No template control
No template control
Threshold
Fluorescence
Cycles

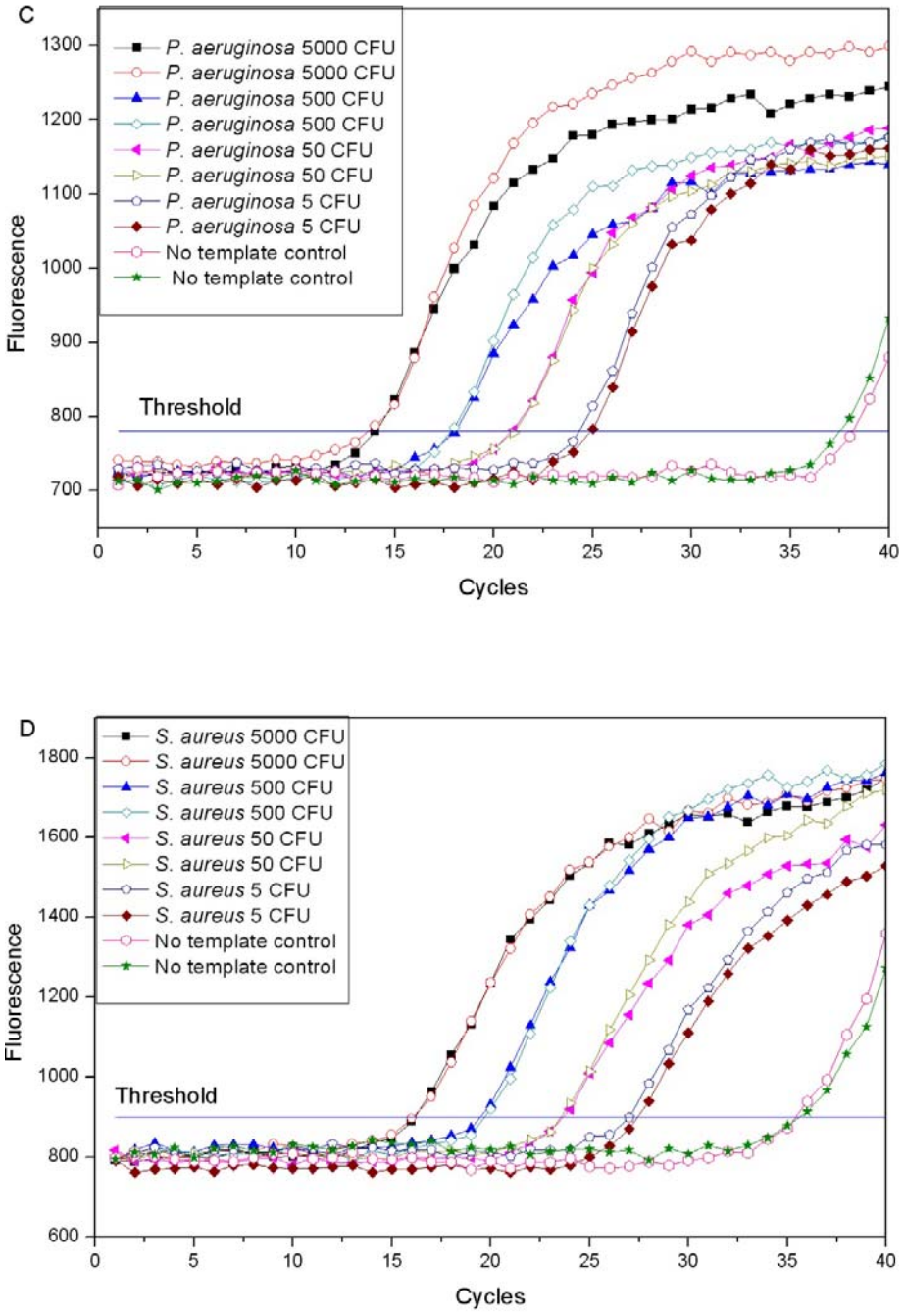

Fig. 4-23 On-chip q-PCR amplification of genomic DNA isolated from 5000 to 5 *P.aeruginosa and S. aureus* (A and B) and q-RT-PCR amplification of RNA isolated from 5000 to 5 *P.aeruginosa and S. aureus* (C and D).

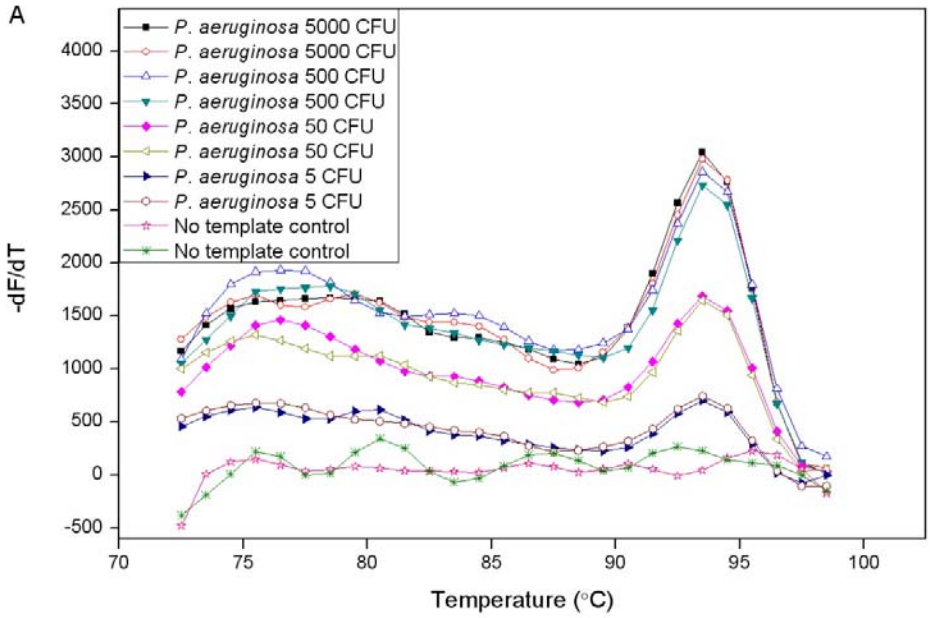
A
P. aeruginosa 5000 CFU
P. aeruginosa 5000 CFU
P. aeruginosa 500 CFU
P. aeruginosa 500 CFU
P. aeruginosa 50 CFU
P. aeruginosa 50 CFU
P. aeruginosa 5 CFU
P. aeruginosa 5 CFU
No template control
No template control
-dF/dT
4000
3500
3000
2500
2000
1500
1000
500
0
-500
70
75
80
85
90
95
100
Temperature (°C)

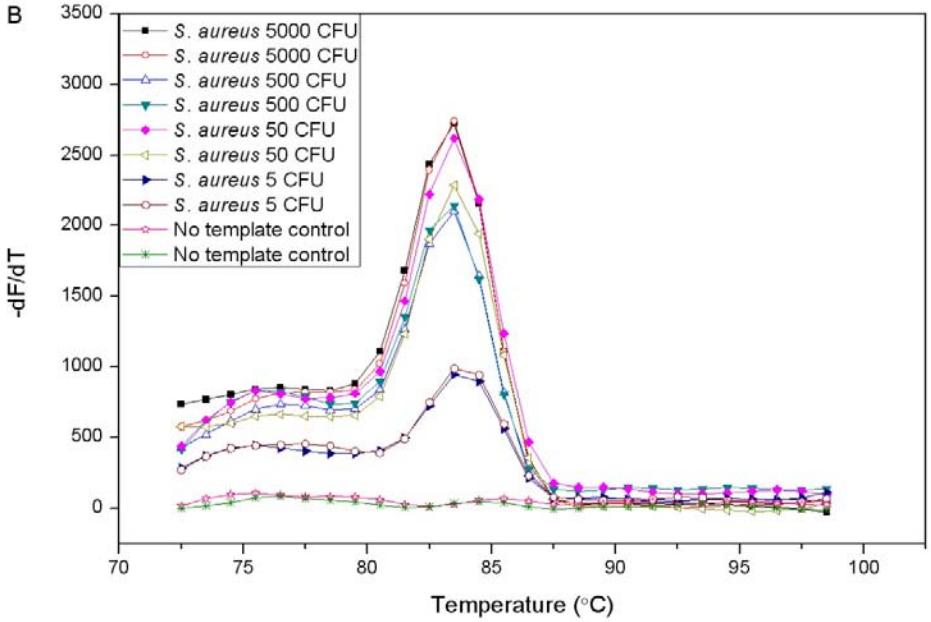
B
S. aureus 5000 CFU
S. aureus 5000 CFU
S. aureus 500 CFU
S. aureus 500 CFU
S. aureus 50 CFU
S. aureus 50 CFU
S. aureus 5 CFU
S. aureus 5 CFU
No template control
No template control
-dF/dT
3500
3000
2500
2000
1500
1000
500
0
70
75
80
85
90
95
100
Temperature (°C)

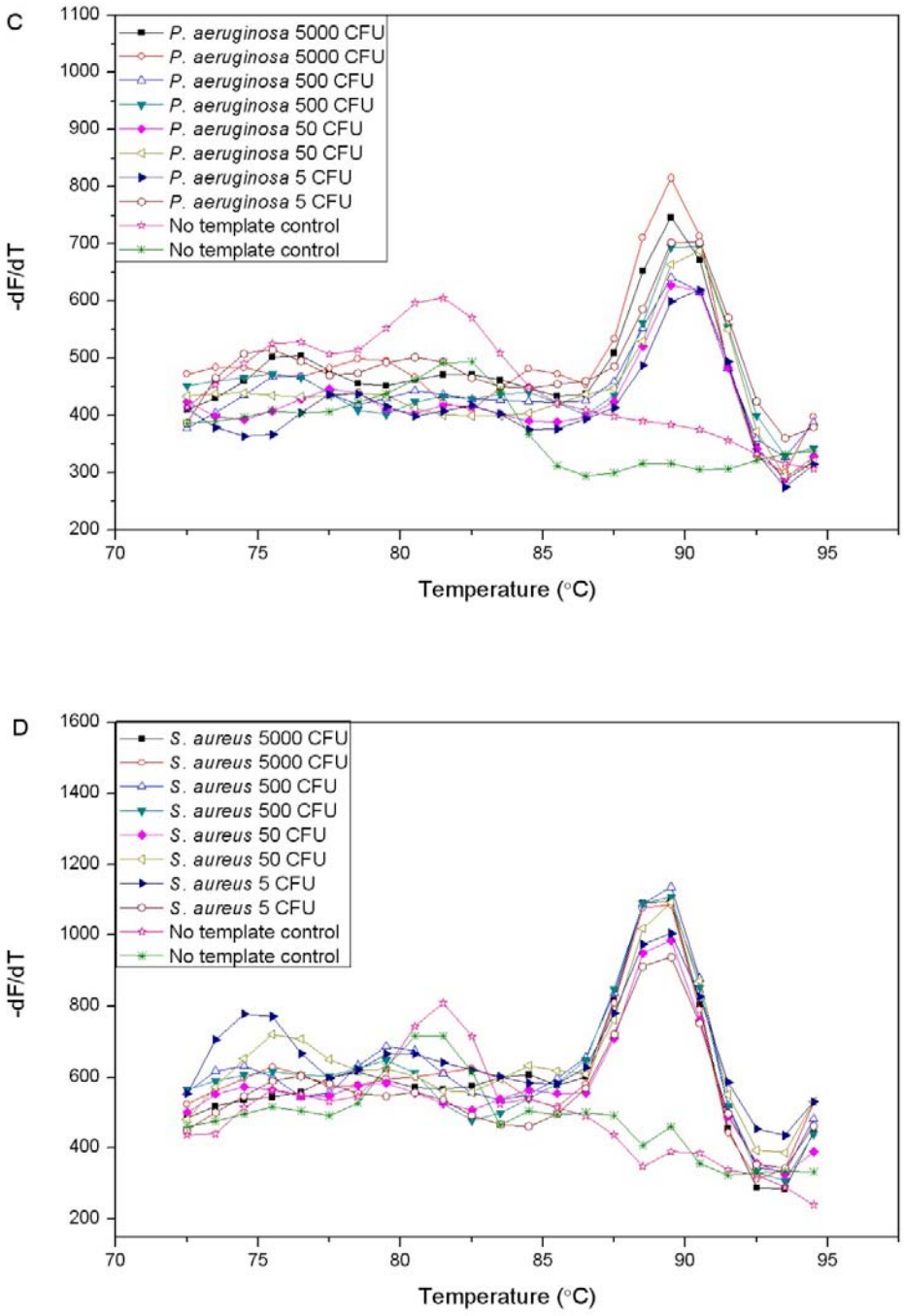

Fig. 4-24 On-chip melting curve analysis of PCR product with genomic DNA isolated from 5000 to 5 *P.aeruginosa and S. aureus* (A and B) and RNA isolated from 5000 to 5 *P.aeruginosa and S. aureus* (C and D) to test the purity of the amplified product.

4.3.3 Nucleic acid isolation from single bacterium

It is well recognized that q-PCR assay can be applied to amplify target sequence of a single DNA molecule. However, quantification of RNA from single bacterium by q-RT-PCR assay has only been proven to be possible by Gao et al recently [90]. In their research, single bacterial cell was selected by vision based aspiration and dispensing technique under the microscope followed by RNA extraction using the column based nucleic acid purification technique. Therefore, only a limited number of single bacterial cells can be studied each time. In addition, the RNA recovery rate and possible false positive signal generated by DNA contamination were not verified. To validate whether the proposed chip based liquid phase nucleic acid purification method can reach single bacterium sensitivity as a possible way to study DNA and RNA heterogeneity in microbial populations, the nucleic acid purification chip was redesigned into a 2D format with 900 micro-wells to hold the sample volume of 125 nl/well. Similar to the on-chip bacterial lysis method as described in section 3.3.2, enzyme mixture of lysozyme-proteinase K and lysostaphin-proteinase K were pre-dried in the micro-wells and were resuspended when *P. aeruginosa* and *S. aureus* cell suspension were loaded into the chip. The bacterial cell densities were adjusted to less than 0.3 CFU/well so that single bacterium can be captured in microwells [120] and lysed for onchip liquid phase nucleic acid purification (Fig. 4-25). The pre-dried enzyme in the micro-wells retained in both activity and quantity during the following sample loading step as assessed according to the same procedure as described in section 3.3.2. *P. aeruginosa* and *S. aureus* RNA were stabilized by adding 1/5 volume of ice cold phenol: ethanol (5:95) [133]. The organic phase with corresponding pH was introduced in the headspace through the inlet capillary

channel with continuous forward and backward flow at 0.65 ml/min to selectively isolate target nucleic acids from single bacterium. The 2D nucleic acid purification chip was then washed twice with 70% ethanol to remove the residual organic phase. The nucleic acids extracted from single bacterial cells were analyzed by on-chip q-PCR and q-RT-PCR analysis as described in Fig. 3-5. Taqman q-RT-PCR was performed in replacement of Sybre green assay for single bacterium RNA analysis to eliminate the primer dimer interference. The primers and probes were adopted from previously published papers [146, 147]. Bacterial cell densities were confirmed by CFU counting on LB agar. The overall success rate in obtaining DNA and RNA isolated from single *P. aeruginosa* was 92% and 85%, respectively, while 87% and 71% of micro-wells trapping single *S. aureus* showed positive amplifications for DNA and RNA, respectively, as calculated according to Poisson statistics [120]. The relatively lower success rate for RNA isolation from single bacterium may have resulted from insufficient cell lysis or incomplete removal of endogenous RNase. The absence of DNA contamination in RNA isolated from single bacterium was confirmed by no positive on-chip amplification when loading q-RT-PCR reaction mixture with SuperScript III RT/Platinum® *Taq* Mix replaced by 2 units of Platinum® *Taq* DNA polymerase as described in section 4.2.3.2 (Fig. 4-26). Fig. 4-25 served as the positive control for Fig. 4-26 as these two experiments were performed side by side. The standard deviations of the Ct values obtained from q-PCR amplifications with genomic DNA from single *P. aeruginosa* and *S. aureus* were 0.45 and 0.57 respectively, and the standard deviations of the Ct values obtained from q-PT-PCR amplifications with RNA from single *P. aeruginosa* and *S. aureus* were 0.62 and 0.68

respectively, indicating good reproducibility of the chip based liquid phase nucleic acid purification method.

4.3.4 Quantification of *rmd* gene transcripts of *P. aeruginosa* adhered single A549 cells

P. aeruginosa encodes and expresses various virulence factors that are related to pathogenesis. For example, it expresses Lipopolysaccharide (LPS) which functions similarly as an adhesin to bind to epithelial surface glycolipid asialo-GM1 [96]. LPS is well-characterized as one of the virulence factors of *P. aeruginosa*. It is located on the outer membrane of the bacterium and plays an important role in pathogen-host interactions. LPS is composed of a hydrophobic lipid A region, a core oligosaccharide, and an O polysaccharide (or O antigen). It has low permeability to antibiotics, and thus contributes to the high antibiotic resistance of *P. aeruginosa*. Early study has shown that the 50% lethal dosage for a mutant strain with damaged LPS is reduced to 1000 fold of that for its wild type [148]. Around 26 genes are reported to be involved in LPS biosynthesis, which is regulated by various environmental stimuli [149]. In this study, the mRNA transcript level of an important gene involved in O antigen synthesis, named *rmd*, which is responsible for the regulation of the synthesis of sugar nucleotide precursors for O antigen [149] was quantified. First, the average *rmd* transcription of *P. aeruginosa* adhered to the whole population of A549 cells was evaluated. At the endpoint of 2h, 4h, and 6h of infection, A549 cells were washed to eliminate the unbound bacteria, and the total RNA (both host and bacteria) was isolated by Qiagen RNeasy Mini Kit following the manufacturer's protocol. The relative gene transcription level was evaluated using multiplexing q-RT-PCR method as described in section 3.3.6 using *P. aeruginosa* 16S rRNA as the reference gene [150], and presented as relative gene transcription ratio with

the *rmd* gene transcription level of *P. aeruginosa* adhered to A549 cells after 2 hours infection defined as 1. The average number of *P. aeruginosa* adhered per A549 cell was determined by CFU counting assay. As shown in Fig. 4-27, *rmd* was up-regulated up to 6 folds as increasing number of *P. aeruginosa* cells became attached with the progression of infection, indicating that this gene may be closely regulated in accordance with *P. aeruginosa* adhesion to the host cells.

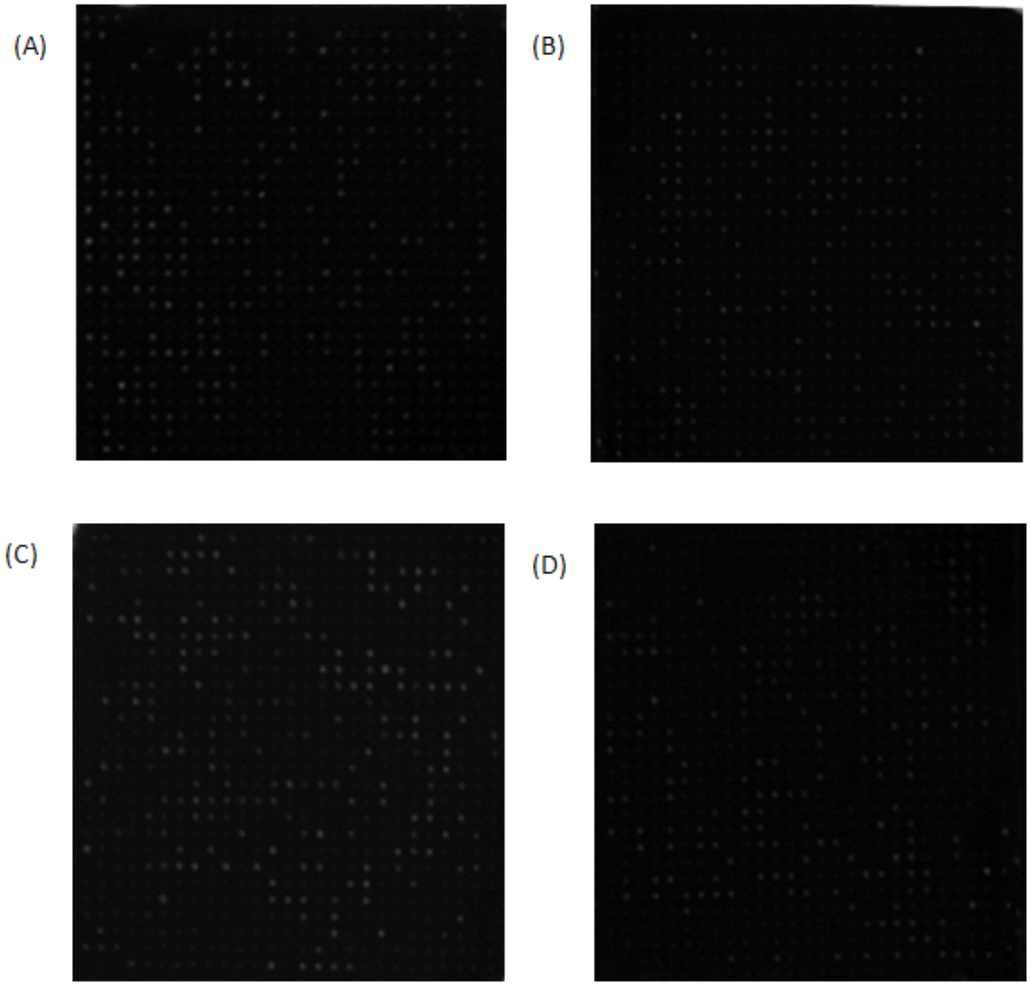

Fig. 4-25 On-chip amplification of DNA isolated from single *P. aeruginosa* (A) and *S. aureus* (C) and On-chip q-RT-PCR amplification of RNA isolated from single *P. aeruginosa* (B) and *S. aureus* (D).

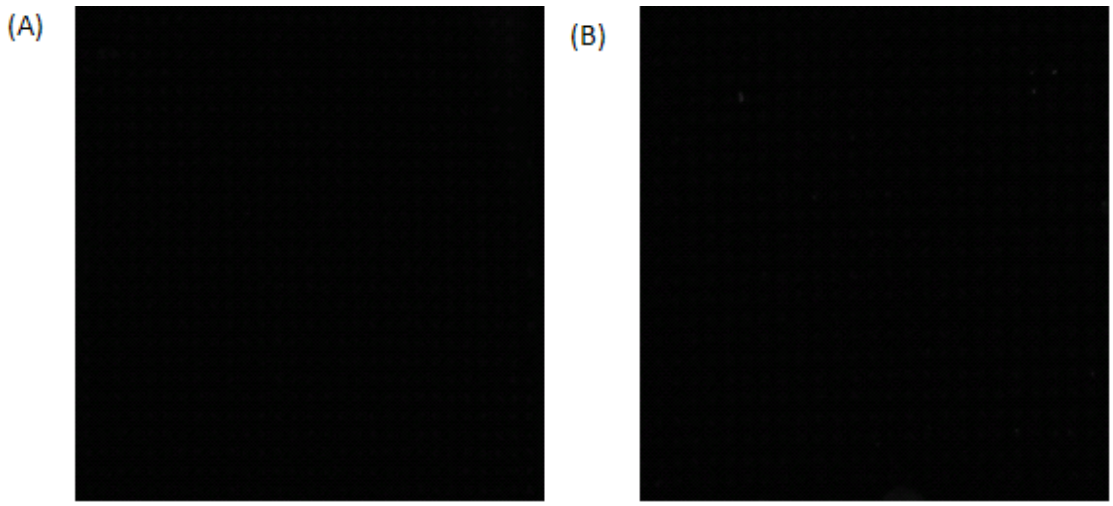

Fig. 4-26 DNA contamination in RNA isolated from single *P. aeruginosa* (A) and *S. aureus* (B) as assessed by on-chip amplification using q-RT-PCR reaction mixture with SuperScript III RT/Platinum® *Taq* Mix replaced by 2 units of Platinum® *Taq* DNA polymerase

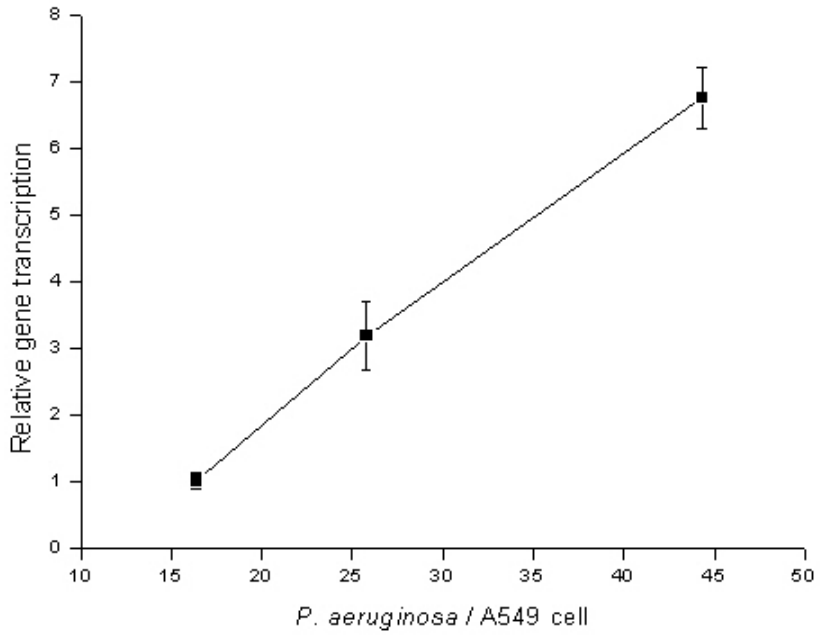

Fig. 4-27 Relative *rmd* gene transcription ratio of *P. aeruginosa* adhered to A549 cells by multiplex q-RT-PCR assay. The gene transcription data are expressed as the mean± standard error of the mean of three experiments.

Following this, the proposed 2D microfluidic nucleic acid purification chip was applied to quantify the level of *rmd* gene transcript from *P. aeruginosa* cells attached to single A549 cells. At the endpoint of *P. aeruginosa* infection at different time intervals, A549 cells were washed, collected by centrifugation and loaded into the 2D nucleic acid purification chip with the cell density pre-adjusted to less than 0.3 cell/well. RNA was isolated as described in section 4.2.5 followed by on-chip multiplex q-RT-PCR assay. The relative gene transcription ratio was calculated using the equation described in section 4.2.6. The number of *P. aeruginosa* associated with single A549 cells was estimated by the Ct value of 16S rRNA and the corresponding q-RT-PCR standard curve constructed as described in section 3.2.5, based on the fact that the quantities of 16S rRNA correlated linearly with the number of bacteria [151]. The standard curve was considered adequate to be used as the reference to quantify *P. aeruginosa* as the number of bacteria attached to single A549 cell is within the defined range as determined in the earlier stage of this study (Fig. 3-28). The *rmd* transcriptional profiles of *P. aeruginosa* adhered to single A549 cells over 2 h, 4h and 6h are shown in Fig. 4-28 with each dot representing a single A549 cell with the number of *P. aeruginosa* matched in the horizontal axis and the relative gene transcription ratio matched in the vertical axis. Up regulation of *rmd* gene in response to greater adherence of *P. aeruginosa* population to a single A549 cell was confirmed by positive correlation between the number of *P. aeruginosa* adhered and the relative gene transcription ratio. Unlike the data in Fig. 4-27 which reflected the overall increase in *rmd* transcription as the average number of adhered *P. aeruginosa* per host cell increased, Fig. 4-28 was able to highlight the fact that within the host A549 cell population, those with less *P. aeruginosa* attached did not induce as much *rmd* transcription as those with more

P. aeruginosa attached. This experiment demonstrated clearly the utility of the 2D liquid phase nucleic acid purification chip that have been developed in this study in providing biological perspectives at the single cell level.

As the in-house real time PCR thermal cycler was designed with only two-fluorescent-color detection system, gene transcription of *P. aeruginosa* in mixed infection with *S. aureus* was not included in this study. However, the above experiment has shown that it is in principle possible to use the platform to profile transcription of the two bacteria attached to the same single host cells during co-infection.

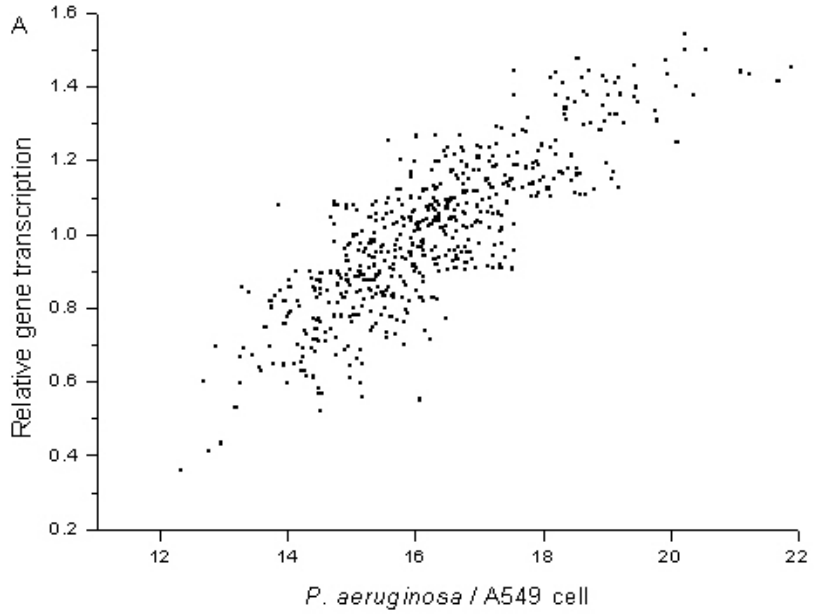

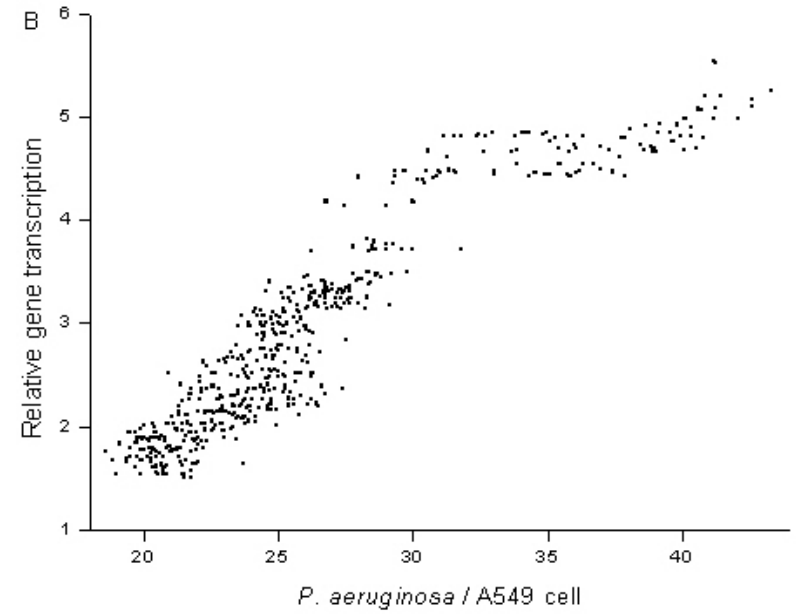

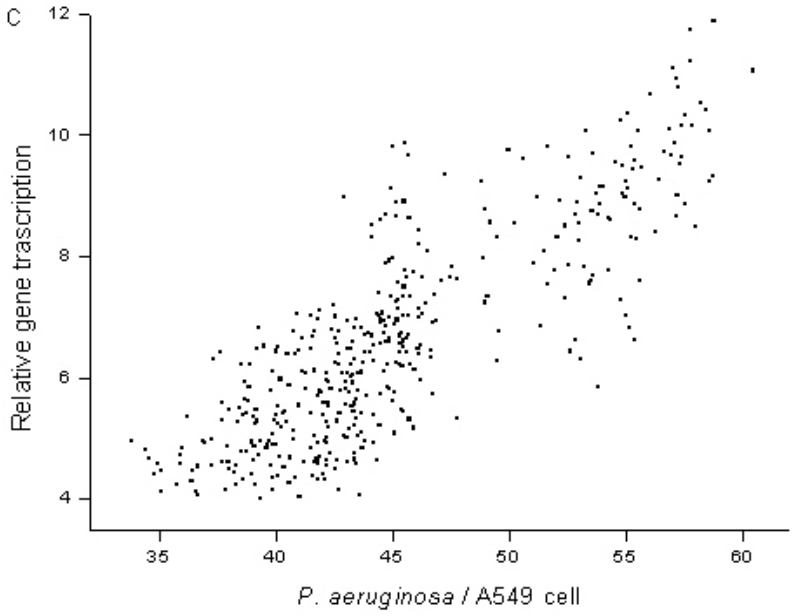

Fig. 4-28 Relative *rmd* gene transcription ratio of *P. aeruginosa* to single A549 cells at the end of 2h (A), 4h (B) and 6h (C) infection.

4.4 Application of the liquid phase nucleic acid purification chip to detect *P. aeruginosa* and *S. aureus* in urine samples by DNA based q-PCR assay

Although the scope of this thesis was to develop a microfluidic platform to study pathogen-host interactions at single cell level for fundamental biological research purpose only, the possibility to use the liquid phase nucleic acid purification chip to detect *P. aeruginosa* and *S. aureus* in urine samples by DNA based q-PCR assay was also explored. DNA based q-PCR assay is considered with priority for bacterial diagnostics in clinical samples [152, 153] due to the better accuracy and reliability as compared with RNA based q-RT-PCR assay.

Isolation of DNA from low quantities of target bacterial cells accompanied by other contaminant cells is important in demonstrating the diagnostic potential of q-PCR method in clinical samples. In order to check that aspect of the liquid phase nucleic acid chip developed in this study, *P. aeruginosa* and *S. aureus*, both important human pathogens associated with severe urinary tract infections, were used as the model microorganisms to evaluate the chip's performance to isolate DNA from the target cells in the presence of *Klebsiella pneumoniae* and *Escherichia coli* at high contamination level, to mimic the scenario of co-infection in real clinical samples. Briefly, 1 µl *P. aeruginosa* or *S. aureus* at the cell densities of 100 CFU or 10 CFU was mixed with *K. pneumoniae* and *E. coli* of 1000 CFU each. Bacterial cells were then lysed followed by chip based liquid phase DNA extraction as described in section 4.2.3.1, and submitted to q-PCR assay as described in section 4.2.3.2. The primers targeting the PA0708 gene and VicK gene as listed in table 4-1 were validated to be specific for *P. aeruginosa* and *S. aureus* respectively prior to q-PCR assay. DNA recovery was calculated as described in section

4.3.1.3. DNA isolated from *P. aeruginosa* and *S. aureus* in the absence of the contaminant bacterial cells served as a control for this experiment. As shown in Fig 4-29, the DNA purified from *P. aeruginosa* or *S. aureus* at the cell densities of both 100 CFU/µl and 10 CFU/µl in the presence of the contaminant bacteria was comparable to those obtained in the absence of the contaminant bacteria with high recovery yield of 90%-100%. These findings suggested that the liquid phase nucleic acid purification chip may potentially be applied to identify suspected bacterial pathogens in complex matrices of microbial communities in clinical samples.

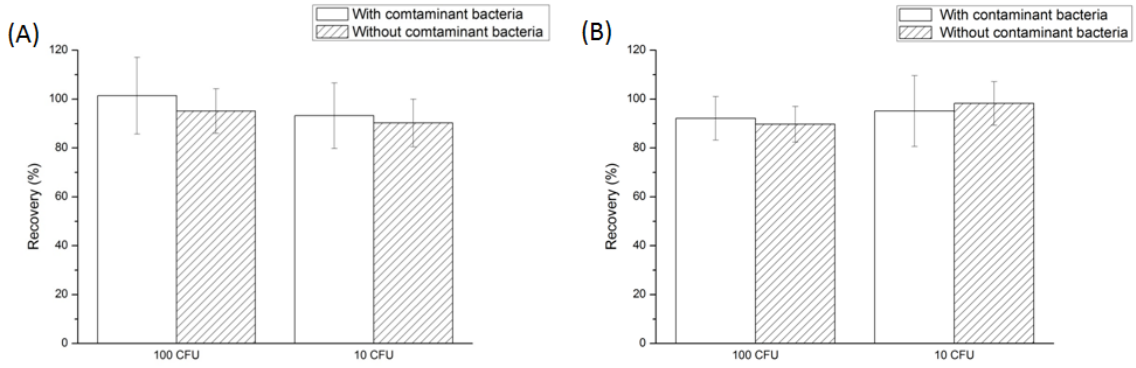

Fig 4-29. Recovery of DNA isolated by chip based liquid phase nucleic acid purification method from *P. aeruginosa* of 100 CFU and 10 CFU (A) and *S. aureus* of 100 CFU and 10 CFU (B) in the absence or presence of bacterial mixture of *K. pneumoniae* and *E. coli* at high contamination level of 1000 CFU each.

To further make the technology more convincing for use by clinicians, the possibility to apply the 2D liquid phase nucleic acid purification chip in urine samples was assessed. *P. aeruginosa* or *S. aureus* were spiked into the self collected urine samples at the cell densities of 100 CFU/ml or 10 CFU/ml along with *K. pneumoniae* and *E. coli* at1000 CFU/ml each. The spiked urine sample was directly loaded into the 2D liquid phase nucleic acid purification chip followed by phase partitioning and on-chip q-PCR as

described in section 4.2.5. According to Poisson statistics, the majority of the micro-wells contain no more than a single bacterium in this condition [120] so that the absolute quantification could be achieved by counting the number of micro-wells showing positive amplifications. Urine samples containing only contaminant bacteria served as the negative control for this experiment. As a comparison, DNA of the spiked bacteria was also purified by Qiagen DNeasy Blood & Tissue Kit according to the manufacturer's protocol and quantified by q-PCR. As illustrated in Table 4-3, the number of bacteria quantified by the 2D nucleic acid purification chip was comparable to the expected number of target bacteria at the cell density of 100 CFU/ml, which showed improved accuracy compared to the Qiagen solid phase extraction method. The sensitivity of the liquid phase nucleic acid purification chip for bacterial detection in urine samples also outperformed the previously reported solid phase extraction using magnetic beads [154]. As the total volume of all micro-wells in the 2D nucleic acid purification chip is around 112.5 μl, it can be expected that bacteria at the concentration below 10 CFU/ml (equivalent to 1 CFU/100 μl) may not be correctly quantified. The negative control of contaminant bacteria spiked in urine samples did not show any positive amplification, indicating that the number of bacteria quantified by the 2D nucleic acid purification chip was truly representative of the specific microorganisms of interest, and the presence of contaminant bacteria would not lead to compromised accuracy.

Table 4-3 Quantification of bacteria spiked in urine samples by the 2D nucleic acid purification chip and Qiagen solid phase extraction method. Each point represents the mean ± standard error of three replicated experiments.

Target microorganism	Cell density of bacteria spiked in urine samples (CFU/ml)	Cell density of bacteria as quantified by 2D nucleic acid purification chip (CFU/ml)	Cell density of bacteria as quantified Qiagen solid phase extraction method (CFU/ml)	Negative control of contaminant bacteria only
P. aeruginosa	100	92.0±5.1	15.4±3.2	No positive amplification
	10	Undetectable	Undetectable	No positive amplification
S. aureus	100	80±8.9	18.6±4.1	No positive amplification
	10	Undetectable	Undetectable	No positive amplification

4.5 Conclusion

A microfluidic liquid phase nucleic acid purification chip was developed to selectively isolate DNA or RNA from a small number of bacterial cells (ranging from 5000 down to single bacterium) in 1 µl or 125 nl sample volume, which allows the nucleic acids isolated to be detectable by on-chip quantitative PCR in the same micro-wells. From both gram-negative (*P. aeruginosa*) and gram-positive (*S. aureus*) bacterial cells ranging from 5000 to 5 CFU in 1 µl sample volume, 85%−120% of nucleic acids could be recovered (with the only exception of 70%−80% for *S. aureus* RNA recovery) using the 1D nucleic acid purification chip. This contrasted with the significantly compromised nucleic acid recovery using conventional Qiagen nucleic acid purification technique which could only achieve 10-18% in DNA recovery for 50 bacteria and 15-20% in RNA recovery for 5 bacteria. Furthermore, DNA extracted from 5 bacteria using Qiagen nucleic

acid purification technique cannot be detected by q-PCR assay. Successful high throughput RNA extraction from single bacterium with compatible on-chip q-RT-PCR assay was achieved for the first time, using the nucleic acid purification device in a 2D format of 900 micro-well array holding the sample volume of 125 nl/well, with single bacterium trapped in individual wells by loading at a cell density of less than 0.3 CFU/ml. False positive signals generated from DNA in q-RT-PCR assays can be effectively removed without the need for additional DNase treatment. The microfluidic liquid phase nucleic acid purification chip has valuable automation potential for applications such as bacterial detection and high throughput mRNA quantification from single bacterium, with minimum user exposure to the hazardous reagent. In addition, the proposed liquid phase nucleic acid purification chip can be also applied to investigate gene transcription profiling of bacteria adhered to single host cells for better understanding of pathogenesis mechanism in biological laboratory.

Chapter 5 Conclusion and future work

5.1 Conclusions

In this study, a high throughput PDMS array chip was designed and fabricated to analyze two biological perspectives of the interactions of *P. aeruginosa* to human lung epithelial A549 cells – adherence and gene transcription – at single cell level in either single or mixed infection context with *S. aureus*. The proposed PDMS array chip is simply structured with 900 micro-wells, one inlet and one outlet micro-channels. Bacterial adherence to single A549 cells was quantified by one step label-free on-chip q-PCR assay. At the endpoint of bacterial infection of 2h, 4h and 6h, single A549 cells was isolated in the individual micro-wells of the array chip probabilistically by vacuum driven microfluidic sample loading controlled by an external mechanical valve when cell density was pre-adjusted to less than 0.3 cell/well. DNA isolation of adhered *P. aeruginosa* was directly incorporated into the initial PCR cycling at 95˚C for 5 minutes with satisfactory extraction efficiency. While *S. aureus* DNA extraction was facilitated by pre-treatment of the bacterial cells with lysostaphin at optimal concentration of 50 μg/ml without significant downstream q-PCR inhibition. To avoid bacterial dissociation prior to single cell isolation, lysostaphin was pre-loaded and dried in micro-wells. Although all micro-wells are temporarily connected during the following sample loading step, the activity and quantity of this enzyme were well retained without cross-well contamination due to the non-specific interactions between protein and glass substrate. *P. aeruginosa* and *S. aureus* DNA of various concentrations were tested by q-PCR assay with good reproducibility of Ct values obtained. The success rate for single *P. aeruginosa* and *S. aureus* detection was

90% and 94% respectively, which is comparable to the sensitivity of microfluidic digital PCR platforms reported previously [32, 155]. With this new device, the association profiling of *P. aeruginosa* and *S. aureus* in both single and mixed infection contexts to single A549 cells at different time point of infection was successfully obtained. It was demonstrated that *P. aeruginosa* and *S. aureus* interact with the host A549 cells in distinguishing infection behaviors. When challenged with prolonged period of infection with *P. aeruginosa*, increasing population of A549 cells become more prone to bacterial association by opportunity. On the contrary, differentiation of the infected A549 cells in bacterial attachment emerged at the early endpoint of 2h infection of *S. aureus*, followed by a rapid association up to 4 hours of infection. However, this differentiation of the host cells in bacteria attachment was reduced as infection progressed to 6 hours. Inhibition of *P. aeruginosa* adherence in the presence of *S. aureus* was confirmed by measuring the binding kinetics of both bacteria in mixed infection context using on-chip multiplex q-PCR assay.

Liu et al. [45] previously established a simple and reliable method to load and seal a 2D matrix with DNA or RNA extracts. The 2D matrix consisted of an array of nanoliter micro-wells, one inlet channel, three outlet channels and one open headspace channel. Exterior vacuum enclosure was required to load the sample liquid into the micro-wells by vacuum driven microfluidics. This technology was further developed in this study with a new design of an enclosed headspace channel, an inlet micro-channel connected to sample reservoir and an outlet micro-channel connected directly to vacuum so that the sample loading process can be significantly simplified without the necessity to use the external vacuum attachment. Most importantly, the novel microfluidic liquid phase partitioning

method developed in this study can be incorporated into the newly designed array chip to perform multiple functionalities including single bacterium isolation and lysis, high throughput nucleic acid purification and on-chip quantitative PCR assay. As a result, "all-in-one" solution for high throughput extraction of RNA coupled with direct on-chip PCR analysis from single bacterial cells could be achieved for the first time (manuscript published in Analytical Chemistry), which is not feasible in Liu's array matrix or other previously published single cell analytical chips.

Thermal lysis technique was used in this study to release the nucleic acids from bacterial cells with the advantage of reduced engineering complexity in the nucleic acid purification chip design. When pre-treated with appropriate enzymes, bacterial cells can be thermally lysed effectively in the optimized lysis buffer with minimal nucleic acid degradation. The bacterial cell lysate was then isolated in an array of micro-well, after which the organic phase was introduced into a headspace channel connecting the micro-well array with continuous flow to increase the contact area between the phases to achieve purification of the target nucleic acids in the micro-wells. The partitioning efficiency of three types of analytes – DNA, RNA and protein – as the model macro-biomolecules present in bacterial lysate with the organic phase at the different flow rates of 0.25 ml/min 0.45 ml/min, and 0.65 ml/min were examined. At optimal organic phase flow rate of 0.65 ml/min, more than 90% DNA or RNA can be selectively recovered with 99% protein removal in a pH dependent manner. Residual organic phase can be eliminated by repeated washing and vacuum evaporating with 70% ethanol with purified nucleic acid dried in the micro-wells. PCR reaction mixture was then distributed into the micro-wells by vacuum facilitated microfluidics for on-chip PCR amplification assay in the same micro-wells in

which nucleic acids were isolated to avoid sample loss caused by liquid transfer. Up to 10 folds enhanced nucleic acid recovery was achieved with this chip based nucleic acid purification technique than conventional column based nucleic acid extraction method. DNA or RNA isolated from *P. aeruginosa* and *S. aureus* in the range of 5000 to 5 CFU in 1µl sample volume can be selectively extracted and amplified by both off-chip and on-chip quantitative PCR assay. To accomplish high throughput nucleic acid analysis from single bacterium, the nucleic acid purification device was further modified into a two dimensional format with 900 micro-wells to hold the liquid of around 125 nl. Single bacterium was trapped in the individual wells by loading the diluted samples of less than 0.3 bacteria per well. This chip was applied to investigate the transcriptional regulation of the *rmd* gene of *P. aeruginosa* adhered to single A549 cells and the up regulation of this gene in response to greater adherence of *P. aeruginosa* population was reported.

5.2 Future work

5.2.1 Further miniaturization of the microfluidic PDMS array chip to increase the throughput for single cell analysis

The micro-well in the current PDMS array chip is 0.5 mm × 0.5 mm ×0.5 mm to hold the liquid volume of around 125 nl. Further miniaturization of the micro-well to cylinder shape with the radius and height of 0.1 mm to hold the sample volume of around 3 nl will allow millions of single cells to be analyzed simultaneously in the array chip with same size of 40 mm ×40 mm. As it is reported that 86 pl is the lowest limit volume to carry out successful PCR [43], the modified chip is also suitable for high throughput PCR based nucleic acid analysis. Besides, the local concentration of the target molecules of

interest will be concentrated to around 40 times in the miniaturized micro-wells so that significant enhancement of detection sensitivity can be expected. Single A549 cells were successfully isolated (Fig. 5-1) using the modified chip with miniaturized micro-wells based on the same single step vacuum driven microfluidics proposed in this study (Fig. 3-5). New generation of quantitative PCR thermal cycler with enhanced fluorescence detection resolution for the miniaturized PDMS array chip is now under development.

5.2.2 Modification of the liquid phase nucleic acid purification chip to perform high throughput q-RT-PCR based mRNA quantification

The current chip is designed in a way to analyzed one mRNA gene transcript of a single cell. Innovative microfluidic liquid transference and mixing method is now under development to distribute RNA isolated from single cells into multiple wells for high throughput gene transcriptional regulation investigations.

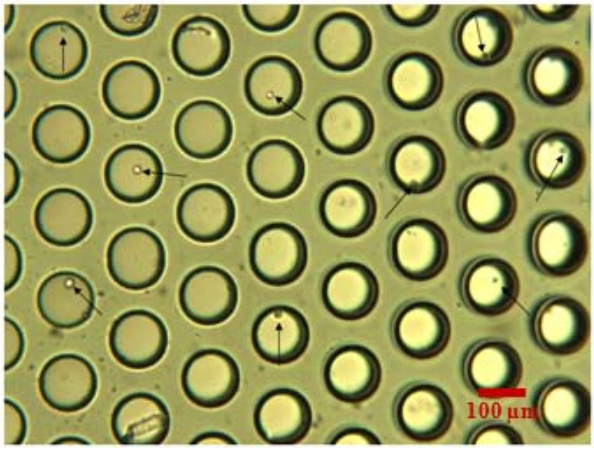

Fig. 5-1 Observation of single A549 cells isolated into the individual minitrized micro-wells of cylindar shape with the radius and height of 0.1 mm. Cells were isolated in one/zero per well pattern by portability based on single step vaccum driven microfluidics. Single cells isolated in micro-wells were arrowed.

5.2.3 Bacterial association and gene transcriptional profiling of cytotoxic *P. aeruginosa* PA103 to A549 cells using the 2D nucleic acid purification device

Studies on in vitro interaction of *P. aeruginosa* with human airway epithelial cells revealed distinguished infectious behavior of cytotoxic and invasive strains, although both could induce morbidity in animal models [122]. Cytotoxic *P. aeruginosas* strains cause lung epithelial cells death within only a short period of infection, while invasive strains do not stimulate viability changes of the host [156]. The *P.aeruginosa* PAO1 used this study belongs to the invasive strain. Further studies of the bacterial association and gene transcription profiling of both invasive and cytotoxic *P. aeruginosa* as a consequence of infection to single A549 cells using the proposed 2D nucleic acid purification chip will provide better insights to understand the strategies that *P. aeruginosa* adopt to enter and survive in mammalian cells as well as the host defense mechanism. It was demonstrated that the adhesion of *S. aureus* was enhanced in the presence of cytotoxic *P. aeruginosa* PA103 at the in MOI of 400 (Fig.5-2), which further highlighted the importance to study bacterial association to the host cells in polymicrobal infection. The proposed PDMS array chip will be used to analyze bacterial adhesion profile of *P. aeruginosa*, including both invasive and cytotoxic strains, and *S. aureus* in mixed infection contexts to single A549 cells for better understanding of lung infection induced by bacterial community.

5.2.4 Single cell analysis from more challenging sources including blood and urine

Single cell isolation and characterization is important in early stage disease diagnostic, as exampled by circulating tumor cell detection [157]. However, single cell nucleic acid analysis from blood and urine sample in the presence of various PCR

inhibitors is quite difficult. The proposed high throughput liquid phase nucleic acid purification chip shows promising potentials to remove PCR inhibitors that can be partitioned from the aqueous phase into the organic phase, including some well recognized protein inhibitors such as the anti-anticoagulant heparin. Optimal protocol for single cell nucleic acid purification (including both mammalian cell and bacterial cell) from blood and urine sample is under development for routine diagnostic application of this device in clinical laboratories.

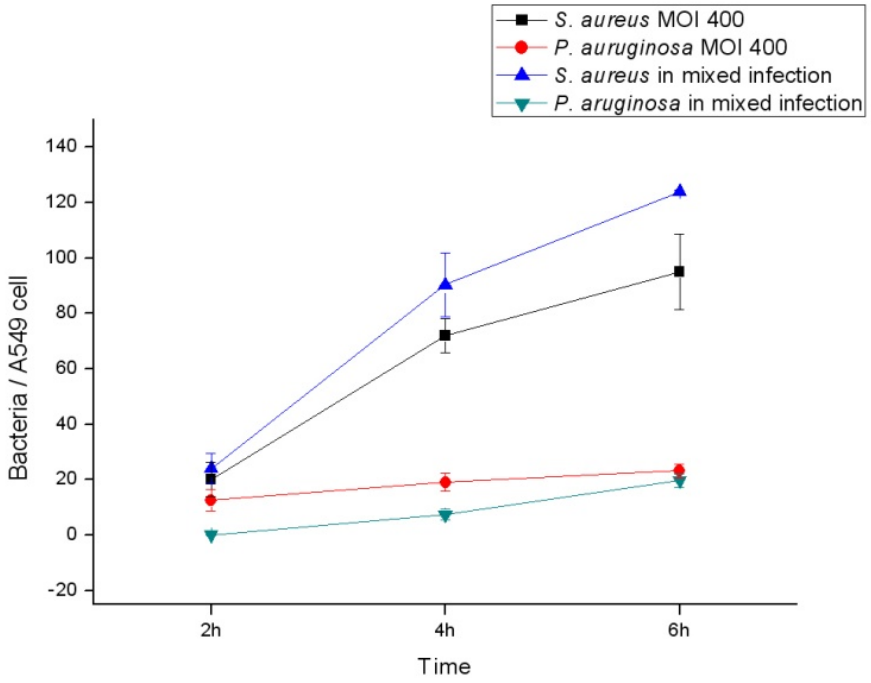

Fig.5-2 The association of *P. aeruginosa* and *S. aureus* with A549 cells in mixed infection. Cultured A549 cells were incubated with bacterial mixtures containing *P. aeruginosa* and *S. aureus* with the MOI of 400. The binding data are expressed as the mean± standard error of the mean of three experiments.

In summary, the proposed microfluidic PDMS array chip is simple, cost-effective and allows high throughput and label-free quantification of bacterial adherence to single

host cells. With integrated microfluidic phase partitioning technology, DNA or RNA from a small number of bacteria in minute sample volume can be selectively isolated with significantly enhanced recovery yield as compared with conventional column based solid phase nucleic acid extraction method. Successful on-chip PCR assay in the same micro-wells in which the nucleic acids were isolated was carried out by one step vacuum driven microfluidics. Achievement of high throughput RNA extraction from single bacterium with compatible on-chip quantitative PCR analysis was reported for the first time. The proposed microfluidic platform offered a convenient and effective "all-in-one" solution to study bacteria-host interactions at single cell level and can also be applied to other PCR based single cell analysis.

References

1. Taniguchi, K., T. Kajiyama, and H. Kambara, *Quantitative analysis of gene expression in a single cell by qPCR.* Nat Meth, 2009. **6**(7): p. 503-506.

2. Tang, F., et al., *mRNA-Seq whole-transcriptome analysis of a single cell.* Nat Meth, 2009. **6**(5): p. 377-382.

3. Raj, A., et al., *Imaging individual mRNA molecules using multiple singly labeled probes.* Nat Meth, 2008. **5**(10): p. 877-879.

4. White, A.K., et al., *High-throughput microfluidic single-cell RT-qPCR.* Proceedings of the National Academy of Sciences.

5. Sibley, C.D., et al., *A polymicrobial perspective of pulmonary infections exposes an enigmatic pathogen in cystic fibrosis patients.* Proceedings of the National Academy of Sciences, 2008. **105**(39): p. 15070-15075.

6. Spiller, D.G., et al., *Measurement of single-cell dynamics.* Nature. **465**(7299): p. 736-745.

7. Kalisky, T., P. Blainey, and S.R. Quake, *Genomic Analysis at the Single-Cell Level.* Annual Review of Genetics. **45**(1): p. 431-445.

8. Zare, R.N. and S. Kim, *Microfluidic Platforms for Single-Cell Analysis.* Annual Review of Biomedical Engineering. **12**(1): p. 187-201.

9. Lindstrom, S. and H. Andersson-Svahn, *Overview of single-cell analyses: microdevices and applications.* Lab on a Chip, 2010. **10**(24): p. 3363-3372.

10. Rettig, J.R. and A. Folch, *Large-Scale Single-Cell Trapping And Imaging Using Microwell Arrays.* Analytical Chemistry, 2005. **77**(17): p. 5628-5634.

11. David, C.D., et al., *Rapid prototyping of microfluidic switches in poly(dimethyl siloxane) and their actuation by electro-osmotic flow.* Journal of Micromechanics and Microengineering, 1999. **9**(3): p. 211.

12. Unger, M.A., et al., *Monolithic Microfabricated Valves and Pumps by Multilayer Soft Lithography.* Science, 2000. **288**(5463): p. 113-116.

13. Wu, H., A. Wheeler, and R.N. Zare, *Chemical cytometry on a picoliter-scale integrated microfluidic chip.* Proceedings of the National Academy of Sciences of the United States of America, 2004. **101**(35): p. 12809-12813.

14. Jensen, E.C., et al., *Microvalve Enabled Digital Microfluidic Systems for High-Performance Biochemical and Genetic Analysis.* Journal of the Association for Laboratory Automation. **15**(6): p. 455-463.

15. Takao, H., et al., *A MEMS microvalve with PDMS diaphragm and two-chamber configuration of thermo-pneumatic actuator for integrated blood test system on silicon.* Sensors and Actuators A: Physical, 2005. **119**(2): p. 468-475.

16. Rich, C.A. and K.D. Wise, *A high-flow thermopneumatic microvalve with improved efficiency and integrated state sensing.* Microelectromechanical Systems, Journal of, 2003. **12**(2): p. 201-208.

17. Goll, C., et al., *An electrostatically actuated polymer microvalve equipped with a movable membrane electrode.* Journal of Micromechanics and Microengineering, 1997. **7**(3): p. 224.

18. Yobas, L., et al., *A novel integrable microvalve for refreshable Braille display system.* Microelectromechanical Systems, Journal of, 2003. **12**(3): p. 252-263.

19. Chou, H.-P., M.A. Unger, and S.R. Quake, *A Microfabricated Rotary Pump.* Biomedical Microdevices, 2001. **3**(4): p. 323-330.

20. Tseng, H.-Y., et al., *Membrane-activated microfluidic rotary devices for pumping and mixing.* Biomedical Microdevices, 2007. **9**(4): p. 545-554.

21. Lindström, S., et al., *A microwell array device with integrated microfluidic components for enhanced single-cell analysis.* Electrophoresis, 2009. **30**(24): p. 4166-4171.

22. White, A.K., et al., *High-throughput microfluidic single-cell RT-qPCR.* Proceedings of the National Academy of Sciences, 2011.

23. Fu, A.Y., et al., *An Integrated Microfabricated Cell Sorter.* Analytical Chemistry, 2002. **74**(11): p. 2451-2457.

24. Eyer, K., et al., *A microchamber array for single cell isolation and analysis of intracellular biomolecules.* Lab on a Chip. **12**(4): p. 765-772.

25. Bontoux, N., et al., *Integrating whole transcriptome assays on a lab-on-a-chip for single cell gene profiling.* Lab on a Chip, 2008. **8**(3): p. 443-450.

26. Sugio, Y., et al., *An agar-based on-chip neural-cell-cultivation system for stepwise control of network pattern generation during cultivation.* Sensors and Actuators B: Chemical, 2004. **99**(1): p. 156-162.

27. Chen, C.S., et al., *Geometric Control of Cell Life and Death.* Science, 1997. **276**(5317): p. 1425-1428.

28. Carlo, D.D., L.Y. Wu, and L.P. Lee, *Dynamic single cell culture array.* Lab on a Chip, 2006. **6**(11): p. 1445-1449.

29. Skelley, A.M., et al., *Microfluidic control of cell pairing and fusion.* Nat Meth, 2009. **6**(2): p. 147-152.

30. Chabert, M., K.D. Dorfman, and J.-L. Viovy, *Droplet fusion by alternating current (AC) field electrocoalescence in microchannels.* Electrophoresis, 2005. **26**(19): p. 3706-3715.

31. Link, D.R., et al., *Geometrically Mediated Breakup of Drops in Microfluidic Devices.* Physical Review Letters, 2004. **92**(5): p. 054503.

32. Kumaresan, P., et al., *High-Throughput Single Copy DNA Amplification and Cell Analysis in Engineered Nanoliter Droplets.* Analytical Chemistry, 2008. **80**(10): p. 3522-3529.

33. Edd, J.F., et al., *Controlled encapsulation of single-cells into monodisperse picolitre drops.* Lab on a Chip, 2008. **8**(8): p. 1262-1264.

34. He, M., et al., *Selective Encapsulation of Single Cells and Subcellular Organelles into Picoliter- and Femtoliter-Volume Droplets.* Analytical Chemistry, 2005. **77**(6): p. 1539-1544.

35. Klein, D., *Quantification using real-time PCR technology: applications and limitations.* Trends in Molecular Medicine, 2002. **8**(6): p. 257-260.

36. Kubista, M., et al., *The real-time polymerase chain reaction.* Molecular Aspects of Medicine. **27**(2-3): p. 95-125.

37. Wong, L.-J.C., R.-K. Bai, and V.V. Didenko, *Real-Time Quantitative Polymerase Chain Reaction Analysis of Mitochondrial DNA Point Mutation. Fluorescent Energy Transfer Nucleic Acid Probes*, 2006, Humana Press. p. 187-200.

38. Litt, M.D., et al., *Transitions in histone acetylation reveal boundaries of three separately regulated neighboring loci.* EMBO J, 2001. **20**(9): p. 2224-2235.

39. Northrup, M.A., et al., *A Miniature Analytical Instrument for Nucleic Acids Based on Micromachined Silicon Reaction Chambers.* Analytical Chemistry, 1998. **70**(5): p. 918-922.

40. Daniel, J.H., et al., *Silicon microchambers for DNA amplification.* Sensors and Actuators A: Physical, 1998. **71**(1-2): p. 81-88.

41. Dahl, A., et al., *Quantitative PCR based expression analysis on a nanoliter scale using polymer nano-well chips.* Biomedical Microdevices, 2007. **9**(3): p. 307-314.

42. Nagai, H., et al., *Development of A Microchamber Array for Picoliter PCR.* Analytical Chemistry, 2000. **73**(5): p. 1043-1047.

43. Liu, J., C. Hansen, and S.R. Quake, *Solving the "World-to-Chip" Interface Problem with a Microfluidic Matrix.* Analytical Chemistry, 2003. **75**(18): p. 4718-4723.

44. Shin, Y.S. and et al., *PDMS-based micro PCR chip with Parylene coating.* Journal of Micromechanics and Microengineering, 2003. **13**(5): p. 768.

45. Liu, H.-B., et al., *Rapid distribution of a liquid column into a matrix of nanoliter wells for parallel real-time quantitative PCR.* Sensors and Actuators B: Chemical, 2009. **135**(2): p. 671-677.

46. Mahalanabis, M., et al., *Cell lysis and DNA extraction of gram-positive and gram-negative bacteria from whole blood in a disposable microfluidic chip.* Lab on a Chip, 2009. **9**(19): p. 2811-2817.

47. Liu, R.H., et al., *Self-Contained, Fully Integrated Biochip for Sample Preparation, Polymerase Chain Reaction Amplification, and DNA Microarray Detection.* Analytical Chemistry, 2004. **76**(7): p. 1824-1831.

48. Belgrader, P., et al., *A Minisonicator To Rapidly Disrupt Bacterial Spores for DNA Analysis.* Analytical Chemistry, 1999. **71**(19): p. 4232-4236.

49. Dauphin, L.A., B.D. Moser, and M.D. Bowen, *Evaluation of five commercial nucleic acid extraction kits for their ability to inactivate Bacillus anthracis spores and comparison of DNA yields from spores and spiked environmental samples.* Journal of Microbiological Methods, 2009. **76**(1): p. 30-37.

50. Xiang, X., et al., *Comparison of three methods for respiratory virus detection between induced sputum and nasopharyngeal aspirate specimens in acute asthma.* Journal of Virological Methods, 2002. **101**(1-2): p. 127-133.

51. Blin, N. and D.W. Stafford, *A general method for isolation of high molecular weight DNA from eukaryotes.* Nucleic Acids Research, 1976. **3**(9): p. 2303-2308.

52. Chomczynski, P. and N. Sacchi, *The single-step method of RNA isolation by acid guanidinium thiocyanate-phenol-chloroform extraction: twenty-something years on.* Nat. Protocols, 2006. **1**(2): p. 581-585.

53. Boom, R., et al., *Rapid and simple method for purification of nucleic acids.* Journal of Clinical Microbiology, 1990. **28**(3): p. 495-503.

54. Muyal, J., et al., *Systematic comparison of RNA extraction techniques from frozen and fresh lung tissues: checkpoint towards gene expression studies.* Diagnostic Pathology, 2009. **4**(1): p. 9.

55. Kramvis, A., S. Bukofzer, and M.C. Kew, *Comparison of hepatitis B virus DNA extractions from serum by the QIAamp blood kit, GeneReleaser, and the phenol-chloroform method.* J. Clin. Microbiol., 1996. **34**(11): p. 2731-2733.

56. Xiang, X., et al., *Comparison of different methods of total RNA extraction for viral detection in sputum.* Journal of Virological Methods, 2001. **94**(1-2): p. 129-135.

57. Cady, N.C., S. Stelick, and C.A. Batt, *Nucleic acid purification using microfabricated silicon structures.* Biosensors and Bioelectronics, 2003. **19**(1): p. 59-66.

58. Hindson, B.J., et al., *Development of an automated DNA purification module using a micro-fabricated pillar chip.* Analyst, 2008. **133**(2): p. 248-255.

59. Wolfe, K.A., et al., *Toward a microchip-based solid-phase extraction method for isolation of nucleic acids.* Electrophoresis, 2002. **23**(5): p. 727-733.

60. Breadmore, M.C., et al., *Microchip-Based Purification of DNA from Biological Samples.* Analytical Chemistry, 2003. **75**(8): p. 1880-1886.

61. Wu, Q., et al., *Microchip-Based Macroporous Silica Sol-Gel Monolith for Efficient Isolation of DNA from Clinical Samples.* Analytical Chemistry, 2006. **78**(16): p. 5704-5710.

62. Wen, J., et al., *DNA Extraction Using a Tetramethyl Orthosilicate-Grafted Photopolymerized Monolithic Solid Phase.* Analytical Chemistry, 2006. **78**(5): p. 1673-1681.

63. Wen, J., et al., *Microfluidic-Based DNA Purification in a Two-Stage, Dual-Phase Microchip Containing a Reversed-Phase and a Photopolymerized Monolith.* Analytical Chemistry, 2007. **79**(16): p. 6135-6142.

64. Jiang, G. and D.J. Harrison, *mRNA isolation in a microfluidic device for eventual integration of cDNA library construction.* Analyst, 2000. **125**(12): p. 2176-2179.

65. Liu, C.-J., et al., *Magnetic-bead-based microfluidic system for ribonucleic acid extraction and reverse transcription processes.* Biomedical Microdevices, 2009. **11**(2): p. 339-350.

66. Hong, J.W., et al., *A nanoliter-scale nucleic acid processor with parallel architecture.* Nat Biotech, 2004. **22**(4): p. 435-439.

67. Lee, W.-C., et al., *An integrated microfluidic system using magnetic beads for virus detection.* Diagnostic microbiology and infectious disease, 2008. **60**(1): p. 51-58.

68. Reddy, V. and J.D. Zahn, *Interfacial stabilization of organic-aqueous two-phase microflows for a miniaturized DNA extraction module.* Journal of Colloid and Interface Science, 2005. **286**(1): p. 158-165.

69. Mao, X.L., S. Yang, and J.D. Zahn, *IMECE2006-16084 Experimental Demonstration and Numerical Simulation of Organic-Aqueous Liquid Extraction Enhanced by Droplet Formation in a Microfluidic Channel.* 2006 ASME International Mechanical Engineering Congress and Exposition, 2006. **262**: p. 213-220

70. Morales, M. and J. Zahn, *Droplet enhanced microfluidic-based DNA purification from bacterial lysates via phenol extraction.* Microfluidics and Nanofluidics. **9**(6): p. 1041-1049.

71. Zahn, J. and V. Reddy, *Two phase micromixing and analysis using electrohydrodynamic instabilities.* Microfluidics and Nanofluidics, 2006. **2**(5): p. 399-415.

72. Fan, H.C., et al., *Whole-genome molecular haplotyping of single cells.* Nat Biotech. **29**(1): p. 51-57.

73. Ottesen, E.A., et al., *Microfluidic Digital PCR Enables Multigene Analysis of Individual Environmental Bacteria.* Science, 2006. **314**(5804): p. 1464-1467.

74. Zeng, Y., et al., *High-Performance Single Cell Genetic Analysis Using Microfluidic Emulsion Generator Arrays.* Analytical Chemistry. **82**(8): p. 3183-3190.

75. Marcy, Y., et al., *Nanoliter Reactors Improve Multiple Displacement Amplification of Genomes from Single Cells.* PLoS Genet, 2007. **3**(9): p. e155.

76. Lecault, V., et al., *Microfluidic single cell analysis: from promise to practice.* Current Opinion in Chemical Biology, (0).

77. Marcus, J.S., W.F. Anderson, and S.R. Quake, *Parallel Picoliter RT-PCR Assays Using Microfluidics.* Analytical Chemistry, 2006. **78**(3): p. 956-958.

78. Guo, G., et al., *Resolution of Cell Fate Decisions Revealed by Single-Cell Gene Expression Analysis from Zygote to Blastocyst.* Developmental Cell. **18**(4): p. 675-685.

79. Yoo, A.S., et al., *MicroRNA-mediated conversion of human fibroblasts to neurons.* Nature. **476**(7359): p. 228-231.

80. Dalerba, P., et al., *Single-cell dissection of transcriptional heterogeneity in human colon tumors.* Nat Biotech. **29**(12): p. 1120-1127.

81. Zhang, H., et al., *Massively Parallel Single-Molecule and Single-Cell Emulsion Reverse Transcription Polymerase Chain Reaction Using Agarose Droplet Microfluidics.* Analytical Chemistry. **84**(8): p. 3599-3606.

82. Marcus, J.S., W.F. Anderson, and S.R. Quake, *Microfluidic Single-Cell mRNA Isolation and Analysis.* Analytical Chemistry, 2006. **78**(9): p. 3084-3089.

83. Zhong, J.F., et al., *A microfluidic processor for gene expression profiling of single human embryonic stem cells.* Lab on a Chip, 2008. **8**(1): p. 68-74.

84. Toriello, N.M., et al., *Integrated microfluidic bioprocessor for single-cell gene expression analysis.* Proceedings of the National Academy of Sciences, 2008. **105**(51): p. 20173-20178.

85. Dubnau, D. and R. Losick, *Bistability in bacteria.* Molecular Microbiology, 2006. **61**(3): p. 564-572.

86. Young, J.W., et al., *Measuring single-cell gene expression dynamics in bacteria using fluorescence time-lapse microscopy.* Nat. Protocols. **7**(1): p. 80-88.

87. Teramoto, J., et al., *Single live-bacterial cell assay of promoter activity and regulation.* Genes to Cells. **15**(11): p. 1111-1122.

88. Miao, H., et al., *Dual fluorescence system for flow cytometric analysis of Escherichia coli transcriptional response in multi-species context.* Journal of Microbiological Methods, 2009. **76**(2): p. 109-119.

89. Robertson, K.L. and G.J. Vora, *Locked Nucleic Acid and Flow Cytometry-Fluorescence In Situ Hybridization for the Detection of Bacterial Small Noncoding RNAs.* Applied and Environmental Microbiology. **78**(1): p. 14-20.

90. Gao, W., W. Zhang, and D.R. Meldrum, *RT-qPCR based quantitative analysis of gene expression in single bacterial cells.* Journal of Microbiological Methods. **85**(3): p. 221-227.

91. Bonifacio, S.L., J.A. Kitterman, and P.C. Ursell, *Pseudomonas pneumonia in infants: an autopsy study.* Human Pathology, 2003. **34**(9): p. 929-938.

92. Gibson, R.L., J.L. Burns, and B.W. Ramsey, *Pathophysiology and Management of Pulmonary Infections in Cystic Fibrosis.* American Journal of Respiratory and Critical Care Medicine, 2003. **168**(8): p. 918-951.

93. Hoiby, N., *Recent advances in the treatment of Pseudomonas aeruginosa infections in cystic fibrosis.* BMC Medicine. **9**(1): p. 32.

94. Lyczak, J.B., C.L. Cannon, and G.B. Pier, *Lung Infections Associated with Cystic Fibrosis.* Clinical Microbiology Reviews, 2002. **15**(2): p. 194-222.

95. Hogardt, M. and J. Heesemann, *Adaptation of Pseudomonas aeruginosa during persistence in the cystic fibrosis lung.* International Journal of Medical Microbiology. **300**(8): p. 557-562.

96. Kipnis, E., T. Sawa, and J. Wiener-Kronish, *Targeting mechanisms of Pseudomonas aeruginosa pathogenesis.* Médecine et maladies infectieuses, 2006. **36**(2): p. 78-91.

97. Chi, E., et al., *Interaction of Pseudomonas aeruginosa with A549 pneumocyte cells.* Infect. Immun., 1991. **59**(3): p. 822-828.

98. Hara-Kaonga, B. and T.G. Pistole, *OmpD but not OmpC is involved in adherence of Salmonella enterica serovar Typhimurium to human cells.* Canadian Journal of Microbiology, 2004. **50**(9): p. 719-727.

99. Furugen, M., et al., *Legionella pneumophila infection induces programmed cell death, caspase activation, and release of high-mobility group box 1 protein in A549 alveolar epithelial cells: inhibition by methyl prednisolone.* Respiratory Research, 2008. **9**(1): p. 39.

100. Agerer, F., S. Waeckerle, and C.R. Hauck, *Microscopic quantification of bacterial invasion by a novel antibody-independent staining method.* Journal of Microbiological Methods, 2004. **59**(1): p. 23-32.

101. Cleary, J., et al., *Enteropathogenic Escherichia coli (EPEC) adhesion to intestinal epithelial cells: role of bundle-forming pili (BFP), EspA filaments and intimin.* Microbiology, 2004. **150**(3): p. 527-538.

102. Larrosa, M., et al., *Evaluation of Pseudomonas aeruginosa (PAO1) adhesion to human alveolar epithelial cells A549 using SYTO 9 dye.* Molecular and Cellular Probes. **26**(3): p. 121-126.

103. Fuller, M.E., et al., *Development of a Vital Fluorescent Staining Method for Monitoring Bacterial Transport in Subsurface Environments.* Applied and Environmental Microbiology, 2000. **66**(10): p. 4486-4496.

104. Ulrich, M., et al., *Localization of Staphylococcus aureus in Infected Airways of Patients with Cystic Fibrosis and in a Cell Culture Model of S. aureus Adherence.* American Journal of Respiratory Cell and Molecular Biology, 1998. **19**(1): p. 83-91.

105. Chifiriuc, M.C., et al., *Interaction of bacteria isolated from clinical biofilms with cardiovascular prosthetic devices and eukaryotic cells.* Anaerobe. **17**(6): p. 419-421.

106. Trouillet, S., et al., *A novel flow cytometry-based assay for the quantification of Staphylococcus aureus adhesion to and invasion of eukaryotic cells.* Journal of Microbiological Methods. **86**(2): p. 145-149.

107. Wang, Y., et al., *Past, present and future applications of flow cytometry in aquatic microbiology.* Trends in Biotechnology. **28**(8): p. 416-424.

108. Grün, M., et al., *Flow cytometric quantification of chlamydial infection in cell culture.* Journal of Microbiological Methods, 2009. **78**(3): p. 360-362.

109. Candela, M., et al., *Real-time PCR quantification of bacterial adhesion to Caco-2 cells: Competition between bifidobacteria and enteropathogens.* Research in Microbiology, 2005. **156**(8): p. 887-895.

110. SCHMIDT, M.T., et al., *Evaluation of Quantitative PCR Measurement of Bacterial Colonization of Epithelial Cells.* Polish Journal of Microbiology, 2010. **59**(2): p. 89-93.

111. Shi, X., et al., *Real-time PCR of single bacterial cells on an array of adhering droplets.* Lab on a Chip, 2011. **11**(13): p. 2276-2281.

112. Zeng, Y., et al., *High-Performance Single Cell Genetic Analysis Using Microfluidic Emulsion Generator Arrays.* Analytical Chemistry, 2010. **82**(8): p. 3183-3190.

113. Tokimitsu, Y., et al., *Single lymphocyte analysis with a microwell array chip.* Cytometry Part A, 2007. **71A**(12): p. 1003-1010.

114. Hauser, A.R., *The type III secretion system of Pseudomonas aeruginosa: infection by injection.* Nat Rev Micro, 2009. **7**(9): p. 654-665.

115. Azghani, A.O., E.J. Miller, and B.T. Peterson, *Virulence Factors from Pseudomonas aeruginosa Increase Lung Epithelial Permeability.* Lung, 2000. **178**(5): p. 261-269.

116. Bragonzi, A., et al., *Pseudomonas aeruginosa Microevolution during Cystic Fibrosis Lung Infection Establishes Clones with Adapted Virulence.* American Journal of Respiratory and Critical Care Medicine, 2009. **180**(2): p. 138-145.

117. Al-Aloul, M., et al., *Increased morbidity associated with chronic infection by an epidemic Pseudomonas aeruginosa strain in CF patients.* Thorax, 2004. **59**(4): p. 334-336.

118. Kolak, M., et al., *Molecular typing of the bacterial flora in sputum of cystic fibrosis patients.* International Journal of Medical Microbiology, 2003. **293**(4): p. 309-317.

119. Scott, D.S., et al., *Impact of Pseudomonas and Staphylococcus Infection on Inflammation and Clinical Status in Young Children with Cystic Fibrosis.* The Journal of pediatrics, 2009. **154**(2): p. 183-188.e3.

120. Mazutis, L., et al., *Droplet-Based Microfluidic Systems for High-Throughput Single DNA Molecule Isothermal Amplification and Analysis.* Analytical Chemistry, 2009. **81**(12): p. 4813-4821.

121. Ramalingam, N., et al., *Real-time PCR-based microfluidic array chip for simultaneous detection of multiple waterborne pathogens.* Sensors and Actuators B: Chemical. **145**(1): p. 543-552.

122. Evans, D.J., et al., *Pseudomonas aeruginosa Invasion and Cytotoxicity Are Independent Events, Both of Which Involve Protein Tyrosine Kinase Activity.* Infect. Immun., 1998. **66**(4): p. 1453-1459.

123. Dingle, T., et al., *A real-time quantitative PCR assay for evaluating Clostridium difficile adherence to differentiated intestinal Caco-2 cells.* Journal of Medical Microbiology. **59**(8): p. 920-924.

124. Grégori, G., et al., *Resolution of Viable and Membrane-Compromised Bacteria in Freshwater and Marine Waters Based on Analytical Flow Cytometry and Nucleic Acid Double Staining.* Applied and Environmental Microbiology, 2001. **67**(10): p. 4662-4670.

125. Kim, S.J., et al., *Structures of Staphylococcus aureus Cell-Wall Complexes with Vancomycin, Eremomycin, and Chloroeremomycin Derivatives by 13C{19F} and 15N{19F} Rotational-Echo Double Resonance.* Biochemistry, 2006. **45**(16): p. 5235-5250.

126. Wu, J.A., et al., *Lysostaphin Disrupts Staphylococcus aureus and Staphylococcus epidermidis Biofilms on Artificial Surfaces.* Antimicrobial Agents and Chemotherapy, 2003. **47**(11): p. 3407-3414.

127. Poole, P.L., *The role of hydration in lysozyme structure and activity: Relevance in protein engineering and design.* Journal of Food Engineering, 1994. **22**(1-4): p. 349-365.

128. Wang, X. and B. Seed, *A PCR primer bank for quantitative gene expression analysis.* Nucleic Acids Research, 2003. **31**(24): p. e154.

129. Rogers, G.B., et al., *Characterization of Bacterial Community Diversity in Cystic Fibrosis Lung Infections by Use of 16S Ribosomal DNA Terminal Restriction Fragment Length Polymorphism Profiling.* J. Clin. Microbiol., 2004. **42**(11): p. 5176-5183.

130. Rogers, G.B., et al., *Bacterial Diversity in Cases of Lung Infection in Cystic Fibrosis Patients: 16S Ribosomal DNA (rDNA) Length Heterogeneity PCR and 16S rDNA Terminal Restriction Fragment Length Polymorphism Profiling.* J. Clin. Microbiol., 2003. **41**(8): p. 3548-3558.

131. Strober, W., *Trypan Blue Exclusion Test of Cell Viability*, in *Current Protocols in Immunology*2001, John Wiley & Sons, Inc.

132. Hao-Bing, L. and G. Hai-Qing, *Templateless prototyping of polydimethylsiloxane microfluidic structures using a pulsed CO 2 laser.* Journal of Micromechanics and Microengineering, 2009. **19**(3): p. 037002.

133. Bhagwat, A.A., et al., *Computational methods and evaluation of RNA stabilization reagents for genome-wide expression studies.* Journal of Microbiological Methods, 2003. **55**(2): p. 399-409.

134. Khan, I.U.H. and J.S. Yadav, *Development of a Single-Tube, Cell Lysis-Based, Genus-Specific PCR Method for Rapid Identification of Mycobacteria: Optimization of Cell Lysis, PCR Primers and Conditions, and Restriction Pattern Analysis.* J. Clin. Microbiol., 2004. **42**(1): p. 453-457.

135. De Medici, D., et al., *Evaluation of DNA Extraction Methods for Use in Combination with SYBR Green I Real-Time PCR To Detect Salmonella enterica Serotype Enteritidis in Poultry.* Appl. Environ. Microbiol., 2003. **69**(6): p. 3456-3461.

136. Sung, K., et al., *A simple and efficient Triton X-100 boiling and chloroform extraction method of RNA isolation from Gram-positive and Gram-negative bacteria.* FEMS Microbiology Letters, 2003. **229**(1): p. 97-101.

137. Li, Y. and R.R. Breaker, *Kinetics of RNA Degradation by Specific Base Catalysis of Transesterification Involving the 2' -Hydroxyl Group.* Journal of the American Chemical Society, 1999. **121**(23): p. 5364-5372.

138. Karim, Z., et al., *Acid pH Increases the Stability of BSC1/NKCC2 mRNA in the Medullary Thick Ascending Limb.* Journal of the American Society of Nephrology, 2003. **14**(9): p. 2229-2236.

139. Yonemura, K., K. Matsumoto, and H. Maeda, *Isolation and Characterization of Nucleases from a Clinical Isolate of Serratia marcescens kums 3958.* Journal of Biochemistry, 1983. **93**(5): p. 1287-1295.

140. Davies, R.C., A. Neuberger, and B.M. Wilson, *The dependence of lysozyme activity on pH and ionic strength.* Biochimica et Biophysica Acta (BBA) - Enzymology, 1969. **178**(2): p. 294-305.

141. Manning, K., *Isolation of nucleic acids from plants by differential solvent precipitation.* Analytical Biochemistry, 1991. **195**(1): p. 45-50.

142. Nanassy, O.Z., P.V. Haydock, and M.W. Reed, *Capture of genomic DNA on glass microscope slides.* Analytical Biochemistry, 2007. **365**(2): p. 240-245.

143. Salonen, A., et al., *Comparative analysis of fecal DNA extraction methods with phylogenetic microarray: Effective recovery of bacterial and archaeal DNA using mechanical cell lysis.* Journal of Microbiological Methods. **81**(2): p. 127-134.

144. Amagliani, G., et al., *Detection of Listeria monocytogenes using a commercial PCR kit and different DNA extraction methods.* Food Control, 2007. **18**(9): p. 1137-1142.

145. Phongsisay, V., V.N. Perera, and B.N. Fry, *Evaluation of eight RNA isolation methods for transcriptional analysis in Campylobacter jejuni.* Journal of Microbiological Methods, 2007. **68**(2): p. 427-429.

146. Pérez-Osorio, A.C., K.S. Williamson, and M.J. Franklin, *Heterogeneous rpoS and rhlR mRNA levels and 16S rRNA/rDNA ratios within Pseudomonas aeruginosa biofilms, sampled by laser capture microdissection.* Journal of Bacteriology.

147. Zhang, L., et al., *Regulated gene expression in Staphylococcus aureus for identifying conditional lethal phenotypes and antibiotic mode of action.* Gene, 2000. **255**(2): p. 297-305.

148. Cryz, S.J., Jr., et al., *Role of lipopolysaccharide in virulence of Pseudomonas aeruginosa.* Infect. Immun., 1984. **44**(2): p. 508-513.

149. Rocchetta, H.L., L.L. Burrows, and J.S. Lam, *Genetics of O-Antigen Biosynthesis in Pseudomonas aeruginosa.* Microbiol. Mol. Biol. Rev., 1999. **63**(3): p. 523-553.

150. Goldsworthy, M.J.H., *Gene expression of Pseudomonas aeruginosa and MRSA within a catheter-associated urinary tract infection biofilm model.* Bioscience Horizons, 2008. **1**(1): p. 28-37.

151. Matsuda, K., et al., *Sensitive Quantitative Detection of Commensal Bacteria by rRNA-Targeted Reverse Transcription-PCR.* Applied and Environmental Microbiology, 2007. **73**(1): p. 32-39.

152. Espy, M.J., et al., *Real-Time PCR in Clinical Microbiology: Applications for Routine Laboratory Testing.* Clinical Microbiology Reviews, 2006. **19**(1): p. 165-256.

153. Lacroix, J.-M., et al., *PCR-based technique for the detection of bacteria in semen and urine.* Journal of Microbiological Methods, 1996. **26**(1–2): p. 61-71.

154. Klaschik, S., et al., *Detection and Differentiation of In Vitro-Spiked Bacteria by Real-Time PCR and Melting-Curve Analysis.* Journal of Clinical Microbiology, 2004. **42**(2): p. 512-517.

155. Yung, T.K.F., et al., *Single-Molecule Detection of Epidermal Growth Factor Receptor Mutations in Plasma by Microfluidics Digital PCR in Non-small Cell Lung Cancer Patients.* Clinical Cancer Research, 2009. **15**(6): p. 2076-2084.

156. Fleiszig, S.M., et al., *Pseudomonas aeruginosa invades corneal epithelial cells during experimental infection.* Infect. Immun., 1994. **62**(8): p. 3485-3493.

157. Maimonis, P.J., et al., *Affinity and size capture of circulating tumor cells: A platform for increased sensitivity.* AACR Meeting Abstracts. **2010**(1_Molecular_Diagnostics_Meeting): p. B5-.